Characterization of resistance to Fusarium head blight in bread and durum wheat

A dissertation submitted to the College of
Graduate and Postdoctoral Studies
in partial fulfillment of the requirements
for the degree of Doctor of Philosophy
in the Department of Plant Sciences
University of Saskatchewan
Saskatoon, Saskatchewan, Canada

By
Gurcharn Singh Brar

PERMISSION TO USE

In presenting this dissertation in partial fulfillment of the requirements of a postgraduate degree from the University of Saskatchewan, I agree that the Libraries of this University may make it freely available for inspection. I further agree that permission for copying of this dissertation in any manner, in whole or in part, for scholarly purposes may be granted by the professor or professors who supervised this thesis work, or in their absence, by the Head of the Department or the Dean of the College in which this thesis work was done. It is understood that any copying or publication or use of this dissertation or part thereof for financial gain shall not be allowed without my written permission. It is also understood that due recognition shall be given to me and to the University of Saskatchewan in any scholarly use which may be made of any material in my dissertation.

DISCLAIMER

This dissertation was exclusively created to meet the dissertation and/or exhibition requirements for the degree of Doctor of Philosophy at the University of Saskatchewan. References in this dissertation to any specific commercial products, process, or service by trade name, manufacturer or otherwise, does not constitute or imply endorsement, recommendation, or favoring by the University of Saskatchewan. The views and opinions of the author expressed herein do not reflect those of the University of Saskatchewan and shall not be used for advertising or product endorsement purposes.

Requests for permission to copy or to make other use of material in this dissertation in whole or part should be addressed to:

Head,	OR	Dean
Department of Plant Sciences,		College of Graduate and Postdoctoral Studies
College of Agriculture and Bioresources		University of Saskatchewan
51 Campus Drive,		116 Thorvaldson Building, 110 Science Place
University of Saskatchewan,		Saskatoon, Saskatchewan S7N 5C9
Saskatoon, Saskatchewan, S7N 5A8		Canada
Canada		

ABSTRACT

Fusarium head blight (FHB) caused primarily by *Fusarium graminearum* (*Fg*) Schwabe (telomorph: *Gibberella zeae* Schw. [Petch]) in North America, is one of the most devstating diseases of wheat in Canada. An integrated approach to manage this disease is recommended that combines the adoption of cultural practices (tillage and crop rotation), cultivar resistance, and fungicide application at recommended timings. Resistance to FHB in wheat is a quantitatively inherited trait and highly influenced by environmental conditions. Sources of resistance are available in common wheat but not for durum wheat. There are no commercially available durum cultivars which are moderately resistant in North America which in part, can be explained by a lack of resistance in the primary gene pool. The current study was designed to study the effects (on disease suppression and linkage-drag associated with introgressions) of Sumai 3 derived *Fhb1*, *Fhb2*, and *Fhb5* genes in hard red spring wheat cultivars [near-isogenic lines (NILs) developed in CDC Go and CDC Alsask backgrounds] from western Canada, the interaction of *Fhb1* and *Fhb5* with metconazole fungicide, and the mapping of quantitative trait loci (QTL) from emmer and durum wheat lines. The last part of the study utilized X-ray computed tomography as a tool to image selected NILs in the CDC Alsask background and focused on identification of key tissues conferring Type-II resistance to *Fg*. The phenotypic response of NILs carrying combinations of Sumai 3-derived genes suggested non-additive responses and *Fhb5* was as effective as *Fhb1* in conferring field resistance in both populations. Four to five resistance improving alleles, other than *Fhb1*, *Fhb2*, and *Fhb5*, in both populations were identified and three of five in the CDC Go population were contributed by the susceptible parent. The regions carrying these resistance improving alleles encoded disease resistance proteins, protein kinases, nucleotide-binding and leucine rich repeats' domains. Complex epistatic gene-gene interactions among marker loci (including *Fhb1*, *Fhb2*, *Fhb5*) explained >20% of the phenotypic variation in FHB infection measurements. For the linkage drag experiment, introgressions resulted in lower thousand kernel weight and increased plant height with *Fhb5*. Among end-use quality traits, SDS-sedimentation volume and grain protein content were affected. In addition to *Fhb1*, *Fhb2*, *Fhb5*, we identified 10 loci in CDC Alsask NILs and nine in CDC Go NILs that affected the traits measured and none of these additional loci were common in both populations indicating the presence of multiple alleles in exotic sources that can result in linkage drag. Linkage drag is largely dependent on genetic background and the proportion of donor resistance alleles, thus, we observed more adverse effects among CDC Alsask NILs than among CDC Go NILs. Improvements in FHB resistance can still be made by introgressing the major genes examined in this study by using marker-assisted selection

and selecting rare segregants with improved agronomy and end-use quality. There was an additive effect of Sumai 3-derived genes with metconazole in suppressing FHB and deoxynivalenol (DON) accumulation in the grain. Despite higher fungicide efficacy on moderately susceptible (MS) genotypes, FHB severity was greater on MS as compared to moderately resistant (MR) genotypes. Application of fungicides is warranted even on MR cultivars under moderate and high FHB disease pressure to reduce the amount of Fusarium damaged kernels (FDKs) and DON accumulation. In the QTL mapping study of tetraploid wheat, fifteen QTL (derived from both parents) for FHB resistance were identified on 11 of the 14 chromosomes using saturated linkage maps and a majority of the QTL were consistently detected in multiple environments. The combination of four relative large-effect and promising QTL reduced field FHB index, severity, incidence and visual rating index by 59%, 48%, 30%, and 29%, respectively. The majority of the QTL reported in the current study are novel and represent narrow intervals between the flanking markers; therefore, marker-assisted selection shoulb be of value in breeding FHB resistant durum wheat cultivars. In the final study of this thesis, as a proof-of-concept, we showcased the successful use of synchrotron-based X-ray imaging techniques to study the wheat-*Fg* interaction. This work indicated/re-confirmed the structural role of rachilla and rachis nodes in Type-II resistance to *Fg* in wheat. The results from all these studies will help wheat breeders to make decisions on introgressing exotic FHB resistance genes into common wheat. Additionally, novel QTL identified in tetraploid wheat can be used to enhance resistance in elite durum wheat lines by marker-assisted selection.

DEDICATION

I dedicate this work and dissertation to the great emperor of Sikh Empire, Sher-e-Punjab (Lion of Punjab) Maharaja Ranjit Singh (1780-1839), Maharani Jind Kaur (1817-1863) and their son Maharaja Duleep Singh (1838-1893)

ACKNOWLEDGEMENTS

I would like to express my special appreciation to my co-supervisors Dr. Pierre J. Hucl (Professor and Wheat Breeder, Crop Development Centre) and Dr. Hadley R. Kutcher (Professor and Cereal Pathologist, Crop Development Centre) for their valuable academic guidance, encouragements and tremendous support throughout my degree program. I also extend my sincere thanks to my advisory committee members Dr. Curtis J. Pozniak (Professor and Wheat Breeder, Crop Development Centre), Dr. Chithra Karunakaran (Senior Scientist and Manager, Environmental and Earth Sciences, the Canadian Light Source – National Synchrotron Research Facility, Saskatoon), Drs. Yuguang Bai (Head, Department of Plant Sciences), Dr. Steve Shirtliffe (Acting Head, Department of Plant Sciences), and Dr. Soledade Pedras (Department of Chemistry, University of Saskatchewan) for their scientific advice and insightful comments and suggestions. Special thanks to Dr. Paul Murphy (North Carolina State University, USA) for serving as the external examiner for this dissertation.

I am very grateful to Dr. Pawan K. Singh [Head, Wheat Pathology, International Maize and Wheat Improvement Center (CIMMYT), Mexico], Dr. Anita L. Brûlé-Babel (Wheat Breeder, University of Manitoba), Dr. Maria A. Henriquez (Wheat Pathologist, Agriculture and Agri-Food Canada, Morden Research and Development Center, Morden, MB), Dr. Xinyao He (Wheat Geneticist, CIMMYT, Mexico) for their help in field trials and support in the degree program. I appreciate the technical assistance provided by Mike Grieman, Glenn Trowell, Mallory Dyck, Everett Boots, Angel Liew, Dr. Amidou N'Diaye, Krysta Wiebe, Justin Coulson, Lexie Martin, Connie Briggs, Gene Argnosa, Dr. Amit Deokar as well as the entire staff of the Bread Wheat Field Lab, Cereal Pathology Lab, the Grains Innovation Lab, Wheat Molecular Breeding Lab at the University of Saskatchewan, Mid-IR and BMIT beamlines at the Canadian Light Source, Wheat Pathology Lab at CIMMYT, Mexico. Finally, I would thank my family for their moral support and unconditional love.

I gratefully acknowledge the financial assistance from the University of Saskatchewan Dean's Scholarship for PhD, Saskatchewan Wheat Development Commission (SWDC) Scholarship, Monsanto's Beachell-Borlaug International Scholars Progarm (MBBISP), the Canadian Phytopathological Society (CPS) Graduate Scholarship, Pest Management Award/Scholarship from the Canadian Society of Agronomy (CSA) and other many minor scholarships from the Department of Plant Science, College of Agriculture & Bioresources, and the University of Saskatchewan.

TABLE OF CONTENTS

LIST OF TABLES

LIST OF FIGURES

LIST OF APPENDICES

LIST OF ABBREVIATIONS

3-ADON – 3-acetyl deoxynivalenol

15-ADON – 15-acetyl deoxynivalenol

AACC – American Association of Cereal Chemists

AAFC – Agriculture and Agri-Food Canada

AUDPC – Area under disease progress curve

BC_x - Backcross

BCRIL – Backcross recombinant inbred line

BMIT – Biomedical imaging and therapy

CDC – Crop Development Centre

CIMMYT – International Maize and Wheat Improvement Center

CLS – Canadian Light Source

CT – Computed/Computational tomography

DArT – Diversity Array Technology

DON – Deoxynivalenol

dpi – Days post inoculation

ELISA – Enzyme-linked immunosorbent assay

FDK – Fusarium damaged kernel

FE – Fungicide efficacy

Fg – Fusarium graminearum

FGSC – *Fusarium graminearum* species complex

FHB – Fusarium head blight

GH – Greenhouse

GP – Grain protein

HSD – Tukey's honest significant difference

INC – Incidence

IND - Index

IR – Infrared

IWGSC – International Wheat Genome Sequencing Consortium

LSD – Fisher's least significant difference

MAS – Marker-assisted selection

MB - Manitoba

NIL – Near-isogenic line

NIV – Nivalenol

NRRL – Northern Regional Research Laboratory

PCI – Phase-contrast imaging

PDR – Percent disease reduction

PFT – Pore-forming toxin-like

PITRE – Phase-sensitive X-ray image processing and tomography reconstruction

POTAGE - PopSeq Ordered *Triticum aestivum* Gene Expression

QTL – Quantitative trait loci

ROI – Region of interest

SAS – Statistical analysis software

SEM – Standard error of mean

SEV - Severity

SK – Saskatchewan

SNP – Single nucleotide polymorphism

SSR – Simple sequence repeat or microsatellite

TW – Test weight

TKW – Thousand kernel weight

FN – Hagberg falling number

CHAPTER 1

Introduction

Wheat (*Triticum* spp. L.) is one of the three most important cereal crops in terms of production and consumption, with an average world-wide production of over 650 million tonnes of annual production globally (Shewry 2009). Wheat is adapted to sub-tropical and temperate climates, while rice (*Oryza sativa* L.) can not be grown as successfully in temperate regions. Wheat is one of the most important field crops in Canada, particularly western Canada, in terms of production and area under cultivation (McCallum and DePauw 2008; Beres et al. 2018). Wheat was described by Newman (1928) as "the economic fairy to the industrial and commercial life of Canada, having built practically the whole economic structure of the Prairie Provinces". Common wheat (*Triticum aestivum* L.) in Canada is classified into market/milling classes based on growth habit (winter or spring) and quality factors such as grain protein content, gluten strength, kernel hardness (hard or soft), and color (red or white) (McCallum and DePauw 2008). The wheat cultivars in western Canada are classified into one of the following classes: Canada Northern Hard Red (CNHR), Canada Prairie Spring Red (CPSR), Canada Western Amber Durum (CWAD), Canada Western Hard White Spring (CWHWS), Canada Western Red Spring (CWRS), Canada Western Red Winter (CWRW), Canada Western Soft White Spring (CWSWS), and Canada Western Special Purpose (CWSP). Canada Western Red Spring is the largest wheat class in terms of area under cultivation followed by CWAD.

Wheat production in Canada is affected by several different biotic and abiotic stresses; the major abiotic stresses are frost damage (in winter wheat) and drought/heat stress. Among biotic stresses, diseases caused by fungal pathogens are the most important although wheat streak mosaic virus (WSMV) has caused some localized outbreaks in some years (Burrows et al. 2016). Among diseases caused by fungal plant pathogens, there are five priority-one diseases in Canada for which a minimum level of resistance is required for cultivar registration (Anonymous 2015b). Priority one diseases, in the Canadian context, are defined as those that are considered to cause harm significant enough to warrant regulation through the registration process and generally genetic resistance is only one of a number of effective management strategies. These five priority-one diseases are: Fusarium head blight (FHB, *Fusarium graminearum* Schw. [Petch]), leaf rust (caused by *Puccinia triticina* Eriks.), stem rust (caused by *Puccinia graminis* Pers.: Pers f. sp. *tritici* Eriks. E. Henn), stripe rust (caused by *Puccinia striiformis* Westend f. sp. *tritici* Eriks.), and common bunt (caused by *Tilletia caries* Bjerk. and *Tilletia laevis* Bjerk.).

Fusarium head blight, also known as scab or ear blight, can be caused by several species of Fusarium in the *F. graminearum* species complex (FGSC) (Shen et al. 2012). However, *F. graminearum* (telomorph: *Gibberella zeae* Schw. [Petch]) is the most common species in North America and other warmer wheat growing regions worldwide (McMullen et al. 2012). The pathogen not only results in shriveled light-weight, chalky colored kernels, regarded as Fusarium damaged kernels (FDKs) or tombstone, which reduce yield and also produce harmful mycotoxins. The presence of FDKs result in downgrading of the product at sale because the fungus destroys the starch granules, cell walls and endosperm protein (Bechtel et al. 1985; McMullen et al. 1997). Among the mycotoxins, type-B trichothecenes, namely deoxynivalenol (DON) and its acetylated forms (3-ADON and 15-ADON) are the most common. The DON mycotoxin, also known as vomitoxin, results in feed refusal and poor weight gain in animals and may cause health problems in humans over a certain threshold (McMullen et al. 1997, 2012). Due to concerns over toxin accumulation in the grain, many countries have imposed limits on toxin levels present in food and feed items (reviewed in Gilbert and Haber 2013).

Fusarium head blight did not make any noticeable impact in Canada until 1980 when eastern Canada witnessed the first epidemic followed by epidemics in 1993 and 1996 in western Canada (Sutton 1982; McMullen et al. 1997). Although the incidence of FHB in Manitoba has increased since 1984, the epidemic of 1993 in Manitoba was the worst ever reported in upper Great Plains of North America (Wong et al. 1992; Gilbert et al. 1994). It was after the 1993 and 1996 epidemics that wheat breeders and researchers showed concern and dedicated their efforts to research on this disease and the causal pathogen in addition to starting annual field and seed surveys for FHB (Gilbert and Tekauz 2000). In 1997, researchers working on cereals in western Canada formed the Prairie Fusarium Task Force (PFTF) to identify research priorities and develop collaborative research projects to combat FHB. Since the epidemics of the 1990s in Manitoba, the disease spread westward and has caused epidemics in Saskatchewan and sporadically in Alberta (Gilbert and Haber 2013). The increased prevalence and incidence of FHB in western Canada was attributed to the increased proportion of 3-ADON chemotype producing population of *F. graminearum*, which is more aggressive, thus resulting in higher disease levels (Ward et al. 2008). Until the last few years, the proportion of 3-ADON and 15-ADON chemotypes was 1:1, however, unpublished data from the Cereal and Flax Pathology program suggest that more than 80% of the *F. graminearum* isolates collected were 3-ADON (Gilbert et al. 2014; Randy Kutcher, personal communication).

Given that FHB influences every aspect of the grain industry, it is important to find ways to manage this disease by managing/controlling the pathogen and strengthening host resistance. The resistance to FHB in wheat is quantitative and highly influenced by environmental factors (Buerstmayr et al. 2009). The strategies to mitigate the disease include: judicious use of fungicides and adoption of cultural practices (four-year crop rotations with non-hosts and possibly tillage) to minimize pathogen inoculum from previous crops. Host defense can be strengthened by identification of new sources of resistance, the mapping and introgression of genes from new sources into elite, adapted lines. Several sources of FHB resistance are now available in common wheat, unlike durum wheat (Bai et al. 2018). Resistant germplasm utilized for FHB resistance breeding research can be grouped into: (i) spring wheat genotypes from Asia such as Sumai 3 and its Ning derivatives (China), Nobeoka Bozu (Japan), (ii) spring wheat from Brazil, i.e. Frontana, and (iii) winter wheats from Europe namely Praag 8 and Novokruma (Buerstmayr et al. 2009; Gilbert and Haber 2013). Sumai 3 is the most commonly used source in North American wheat breeding programs (McMullen et al. 2012). At the Crop Development Centre (CDC) of the University of Saskatchewan, the durum and bread wheat breeding groups are continually working to improve genetic resistance to FHB in their elite and advanced breeding lines. Improving resistance in durum wheat is particularly more challenging due to the lack of resistance in adapted elite lines or cultivars. The projects discussed in this dissertation stem from ongoing efforts at CDC to improve and understand the genetics of resistance to FHB in common and durum wheat. To improve resistance in bread wheat, Sumai 3 derived lines 04GC0137 and 04GC0139 were used to pyramid *Fhb1*, *Fhb2*, and *Fhb5* genes, in addition to utilization of resistance (smaller effect) from locally adapted cultivars. For durum wheat, an emmer wheat landrace (BGRC3487) with Type-II resistance to FHB was identified and utilized for genetic mapping. The overall focus of thesis was on various aspects of utilization of an exotic source to improve FHB resistance in local elite wheat cultivars. The specific hypotheses and the corresponding objectives included in this PhD project/dissertation were:

1.1. Project hypotheses

1. The introgression of Sumai 3 derived gene(s) improves genetic resistance to FHB in Canadian hard red spring wheat varieties CDC Go and CDC Alsask, irrespective of their genetic background.
2. The introgression of three genes for resistance to FHB do not result in linkage drag (in terms of agronomic traits and grain quality) in Canadian hard red spring wheats CDC Go and CDC Alsask backgrounds.

3. Three FHB resistance genes, *Fhb1*, *Fhb2*, and *Fhb5*, derived from Sumai 3 do not interaction with triazole fungicides, in terms of disease reduction and DON accumulation.
4. The quantitative trait loci (QTL) for FHB resistance in tetraploid emmer wheat accession BGRC3487 can be mapped using SNP marker saturated genetic maps.
5. The rachilla is the part of the rachis in 'Sumai 3' and its derivatives are responsible for resistance to FHB.

1.2. Project objectives

1. To evaluate FHB resistance and DON accumulation in near-isogenic lines (NILs; in CDC Go and CDC Alsask backgrounds) carrying all possible combinations of *Fhb1*, *Fhb2*, and *Fhb5*.
2. To study linkage drag associated with introgressions of *Fhb1*, *Fhb2*, and *Fhb5*, in hard red spring wheat cultivars CDC Go and CDC Alsask.
3. To study the interaction of *Fhb1* and *Fhb5* in CDC Go NILs with metconazole (triazole) fungicide applied at 50% anthesis.
4. To develop high-density genetic maps of a durum wheat backcross recombinant inbred line (BCRIL) population and map QTL for resistance to FHB and compare it with previously mapped QTL.
5. To determine changes in biopolymer composition and tissue structure (using X-ray phase contrast imaging [PCI] and Fourier-transform infrared [FTIR] spectroscopy) in NILs differing in FHB resistance during *F. graminearum* infection and relate these changes to specific FHB gene(s).

CHAPTER 2

Review of Literature

2.1. Wheat: brief history and production in Canada

There is evidence that wheat cultivation began approximately 10,000 years ago as part of the 'Neolithic Revolution', representing a shift of human activity from hunting and gathering to domestication of crops and settled agriculture (reviewed in Shewry 2009). Diploid einkorn (genome AA) and tetraploid (genome AABB) wheats were the earliest cultivated, which most likely originated in Turkey (Heun et al. 1997; Nesbitt 1998). Hexaploid wheat (genome AABBDD) cultivation occurred approximately 9,000 years ago (Feldman 2001). The earliest cultivated wheats were mainly of landraces from wild populations. Reduced shattering at maturity was the first trait selected followed by the free-threshing kernels. The spread of wheat around the world is summarized by Feldman (2001). Briefly, wheat was introduced to Europe in 8,000 BP, followed by a movement northward to the Danube (7,000 BP) and across Italy, France, and Spain (7,000 BP), and finally to the UK and Scandanavia in about 5,000 BP. Wheat spread into Iran, central Asia, China, and Africa around 3,000 BP. It was introduced into Mexico and North America in 1529 and Australia in 1788.

In 2017, Canada produced approximately 29.9 million tonnes of wheat, including 4.9 million tonnes of durum wheat production (Anonymous 2018b). The majority of the wheat in Canada is spring grown and mainly occupies the area under production in the three Prairie Provinces, i.e. Alberta, Saskatchewan, and Manitoba. The Province of Saskatchewan produces approximately 40% of the spring wheat in Canada. In durum wheat production, Saskatchewan is the leading province with about 83% of the durum production in Canada. Approximately 20.1 million tonnes of wheat, including durum, were exported from Canada in 2017.

2.2. Genomic constitution of wheat

Wheat is an allopolyploid, which means it has more than two complete sets of chromosomes per cell nucleus and has evolved through interspecific or intergeneric hybridization (Shewry 2009; Feldman and Levy 2012). The wild allotetraploid wheat *T. turgidum* ssp. *dicoccoides* (2n=4x=28, AABB), which is the direct progenitor of modern durum (*T. turgidum* L. ssp. *durum*) and bread (*T. aestivum L.*) wheat, evolved through a polyploidization event between *T. urartu* (AA genome) and an *Aegilops speltoides*-related species (BB genome), about half a million years ago (Huang et al. 2002). Allohexaploid bread wheat (2n=6x=42, AABBDD) evolved from a second round of intergeneric hybridization and chromosome doubling between the domesticated allotetraploid wheat, *T. turgidum* (AABB) and the diploid *Ae. tauschii* (2n=2x=14, DD), about 9,000 years ago (Huang et al. 2002; El Baidouri et al. 2016).

The combination of large diploid genomes in the polyploid wheat species resulted in large genomes, varying from 12 Gigabases (Gb) in durum wheat to 17 Gb in hexaploid bread wheat (IWGSC 2014), with a repetitive DNA content of over 80% (Paux et al. 2006).

2.3. Biotic stresses associated with wheat cultivation in Canada

Wheat cultivation in Canada is affected by various biotic and abiotic constraints. Among biotic constraints, several viruses, fungi and bacteria attack wheat crops and result in diseases. The most common diseases are Fusarium head blight (FHB, caused by *Gibberella zeae*), leaf rust (caused by *Puccinia triticina* Eriks.), stem rust (caused by *Puccinia graminis* Pers.: Pers f. sp. *tritici* Eriks. E. Henn), stripe rust (caused by *Puccinia striiformis* Westend f. sp. *tritici* Eriks.), common bunt (caused by *Tilletia caries* Bjerk. and *Tilletia laevis* Bjerk.), tan spot (*Pyrenophora tritici-repentis* [Died.] Drechsler), septoria leaf spot (*Septoria tritici* Desm.), and wheat streak mosaic virus (Anonymous 2015). Among insect-pests, orange wheat blossom midge (*Sitodiplosis mosellana* Gehin) and sawfly (*Cephus cinctus* Norton) are important. In Canada, there are five priority-one diseases [three rusts, FHB, and common bunt] defined by the Prairie Recommending Committee for Wheat, Rye and Triticale (PRCWRT) for which a certain level of resistance is required for cultivar registration. Among these five priority-one diseases, rusts and bunts are relatively easy to breed for, however breeding for FHB resistance is a challenging task. Leaf and stem rusts are very well managed by long-term breeding efforts, however, still priority diseases to maintain good resistance in the germplasm and avoid any future epidemic outbreaks (McCallum et al. 2016; Brar et al. 2018b) The next sections of this Chapter are focussed on FHB.

2.4. Fusarium head blight: causal pathogen and disease epidemiology

The genus 'Fusarium' was named in 1809 when a German mycologist, Link, described a fungus having fusiform spores as *Fusarium roseum* (Booth 1971). Later, Schwabe described *F. graminearum* in 1838. *Fusarium* spp. exist in both anamorphic (asexual) and teleomorphic (sexual) stages. The species overwinters on infested crop debris on the soil surface (Guenther and Trail 2005; Trail et al. 2005). Fusarium head blight (FHB) was first described in 1884 as "scab" by W.G. Smith (Arthur 1891) and later the names "Fusarium blight" and "fusariosis" were introduced by Atanasoff (1920; cited in Stack 2003) and Dounin (1926, cited in Stack 2003). Following first reports of the disease, FHB was widely recognized in 31 states of the USA by 1917. Around the same time, the disease was recognized in other parts of the world including Europe and Japan. The disease made its first noticeable impact when an epidemic occurred in 1919, which affected the provinces of Manitoba and Saskatchewan in Canada (MacInnes and Fogelman 1923; cited in Stack 2003). One of the major factors of the 1919 epidemic was the widespread cultivation of the highly

susceptible spring wheat cultivar 'Marquis', which was introduced in Canada in 1908 (Stack 2003).

The risk of FHB has increased by several factors including changes in agricultural practices during the last few decades, which includes reduced or minimum tillage and a less diverse or complete abandonment of crop rotation (Prat et al. 2014). This is particularly important for the corn belt in the mid-western United States where rotations include only corn and wheat, and as a result produce a large amount of *Fusarium* inoculum (McMullen et al. 1997, 2012). About 80% of the durum in the United States is grown in North Dakota, thus it is even more important to manage FHB in North Dakota and adjoining areas (Otto et al. 2002).

Fusarium ascospores serve as the primary inoculum that infects cereal crops. Epidemics of the disease are governed largely by local and regional environments, although other factors, such as host resistance, pathogen population adaptation and aggressiveness, and the physiological state of the crop play a role (Osborne and Stein 2007). With frequent rains, high relative humidity and temperatures between 15-30˚C during anthesis and soft-dough stages of wheat the disease can devastate a healthy, high-yielding crop within a few weeks (McMullen et al. 1997). Each species in the *F. graminearum* species complex (FGSC) may have different biological and environmental requirements (Osborne and Stein 2007). For example, *F. graminearum* is favored by a wide range of temperature conditions up to 30˚C, whereas *F. poae* can grow well under lower temperature conditions up to 20˚C. That is the reason that *F. poae* is found more frequently in temperate climates and *F. graminearum* can be found in much of the geographical area affected by FHB. In spite of differences in temperature requirements, most of the species causing FHB can be recovered from most infected crops (Dufault et al. 2006 cited in Osborne and Stein 2007).

F. graminearum is a residue-borne fungus, which persists on corn or small grain cereal crop debris (McMullen et al. 1997, 2012) and on some pulse crop residues (mainly roots as the fungus is associated with some root diseases). Prolonged cool and wet conditions favour growth and sporulation of the fungus on residue. Conidia (asexual spores) or more likely ascospores (sexual spores) of the fungus attack cereal crops in favorable weather (Trail et al. 2005). *F. graminearum* can survive on crop debris buried under 20-25 cm of soil, however, its growth is favored only in the upper few centimeters of the soil profile (Leplat et al. 2013). Soil moisture is very important for ascospore production on crop debris, which is maximized when soil moisture is >80% and ceases at <30% (Osborne and Stein 2007). Soil compaction may affect spore production because it affects water availability. *F. graminearum* and *F. nivale* populations are limited in compacted soil due to poor water availability and

poor growth and mobility of the fungus. Soil aeration is important for the growth and survival of the fungus. Soil pH affects the fungal growth.

Mycelial growth and conidia formation of *F. graminearum* is affected by acidic and alkaline conditions, but the fungus can grow in media between pH 4 and 10 (Leplat et al. 2013). Minimum temperatures for ascospore production in residue are 7-10˚C and maximum 15-20˚C. In comparison to other FHB causing fungi, conidia formation and infection rates of *F. graminearum* are favored by relatively warm and wet conditions, only ascospore production is favored by cooler conditions. Ascospore release from fruiting bodies (i.e. perithecia) is inhibited by prolonged high humidity (Osborne and Stein 2007), although ascospore viability depends on high relative humidity. In most of the cases, ascospores are sufficiently robust to retain viability after release from perithecia (Gilbert and Haber 2013).

Burning of crop residue reduces the amount of primary inoculum (Dill-Macky and Salas 2001). Spore (ascospores and conidia) dispersal occurs by wind or rain splash, thus dispersal distance is limited (Xu 2003); however, long distance dispersal of ascospores is also reported in rare cases (Maldonado-Ramirez et al. 2005 cited in Osborne and Stein 2007). Ascospores are ejected a few mm with force from perithecia and wind aids in dispersal to nearby plants (Trail et al. 2005). Rainfall is the major factor inducing rupture of the ascus wall. With increased relative humidity, osmotic pressure rises within the perithecium due to the entry of mannitol, potassium and chloride ions, thus releasing ascospores with force (Gilbert and Haber 2013).

Wheat and barley are most vulnerable to attack by *Fusarium* spp. from anthesis to soft dough stage (Schaafsma and Hooker 2007; McMullen et al. 2012). Wheat is most susceptible to *F. graminearum*, and the period 2-3 days prior to anthesis and a week after anthesis of critical importance (McMullen et al. 2012). Warm and humid weather triggers Fusarium head blight epidemics and the ratio of Fusarium diseased/damaged kernels to DON contamination depends heavily on weather conditions (Mesterházy 2014). The DON content in grain was reported to be much higher in humid weather as compared to dry weather and analyses of long-term weather data indicated that the amount of precipitation is most important factor associated with increased disease incidence and toxin content. Toxin level in grain increases after heavy rains just prior to harvest (Mesterházy 2014). Mycotoxin production requires relatively more specific conditions than fungal growth. Maximum mycotoxin production is reported to be 30˚C. Rainfall is another major factor, in addition to temperature, leading to FHB epidemics. Severe flooding in the states of North Dakota, South Dakota and Minnesota in 1993, and precipitation greater than long-term normals in North

Dakota from 1993-1996, resulted in severe FHB epidemics in these major wheat growing regions of the USA (McMullen et al. 1997).

In addition to favorable environmental conditions, niche availability is another major factor in pathogen abundance in affected areas. In the Great Plains of the USA, maize is largely grown in rotation with wheat (Osborne and Stein 2007; Gilbert and Haber 2013), and it is a host of *F. graminearum*, so there is a regular supply of infected plant material. The maize-wheat rotation is accompanied by zero or minimum tillage practices in the USA, which provides enough crop debris to the over-wintering pathogen for ascospore production. The area under maize production has greatly increased in the northern Great Plains in recent decades. Thus, increased area under maize and zero or minimum tillage practices has led to a large reservoir of fungal biomass (Osborne and Stein 2007).

2.5. FHB management strategies

There is agreement in the literature that no single strategy is sufficient to protect yield and quality in FHB epidemic years; an integration of different strategies is the best (reviewed in McMullen et al. 1997; Gilbert and Tekauz 2000; McMullen et al. 2012; Gilbert and Haber 2013; Wegulo et al. 2015; Dweba et al. 2017). A combination of host resistance (varietal selection), cultural practices (tillage and crop rotation), fungicide application with use of decision forecast systems (e.g. FHB and DON prediction models) can facilitate efficient management of the disease; although the effectiveness of these practices may vary depending on weather conditions during the growing season, particularly just before, at, and just after the anthesis growth stage. In Canada, winter wheat usually escapes FHB damage because the early anthesis stage is asynchronous with the peak inoculum production of most *Fusarium* species (Beres et al. 2018).

Two important cultural practices for the mitigation of FHB of cereal crops are: tillage and crop rotation, both are based on avoiding or limiting the exposure of small grain cereals to spores/inoculum at the anthesis stage (Sutton 1982; Pereyra and Dill-Macky 2008). Tillage operations bury the host crop residue in soil and crop rotation employs the seeding of a non-host crop following wheat. Burning of crop residue decreases the amount of inoculum, however, this is not an environmental acceptable practice (Salas and Dill-Macky 2005). Some other cultural practices to manage FHB such as staggered seeding dates and increasing the fan speed of the combine while harvesting are possible, although not very popular among growers (McMullen et al. 2012; Beres et al. 2018). In Canada, preliminary results indicated some success in escaping FHB in spring wheat by very early planting when soil temperatures are as low as 2°C (Beres et al. 2018). Other than cultural practices, fungicide application and cultivar resistance are the most important strategies of an integrated FHB management plan.

2.6. Management of FHB using fungicides

In spite of efforts to improve FHB resistance in wheat, the majority of cultivars are still intermediate to susceptible in reaction to FHB. Durum wheat in particular is much more susceptible than hard red spring wheat. In epidemic years, fungicides can help to minimize damage (Mesterhazy 2003). During the epidemics of the 1990s in North America, the fungicides available were ineffective in managing FHB (Milus 1994). The use of fungicides for FHB management changed after 1997. Until then pathologists questioned the ability of fungicides to supress FHB and DON production. Although azole fungicides were available prior to 2000, only after numerous studies was fungicide effecacy for FHB management proven (Paul et al. 2008).

Among the azoles, demethylation inhibitor (DMI) fungicides are preferred for control of FHB and to reduce DON accumulation (Boyacioglu et al. 1992; McMullen et al. 2012; Paul et al. 2008). Compared to single site-specific fungicides that can be rendered ineffective due to single point mutations in the genes encoding target proteins, the efficacy of DMIs has decreased relatively slowly and gradually as they target multiple sites (Cools et al. 2013). Prothioconazole + tebuconazole, metconazole, and prothioconazole were proven to perform significantly better than propiconazole or tebuconazole in suppressing FHB severity and DON accumulation in a meta-analysis study (comprised of more than 100 uniform fungicide trials) conducted in the United States (Paul et al. 2008, 2010). A more recent study also reported similar results for the triazoles (Paul et al. 2018). Fungicides in the quinone inhibitor (QoI) class have been shown to result in increased DON concentrations in the grain and therefore are not recommended for FHB and DON suppression (Amarasinghe et al. 2013; Ye et al. 2017; Bissonnette et al. 2018; Paul et al. 2018). Timing and application methodology have a great influence on efficacy of fungicides (reviewed in McMullen et al. 2012). Although 50% anthesis is still the recommended for the timing of application, some studies have reported improved FHB and DON suppression with more than one timing of application or at different crop growth stages. Nozzles angled forward and that deliver coarser sprays have superior fungicide deposition over other configurations. Additionally, a boom height of 30 cm above the crop canopy is more effective than that higher boom heights (find a reference by Tom Wold). Fungicide efficacy is affected by other factors such as environment or cultivar resistance.

Seed treatments are not recommended for FHB control, although Jorgensen et al. (2012) reported that using difenconazole, triticonazole, maneb or fludioxonil significantly improved germination and reduced Fusarium seedling blight in three field trials with 5-45% infected seed; yield improvement was not detected.

2.7. Host resistance

Resistance to FHB in wheat is polygenic and quantitatively inherited (Buerstmayr et al., 2009). Response to FHB in wheat is further complicated by the major influence of environmental conditions, which modulate disease infection and development (McMullen et al. 2012; Gilbert and Haber 2013). Additionally, environmental conditions also affect repeatability and reliability of data, which is compensated for by increasing the numbers of replications or site-years. The complexity of the host reaction makes it very difficult to reliably evaluate material in a few environments and make selections in breeding programs. Host resistance to FHB in wheat is classified into different types and it was Christensen (1963; reviewed in Schroeder and Christensen 1963) that described the first two types, i.e. resistance to initial infection (Type-I) and resistance to fungal spread in the spike after successful initial infection (Type-II). He further reported that cultivars varied independently for either type of resistance. A third type of resistance is resistance to toxin (DON) accumulation or the ability of plants to degrade the toxin (Type-III), which was identified and reported by Miller et al. (1985). Other resistance types (Type-IV for resistance to kernel infection and Type-V for tolerance to yield reduction) have also been proposed (Mesterhazy 1995) but are not as widely used as Types-I, II, and III.

Evaluation of plant material for any particular type of resistance to FHB, requires dedicated protocols, although more than one type can be evaluated from a single experiment. For evaluation of Type-I resistance, spray inoculation methods are used under controlled conditions or FHB incidence is used as a measure in field nurseries. For Type-II resistance, single floret point inoculation is used under controlled conditions or FHB severity is used as an indirect measure from field nurseries (Wang and Miller 1988). From field nurseries, an FHB index is calculated (see Chapters 3-6) from incidence and severity as a combined measure of Type-I + Type-II resistance, often referred to as 'field resistance' (Buerstmayr et al. 2009). Type-III resistance is assessed by quantification of DON accumulation in the grain harvested from inoculated nurseries (Wang and Miller 1988). Type-IV resistance is evaluated by calculating the proportion of FDKs in harvested kernels and yield related measures for assessing Type-V resistance. Usually all types of resistance are positively correlated. In some older literature, Type-III resistance is defined as Type-V. Since early reports on variability in wheat for different types of resistance mechanisms, breeders and pathologists have focussed on in-depth characterization of genetic resistance and the next three sub-sections are focussed on summarizing the results from such resistance mapping studies in wheat and related species.

2.7.1. Hexaploid wheat

Resistance to FHB in hexaploid wheat originated from Asia, Brazil (mainly Frontana), and winter wheats from Europe (Bai and Shaner 2004; Buerstmayr et al. 2009; Jia et al. 2018). Chinese wheat lines Sumai 3, Ning 7840, Ning 8331, Wangshuibai and some other sources (listed in Table 2.1) have remained major sources of resistance utilized by breeders across the globe (Bai and Shaner 2004). The only FHB resistance gene cloned to date (*Fhb1*) was derived from Sumai 3 (Rawat et al. 2016). At present, there are seven genes (*Fhb1* to *Fhb7*) for FHB resistance in wheat that are formally designated as single, Mendelized genes: *Fhb1* was derived from Sumai 3 (Cuthbert et al. 2006), *Fhb2* from Sumai 3 (Cuthbert et al. 2007), *Fhb3* from *Leymus racemosus* (Qi et al. 2008), *Fhb4* from Wangshuibai (Xue et al. 2010a), *Fhb5* from Wangshuibai and Sumai 3 (Xue et al. 2011), *Fhb6* from *Elymus tsukushiensis* (Cainong et al. 2015), and *Fhb7* from *Thinopyrum ponticum* (Guo et al. 2015). These major resistance genes, along with some temporarily designated major QTL (listed in Table 2.1), are amenable to marker-assisted selection to benefit wheat breeding. The QTL mapped until 2009 are summarized in an excellent review paper by Buerstmayr et al. (2009). In Table 2.1, we have summarized all QTL mapped for FHB resistance and DON reduction in hexaploid wheat after 2009 in a similar format following Buerstmayr et al. (2009). We retrieved a total of 34 QTL mapping studies in hexaploid wheat between 2009-2018.

FHB resistance in hexaploid wheat is also influenced by other traits, mainly plant height and anther extrusion (Mesterhazy 1995; Miedaner and Voss 2008; Voss et al. 2008; Srinivasachary et al. 2009; Skinnes et al. 2011; Lu et al. 2011; Lu et al. 2013). The short stature of wheat plants resulting from the introgression of reduced height (*Rht*) genes render them more susceptible to FHB as they are in closer proximity to infected residue on the ground. Additionally, there are studies that have reported co-localization of some FHB resistance QTL with *Rht* alleles (Gervais et al. 2003; Haberle et al. 2009; Mao et al. 2010). Three *Rht* genes derived from Japanese cultivar Norin10, namely, *Rht-B1b* (4B), *Rht-D1b* (4D), and *Rht8c* (2D) are the most widely introgressed genes in elite cultivars worldwide. Among these, *Rht-B1b* and *Rht-D1b* are gibberellic acid (GA)-insensitive, whereas *Rht8c* is GA-sensitive and tightly linked to photoperiod insensitivity gene *Ppd1*. Studies of dwarfing genes and FHB severity have been somewhat inconsistent. Miedaner and Voss (2008) reported that plants with *Rht* alleles had higher FHB severity and concluded that *Rht8c* was the most favourable choice among the three. In their study, the near-isogenic lines (NILs) with *Rht-B1b* were less susceptible than *Rht-D1b*, however, the height reduction associated with *Rht-B1b* was less pronounced than for the other genes. Srinivasachary et al. (2009) reported that both *Rht-B1b* and *Rht-D1b* resulted in lower Type-I resistance, however, only

Rht-B1b significantly improved Type-II resistance. Voss et al. (2008) reported that *Rht-D1b* consistently resulted in higher FHB severity compared with the wild-type allele. He further concluded that plant height *per se* was not responsible for total variation in the material and the genetic linkage with, or pleiotropy of *Rht-D1b* conferring FHB susceptibility or conversely *Rht-D1a* conferring resistance affected variation in the data. In spite of the effects of *Rht* alleles on FHB severity, Miedaner and Voss (2008) and Srinivasachary et al. (2009) concluded that with a less negative effect of *Rht-B1b*, it is possible to select for both improved resistance and reduced height. Another more recently described *Rht* gene, i.e. *Rht24* (6A), was also evaluated for its effect on FHB (Herter et al. 2018). *Rht24*, a GA-sensitive gene, is becoming an important gene in wheat breeding programs as it has been shown to increase yield by increasing thousand-kernel weight (Tian et al. 2017). Herter et al. (2018) proved that *Rht24* does not affect FHB ratings and none of the plant height QTL overlapped with this dwarfing gene in their study.

Studies by Strange and Smith (1971) and Strange et al. (1974) reported the role of wheat anthers in increasing *Fusarium* species infection as a result of choline and betaine presence. A later study by Engle et al. (2004) challenged these studies by reporting no such correlation. More recently, studies by Skinnes et al. (2010) and Lu et al. (2013) reported the role of anther extrusion with FHB resistance in European wheats. The authors reported that lines with low anther extrusion are more susceptible to FHB because anthers trapped between glumes provide a way for the fungus to infect the florets. The low anther extrusion in most durum wheat lines could explain, in part, higher FHB susceptibility than in bread wheat. Contrary to these studies that support the role of anther extrusion in enhanced Type-I resistance, Kubo et al. (2010), who used a spray inoculation method, reported that cleistogamous lines were less often infected with FHB as compared to chasmogamous lines. The relationship of floral opening, anther extrusion and FHB susceptibility is complex and not well-studied in Canadian wheat cultivars. Thus, more dedicated studies are required before breeders can exploit this trait to improve FHB resistance in their material.

Table 2. 1. Quantitative trait loci (QTL) for Fusarium head blight (FHB) resistance mapped in common wheat post year 2009 [following the review by Buerstmayr et al. (2009) that described QTL mapped until 2009].

Source of resistance allele	Chr.[a]	PVE[b]	Markers[c]	Resistance type[d]	Plant material	Phenotyping	References
Wangshuibai	7A	14.6	*wmc168, wmc479*	Type–II	Wangshuibai x Sy95-7 $F_{2:3}$, 194 lines	*Fg*, one field exp.	Zhang et al. (2010)
Wangshuibai	6B	22.4	*wmc486, wmc737*	Type–II	Wangshuibai x Sy95-7 $F_{2:3}$, 194 lines	*Fg*, one field exp.	Zhang et al. (2010)
Wangshuibai	3B	31.7	*wmc623, wmc231*	Type–II	Wangshuibai x Sy95-7 $F_{2:3}$, 194 lines	*Fg*, one field exp.	Zhang et al. (2010)
Wangshuibai	2D	5.0	*wmc503*	Type–II	Wangshuibai x Sy95-7 $F_{2:3}$, 194 lines	*Fg*, one field exp.	Zhang et al. (2010)
Wangshuibai	1B	6.6	*wmc134*	Type–II	Wangshuibai x Sy95-7 $F_{2:3}$, 194 lines	*Fg*, one field exp.	Zhang et al. (2010)
NK93604	1A	-	*wPt-5577, barc213*	Types-II, III	Arina x NK93604 DH, 93 lines	*Fc, Fg*, five field exp.	Skinnes et al. (2010)
Arina	1B	-	*barc188, wmc766*	Type-II	Arina x NK93604 DH, 93 lines	*Fc, Fg*, five field exp.	Skinnes et al. (2010)
Arina	7A	-	*DuPw226, gwm276*	Type-II	Arina x NK93604 DH, 93 lines	*Fc, Fg*, five field exp.	Skinnes et al. (2010)
T. macha	2A	11.5	*Xs11m24_10*	Type-II	*T. macha* x *T. aestivum* cv. Furore, $BC_1F_{3:5}$, 321 lines	*Fg*, *Fc*, seven field exp.	Buerstmayr et al. (2011)
T. macha	2BS	7.1	*Xs20m13_4*	Type-II	*T. macha* x *T. aestivum* cv. Furore, $BC_1F_{3:5}$, 321 lines	*Fg*, *Fc*, seven field exp.	Buerstmayr et al. (2011)
T. macha	2BL	9.7	*Xs24m19_6*	Type-II	*T. macha* x *T. aestivum* cv. Furore, $BC_1F_{3:5}$, 321 lines	*Fg*, *Fc*, seven field exp.	Buerstmayr et al. (2011)
T. macha	5AL	22.7	*q*	Type-II	*T. macha* x *T. aestivum* cv. Furore, $BC_1F_{3:5}$, 321 lines	*Fg*, *Fc*, seven field exp.	Buerstmayr et al. (2011)
T. macha	5B	9.3	*gwm497e*	Type-II	*T. macha* x *T. aestivum* cv. Furore, $BC_1F_{3:5}$, 321 lines	*Fg*, *Fc*, seven field exp.	Buerstmayr et al. (2011)
Furore	2D	3.2	*gwm261*	Type-II	*T. macha* x *T. aestivum* cv. Furore, $BC_1F_{3:5}$, 321 lines	*Fg*, *Fc*, seven field exp.	Buerstmayr et al. (2011)
PI 277012	5AS	20.0	*barc40*	Types–II, III, IV	Grandin x PI 277012 DH, 130 lines	*Fg*, three GH and two field exp.	Chu et al. (2011)
PI 277012	5AL	32.0	*Q, Xcfd39*	Types–II, III, IV	Grandin x PI 277012 DH, 130 lines	*Fg*, three GH and two field exp.	Chu et al. (2011)
Haiyanzhong	7D	22.6	*Xcfd46, wmc702*	Type-II	Wheaton x Haiyanzhong F_8, 136 lines	*Fg*, three GH and one field exp.	Li et al. (2011)
Haiyanzhong	6B1	4.1	*gwm705, wmc104*	Type-II	Wheaton x Haiyanzhong F_8, 136 lines	*Fg*, three GH and one field exp.	Li et al. (2011)
Haiyanzhong	6B2	7.2	*gwm644, barc223.1*	Type-II	Wheaton x Haiyanzhong F_8, 136 lines	*Fg*, three GH and one field exp.	Li et al. (2011)
Haiyanzhong	5A	7.4	*gwm129*	Type-II	Wheaton x Haiyanzhong F_8, 136 lines	*Fg*, three GH and one field exp.	Li et al. (2011)
Haiyanzhong	1A	5.5	*wmc120.1, wmc24*	Type-II	Wheaton x Haiyanzhong F_8, 136 lines	*Fg*, three GH and one field exp.	Li et al. (2011)
CS- Sumai 3-7ADSL	3BS	35.0	*umn10*	Types–II, III, IV	Chinese Spring x CS- Sumai 3-7ADSL $F_{4:5}$, $F_{6:7}$, $F_{6:8}$, 191 lines	*Fg*, three GH exp.	Jayatilake et al. (2011)
CS- Sumai 3-7ADSL	7AC	24.0	*barc174*	Types–II, III, IV	Chinese Spring x CS- Sumai 3-7ADSL $F_{4:5}$, $F_{6:7}$, $F_{6:8}$, 191 lines	*Fg*, three GH exp.	Jayatilake et al. (2011)
Avle	2BL	15.3	*gwm382b, barc122*	Type-II	Line 685 x Avle DH, 171 lines	*Fc, Fg,* six field exp.	Lu et al. (2011)
Line 685	2D	9.7	*gwm539, cfd233*	Type-II	Line 685 x Avle DH, 171 lines	*Fc, Fg,* six field exp.	Lu et al. (2011)
Line 685	3BS	13.6	*umn10, barc147*	Type-II	Line 685 x Avle DH, 171 lines	*Fc, Fg,* six field exp.	Lu et al. (2011)
Avle	4D	38.2	*Rht-D1, wPt-5809*	Type-II	Line 685 x Avle DH, 171 lines	*Fc, Fg,* six field exp.	Lu et al. (2011)
Line 685	5A	16.6	*barc56, barc40, gwm156, barc141*	Type-II	Line 685 x Avle DH, 171 lines	*Fc, Fg,* six field exp.	Lu et al. (2011)
Huangfangzhu	3BS	35.6	*umn10, barc147*	Type-II	Wheaton x Huangfangzhu F_8, 106 lines	*Fg*, three GH and one field exp.	Li et al. (2012)
Huangfangzhu	7AL	18.2	*gwm276, barc121*	Type-II	Wheaton x Huangfangzhu F_8, 106 lines	*Fg*, three GH and one field exp.	Li et al. (2012)
Huangfangzhu	1B	9.9	*barc207*	Type-II	Wheaton x Huangfangzhu F_8, 106 lines	*Fg*, three GH and one field exp.	Li et al. (2012)
Huangfangzhu	1AS	11.1	*wmc120.2, wmc24*	Type-II	Wheaton x Huangfangzhu F_8, 106 lines	*Fg*, three GH and one field exp.	Li et al. (2012)
Huangfangzhu	5AS	7.3	*barc186, barc117*	Type-II	Wheaton x Huangfangzhu F_8, 106 lines	*Fg*, three GH and one field exp.	Li et al. (2012)
Baishanyuehuang	3BS	15.7	*gwm533, gwm493*	Type-II	Baishanyuehuang x Jagger $F_{6:7}$, 188 lines	*Fg*, three GH exp.	Zhang et al. (2012a)

Baishanyuehuang	3BSc	8.5	*gwm566*	Type-II	Baishanyuehuang x Jagger $F_{6:7}$, 188 lines	*Fg*, three GH exp.	Zhang et al. (2012a)
Baishanyuehuang	3A	7.5	*wmc651, barc356*	Type-II	Baishanyuehuang x Jagger $F_{6:7}$, 188 lines	*Fg*, three GH exp.	Zhang et al. (2012a)
Baishanyuehuang	5A	4.5	*gwm304, barc141*	Type-II	Baishanyuehuang x Jagger $F_{6:7}$, 188 lines	*Fg*, three GH exp.	Zhang et al. (2012a)
Frontana	2B1	9.6	*gwm120, Xs12m19_9*	Types–II, IV	Frontana x Remus DH, 210 lines	*Fg*, *Fc*, six field exp.	Szabo-Hever et al. (2012)
Frontana	2B2	8.6	*gwm526*	Types–II, IV	Frontana x Remus DH, 210 lines	*Fg*, *Fc*, six field exp.	Szabo-Hever et al. (2012)
Frontana	3A	8.2	*gwm1121, gwm779*	Type-II	Frontana x Remus DH, 210 lines	*Fg*, *Fc*, six field exp.	Szabo-Hever et al. (2012)
Frontana	3D	9.7	*Xs12m19_5, gwm341*	Type-IV	Frontana x Remus DH, 210 lines	*Fg*, *Fc*, six field exp.	Szabo-Hever et al. (2012)
Frontana	4A	9.5	*Xwg232*	Type-II	Frontana x Remus DH, 210 lines	*Fg*, *Fc*, six field exp.	Szabo-Hever et al. (2012)
Frontana	4B	9.4	*Xs13m26_7, Xs13m18_9*	Types–II, IV	Frontana x Remus DH, 210 lines	*Fg*, *Fc*, six field exp.	Szabo-Hever et al. (2012)
Frontana	5A	7.2	*gwm293, Xs24m19_5*	Types–II, IV	Frontana x Remus DH, 210 lines	*Fg*, *Fc*, six field exp.	Szabo-Hever et al. (2012)
Frontana	6B	6.8	*Xs13m14_10, Xs23m14_4*	Type-II	Frontana x Remus DH, 210 lines	*Fg*, *Fc*, six field exp.	Szabo-Hever et al. (2012)
Frontana	7B	11.1	*Xs12m25_2*	Types–II, IV	Frontana x Remus DH, 210 lines	*Fg*, *Fc*, six field exp.	Szabo-Hever et al. (2012)
Frontana	ND	7.3	*Xs12m15_4*	Type-IV	Frontana x Remus DH, 210 lines	*Fg*, *Fc*, six field exp.	Szabo-Hever et al. (2012)
Heyne	3AS	17.9	*barc86, wmc428*	Type-II	Trego x Heyne RIL, 94 lines	*Fg*, two GH and two field exp.	Zhang et al. (2012b)
Heyne	4DL	23.4	*wmc331, wmc720*	Type-II	Trego x Heyne RIL, 94 lines	*Fg*, two GH and two field exp.	Zhang et al. (2012b)
Heyne	4AL	18.1	*wmc219, gwm160, barc78*	Type-II	Trego x Heyne RIL, 94 lines	*Fg*, two GH and two field exp.	Zhang et al. (2012b)
VA00W-38	1BL	8.7	*gwm273, barc120*	Type-II	VA00W-38 x Pioneer 26R46 $F_{4:5}$, $F_{5:6}$, 182 lines	*Fg*, four field exp.	Liu et al. (2012)
VA00W-38	2AS	7.8	*wPt733314, gwm210*	Type-IV	VA00W-38 x Pioneer 26R46 $F_{4:5}$, $F_{5:6}$, 182 lines	*Fg*, four field exp.	Liu et al. (2012)
VA00W-38	2ASc	6.5	*gwm448, gpw5177a*	Types–III, IV	VA00W-38 x Pioneer 26R46 $F_{4:5}$, $F_{5:6}$, 182 lines	*Fg*, four field exp.	Liu et al. (2012)
VA00W-38	2AL	13.4	*wPt5865, gwm312, wPt742893*	Type-III	VA00W-38 x Pioneer 26R46 $F_{4:5}$, $F_{5:6}$, 182 lines	*Fg*, four field exp.	Liu et al. (2012)
VA00W-38	2DL	13.3	*wPt1301, wPt667765, gwm349, wPt731220, wPt0153*	Types–I, II	VA00W-38 x Pioneer 26R46 $F_{4:5}$, $F_{5:6}$, 182 lines	*Fg*, four field exp.	Liu et al. (2012)
VA00W-38	5B	12.9	*wPt9205, wPt6001*	Types–I, III	VA00W-38 x Pioneer 26R46 $F_{4:5}$, $F_{5:6}$, 182 lines	*Fg*, four field exp.	Liu et al. (2012)
VA00W-38	6A	15.9	*wPt730772, wPt0902*	Type-IV	VA00W-38 x Pioneer 26R46 $F_{4:5}$, $F_{5:6}$, 182 lines	*Fg*, four field exp.	Liu et al. (2012)
VA00W-38	7A	15.2	*wPt4345, wPt7076*	Type-II	VA00W-38 x Pioneer 26R46 $F_{4:5}$, $F_{5:6}$, 182 lines	*Fg*, four field exp.	Liu et al. (2012)
VA00W-38	2BSc	7.8	*wmc477, gwm319*	Type-I	VA00W-38 x Pioneer 26R46 $F_{4:5}$, $F_{5:6}$, 182 lines	*Fg*, four field exp.	Liu et al. (2012)
Pioneer 26R46	4BL	7.3	*wmc657, gwm513*	Type-I	VA00W-38 x Pioneer 26R46 $F_{4:5}$, $F_{5:6}$, 182 lines	*Fg*, four field exp.	Liu et al. (2012)
Pioneer 26R46	6A	16.7	*wPt5964, wPt6668*	Type-I	VA00W-38 x Pioneer 26R46 $F_{4:5}$, $F_{5:6}$, 182 lines	*Fg*, four field exp.	Liu et al. (2012)
Massey	2DS	-	*Ppd-D1, Rht8*	Type-I	Becker x Massey $F_{7:14}$, 152 lines	*Fg*, one GH and eight field exp.	Liu et al. (2013a)
Becker	4BS1	-	*Rht-B1, wPt1708*	Type-I	Becker x Massey $F_{7:14}$, 152 lines	*Fg*, one GH and eight field exp.	Liu et al. (2013a)
Massey	1DS	-	*wPt1595, wPt7946*	Type-II	Becker x Massey $F_{7:14}$, 152 lines	*Fg*, one GH and eight field exp.	Liu et al. (2013a)
Massey	3BL	-	*wPt4048, barc164*	Type-II	Becker x Massey $F_{7:14}$, 152 lines	*Fg*, one GH and eight field exp.	Liu et al. (2013a)
Massey	1AS	-	*wPt4735, wPt3870*	Type-II	Becker x Massey $F_{7:14}$, 152 lines	*Fg*, one GH and eight field exp.	Liu et al. (2013a)
Becker	2BL	-	*wPt0628, wPt2528*	Type-II	Becker x Massey $F_{7:14}$, 152 lines	*Fg*, one GH and eight field exp.	Liu et al. (2013a)
Becker	4BS2	-	*tPt0602, wPt3908, wPt6149*	Types–II, IV	Becker x Massey $F_{7:14}$, 152 lines	*Fg*, one GH and eight field exp.	Liu et al. (2013a)
Massey	4DS	-	*Rht-D1, rPt4471*	Type-II	Becker x Massey $F_{7:14}$, 152 lines	*Fg*, one GH and eight field exp.	Liu et al. (2013a)
Massey	6BL	-	*wPt5176, wPt8268*	Type-II	Becker x Massey $F_{7:14}$, 152 lines	*Fg*, one GH and eight field exp.	Liu et al. (2013a)
Massey	4DL	-	*wPt3743, wPt6059*	Type-III	Becker x Massey $F_{7:14}$, 152 lines	*Fg*, one GH and eight field exp.	Liu et al. (2013a)
MO 94-317	4BS	-	*Rht-B1, gwm513*	Types–I, II, III, IV	Ernie x MO 94-317 F_{11}, 231 lines	*Fg*, one GH and eight field exp.	Liu et al. (2013a)
Ernie	4DS	-	*Rht-D1, barc334b*	Types–I, II, III, IV	Ernie x MO 94-317 F_{11}, 231 lines	*Fg*, one GH and eight field exp.	Liu et al. (2013a)
Ernie	5AL	-	*gwm291-B1*	Types–I, II	Ernie x MO 94-317 F_{11}, 231 lines	*Fg*, one GH and eight field exp.	Liu et al. (2013a)
Ernie	2DS	-	*Ppd-D1*	Types–I, II	Ernie x MO 94-317 F_{11}, 231 lines	*Fg*, one GH and eight field exp.	Liu et al. (2013a)
Ernie	3BL	-	*wmc307, wmc1, wmc653*	Types–II, III, IV	Ernie x MO 94-317 F_{11}, 231 lines	*Fg*, one GH and eight field exp.	Liu et al. (2013a)
Ernie	6AL	-	*XE37M59_4, barc171*	Type-III	Ernie x MO 94-317 F_{11}, 231 lines	*Fg*, one GH and eight field exp.	Liu et al. (2013a)
Catbird	7DS	18.0	*barc128, wmc702, cfd14*	Type-II	Catbird x Milan DH, 102 lines	*Fg*, three GH exp.	Cativelli et al. (2013)

Catbird	3BS	9.0	*barc133, wmc754, gwm493*	Type-II	Catbird x Milan DH, 102 lines	*Fg*, three GH exp.	Cativelli et al. (2013)
Catbird	5DL	15.0	*gdm153, wmc215, Vrn-D1*	Type-II	Catbird x Milan DH, 102 lines	*Fg*, three GH exp.	Cativelli et al. (2013)
Naxos	1AL.1	2.6	*wPt-8797, wPt-7030*	Type-III	'Shangai-3/Catbird' x Naxos F_6, 181 lines	*Fg, Fc,* six field exp.	Lu et al. (2013)
Naxos	1BS	5.7	*gwm550, wmc619*	Types-II, III	'Shangai-3/Catbird' x Naxos F_6, 181 lines	*Fg, Fc,* six field exp.	Lu et al. (2013)
Naxos	2AS	9.3	*gwm636, barc124*	Types-III, IV	'Shangai-3/Catbird' x Naxos F_6, 181 lines	*Fg, Fc,* six field exp.	Lu et al. (2013)
Naxos	2BL	5.2	*wmc441, gwm1267b*	Type-III	'Shangai-3/Catbird' x Naxos F_6, 181 lines	*Fg, Fc,* six field exp.	Lu et al. (2013)
Naxos	2DL	3.1	*gwm265, mag3616*	Type-II	'Shangai-3/Catbird' x Naxos F_6, 181 lines	*Fg, Fc,* six field exp.	Lu et al. (2013)
Naxos	3AS	4.4	*wmc489b, wmc695b*	Type-III	'Shangai-3/Catbird' x Naxos F_6, 181 lines	*Fg, Fc,* six field exp.	Lu et al. (2013)
Naxos	4BS	11.2	*Rht-B1, gwm368*	Type-II	'Shangai-3/Catbird' x Naxos F_6, 181 lines	*Fg, Fc,* six field exp.	Lu et al. (2013)
Naxos	5AS	11.5	*wmc489d, wPt-8226*	Types-III, IV	'Shangai-3/Catbird' x Naxos F_6, 181 lines	*Fg, Fc,* six field exp.	Lu et al. (2013)
Naxos	5BL	7.0	*barc275, barc232*	Types-II, III	'Shangai-3/Catbird' x Naxos F_6, 181 lines	*Fg, Fc,* six field exp.	Lu et al. (2013)
Naxos	5DL	3.5	*gwm174, wPt-1400*	Type-II	'Shangai-3/Catbird' x Naxos F_6, 181 lines	*Fg, Fc,* six field exp.	Lu et al. (2013)
Naxos	7AL.1	16.2	*wmc603, barc292*	Type-III	'Shangai-3/Catbird' x Naxos F_6, 181 lines	*Fg, Fc,* six field exp.	Lu et al. (2013)
'Shangai-3/Catbird'	1AL.2	9.3	*wPt-8016, wPt-2847*	Type-II	'Shangai-3/Catbird' x Naxos F_6, 181 lines	*Fg, Fc,* six field exp.	Lu et al. (2013)
'Shangai-3/Catbird'	2DLc	24.3	*wmc18, wmc41*	Types-II, III	'Shangai-3/Catbird' x Naxos F_6, 181 lines	*Fg, Fc,* six field exp.	Lu et al. (2013)
'Shangai-3/Catbird'	3DL	3.8	*cfd9, barc323*	Type-II	'Shangai-3/Catbird' x Naxos F_6, 181 lines	*Fg, Fc,* six field exp.	Lu et al. (2013)
'Shangai-3/Catbird'	4AL	10.5	*gwm160, wPt-5172*	Type-II	'Shangai-3/Catbird' x Naxos F_6, 181 lines	*Fg, Fc,* six field exp.	Lu et al. (2013)
'Shangai-3/Catbird'	5AL	6.8	*gwm617, gwm291*	Type-II	'Shangai-3/Catbird' x Naxos F_6, 181 lines	*Fg, Fc,* six field exp.	Lu et al. (2013)
'Shangai-3/Catbird'	6AS	7.1	*wPt-0832, wPt-6904*	Type-II	'Shangai-3/Catbird' x Naxos F_6, 181 lines	*Fg, Fc,* six field exp.	Lu et al. (2013)
'Shangai-3/Catbird'	6ASc	2.6	*barc37, wmc748a*	Type-III	'Shangai-3/Catbird' x Naxos F_6, 181 lines	*Fg, Fc,* six field exp.	Lu et al. (2013)
'Shangai-3/Catbird'	7AL.2	2.8	*barc121, wPt-8399*	Type-II	'Shangai-3/Catbird' x Naxos F_6, 181 lines	*Fg, Fc,* six field exp.	Lu et al. (2013)
Frontana	1A	9.5	*wPt-734078, wPt-731843, wPt-672089*	Types–II, IV	Mini Mano x Frontana DH, 168 lines	*Fg*, *Fc*, two field exp.	Ágnes et al. (2014)
Frontana	1B	18.0	*wPt-5347, wPt-2315, wPt-2597, wPt-0705, wPt-9857*	Types–II, III, IV	Mini Mano x Frontana DH, 168 lines	*Fg*, *Fc*, two field exp.	Ágnes et al. (2014)
Frontana	2D	23.0	*wPt-732882, wPt-667765, wPt-732603, wPt-733932*	Types–II, III, IV	Mini Mano x Frontana DH, 168 lines	*Fg*, *Fc*, two field exp.	Ágnes et al. (2014)
Frontana	2D	12.4	*wPt-3812, wPt-732411, gwm261*	Types–III, IV	Mini Mano x Frontana DH, 168 lines	*Fg*, *Fc*, two field exp.	Ágnes et al. (2014)
Frontana	3B	11.1	*gwm533, wPt-3921*	Types–II, III, IV	Mini Mano x Frontana DH, 168 lines	*Fg*, *Fc*, two field exp.	Ágnes et al. (2014)
Frontana	4A	14.8	*wPt-800509, wPt-2780, wPt-0804*	Type-II	Mini Mano x Frontana DH, 168 lines	*Fg*, *Fc*, two field exp.	Ágnes et al. (2014)
Frontana	4B1	9.1	*wPt-5334, wPt-4243, wPt-6209*	Type-II	Mini Mano x Frontana DH, 168 lines	*Fg*, *Fc*, two field exp.	Ágnes et al. (2014)
Frontana	4B2	7.5	*wPt-732448, wPt-6869, wPt-3439*	Type-III	Mini Mano x Frontana DH, 168 lines	*Fg*, *Fc*, two field exp.	Ágnes et al. (2014)
Frontana	5A	13.7	*gwm205, gwm156, gwm293, gwm129*	Types–II, III, IV	Mini Mano x Frontana DH, 168 lines	*Fg*, *Fc*, two field exp.	Ágnes et al. (2014)
Frontana	5B	15.2	*wPt-741134, wPt-5896, wPt-7240, wPt-2586*	Types–II, III, IV	Mini Mano x Frontana DH, 168 lines	*Fg*, *Fc*, two field exp.	Ágnes et al. (2014)
Frontana	6A	14.2	*wPt-7204, wPt-744786*	Types–II, IV	Mini Mano x Frontana DH, 168 lines	*Fg*, *Fc*, two field exp.	Ágnes et al. (2014)
Frontana	6B	20.5	*wPt-6039, gwm88*	Types–II, III, IV	Mini Mano x Frontana DH, 168 lines	*Fg*, *Fc*, two field exp.	Ágnes et al. (2014)
Frontana	7A	5.9	*wPt-7763, wPt-1601*	Type-III	Mini Mano x Frontana DH, 168 lines	*Fg*, *Fc*, two field exp.	Ágnes et al. (2014)
Frontana	7B1	15.3	*wPt-9925, wPt-5922, wPt-5646, wPt-4045*	Types–II, IV	Mini Mano x Frontana DH, 168 lines	*Fg*, *Fc*, two field exp.	Ágnes et al. (2014)
Frontana	7B2	10.3	*wPt-9467, wPt-5283, wPt-7318*	Type-III	Mini Mano x Frontana DH, 168 lines	*Fg*, *Fc*, two field exp.	Ágnes et al. (2014)
Frontana	7D	8.7	*wPt-0934, wPt-744219, wPt-743601*	Types–III, IV	Mini Mano x Frontana DH, 168 lines	*Fg*, *Fc*, two field exp.	Ágnes et al. (2014)
Frontana	NA1	9.0	*wPt-744219, gwm44*	Types–II, IV	Mini Mano x Frontana DH, 168 lines	*Fg*, *Fc*, two field exp.	Ágnes et al. (2014)

Frontana	NA2	11.1	*wPt-666593, wPt-664682*	Types–II, IV	Mini Mano x Frontana DH, 168 lines	*Fg*, *Fc*, two field exp.	Ágnes et al. (2014)
NX188	2D	4.7	*wmc111, wmc112*	Type-II	YZ1 x NX188 $F_{7:8}$, 199 lines	*Fg*, *Fc*, *Fa*, four field exp.	Lv et al. (2014)
NX188	4B	5.7	*gwm0925, gwm0898*	Type-II	YZ1 x NX188 $F_{7:8}$, 199 lines	*Fg*, *Fc*, *Fa*, four field exp.	Lv et al. (2014)
YZ1	4D	9.3	*psp3007, DFMR2*	Type-II	YZ1 x NX188 $F_{7:8}$, 199 lines	*Fg*, *Fc*, *Fa*, four field exp.	Lv et al. (2014)
YZ1	5B	1.0	*wmc235, wmc28*	Type-II	YZ1 x NX188 $F_{7:8}$, 199 lines	*Fg*, *Fc*, *Fa*, four field exp.	Lv et al. (2014)
YZ1	5D	12.9	*gwm292, Vrn-D1*	Type-II	YZ1 x NX188 $F_{7:8}$, 199 lines	*Fg*, *Fc*, *Fa*, four field exp.	Lv et al. (2014)
Huangcandou	*Fhb1*	26.1	*gwm493, gwm533*	Type-II	Huangcandou x Jagger $F_{5:7}$, 190 lines	*Fg,* three GH exp.	Cai and Bai (2014)
Huangcandou	3BSc	6.6	*wmc777, barc139*	Type-II	Huangcandou x Jagger $F_{5:7}$, 190 lines	*Fg,* three GH exp.	Cai and Bai (2014)
Huangcandou	3AS	10.0	*cfa2134, gwm2*	Type-II	Huangcandou x Jagger $F_{5:7}$, 190 lines	*Fg,* three GH exp.	Cai and Bai (2014)
Jagger	2D	9.5	*wmc112, wmc25*	Type-II	Huangcandou x Jagger $F_{5:7}$, 190 lines	*Fg,* three GH exp.	Cai and Bai (2014)
Jagger	6D	6.7	*cfd76, barc175*	Type-II	Huangcandou x Jagger $F_{5:7}$, 190 lines	*Fg,* three GH exp.	Cai and Bai (2014)
DH81 (*T. macha*)	4AS	30.2	*BS00011173, TC93568*	Type–I, II, AUDPC	HS x DH81 F_5, 39 and 78 lines	*Fc*, three field exp.	Burt et al. (2015)
HS	4AS	22.0	*wmc48, BS00003623*	Type–I, II, AUDPC	HS x DH81 F_5, 39 and 78 lines	*Fc*, three field exp.	Burt et al. (2015)
Arina	1BS	5.6	*tPt-5080, wPt-3103, wPt-6117*	Type-II	Capo x Arina, $F_{5:7}$, 171 lines	*Fc*, three field exp.	Buerstmayr and Buerstmayr (2015)
Arina	2AS	7.6	*wPt-7721, tPt-3109, wPt-8490, tPt-8937*	Type-II	Capo x Arina, $F_{5:7}$, 171 lines	*Fc*, three field exp.	Buerstmayr and Buerstmayr (2015)
Arina	3B	6.4	*wPt-10323, wPt-2372, wPt-0065, wPt-7688*	Type-II	Capo x Arina, $F_{5:7}$, 171 lines	*Fc*, three field exp.	Buerstmayr and Buerstmayr (2015)
Capo	3D	7.1	*wPt-741038, wPt-4544*	Type-II	Capo x Arina, $F_{5:7}$, 171 lines	*Fc*, three field exp.	Buerstmayr and Buerstmayr (2015)
Arina	4AL	8.6	*wPt-2345, wPt-2903, wPt-4828*	Type-II	Capo x Arina, $F_{5:7}$, 171 lines	*Fc*, three field exp.	Buerstmayr and Buerstmayr (2015)
Capo	5AL	6.9	*wPt-1200, gwm291, wPt-5096, tPt-4184*	Type-II	Capo x Arina, $F_{5:7}$, 171 lines	*Fc*, three field exp.	Buerstmayr and Buerstmayr (2015)
Arina	6BL	5.4	*wmc389, gwm518, barc24, wPt-6039, tPt-3689*	Type-II	Capo x Arina, $F_{5:7}$, 171 lines	*Fc*, three field exp.	Buerstmayr and Buerstmayr (2015)
Arina	7D	8.3	*wPt-743857, wPt-1859*	Type-II	Capo x Arina, $F_{5:7}$, 171 lines	*Fc*, three field exp.	Buerstmayr and Buerstmayr (2015)
NC-Neuse	1A	11.4	*IWA3805, IWA6152*	Types–I, II, III, IV	NC-Neuse x AGS 2000 F_5, 170 lines	*Fg*, seven field exp.	Peterson et al. (2016),
NC-Neuse	1B	9.5	*IWA6290, wmc419*	Types–III, IV	NC-Neuse x AGS 2000 F_5, 170 lines	*Fg*, seven field exp.	Peterson et al. (2016)
AGS 2000	1D.2	10.8	*wPt2206, IWA1386, wPt671990*	Types–III, IV	NC-Neuse x AGS 2000 F_5, 170 lines	*Fg*, seven field exp.	Peterson et al. (2016)
NC-Neuse	2A	9.7	*wmc522, IWA2612*	Types–II, III	NC-Neuse x AGS 2000 F_5, 170 lines	*Fg*, seven field exp.	Peterson et al. (2016)
NC-Neuse	4A	19.5	*barc170, IWA4480, IWA2900*	Types–III, IV	NC-Neuse x AGS 2000 F_5, 170 lines	*Fg*, seven field exp.	Peterson et al. (2016)
AGS 2000	5B	18.2	*IWA2500, IWA4793, Vrn_B1, wPt5896*	Types–I, III	NC-Neuse x AGS 2000 F_5, 170 lines	*Fg*, seven field exp.	Peterson et al. (2016)
NC-Neuse	6A	11.1	*IWA3483, wmc256, IWA4036*	Types–I, II	NC-Neuse x AGS 2000 F_5, 170 lines	*Fg*, seven field exp.	Peterson et al. (2016)
INW0412	1AS	12.2	TP126266	Type-I	INW0412 x 992060G1 $F_{6:8}$, 198 lines	*Fg*, two GH and two field exp.	Sun et al. (2016)
INW0412	1BL	11.4	TP188538	Type-I	INW0412 x 992060G1 $F_{6:8}$, 198 lines	*Fg*, two GH and two field exp.	Sun et al. (2016)
INW0412	2BL	11.7	TP97022	Type-I	INW0412 x 992060G1 $F_{6:8}$, 198 lines	*Fg*, two GH and two field exp.	Sun et al. (2016)
INW0412	3AS	8.5	TP228487	Type-I	INW0412 x 992060G1 $F_{6:8}$, 198 lines	*Fg*, two GH and two field exp.	Sun et al. (2016)
Haiyanzhong	5AS	16.0	*GSB3127, barc316*	Type-II	Wheaton x Haiyanzhong F_8, 186 lines	*Fg*, three GH exp.	Cai et al. (2016)

Haiyanzhong	6BS	11.1	*GBS4963, GBS3704*	Type-II	Wheaton x Haiyanzhong F_8, 186 lines	*Fg*, three GH exp.	Cai et al. (2016)
Haiyanzhong	7DL	7.5	*cfd46, wmc702*	Type-II	Wheaton x Haiyanzhong F_8, 186 lines	*Fg*, three GH exp.	Cai et al. (2016)
Wheaton	2B-1	5.8	*GBS1340, GBS0835*	Type-II	Wheaton x Haiyanzhong F_8, 186 lines	*Fg*, three GH exp.	Cai et al. (2016)
Wheaton	2B-2	7.8	*GBS5561, GBS0848*	Type-II	Wheaton x Haiyanzhong F_8, 186 lines	*Fg*, three GH exp.	Cai et al. (2016)
Haiyanzhong	4D	14.5	*GBS3223, GBS4883*	Type-II	Wheaton x Haiyanzhong F_8, 186 lines	*Fg*, three GH exp.	Cai et al. (2016)
Haiyanzhong	3B	8.2	*GBS1778, GBS3048*	Type-II	Wheaton x Haiyanzhong F_8, 186 lines	*Fg*, three GH exp.	Cai et al. (2016)
Haiyanzhong	4B	5.6	*GBS2348, GBS3434*	Type-II	Wheaton x Haiyanzhong F_8, 186 lines	*Fg*, three GH exp.	Cai et al. (2016)
Yumechikara	1BS	36.4	*Glu-B3, Rg-B1*	Type-II	Yumechikara x Kitahonami RIL	Five field exp.	Nishio et al. (2016)
Kitahonami	3BS	11.2	*hbg406, barc87*	Type-II	Yumechikara x Kitahonami RIL	Five field exp.	Nishio et al. (2016)
Truman	1BSc	10.9	*wmc269*	Type-II	Truman x MO 94-317 $F_{8\text{-}10}$, 167 lines	*Fg*, two GH and two field exp.	Islam et al. (2016)
Truman	2BL	16.1	*wmc592*	Type-II	Truman x MO 94-317 $F_{8\text{-}10}$, 167 lines	*Fg*, two GH and two field exp.	Islam et al. (2016)
Truman	2DS1	30.7	*wPt666223, Ppd-D1*	Types–I, II, III	Truman x MO 94-317 $F_{8\text{-}10}$, 167 lines	*Fg*, two GH and two field exp.	Islam et al. (2016)
Truman	3BSc1	10.3	*wmc615*	Types–II, III	Truman x MO 94-317 $F_{8\text{-}10}$, 167 lines	*Fg*, two GH and two field exp.	Islam et al. (2016)
Truman	2ASc	12.3	*wPt8826, gwm095*	Types–I, III	Truman x MO 94-317 $F_{8\text{-}10}$, 167 lines	*Fg*, two GH and two field exp.	Islam et al. (2016)
Truman	3DS	10.0	*wPt5390, cfd055*	Type-I	Truman x MO 94-317 $F_{8\text{-}10}$, 167 lines	*Fg*, two GH and two field exp.	Islam et al. (2016)
Truman	3BSc2	10.2	*gwm285*	Type-II	Truman x MO 94-317 $F_{8\text{-}10}$, 167 lines	*Fg*, two GH and two field exp.	Islam et al. (2016)
Truman	2DS2	7.5	*gwm102*	Type-IV	Truman x MO 94-317 $F_{8\text{-}10}$, 167 lines	*Fg*, two GH and two field exp.	Islam et al. (2016)
Truman	3BLc	9.6	*wPt9433, barc164*	Type-IV	Truman x MO 94-317 $F_{8\text{-}10}$, 167 lines	*Fg*, two GH and two field exp.	Islam et al. (2016)
Truman	1BLc	7.4	*wmc694*	Type-IV	Truman x MO 94-317 $F_{8\text{-}10}$, 167 lines	*Fg*, two GH and two field exp.	Islam et al. (2016)
Truman	6ALc	6.7	*barc146*	Type-III	Truman x MO 94-317 $F_{8\text{-}10}$, 167 lines	*Fg*, two GH and two field exp.	Islam et al. (2016)
Naxos	2AS	5.9	*Ex_c18324_390, BS00022331_51*	Type-II	Soru#1 x Naxos F6, 131 lines	*Fg*, six field exp.	He et al. (2016)
Naxos	2DL	8.2	*BS00021881_51, Kukri_c31995_1948*	Types-II, III	Soru#1 x Naxos F6, 131 lines	*Fg*, six field exp.	He et al. (2016)
Naxos	2DS	13.5	D_F1BEJMU02GB94Z_188	Type-II	Soru#1 x Naxos F6, 131 lines	*Fg*, six field exp.	He et al. (2016)
Soru#1	2DLc	17.1	*W_Ku_c8712_14751858, GENEU0808_728*	Types–II, III, IV	Soru#1 x Naxos F6, 131 lines	*Fg*, six field exp.	He et al. (2016)
Soru#1	4DS	5.4	*Rht_D1, D_c56766_278*	Types–II, III	Soru#1 x Naxos F6, 131 lines	*Fg*, six field exp.	He et al. (2016)
Soru#1	5AL	6.8	*Ku_c12469_983, IAAV4799*	Types–II, III	Soru#1 x Naxos F6, 131 lines	*Fg*, six field exp.	He et al. (2016)
Soru#1	5DL	6.4	*Ra_c27043_437, IAAV2323*	Types–II, III	Soru#1 x Naxos F6, 131 lines	*Fg*, six field exp.	He et al. (2016)
Soru#1	3AS	9.9	*Kukri_c96747_274, wC11_r_c4157_1965583*	Type-II	Soru#1 x Naxos F6, 131 lines	*Fg*, six field exp.	He et al. (2016)
Soru#1	4AL	6.6	*Ex_c11968_204, RAC875_c35979_263*	Type-II	Soru#1 x Naxos F6, 131 lines	*Fg*, six field exp.	He et al. (2016)
Soru#1	5AL	12.3	*Vrn-A1, Ex_c7729_144*	Type-II	Soru#1 x Naxos F6, 131 lines	*Fg*, six field exp.	He et al. (2016)
SYN1	2D	25.0	*wmc41,* 1103038|F|0	Type-II	SYN1 x Ocoroni DH, 169 lines	*Fg*, two field exp.	Zhu et al. (2016)
SYN1	7A	8.5	1090541|F|0	Type-II	SYN1 x Ocoroni DH, 169 lines	*Fg*, two field exp.	Zhu et al. (2016)
SYN1	1B	4.8	1000810|F|0	Type-II	SYN1 x Ocoroni DH, 169 lines	*Fg*, two field exp.	Zhu et al. (2016)
PI 672538	2B	11.6	*barc55*	Type-II	L661 x PI 672538 F_2, $F_{2:3}$, 229 lines	*Fg*, four field exp.	Li et al. (2017)
PI 672538	3B	10.0	*wmc54, wmc615, gwm566*	Types–II, IV	L661 x PI 672538 F_2, $F_{2:3}$, 229 lines	*Fg*, four field exp.	Li et al. (2017)
NC-Neuse	1A	18.0	*IWB29758, IWB73950, IWB36272*	Types–I, III	NC-Neuse x Bess DH, 98 lines	*Fg*, seven field exp.	Peterson et al. (2017)
Bess	1B.4	11.0	*IWB31692, IWB9040, IWB38247*	Types–I, IV	NC-Neuse x Bess DH, 98 lines	*Fg*, seven field exp.	Peterson et al. (2017)
NC-Neuse	2A.3	13.0	*IWB42392, IWB3746, IWB836*	Types–I, IV	NC-Neuse x Bess DH, 98 lines	*Fg*, seven field exp.	Peterson et al. (2017)
Bess	2B.1	21.1	*IWB31987, IWB40514, IWA5830*	Types-II, III, IV	NC-Neuse x Bess DH, 98 lines	*Fg*, seven field exp.	Peterson et al. (2017)
Bess	3B.2	16.1	*IWB35616, IWA4267, IWB57595*	Type-II	NC-Neuse x Bess DH, 98 lines	*Fg*, seven field exp.	Peterson et al. (2017)

NC-Neuse	4A.2a	23.3	*IWA2106, IWB26481, IWB44184, IWB29438*	Types–I, II, III, IV	NC-Neuse x Bess DH, 98 lines	*Fg*, seven field exp.	Peterson et al. (2017)
NC-Neuse	4A.2b	20.0	*IWB12132, IWA4859, IWB36777, IWB28864*	Types–II, III	NC-Neuse x Bess DH, 98 lines	*Fg*, seven field exp.	Peterson et al. (2017)
Bess	4D.1	10.0	*IWB49801, IWB61486, IWB54349, IWB53820*	Types–II, IV	NC-Neuse x Bess DH, 98 lines	*Fg*, seven field exp.	Peterson et al. (2017)
NC-Neuse	5B.1	15.1	*IWB51347, IWB8972*	Type-IV	NC-Neuse x Bess DH, 98 lines	*Fg*, seven field exp.	Peterson et al. (2017)
Bess	5D.1	26.7	*IWB50247, IWB54292, IWB61072*	Types-I, II, III	NC-Neuse x Bess DH, 98 lines	*Fg*, seven field exp.	Peterson et al. (2017)
NC-Neuse	6A.2	21.2	*IWB12224, IWB74194, IWB2543*	Types-I, II, III, IV	NC-Neuse x Bess DH, 98 lines	*Fg*, seven field exp.	Peterson et al. (2017)
NC-Neuse	6A.3	17.1	*IWA6517, IWA3585, IWB39452*	Types–III, IV	NC-Neuse x Bess DH, 98 lines	*Fg*, seven field exp.	Peterson et al. (2017)
Stettler	2BL	16.2	*Excaliber_rep_c108662_132, RAC875_c25277_324, Tdurum_contig7144_602, wsnp_Ex_c41558_48356869*	Type-II	FL62R1 x Stettler DH, 185 lines	*Fg*, two GH exp.	Zhang et al. (2018)
FL62R1	2AS	6.0	*RAC875_c54668_102, GENE-0137_147*	Type-II	FL62R1 x Stettler DH, 185 lines	*Fg*, two GH exp.	Zhang et al. (2018)
FL62R1	5AL	6.3	*BS00036839_51, BobWhite_c2236_111*	Type-II	FL62R1 x Stettler DH, 185 lines	*Fg*, two GH exp.	Zhang et al. (2018)
FL62R1	1AL	7.5	*RAC875_c68350_61, Tdurum_contig52086_129*	Type-II	FL62R1 x Stettler DH, 185 lines	*Fg*, two GH exp.	Zhang et al. (2018)
FL62R1	4A	8.6	*Kukri_c29142_473, RAC875_c30110_156*	Type-II	FL62R1 x Stettler DH, 185 lines	*Fg*, two GH exp.	Zhang et al. (2018)
ND2710	3B	20.0	*umn10*	Type-II	Bobwhite x ND2710 RIL, 233 lines	*Fg*, three GH and one field exp.	Zhao et al. (2018)
ND2710	6B	12.0	*Fhb2-CAPS3, gwm644*	Type-II	Bobwhite x ND2710 RIL, 233 lines	*Fg*, three GH and one field exp.	Zhao et al. (2018)
ND2710	2A	6.0	wsnp_Ex_rep_c103167_88182254	Type-II	Bobwhite x ND2710 RIL, 233 lines	*Fg*, three GH and one field exp.	Zhao et al. (2018)
ND2710	6A	8.0	*tplb0037a05_913*	Type-II	Bobwhite x ND2710 RIL, 233 lines	*Fg*, three GH and one field exp.	Zhao et al. (2018)
AQ24788-83	7DL	32.2	*gwm428*	Type-II	Luke x AQ24788-83 F_6, 272 lines	*Fg*, two GH and six field exp.	Ren et al. (2018)
AQ24788-83	1AS	7.0	*IWB63682*	Type-II	Luke x AQ24788-83 F_6, 272 lines	*Fg*, two GH and six field exp.	Ren et al. (2018)
Luke	5AS	9.8	*IWA7777*	Type-II	Luke x AQ24788-83 F_6, 272 lines	*Fg*, two GH and six field exp.	Ren et al. (2018)
Yangmai 13	1AL	10.8	*RAC875_c6338_1887*	Type-II	C615 x Yangmai 13 F_7, 198 lines	*Fg*, three field exp.	Yi et al. (2018)
C615	2DS-1	5.4	*Kukri_c60627_74*	Type-II	C615 x Yangmai 13 F_7, 198 lines	*Fg*, three field exp.	Yi et al. (2018)
C615	2DL-1	11.8	*TA001163-0861*	Type-II	C615 x Yangmai 13 F_7, 198 lines	*Fg*, three field exp.	Yi et al. (2018)
C615	4AL-1	9.6	*BS00041735_51*	Type-II	C615 x Yangmai 13 F_7, 198 lines	*Fg*, three field exp.	Yi et al. (2018)
Yangmai 13	5AL-1	8.7	*BS00069175_51*	Type-II	C615 x Yangmai 13 F_7, 198 lines	*Fg*, three field exp.	Yi et al. (2018)
C615	5DL-1	7.3	*D_F1BEJMU02IBF8G_328*	Type-II	C615 x Yangmai 13 F_7, 198 lines	*Fg*, three field exp.	Yi et al. (2018)
Yangmai 13	6AS-1	9.3	*Tdurum_contig55193_296*	Type-II	C615 x Yangmai 13 F_7, 198 lines	*Fg*, three field exp.	Yi et al. (2018)
C615	1AS	9.6	*BS00026456_51*	Type-II	C615 x Yangmai 13 F_7, 198 lines	*Fg*, three field exp.	Yi et al. (2018)
Yangmai 13	1AL	7.5	*wsnp_CAP12_c2438_1180601*	Type-II	C615 x Yangmai 13 F_7, 198 lines	*Fg*, three field exp.	Yi et al. (2018)
C615	2AL	9.3	*BS00022896_51*	Type-II	C615 x Yangmai 13 F_7, 198 lines	*Fg*, three field exp.	Yi et al. (2018)
C615	6AS-1	7.3	*tplb0031m24_341*	Type-II	C615 x Yangmai 13 F_7, 198 lines	*Fg*, three field exp.	Yi et al. (2018)
Solitar, Bussard	5B	13.9	*M2441, M2290*	Type-II	Solitar x Bussard RIL, 157 lines	*Fc,* four field exp.	Herter et al. (2018)
Solitar, Bussard	2D	14.3	*M425, M615*	Type-II	Solitar x Bussard RIL, 157 lines	*Fc,* four field exp.	Herter et al. (2018)
Solitar, Bussard	7D	12.1	*M2491, M791*	Type-II	Solitar x Bussard RIL, 157 lines	*Fc,* four field exp.	Herter et al. (2018)

Abbreviations: DH - double haploid, *Fc – Fusarium culmorum*, *Fg – Fusarium graminearum*, GH – greenhouse, RIL - recombinant inbred line.

[a]Chromosome where QTL is mapped. [b]Percent phenotypic variation (maximum) explained by the QTL.

[c]Repersents flanking markers and/or markers in the QTL interval and/or markers in the QTL peak. For He et al. (2016), Zhao et al. (2018), Zhang et al. (2018) and Yi et al. (2018), only the closest marker is listed, for all co-segregating markers, refer to their original papers.

[d]Type – I, Types – II, Type – III, and Type – IV represent resistance to initial infection, spread within spike after initial infection, ability to degrade to accumulated toxin or resistance to toxin accumulation, and resistance to kernel infection, respectively.

2.7.2. Tetraploid wheat

FHB is particularly of concern in durum wheat, which is predominantly used for pasta and semolina making, and intended for direct human consumption (Prat et al. 2014). Thus, managing FHB in durum remains challenging because fungicides have limited effectiveness on the disease. Thus, breeding for host resistance in durum is pivotal. Higher susceptibility of durum to FHB was reported as early as the 1920s and even today, the majority of durum wheat cultivars are susceptible (Atanasoff 1920; Gilbert and Haber 2013; Anonymous 2018a). The reason modern durum cultivars are susceptible to FHB could be attributed to the narrow genetic base of resistance (Prat et al. 2014). The lack of resistance sources detected in durum wheat after many phenotyping studies led to the conclusion that durum wheat either lacks resistance or may actually carry susceptibility factors (suppressors that mask the effect of resistance QTL, if present) (Stack et al. 2002; Kishii et al. 2005; Garvin et al. 2009; Ghavami et al. 2011; Zhu et al. 2016b).

Durum wheat breeders are particularly challenged to improve FHB resistance in their breeding material along with improvement in other traits. The prerequisite for resistance breeding is to identify resistant donors followed by genetic mapping (Buerstmayr et al. 2009). Elite durum wheat cultivars and germplasm from the primary gene pool have little to no variation for the trait (Prat et al. 2014). Efforts to identify accessions with improved FHB resistance were not successful in the past. Efforts to identify accessions with improved FHB resistance have been unsuccessful in the past. After screening a large collection of durum wheat lines, Elias et al. (2005) did not identify any with significant resistance. Later, five accessions of Tunisian wheat lines with moderate Type-II resistance were identified among thousands of lines from CIMMYT and ICARDA gene banks (Elias et al. 2005; Huhn et al. 2012). Similarly, Talas et al. (2011) identified four Syrian landraces with some level of FHB resistance.

Investment of greater resources and variation for FHB resistance in hexaploid wheat resulted in identification of a large number of QTL (Buerstmayr et al. 2009; Gilbert and Haber 2013). Buerstmayr et al. (2009) did an extensive of review of 52 FHB QTL mapping studies, including six of durum wheat. Until 2014, there were only 10 QTL mapping studies in durum wheat (Prat et al. 2014). We have summarized QTL mapped for FHB resistance following a review by Prat et al. (2014) in tetraploid wheat (Tables 2.2 and 2.3). Since the publication of Prat et al. (2014), seven studies (Table 2.2) that utilized emmer and elite durum wheats (carrying some level of FHB resistance/tolerance) for mapping FHB resistance loci in tetraploid wheat have been reported in the literature (Table 2.3)

Table 2. 2. Mapping populations and the phenotyping methods performed to map Fusarium resistance quantitative trait loci in tetraploid wheat from 2014 to the present [following the review by Prat et al. (2014) that described QTL mapped up to an including 2013].

Plant material		Phenotyping			Reference
Parents	**Population**	**No. of experiments**	**method[a]**	**Fusarium species**	
Ben/PI 41025	200 RILs F_8	3 GH, 1 field	SFI, spray	*Fg*	Zhang et al. (2014)
Tunisian108/Ben//Ben	171 BCRILs BC_1F_7	2GH, 2 field	SFI, spray	*Fg*	Pirseyedi (2014)
Tunisian108/Lebsock//Lebsock	172 BCRILs BC_1F_7	2GH, 2 field	SFI, spray	*Fg*	Pirseyedi (2014)
Langdon(Dic-3a)/Langdon	83 RILs	2GH	SFI	*Fg*	Zhu et al. (2016a)
02-5B-318 (Sumai 3 derivative)/Saragolla	135 RILs $F_{2:7}$	4 field	Spray	*Fg*	Giancaspro et al. (2016)
DBC-480 (Sumai 3 derivative tetraploid wheat)/Karur	111 RILs F_7	3 GH, 3 field	SFI, spray	*Fc*	Prat et al. (2017)
DBC-480 (Sumai 3 derivative tetraploid wheat)/Durobonus	100 RILs F_7	3 field	Spray	*Fc*	Prat et al. (2017)
DBC-480 (Sumai 3 derivative tetraploid wheat)/SZD1029K	100 RILs F_7	3 field	Spray	*Fc*	Prat et al. (2017)
Joppa/10Ae564	205 RILs $F_{2:7}$	2GH, 2 field	SFI, spray	*Fg*	Zhao et al. (2018)
DT707/DT696	121 DH lines, later increased to 423 DH lines	5 field	Spray	*Fg*	Sari et al. (2018)
Strongfield/*T. turgidum* ssp. *carthlicum* cv. Blackbird	90 DH lines, later increased to 102 lines	2 field	Spray	*Fg*	Sari et al. (2018)

Abbreviations: DH - double haploid, *Fc – Fusarium culmorum*, *Fg – Fusarium graminearum*, GH – greenhouse, RIL - recombinant inbred line, SFI – single floret inoculation.
[a]Method of plant inoculations.

Table 2. 3. Quantitative trait loci (QTL) for Fusarium head blight resistance mapped in tetraploid wheat from 2014 to the present [following the review by Prat et al. (2014) that described QTL mapped up to an including 2013].

Source of resistance	Chr.[a]	Markers[b]	PVE[c]	Resistance types[d]	Comments	Reference
T. turgidum subsp. *dicoccum* accession PI 41025	3A	*IWA7649, IWA5039, IWA8624, gwm5*	8.0	Type-II		Zhang et al. (2014)
T. turgidum subsp. *dicoccum* accession PI 41025	5A	*wmc110, IWA7009, fcp650(Q), IWA1942, IWA821*	35.0	Type-II	Mapped near domestication gene *Q*	Zhang et al. (2014)
T. turgidum subsp. *durum* cv. Ben	2A	*IWA1103, IWA111, IWA2604, IWA5993, IWA2948, gwm473, IWA549*	9.0	Type-II		Zhang et al. (2014)
Tunisian108	2B	*wmc96, barc353, gwm71, barc297*	10.0	Types–II, III, IV		Pirseyedi (2014)
Tunisian108	3B	*wpt0384, barc229*	10.8	Types–II, III		Pirseyedi (2014)
Tunisian108	5A	*barc2187, barc141, wpt4248*	23.7	Types–II, IV		Pirseyedi (2014)
T. turgidum subsp. *durum* cv. Ben	5B	*wpt5928, wpt5604*	5.1	Type-II		Pirseyedi (2014)
Tunisian108	5B	*wpt6902, wpt5514*	7.8	Type-IV		Pirseyedi (2014)
T. turgidum subsp. *durum* cv. Ben	7B	*wpt7975, wpt5846*	9.5	Type-II		Pirseyedi (2014)
Tunisian108	7B	*gpw1054, wpt0884*	9.7	Type-II		Pirseyedi (2014)
T. turgidum subsp. *durum* cv. Ben	1B	*wpt1818, wpt5061*	16.3	Type-II		Pirseyedi (2014)

Tunisian108	1B	*gwm264, wpt3451*	11.7	Type-IV		Pirseyedi (2014)
T. turgidum subsp. *durum* cv. Ben	1A	*wpt7784, wpt6853*	4.8	Type-III		Pirseyedi (2014)
Tunisian108	1B	*wPt0506, wPt5485, wPt1818*	5.4	Type-II		Pirseyedi (2014)
Tunisian108	1A	*wPt5876, wPt6280*	5.1	Type-II		Pirseyedi (2014)
Tunisian108	1A	*wPt4886, wPt3698*	9.3	Type-II		Pirseyedi (2014)
Tunisian108	6B	*rPt1040, wPt8976*	5.5	Type-II		Pirseyedi (2014)
T. turgidum subsp. *durum* cv. Lebsock	3B	*wPt0384, wPt6981*	9.3	Type-II		Pirseyedi (2014)
Tunisian108	4A	*wmc96, wPt0054*	6.3	Type-II		Pirseyedi (2014)
Tunisian108	5A	*wPt2357, gwm291*	4.3	Type-II		Pirseyedi (2014)
T. turgidum subsp. *durum* cv. Lebsock	1A	*wPt3870, wPt4886*	8.5	Type-II		Pirseyedi (2014)
T. turgidum subsp. *durum* cv. Lebsock	3B	*wPt0250, wPt10965*	4.7	Type-II		Pirseyedi (2014)
Tunisian108	5A	*wPt5309, gwm156*	9.9	Type-II		Pirseyedi (2014)
Tunisian108	3A	*tPt7492, wPt0819*	7.3	Type-II		Pirseyedi (2014)
T. turgidum subsp. *durum* cv. Lebsock	3A	*wPt8876, wPt2562*	6.9	Type-II		Pirseyedi (2014)
Tunisian108	3B	*wPt10687, wPt11451*	5.1	Type-III		Pirseyedi (2014)
Tunisian108	3B	*wPt10325, tPt9948*	6.5	Type-III		Pirseyedi (2014)
T. turgidum subsp. *durum* cv. Lebsock	3A	*wPt2938, tPt1143*	6.9	Type-III		Pirseyedi (2014)
T. dicoccoides Israel A	3AS	*wgc501, wgc510, wgc1226*	46.9	Type-II	Refined map from Otto et al. (2002) and Chen et al. (2007)	Zhu et al. (2016a)
Triticum aestivum line 02-5B-318	2AS	*1WB63138*	12.0	Types–I, II	Co-localize with *WheatPME1* genes encoding pectin methylesterase	Giancaspro et al. (2016)
Triticum aestivum line 02-5B-318	3AL	*IWB37509*	11.0	Type-I		Giancaspro et al. (2016)
Triticum aestivum line 02-5B-318	3BS	*IWB64332*	9.0	Type-I		Giancaspro et al. (2016)
Triticum aestivum line 02-5B-318	5BL	*IWB72334*	9.0	Type-I		Giancaspro et al. (2016)
Triticum aestivum line 02-5B-318	6BS	*IWA1721*	8.0	Type-I		Giancaspro et al. (2016)
T. turgidum subsp. *durum* cv. Saragolla	7AL	*IWB43304*	9.0	Type-I		Giancaspro et al. (2016)
T. turgidum subsp. *durum* cv. Saragolla	2BS	*IWB55365*	12.0	Type-II	Co-localize with *WheatPME1* genes encoding pectin methylesterase	Giancaspro et al. (2016)
Triticum aestivum line 02-5B-318	1BL	*IWB65943*	9.0	Type-II		Giancaspro et al. (2016)
Triticum aestivum line 02-5B-318	4BL	*IWB48353*	12.0	Type-II		Giancaspro et al. (2016)
Triticum aestivum line 02-5B-318	5BS	*IWB816*	8.0	Type-II		Giancaspro et al. (2016)
DBC-480	2BL	*1072874*	7.2	Type-II		Prat et al. (2017)
DBC-480	3BS	*4410793, barc147, umn10*	16.0	Type-II	Co-localize with *Fhb1*	Prat et al. (2017)
DBC-480	4AL	*4541598*	18.8	Type-II		Prat et al. (2017)
DBC-480	4BS	*RhtB1*	69.0	Type-II	Co-localize with reduced height gene *Rht-B1*	Prat et al. (2017)
DBC-480	5AL	*1111359*	15.0	Type-II		Prat et al. (2017)
DBC-480	6AS	*4008755*	28.0	Type-II		Prat et al. (2017)
T. turgidum subsp. *durum* cv. Joppa	2A	*IWB73981, IWB10237, IWB65481*	15.0	Types–II, III		Zhao et al. (2018)
10Ae564	5A	*IWB71377, IWB26525, IWB8656*	19.0	Types–II, III		Zhao et al. (2018)
10Ae564	7A	*IWB72301, IWB74024, IWB58523*	11.0	Type-II		Zhao et al. (2018)
T. turgidum subsp. *durum* line DT696	1B	*IAAV7541*	4.3	Type-II		Sari et al. (2018)
T. turgidum subsp. *durum* line DT696	2B	*Kukri_c28077_282, Kukri_c44368_180 Kukri_c50943_853*	3.0	Type-II		Sari et al. (2018)

T. turgidum subsp. *durum* line DT696	5A1	*Ex_c6161_335, GENE-3101_854, IACX815, IAAV3512, tplb0039m09_92*	20.8	Types–I, II	Co-localized with QTL for plant height	Sari et al. (2018)
T. turgidum subsp. *durum* line DT696	5A	*IACX9023, IAAV3365, IAAV3043, IACX10100, IAAV8669, JD_c889_708*	25.7	Types–I, II	Co-localized with QTL for maturity	Sari et al. (2018)
T. turgidum subsp. *durum* line DT696	7A	*IAAV3305, TA006231-0789*	4.7	Type-II	Co-localized with QTL for maturity	Sari et al. (2018)
T. turgidum ssp. *carthlicum* cv. Blackbird	1A	*BS00012321_51, BS00000713_51, BS00014831_51, BS00080187_51*	26.8	Types–I, II	Co-localized with QTL for maturity	Sari et al. (2018)
T. turgidum ssp. *carthlicum* cv. Blackbird	2A	*wsnp_Ex_c4847_8646583, RAC875_rep_c101689_504*	11.8	Type-II	Co-localized with QTL for plant height	Sari et al. (2018)
T. turgidum subsp. *Durum* cv. Strongfield	2B	*Tdurum_contig27844_127, wsnp_Ex_c6471_11241582, Jagger_c6853_60*	15.9	Type-II		Sari et al. (2018)
T. turgidum ssp. *carthlicum* cv. Blackbird	3A	*Excalibur_c27972_654, IAAV2646, D_contig16408_629*	12.6	Type-II		Sari et al. (2018)
T. turgidum subsp. *Durum* cv. Strongfield	6A	*Tdurum_contig27441_373, Bobwhite_c4255_127*	11.8	Type-II		Sari et al. (2018)
T. turgidum ssp. *carthlicum* cv. Blackbird	6B	*RAC875_c54818_481, GENE-3716_393*	16.9	Type-II		Sari et al. (2018)
T. turgidum subsp. *Durum* cv. Strongfield	7B	*Tdurum_contig19413_163, wsnp_CAP8_c334_304253*	14.3	Types–I, II	Co-localized with QTL for maturity	Sari et al. (2018)

[a]Chromosome where QTL is mapped.

[b]Repersents flanking markers and/or markers in the QTL interval and/or markers in the QTL peak. For Sari et al. (2018) and Zhao et al. (2018), only a few co-segregating markers are listed. For complete list, refer to the original papers.

[c]Percent phenotypic variation (maximum) explained by the QTL.

[d]Type – I, Types – II, Type – III, and Type – IV represent resistance to initial infection, spread within spike after initial infection, ability to degrade to accumulated toxin or resistance to toxin accumulation, and resistance to kernel infection, respectively.

2.7.3. Wheat relative species

In addition to cultivated wheats, researchers have also looked for resistance in wheat related species and many of these have been identified as highly effective sources of resistance (reviewed in Oliver et al. 2005; Cai et al. 2005; Fedak et al. 2007). Wan et al. (1997) evaluated 1463 accessions from 17 genera of *Triticum* and 85 species and reported 18 resistant or highly resistant accessions. Gilchrist et al. (1999) credited *Aegilops tauchii* for FHB resistance observed in synthetic hexaploid wheat lines developed at CIMMYT. Recently, Brisco et al. (2017) screened 109 accessions of *A. tauschii* and reported five as resistant and seven as moderately resistant to FHB; all expressing Type-II resistance. Ban (1997) evaluated four indigenous species of the genus *Elymus* from Japan and reported *E. humidus* (2n=6x=42, SSHHYY) and *E. racemifer* (2n=4x=28, SSYY) as highly resistant to FHB. Fedak (2000) reported *E. humidus* as immune to FHB after point inoculation. Brar and Hucl (2017) reported a putative intergeneric line (00Ar134-1) derived from a cross of an elite wheat with *Elymus repens*, comparable to elite cultivars from western Canada and carrying Type-II resistance. Among other *Triticum* related genera, *Thinopyrum*, *Roegneria*, *Leymus*, and *Elymus* have been major targets in resistance breeding (Wan et al. 1997; Jauhar and Peterson 1998; Chen and Liu 2000; Chen et al. 2005; McArthur et al. 2012; Turner et al. 2013; Zeng et al. 2013). Three of the seven formally designated FHB resistance genes in wheat are derived from wheat relatives i.e. *Fhb3* from *Leymus racemosus* (Qi et al. 2008), *Fhb6* from *Elymus tsukushiensis* (Cainong et al. 2015), and *Fhb7* from *Thinopyrum ponticum* (Guo et al. 2015).

2.7.4. Expressed proteins and hormones related to FHB resistance

Host resistance to pathogen infection is a regulated process that results in a number of cellular events. Numerous studies have tried to identify FHB resistance-related genes and hormones in the wheat-*Fusarium* pathosystem (Schweiger et al. 2013; Dhokane et al. 2016; Schweiger et al. 2016; Samad-Zamini et al. 2017; Li et al. 2018; reviewed in Jia et al. 2018). Important genes were identified as differentially expressed in wheat lines with and without *Fhb1* and *Fhb5* genes (e.g.: UDP-glycosyltansferase, receptor-like protein kinases, phenylpropanoids). These are proteins that are associated with, or related to defence, oxidative stress, photosynthesis, translation or cell-wall biosynthesis.

Lignin is a major component of the cell-wall and is involved in defence against pathogen attack, many of the above-mentioned studies reported up-regulation of lignin related proteins, however, mostly as a part of basal resistance. Dhokane et al. (2016) identified six expressed genes (4-Coumarate ligase, callose synthase, basic helix loop helix transcription factor, glutathione S-transferase, ABC transporter, and cinnamyl alcohol

dehydrogenase) associated with *Fhb2* and later on Zhao et al. (2018) confirmed two (Glutathione S-transferase, and Cinnamyl alcohol dehydrogenase) of these six in the re-mapping of *Fhb2*. Differentially expressed genes for QTL derived from Wangshuibai belonged to salicylic acid signaling/biosynthesis, jasmonic acid biosynthesis, antimicrobial compound synthesis, protein kinases, antioxidative stress, genes for cell-wall fortification, and defence related genes. The mechanism of resistance to biotrophs and necrotrophs is mostly governed by salicylic acid and ethylene/jasmonic acid pathways, respectively (Brewer and Hammond-Kosack 2015).

It becomes more challenging to study pathways for *Fusarium* species because it is hemi-biotroph. A transcriptomic analysis showed that defence pathways mediated by calcium ions, salicylic acid, jasmonic acid are all required for resistant responses to infection by *F. graminearum* in corroboration with many other studies (Steiner et al. 2009; Zhang et al. 2013; Xiao et al. 2013; Dhokane et al. 2016). Based on these studies, it was postulated that timely and orderly activation of jasmonic and salicylic acid pathways is critical for FHB resistance in wheat (Jia et al. 2018). Thus far, a large number of genes inducible following *Fusarium* infection are catalogued (reviewed/listed in aforementioned references) and many of the gene classes are common for QTL derived from different resistant donors. It is important to note that despite some common findings in the studies, the results on gene expression of important candidate proteins are inconsistent among studies and the challenge is to functionally verify the association of these genes with FHB response.

2.8. Implications of using FHB resistance QTL/gene(s)

Breeding for FHB resistance is a very challenging task as resistance to FHB is a quantitative trait, which is highly influenced by environment (McMullen et al. 2012). Apart from many 'small-effect' or 'minor' QTL there are some 'major' QTL that confer resistance to FGSC (Buerstmayr et al. 2009). Of these major QTL, *Qfhs.ndsu-3BS* (syn. *Fhb1*), which confers Type-II resistance, is the most effective and most widely used in breeding programs worldwide. Other major QTL are *Fhb2* on chromosome 6BS, *Qfhs.ifa-5A* on 5AS, and *Fhb4* on 4B conferring Type-II, I and II resistance, respectively (Buertsmayr et al. 2009). One of the biggest challenges associated with the introgression of QTL conferring FHB resistance from a wide range of germplasm to adapted wheat varieties is linkage drag (unwanted side-effects) and pleiotropy in terms of agronomic, quality and other traits (Salameh et al. 2011). Sumai 3 is the most widely utilized source of FHB resistance in hexaploid wheat in North America and breeders have expressed their concern about its susceptibility to other diseases and it association with seed shattering, in addition to its negative effects on quality and agronomic traits (McMullen et al. 2012). Several studies reported enhanced effects of

combining QTL to improve resistance to FHB (Buerstmayr et al. 2003; McCartney et al. 2007; Xue et al. 2010b; Salameh et al. 2011).

A study by Salameh et al. (2011) examined the effect of combining *Fhb1* and QTL on 5AS, for FHB resistance, and on agronomic and quality traits, in a series of backcross-derived sister lines based on nine European winter wheat breeding lines. Although most of the lines had greater FHB resistance with the combination of these two major QTL, they reported some lines where *Fhb1* alone provided the same level of resistance as the combination of *Fhb1* plus QTL on 5AS. This was attributed to the genetics of the recurrent parents used in the study. The effect of these QTL on grain yield, thousand kernel weight and protein content was insignificant. However, QTL on 5AS increased height by an average of 4 cm. Similarly, a study by McCartney et al. (2007) reported a greater effect of the *Fhb4* (4B) QTL in decreasing FHB index, FDK and DON in a breeding population relative to the Nyuubai derived *Fhb1* and 3BSc QTL. Also, an increase of 9 cm and 6 cm plant height was associated with QTL on 4B (derived from Wuhan-1) and 3BSc (derived from Nyuubai). However, the 3BS QTL was associated with a 3.5 cm reduction in plant height. The epistatic effect of QTL was significant for plant height, FHB index, FDK and DON and non-significant for anthesis date, although in a very few studies the results were contrasting and depended on the genetic background of the recurrent parents. The Sumai-3 derived 5AS QTL reduced grain protein content and thousand kernel weight, whereas the Nyuubai 5AS allele did not. Suzuki et al. (2012) reported linkage-drag associated with Sumai-3 alleles on 4BS and 5AS in an F_1-derived double-haploid population of 233 lines. Introgressions of 4BS and 5AS QTL increased stem and spike length, whereas the 2DL QTL significantly decreased grain weight, and the 6BS QTL delayed heading. Miedaner et al. (2011) also studied the effect of introgression of 3BS (*Fhb1*) and 5AS QTL in European elite spring and winter wheat lines. A small negative effect of the 3BS QTL on yield was observed, dispite this however, they concluded MAS is a good strategy to improve FHB resistance and germplasm development. It is important to study linkage drag associated with introgressions of exotic FHB resistance genes or QTL into elite backgrounds before their utilization in wheat breeding.

2.9. Synchrotron-based technologies to study *Fg*-wheat pathosystem

The susceptibility of wheat florets at anthesis and the general progression of Fusarium head blight has been recognized for over a century (Arthur 1891; Atanasoff 1920; Pugh et al. 1933; Anderson 1948). The histology of spike infection has been studied extensively in the last decade, revealing the infection route of the two main species responsible for FHB, i.e. *F. graminearum* and *F. culmorum* (Kang and Buchenauer 2000; Ribichich et al. 2000; Miller et

al. 2004; Jansen et al. 2005; Brown et al. 2010). Post-floral invasion, these pathogens spread throughout the spikelet inter- and intra-cellularly down the rachis through the rachis node. In anatomical and histological studies published between 2000 and 2010, the authors concluded that spikelet to spikelet spread of the fungus was inhibited in cultivars with Type-II resistance. The limited number of studies that included cultivars with differential susceptibility to FHB, indicated that the cellular changes in those cultivars are generally similar and the only difference is in the rate of disease progression (Kang amd Buchenauer 2000; Ribichich et al. 2000). Cultivars with Type-II resistance resist pathogen spread in the rachis thus slowing disease development or progression. Anatomical features associated with Type-II resistance include: spike traits such as dense vascular bundles in the rachis, small diameter vessels, strong and thick cortical sclerenchyma cell-walls, and short internodes in the upper part of the rachis (Zhang and Ye 1993; Yu et al. 1996). Studies by Jansen et al. (2005) and Zhang et al. (2008) pointed to the rachis node as an important part of the spike resisting fungal spread. Earlier, histopathology studies were mostly aimed at understanding the host-pathogen interaction and pathogen infection processes (Arthur 1891; Atanasoff 1920; Pugh et al. 1933; Anderson 1948; Kang and Buchenauer 2000; Ribichich et al. 2000; Miller et al. 2004; Jansen et al. 2005; Brown et al. 2010).

Synchrotrons are descendent of the cyclotron and modern synchrotron facilities are powerful machines that work as cyclic particle accelerators (Miller and Dumas 2006; Vijayan et al. 2015). Synchrotrons accelerate charged particles such as electrons in a cyclic trajectory at near the speed of light. Intense beamlines or light radiation ranging in the energies of infrared (IR) to X-ray are generated from these accelerated electrons. Electromagnetic radiation from the emission device to the end-station are carried along a synchrotron beamline, where they are used to illuminate sample material in a spectrometer or microscope. As compared to traditional laboratory-based spectroscopic and imaging technologies such as optical infrared, X-ray and electron microscopy; synchrotron radiation is much brighter, and more cohesive, with more polarization, and greater resolution (Miller and Dumas 2006). Conventional mid-IR beamlines can achieve a spatial resolution of approximately 20 μm, whereas synchrotron light is capable of attaining spatial resolution from 1-10 μm in mid-IR and up to 5 nm in soft X-ray imaging (Vijayan et al. 2015). Currently, there are 47 synchrotron facilities in operation worldwide (http://www.lightsources.org). A variety of beamlines are available for biological research at the Canadian Light Source located on the University of Saskatchewan campus (http://www.lightsource.ca).

Fourier Transformed Infrared spectroscopy is a physico-chemical analytical technique (Lahlali et al. 2015) and is very efficient for non-destructive analyses of biological samples

(Baker et al. 2014). In FTIR imaging, an infrared beamline is passed through a sample of interest; some portion of the radiation is absorbed and some is transmitted (Anonymous 2001). The spectrum produced is a result of the different functional groups and chemically different compounds in the sample. The spectra serve as fingerprints of the compound, and as no two fingerprints are similar, the FTIR spectrum is also different for different organic compounds. Therefore, an FTIR spectral analyses provides a unique method to study biopolymers in biological samples. An FTIR spectra can be divided into five zones (Taoutaou et al. 2012). The first zone is called the fingerprinting zone, ranging from 600-900 cm^{-1} wavelength. The second zone ranges from 900-1200 cm^{-1} and constitutes a spectrum resulting from the changes in polysaccharides and carbohydrates. The third zone lies between 1200-1500 cm^{-1} and is a mixed region with changes in proteins, fatty acids, nucleic acids (DNA and RNA) and phosphorous compounds. The fourth zone at 1500-1800 cm^{-1} characterizes the changes in amides and proteins (amide I, amide II, peptides) and phenols and polyphenols. The last region characterizes changes in fatty acids with a wavelength ranging between 2800 and 3200 cm^{-1}.

The FTIR spectral analyses is used in a number of studies focussing on plant host-pathogen interactions (Martin et al. 2005; Taoutaou et al. 2012), such as to differentiate fungal potato pathogens (Erukhimovitch et al. 2010). FTIR was used in various other biological studies (Miller and Dumas 2006). So far, there are only two reports on the use of FTIR spectroscopy to study FHB of wheat (Lahlali et al. 2015, 2016). Another study demonstrated differences between sound and fusarium damaged kernels using FTIR (Peiris et al. 2012; Clark et al. 2016). Imaging technologies have advanced the field of plant biology by making non-destructive analyses of plants organs and biological phenomena possible (Tanino et al. 2017). The non-destructive analyses of plant parts can be achieved by X-ray phase contrast imaging (PCI) and computed tomography (CT) from either conventional lab-based or synchrotron sources. Given that *F. graminearum* infection results in structural changes in wheat spike tissue, this pathosystem can be subjected to proof-of-concept experiments utilizing imaging and spectroscopic techniques.

CHAPTER 3

Evaluation of Fusarium head blight resistance genes *Fhb1*, *Fhb2*, and *Fhb5* introgressed into elite Canadian hard red spring wheats: Part I. Effect on disease severity and deoxynivalenol accumulation as affected by genetic background and epistatic interactions*

*The content of this Chapter is published as a full-length research article in 'BMC Plant Biology' journal (See Brar et al. 2019a).

3.1. Preface

In terms of resistance breeding, Fusarium head blight (FHB) is one of the most challenging trait to work with due to quantitative nature of resistance in wheat. Although approximately 250 QTL (many are co-incident) for FHB are mapped in common wheat, only seven are formally designated as single genes including Sumai 3 derived genes *Fhb1*, *Fhb2*, and *Fhb5*. Distinct behavior of these genes in different genetic backgrounds has been reported in literature and there is scarcity of studies showing effect of these genes in Canadian hard red spring wheat backgrounds. This Chapter presents results on the development of near-isogenic lines carrying all possible combinations of aforementioned three genes in two hard red spring wheat backgrounds and their effect on suppression of FHB and deoxynivalenol accumulation. The Chapter also investigated factors that affect the gene expression in the backgrounds.

3.2. Abstract

Fusarium head blight resistance genes, *Fhb1* (for Type-II resistance), *Fhb2* (Type-II), and *Fhb5* (Type-I plus some Type-II), which originate from Sumai 3, are among the most important that confer resistance in hexaploid wheat. Near-isogenic lines (NILs), in the CDC Alsask (susceptible; n= 32) and CDC Go (moderately susceptible; n= 38) backgrounds, carrying these genes in all possible combinations were developed solely using flanking microsatellite markers and evaluated for their response to FHB and deoxynivalenol (DON) accumulation in eight environments. Genotyping using 81,857 single nucleotide polymorphism (SNP) markers revealed polymorphism on all chromosomes and that the NILs carried <3% of alleles from the resistant donor. Significant improvement in field resistance (Type-I + Type-II) resulted only among the CDC Alsask NILs, not the CDC Go NILs. The phenotypic response of NILs carrying combinations of Sumai 3 derived genes suggested non-additive responses and *Fhb5* was as good

as *Fhb1* in conferring field resistance in both populations. In addition to *Fhb1*, *Fhb2*, and *Fhb5,* four to five resistance improving alleles in both populations were identified and three of five in CDC Go were contributed by the susceptible parent. The introgressed chromosome regions carried genes encoding disease resistance proteins, protein kinases, nucleotide-binding and leucine rich repeats' domains. Complex epistatic gene-gene interactions among marker loci (including *Fhb1*, *Fhb2*, *Fhb5*) explained >20% of the phenotypic variation in FHB measurements. Results verified that marker-assisted selection is possible for the introgression of exotic FHB resistance genes, however, the genetic background of the recipient line and epistatic interactions can have a strong influence on expression and penetrance of any given gene.

3.3. Introduction

Wheat (*Triticum* spp. L.) is one of the most important field crops worldwide as it serves as staple food for a large proportion of the global population. Wheat production is challenged by several constraints and Fusarium head blight is one of the major biotic limitations. There are several *Fusarium* spp. that cause head blight or scab; *Fusarium graimnearum* Schwabe (telomorph: *Gibberella zeae* Schw. [Petch]) is the main culprit in North America, and it is also hosted by maize (*Zea mays* L.) and barley (*Hordeum vulgare* L.) (McMullen et al. 2012; Gilbert and Haber 2013). Direct yield loss from the disease is due to shrivelled grain with lower test weight or even failure of seed formation. Loss in marketability from mycotoxins contamination is an even bigger concern from an international trade perspective. The accumulation of harmful mycotoxins, particularly deoxynivalenol (DON) and its acetylated forms (3-ADON and 15-ADON), may render the grain unsuitable for food or feed. The majority of wheat growing countries have defined certain threshold limits for the presence of DON in the grain to be able to export or import across international boundaries and many beverage and food industries have self-imposed even greater restrictions (McMullen et al. 2012).

An integrated approach for FHB management is imperative and genetic resistance is an integral part of such disease management approach. Resistance to FHB in wheat is inherited quantitatively and strongly influenced by the environment (Buerstmayr et al. 2009). Genetic studies in wheat have identified many useful loci for improvement in complex traits, such as FHB; unfortunately, many of them remain un- or under-utilized in plant breeding programs mainly because of the complex nature of resistance (Buerstmayr et al. 2009). In spite of a tremendous amount of FHB resistance breeding efforts, genetic gain has been moderate (Bai et al. 2018). Efficient introgression of QTL associated with FHB resistance into elite germplasm requires the use of linked genetic markers to facilitate marker-assisted selection (MAS);

however, the linkage phase between the marker(s) and the QTL cannot always be inferred among genetic backgrounds, unless strong linkage disequilibrium exists (Beavis 1998). Of more than 100 QTL identified for resistance to FHB, only seven have been formally designated as Mendelized genes: *Fhb1* derived from Sumai 3 (Cuthbert et al. 2006), *Fhb2* from Sumai 3 (Cuthbert et al. 2007), *Fhb3* from *Leymus racemosus* (Qi et al. 2008), *Fhb4* from Wangshuibai (Xue et al. 2010a), *Fhb5* from Wangshuibai and Sumai 3 (Xue et al. 2011), *Fhb6* from *Elymus tsukushiensis* (Cainong et al. 2015), and *Fhb7* from *Thinopyrum ponticum* (Guo et al. 2015). Based on host response, the expression of resistance is classified into five different types: Type-I (resistance to initial pathogen infection), Type-II (resistance to fungal spread in the spike), Type-III (resistance to toxin accumulation or the ability to degrade the mycotoxins), Type-IV (resistance to kernel infection), and Type-V (tolerance to yield loss) (Schroeder and Christensen 1963; Miller et al. 1985; Mesterhazy et al. 1999). Type-I and Type-II resistance are more widely exploited and Type-III resistance has gained importance as it is important to maintain grain end-use quality. All types of resistance are generally strongly correlated.

The discovery of promising QTLs is a preliminary step in a MAS program, but validation of such loci in multiple genetic backgrounds and environments is equally important (Bernardo 2008). The actual effect of the QTL, usually identified from bi-parental populations such as recombinant inbred lines or double haploid lines, is dependent on the alleles and allelic frequencies present at the locus, as well as epistatic interactions among QTL and other genes, which are usually over-estimated in the original mapping population (Beavis 1998). Near-isogenic lines (NILs) are advantageous for studying phenotypic effects attributable to a specific QTL or gene as the genetic background is fixed, which in turn maintains morphological and phenological traits of the plants that might influence the trait under study (Kaeppler et al. 1993). NILs are particularly attractive to breeders for traits that are introduced from exotic parents or wide crosses as they allow confirmation of allelic effects on traits of interest. Additionally, by fixing the genetic background, NILs serve as an ideal source for fine-mapping, gene expression profiling, and hypothesis-driven biological experimentation (Pumphrey et al. 2007).

Canadian wheat growers have witnessed several FHB epidemics in the last two decades, particularly in eastern Canada and the province of Manitoba in western Canada (Gilbert and Haber 2013; Gilbert et al. 2014). However, in last 10-15 years, FHB epidemics in Saskatchewan are not uncommon; attributable to the increasing proportion of the more aggressive 3-ADON chemotype in the *F. graminearum* population (Ward et al. 2008; Gilbert et al. 2014). These epidemics spurred research to improve genetic resistance and management options for FHB. The majority of the resistance genes currently available originate from Asian or Brazilian wheats;

however, breeders in North America are reluctant to use exotic sources in their programs due to linkage drag (for example, shattering and susceptibility of Sumai 3 to other pathogens). In an effort to introgress resistance into Canadian hard red spring wheat, the bread wheat breeding program at the Crop Development Centre (CDC) utilized 04GC0139 (pedigree: ND2710/RL4851//BW278; carrying *Fhb1*, *Fhb2*, and *Fhb5*), a derivative of Sumai 3, to cross with CDC wheat cultivars. The current project used NILs in CDC Alsask and CDC Go backgrounds to study the effects of these three major genes and their combinations: *Fhb1*, *Fhb2*, and *Fhb5*. The effects of introgressing *Fhb1* and *Fhb5* on disease resistance are reported in previously published studies from North America (McCartney et al. 2007; Pumphrey et al. 2007; Balut et al. 2013), Europe (Miedaner et al. 2006; Salameh et al. 2011), and China (Xue et al. 2010b). The majority of these studies used RILs/NILs from F_2 derived inbreds through enforced inbreeding or doubled haploid lines and only Salameh et al. (2011) and Xue et al. (2010b) used BC_2 or BC_3 derived NILs; thus, a greater proportion of the resistant donor alleles was expected in these studies, which influenced the overall phenotypic expression of the lines. Additionally, these studies utilized only microsatellite (SSR) markers spanning a large physical interval, unlike modern KASP/SNP markers associated with a single gene region. Microsatellite markers target more than one allele of the gene in the genome thus potentially enhancing the proportion of donor genome in the progenies derived (McCartney et al. 2004). Therefore, to precisely quantify the effect of major FHB resistance genes or QTL, it is imperative to reduce the proportion of other alleles as much as possible. At the same time, it is practically impossible (with repeated backcrossing or other classical breeding approaches) to introgress only genes of interest in any given genetic background, thus, one should account for the effect of other alleles and their interaction with genes of interest to influence phenotypic expression.

The current study presents the results of a marker-based introduction of Sumai 3-derived genes in Canadian hard red spring wheats and their effects on the disease (Part-I) and Chapter 4 entitled "**Evaluation of Fusarium head blight resistance genes *Fhb1*, *Fhb2*, and *Fhb5* introgressed into elite Canadian hard red spring wheats: Part II. Effect on agronomic and end-use quality traits and implications for breeding"** presents effects on agronomic and end-use quality. The specific objectives of the current study (Part-I) were: (i) to examine the phenotypic effect on FHB resistance from the introgression of Sumai 3-derived genes in multiple elite backgrounds with differential susceptibility, (ii) to determine the allelic proportion in two backgrounds, derived from the resistant donor parent, and (iii) to examine single marker-effect and marker-marker interactions for all polymorphic markers among NIL entries. Here, we report the effect of *Fhb1*, *Fhb2*, and *Fhb5* genes on FHB severity and DON accumulation in two hard

red spring wheat cultivars, one that was moderately susceptible (MS) and the other susceptible (S) to the disease. The genomic composition of the NILs was thoroughly analyzed for allelic effects and the proportions of alleles from each parent. The study essentially characterized the complexity of the trait through gene-gene interactions and identified loci other than *Fhb1*, *Fhb2*, and *Fhb5* that contribute to improved FHB resistance.

3.4. Materials and methods

3.4.1. NIL development using marker-assisted background selection

F_4 populations were developed from two backcross populations CDC Go*4/04GC0139 and CDC Alsask*4/04GC0139. Line 04GC0139 (*Triticum aestivum* L.) was derived from Sumai 3 and has a high level of resistance to FHB, kindly provided by Dr. Julian Thomas (retired) of the Cereal Research Centre, Agriculture and Agri-Food Canada, Winnipeg, Manitoba. Line 04GC0139 has ND2710 and BW278 (pedigree: AC Domain*2/Sumai 3) in its pedigree which are both derivatives of Suami3. Line RL4851 has Grandin (also in pedigree of CDC Go) and AC Domain in its pedigree. The line 04GC0139 carries three well-characterized genes for resistance to FHB on chromosomes 3BS (*Fhb1)*, 6BS (*Fhb2)* and 5AS (*Fhb5)* (G.S. Brar, unpublished data). The hard red spring wheat cultivar CDC Go (pedigree: Grandin/SD3055) is moderately susceptible (MS) to FHB, and CDC Alsask (pedigree: AC Elsa/AC Cora) is susceptible (S) (Anonymous 2015a). The NILs were developed by backcrossing F_1 plants to the recurrent parents (CDC Go or CDC Alsask) and the F_1 at each BC cycle was screened with microsatellite markers flanking *Fhb1*, *Fhb2* and *Fhb5*. Approximately 2,100 BC_2F_1 and 1,300 BC_3F_1 hybrid seeds were generated by hand crossing and 90% of the seeds were germinated and haplotyped. During the selfing process, 123 BC_3F_1-derived families were advanced and approximately 7,000 F_2 seedlings were grown, which were used to generate seed for F_3 plots grown in the field in 2009. Two hundred spikes were harvested from each plot and haplotyped in the F_4 generation. A total of 70 lines (38 from CDC Go and 32 from CDC Alsask) representing all eight possible combinations of FHB genes were recovered.

3.4.2. Microsatellite and SNP genotyping

Genomic DNA was extracted from grain and/or leaf tissue with the DNeasy 96 Plant Kit (Qiagen, Mississauga, ON). Quantification of DNA was done by fluorometry using Hoechst 33258 stain. During population development, a total of seven simple sequence repeats markers associated with *Fhb1*, *Fhb2*, or *Fhb5* were screened on genomic DNA. Markers *umn10* for *Fhb1* on chromosome *3BS* (Liu et al. 2008), *gwm133* and *gwm644* for *Fhb2* on chromosome 6BS (Cuthbert et al. 2007), and *gwm304*, *barc117*, *wmc705* and *gwm293* for *Fhb5* on chromosome

5AS were used (Xue et al. 2011). Each SSR primer pair was modified by addition of the M13 sequence to the 5' end of the forward primer during synthesis. Fluorescent dye (either HEX, FAM or NED) was used to label the universal M13 primer. The PCR reactions consisted of 1.5 µl 10× PCR buffer, 1.5 (or 0) mM of $MgCl_2$, 0.2 mM of each dNTP, 0.04 µM of M13 sequence-modified forward primer, 0.16 µM of reverse primer, 0.152 µM of universal dye-labelled M13 primer, 1 U of *Taq* DNA polymerase, and 50 ng of genomic DNA. The total PCR volume was 15 µL. Temperature cycling included 94°C for 30 s, 56°C (or 62°C) for 50 s, 72°C for 55 s, 94°C for 30 s, 54°C (or 60°C) for 50 s, 72°C for 55 s, 94°C for 30 s, 52°C (or 58°C) for 50 s, 72°C for 55 s, 94°C for 30 s, 50°C (or 56°C) for 50 s, 72°C for 55 s, then 25 cycles of 94°C for 30 s, 51°C for 50 s, 72°C for 55 s, then 1 cycle of 72°C for 10 min. Primers were first assessed for polymorphism on 2% (*w/v*) agarose gel stained with 0.5 µg/ml ethidium bromide, then further tested for polymorphism by capillary electrophoresis (CE) using an AB13100 Genetic Analyzer (Applied Biosystems). For CE, 1 µL of diluted PCR product (diluted 1/5, 1/10 or 1/20 in deionized water depending on band intensity visualized on agarose gel) was combined with 9.0 µL HiDi formamide (ABI, Foster City, CA, USA) and 0.09 µL of 500 ROX size standard. Samples were run on a 36 cm capillary array, processed with Applied Biosystems Data Collection Software version 2.0, and genotyped using GeneMapper version 3.0. The presence of *Fhb1* in NILs was also confirmed with the KASP assay (Liu et al. 2008).

The NILs were genotyped with seven microsatellite markers while in the developmental phase in 2008-2011. To confirm the genotype of the NILs, some additional microsatellite markers (from fine-mapping studies reporting a narrow QTL interval) were used in 2017-2018 i.e. *gwm493*, *gwm533*, and functional marker for pore-forming toxin (PFT) protein for *Fhb1* (Cuthbert et al. 2006; Rawat et al. 2016), *Fhb2-CAPS3* for *Fhb2* (Zhao et al. 2018), *barc180* and *barc186* for *Fhb5* (Buerstmayr et al. 2017). Additionally, the NILs were genotyped along with the parents using the wheat 90,000 iSelect assay comprised of 81,587 SNPs (Wang et al. 2014) to better understand the genomic composition and haplotype structure of the NILs. The SNP alleles were called using GenomeStudio (Illumina Inc., San Diego, CA, USA) and filtered based on polymorphisms between parents.

3.4.3. Greenhouse FHB evaluations

The 38 CDC Go and 32 CDC Alsask NILs, the parents and a number of check cultivars [CDC Teal as susceptible check, AC Barrie as intermediate (I)/moderately resistant (MR) check, and ND2710 as resistant (R) check] were assessed for FHB symptoms in 2010 in a greenhouse (GH) equipped with incandescent lamps, 16 h photoperiod and 22/16°C day/night temperatures. Two isolates of *F. graminearum*, M09-07-1, a 3-ADON chemotype (NRRL 52068) and M1-07-2, a

15-ADON chemotype (NRRL 47847), were used for inoculations (Gilbert et al. 2014). At 50% anthesis, a main stem spike (two florets leaving lower two-third of the spike) on each plant was inoculated with a 10 µl macroconidial spore suspension (50,000 spores/ml) containing 0.02% Tween 20. The inoculations were performed as described in Cuthbert et al. (2006). A total of three plants per replication were inoculated and there were three replications in total. The FHB severity was rated as the percentage of infected spikelets per spike at 7 (GH7), 14 (GH14) and 21 days (GH21) post inoculation. Area under disease progress curve (GH_AUDPC), used as a measure of FHB severity over time, was calculated according to Buerstmayr et al. (2000).

3.4.4. Field FHB evaluations

The same NILs, parents and check cultivars evaluated in the greenhouse were also assessed in the field nursery at Carman, MB from 2010-2013 and 2016, Saskatoon, SK in 2016, and at Morden, MB in 2015. In 2010, the CDC Alsask population was not evaluated in the field because the seed under multiplication in the greenhouse was not ready for field planting. The field trial was set up as a randomized complete block design with two replicates in Carman and four replicates in Morden and Saskatoon. Plots at Morden and Carman consisted of single 1.5 m and 1 m rows, respectively, and in the Saskatoon nursery in hills. Sowing density was approximately 80 seeds per row and 30 seeds per hill. At Carman, every plot in the nursery was artificially inoculated with a suspension of *F. graminearum* macro-conidia prepared with the isolates M9-07-1 (3-ADON), M7-07-1 (3-ADON), M1-07-1 (15-ADON) and M3-07-2 (15-ADON). The isolates used were originally provided by Dr. Jeannie Gilbert at the CRC-AAFC. Isolates were cultured in Spezieller Nährstoffarmer Agar (SNA) for seven days and then incubated in Carboxymethyl Cellulose (CMC) media for another seven to ten days. The number of spores was counted to calculate their concentration. Prior to field application, the suspension of the four isolates was mixed in equal proportions (based on macro-conidia concentration) to provide a total concentration of 50,000 macro-conidia spores/ml. The field application was achieved using a CO_2 backpack sprayer and directed to the wheat spikes at flowering (anthesis) stage. A second application was performed to the same rows three days later. After each inoculation, plots were mist irrigated overnight. Visual assessments of disease incidence (% of infected spikes in the plot) and severity (% of spikelets infected on the infected spikes) were made on each plot 18-21 days after the first inoculation. Fusarium head blight index for each plot was calculated as follows: (disease incidence x disease severity)/100. At Morden, MB and Saskatoon, SK, irrigated nurseries were inoculated with air-dried corn spawn (colonized by *F. graminearum*) at 50% anthesis. Each plot was assessed using an FHB index (%incidence x %severity/ 100) (FLD_IND) based on disease incidence (%) (FLD_INC) and severity (%)

(FLD_SEV) at 21 to 23 dpi. Cultivars CDC Teal (S), AC Barrie (moderately resistant, MR), and ND2710 (resistant, R) were included as checks in Morden and Saskatoon. Cultivars AC Vista, and CDC Teal were used as S check, AC Cora as I check, 5602HR as MR, and FHB37 as R check in Carman nursery. Up to 50 spikes of each NIL were harvested by hand and retained for DON quantification (FLD_DON).

3.4.5. DON quantification

The spikes of each NIL were harvested from two replicates at the fully ripe stage (BBCH 92, Lancashire et al. 1991) and dried to minimal water content. Approximately 50-100 g samples of each NIL were ground to a fine powder with a laboratory mill and stored at -20°C until further processing. Analysis of DON was carried out using ELISA based assays (Sinha et al. 1995) and a Neogen commercial kit. Measurements were performed in two replications. Detailed information on the Neogen ELISA assay are found in Appendix A.

3.4.6. Physical mapping and functional annotation

All SNP markers from the wheat 90K assay were physically positioned on the Chinese Spring wheat reference genome sequence. The SNP-bearing sequences were probed to the entire bread wheat NRGene genome assembly RefSeq ver. 1.0 (International Wheat Genome Sequencing Consortium, https://wheat-urgi.versailles.inra.fr/Seq-Repository/Assemblies) using an *in-house* BLAST portal. The best hits, based on sequence similarity and cumulative alignment length percentage of matches, were considered. For annotation, the wheat genome scaffolds carrying the marker were retrieved from the BLAST searches and used to find genes expressed on the scaffolds using POTAGE (PopSeq Ordered *Triticum aestivum* Gene Expression) (Suchecki et al. 2017). POTAGE integrates map location with gene expression, infers functional annotation and visualizes these data through a web browser interface. The map location (implemented in POTAGE) were based on the wheat POPSEQ map of the 90 double haploid individuals of the synthetic W7984 X Opata M85 population, where SNP markers are anchored to contigs in linear order (Chapman et al. 2015).

3.4.7. SNP data and marker-marker epistatic interaction analyses

For haplotype analyses and to assign each NIL entry to a QTL class, SNP markers tightly linked to SSR markers or mapped to *Fhb1*, *Fhb2*, and *Fhb5* regions were considered (Buerstmayr et al. 2017; Zhao et al. 2018; Ron Knox, unpublished data). The SNP markers flanking the *Fhb1* region of Carberry were provided by Dr. Ron Knox (AAFC, Swift Current) and were also mapped in ND2710 by Zhao et al. (2018). The introgressed haplotypes from the resistant donor parent were visualized using Graphical Genotypes software ver. 2.0 (Van Berloo 2008). To analyze the phenotypic data as influenced by all polymorphic markers, genotypic and phenotypic

data were used to test for epistatic interactions. Epistatic interactions between markers with significant main effects (*Fhb1*, *Fhb2*, and *Fhb5*) were tested as well as all other markers regardless of significance. A linear regression model was used to calculate *P*-values for pairwise marker interactions using an *in-house* designed script in the R environment (the R Core Team 2018). A false discovery rate of 0.05 was used as a threshold for significant interactions. Epistatic interactions were analyzed according to Xu and Jia (2007) and modeled as follows:

$$y = 1\mu + Z_l\gamma_l + (Z_l \times Z_{l'})\gamma_{ll'} + e$$

Where: y is the n × 1 vector for phenotypic observation, μ is the population mean, $Z_l$is a vector $(Z_{1l}\ldots Z_{nl})^T$, for the genotype indicators of locus l, Z_{il} takes one of two values (-1, +1) depending on which parental allele was passed on to line i, for locus l, γ_l is the additive (main) effect of locus l, $\gamma_{ll'}$ is the epistatic effect between loci l and l', and e is the residual error vector. From each chromosome, one marker from each group of redundant/co-segregating markers was chosen for the epistatic interaction analyses. Any marker-marker interaction for a given phenotype was declared significant at $P = 0.001$.

3.4.8. Statistical and phenotypic data analyses

The phenotypic data collected from field and greenhouse evaluations was subjected to correlation and analysis of variance (ANOVA). Before conducting ANOVA, assumptions of independence, normal distribution and homogeneity of residuals for all class variables were verified using Shapiro-Wilk and Levene's tests implemented in procedure UNIVARIATE in SAS (Statistical Analytical Software) ver. 9.4 (SAS Institute, Inc., Cary, NC). Heterogeneous variances, if any, were modeled using the 'repeated/group=effect' statement in procedure MIXED (Littell et al. 2006). Variance component estimates and corresponding *F*-values were calculated using the procedure MIXED in SAS ver. 9.4 with the 'ddfm= kenwardroger' option to approximate degrees of freedom. Mean separation was conducted using the least significant difference (LSD) test (Fisher's least significant difference). All tests used a nominal alpha level of 0.05. Pearson's correlation coefficients among various parameters were calculated using procedure CORR in SAS. Associations among environments, genotypes, and the genotype by environment interaction were analyzed and visualized using biplot analyses (Yan and Tinker 2006) in the R environment using the GGEBiplotGUI package (Frutos et al. 2014; the R Core Team, 2018). For biplot analyses, the following settings were used: singular value portioning, environment-metric preserving; and genotype by environment scaling, according to the standard deviation; centered by environment (G+G*E). Broad-sense heritability (H^2) was estimated as described in Brar et al. (2018a).

3.5. Results

3.5.1. Marker analyses

Molecular characterization of the NILs in both populations using gene-specific microsatellite or SNP markers assisted in their classification into individual gene and gene combination classes. Additional genotypic data were generated with the 90K iSelect wheat assay (Wang et al. 2014) to determine the genomic composition and the haplotype structure of the NILs compared to their recurrent parents. The SNP markers were assigned to chromosomes using the reference sequence assembly of Chinese Spring RefSeq ver. 1 (International Wheat Genome Sequencing Consortium, https://wheat-urgi.versailles.inra.fr/Seq-Repository/Assemblies). Polymorphisms among NILs were present on all 21 chromosomes in both NIL populations (Fig. 3.1; Appendices B – D). A total of 10,535 SNPs were polymorphic among parents in the CDC Alsask population and 8,686 SNPs in the CDC Go population; however, only 3,667 and 1,454 were polymorphic among the NILs (Fig. 3.1). Of the polymorphic SNPs among the NILs, most of the markers were located on Chromosomes 3B (452), 5A (444), 5B (341), and 6B (510) in CDC Alsask, and on 1A (127), 2A (167), 3B (83), 5A (226), and 7A (188) in CDC Go. The chromosomes 3B, 5A, 6B carrying *Fhb1*, *Fhb5*, and *Fhb2* were anchored with 38% of the total polymorphic SNPs in CDC Alsask and 26% in CDC Go.

With the help of previously published studies or the use of a consensus map and physical location of the SNPs, the markers on Chromosomes 3BS, 5AS, and 6BS from the 90K assay were identified and used to define haplotype segments carrying *Fhb1*, *Fhb2*, and *Fhb5* in both populations (Fig. 3.2) (Macferri et al. 2015; Buerstmayr et al. 2017; Zhao et al. 2018; Ron Knox, unpublished data). The classification of the NILs into gene classes using microsatellite markers was in agreement with SNP markers for all three genes in both populations with the exception of *Fhb1* in two NIL entries (Go2 and Go6) in the CDC Go background. The two inconsistent NIL entries for presence/absence of *Fhb1* were classified using the functional gene-specific, pore-forming toxin (PFT) protein marker (Rawat et al. 2016). The CDC Alsask NILs carried more alleles (higher recombination rate, a function of genetic background) from the donor parent as compared to the CDC Go NILs (Fig. 3.2; Appendices B - D). The genomes of the CDC Alsask NILs carried up to 2.7% of the resistant donor's alleles and the CDC Go NILs 0.9% (Appendices B - C). On Chromosomes 3B (carrying *Fhb1*), 5A (carrying *Fhb5*), and 6B (carrying *Fhb2*), the CDC Alsask NILs had up to 9.9, 11.6, and 12.6% of the resistant donor parent alleles, respectively, while the CDC Go NILs had 2.2, 6.7, and 1.7%.

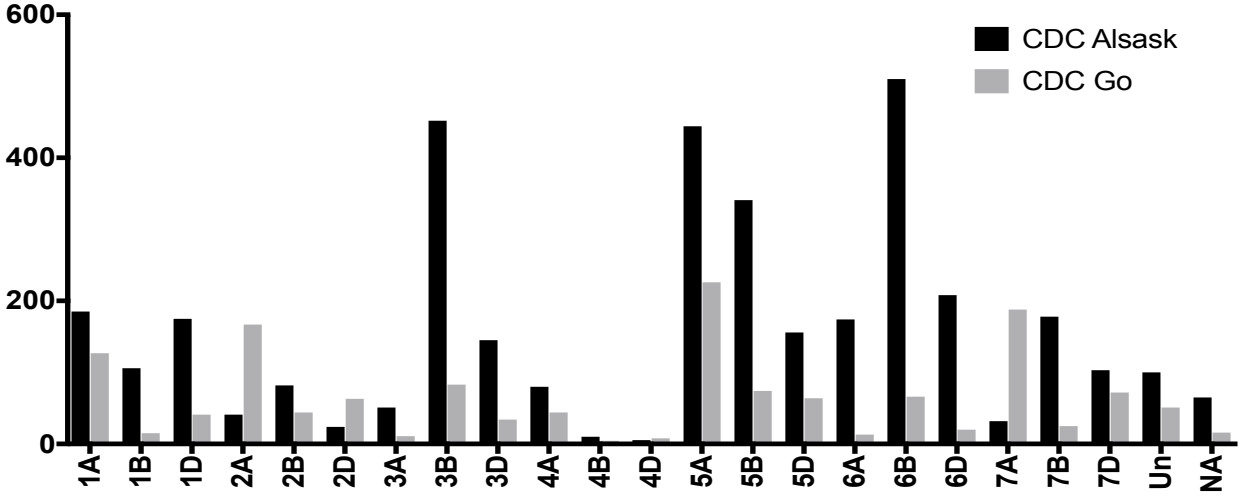

Figure 3.1. Number of polymorphic (among near-isogenic lines and recurrent parents only) single nucleotide polymorphism (SNP) markers in CDC Alsask and CDC Go near-isogenic lines segregating for *Fhb1* (3B), *Fhb2* (6B), and *Fhb5* (5A).

3.5.2. FHB evaluations and heritability estimates

In all environments, FHB inoculations were successful and there was sufficient disease pressure in all environments to discriminate NIL entries as indicated by longer environmental vectors in biplots which were proportional to the standard deviation in the phenotypic data (Fig. 3.3). Also, there was positive and significant correlations ($P = 0.05$) among most of the environments in both CDC Go and CDC Alsask populations, indicated by acute angles between environmental vectors. Two axes of the biplots explained ~56% of the phenotypic variation in both populations. For GH evaluations, *F*-values were significant for variation among gene classes in both NIL populations for GH14, GH21, and GH_AUDPC (Table 3.1). The *F*-values for entry nested within gene class were significant for GH14, GH21, and GH_AUDPC in the CDC Go population, but only for GH_AUDPC in the CDC Alsask population. The two *F. graminearum* chemotypes differed for GH14 and GH_AUDPC in both populations, whereas the interaction of chemotype by gene was significant only for GH_AUDPC in the CDC Alsask population. For field evaluations, *F*-values were significant only for gene classes for all FHB parameters in both populations. Insignificant *F*-values for entry nested within gene class for INC, SEV, IND, and DON indicated that the NIL entries within any given gene class behaved similarly. Broad-sense heritability (H^2) estimates were high for GH14, GH21, GH_AUDPC, moderate for INC, SEV, IND and weak for DON. In both GH and field evaluations, the random effect of environment (site-year) was significant ($P = 0.05$; data not presented).

In the CDC Alsask population, for GH14, NILs carrying *Fhb1*, *Fhb5*, *Fhb2*+*Fhb5* and *Fhb1*+*Fhb2*+*Fhb5* reduced FHB severity (SEV) as compared to the recurrent parent and the

susceptible checks (Table 3.2). Other genes or gene combinations tended to lower the disease as compared to the recurrent parent and the susceptible checks, but differences were not statistically significant. For GH21 and GH_AUDPC, all genes and their combinations reduced disease compared to the recurrent parent and the susceptible check. For the CDC Go population, except for *Fhb2*, all other genes or their combinations reduced disease severity in GH14. For GH21, only NILs carrying all three genes reduced FHB severity and for GH_AUDPC, all genes classes except *Fhb1* and *Fhb2* had lower disease severity than the recurrent parent or the susceptible check. Pyramiding *Fhb1+Fhb2+Fhb5* in the CDC Alsask background reduced severity (relative to the recurrent parent) by 37% for GH14, 27% for GH21, and 39% for GH_AUDPC, and in the CDC Go background by 62, 33, and 49%, respectively. Although NILs carrying all three genes performed better than the intermediate/moderately resistant (MR) check, i.e. AC Barrie, the improvement was not comparable to the resistant check or the resistant donor parent. It is important to mention that the NILs that did not carry *Fhb1*, *Fhb2*, or *Fhb5* also reduced disease by 1-13% in both populations, and the combination of any two of these genes in the CDC Alsask population did not improve resistance as compared to NILs carrying the genes singly, which indicated significant gene interactions. The 3-ADON chemotype resulted in higher FHB severity, for GH14 and GH_AUDPC, as compared to the 15-ADON chemotype in both populations (Fig. 3.4).

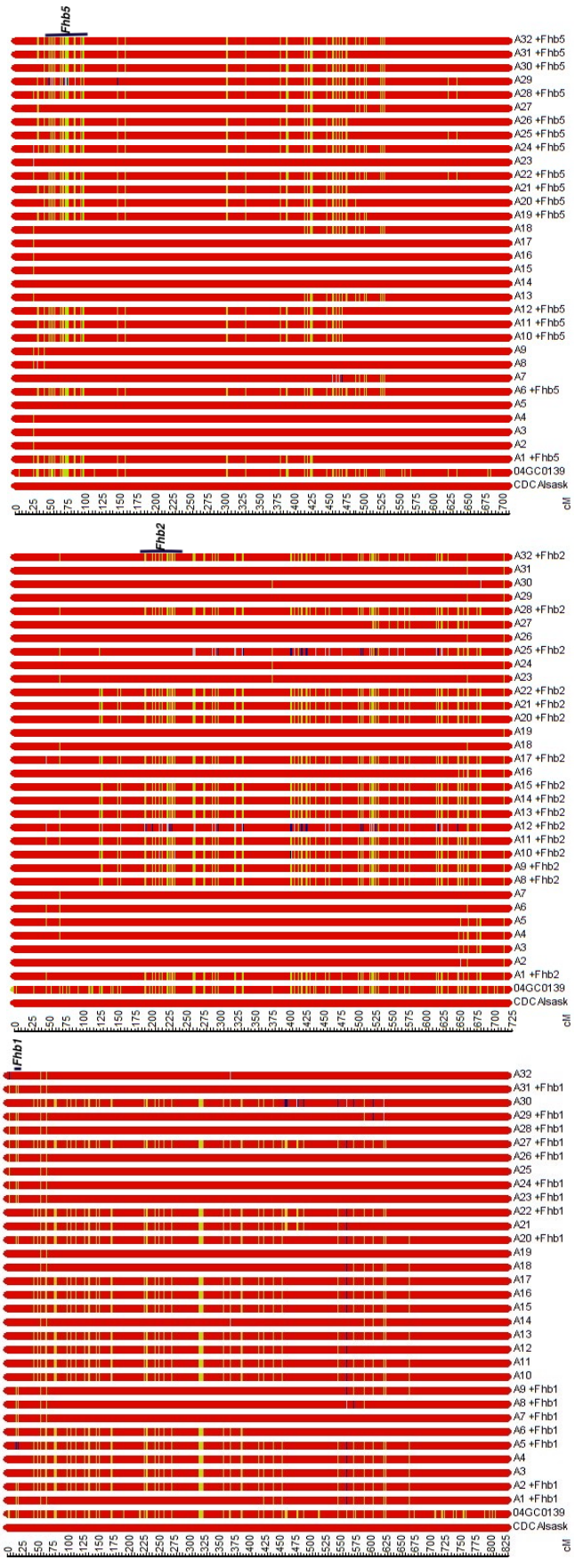
Fhb5
A32 +Fhb5
A31 +Fhb5
A30 +Fhb5
A29
A28 +Fhb5
A27
A26 +Fhb5
A25 +Fhb5
A24 +Fhb5
A23
A22 +Fhb5
A21 +Fhb5
A20 +Fhb5
A19 +Fhb5
A18
A17
A16
A15
A14
A13
A12 +Fhb5
A11 +Fhb5
A10 +Fhb5
A9
A8
A7
A6 +Fhb5
A5
A4
A3
A2
A1 +Fhb5
04GC0139
CDC Alsask
0 25 50 75 100 125 150 175 200 225 250 275 300 325 350 375 400 425 450 475 500 525 550 575 600 625 650 675 700
cM
Fhb2
A32 +Fhb2
A31
A30
A29
A28 +Fhb2
A27
A26
A25 +Fhb2
A24
A23
A22 +Fhb2
A21 +Fhb2
A20 +Fhb2
A19
A18
A17 +Fhb2
A16
A15 +Fhb2
A14 +Fhb2
A13 +Fhb2
A12 +Fhb2
A11 +Fhb2
A10 +Fhb2
A9 +Fhb2
A8 +Fhb2
A7
A6
A5
A4
A3
A2
A1 +Fhb2
04GC0139
CDC Alsask
0 25 50 75 100 125 150 175 200 225 250 275 300 325 350 375 400 425 450 475 500 525 550 575 600 625 650 675 700 725
cM
Fhb1
A32
A31 +Fhb1
A30
A29 +Fhb1
A28 +Fhb1
A27 +Fhb1
A26 +Fhb1
A25
A24 +Fhb1
A23 +Fhb1
A22 +Fhb1
A21
A20 +Fhb1
A19
A18
A17
A16
A15
A14
A13
A12
A11
A10
A9 +Fhb1
A8 +Fhb1
A7 +Fhb1
A6 +Fhb1
A5 +Fhb1
A4
A3
A2 +Fhb1
A1 +Fhb1
04GC0139
CDC Alsask
0 25 50 75 100 125 150 175 200 225 250 275 300 325 350 375 400 425 450 475 500 525 550 575 600 625 650 675 700 725 750 775 800 825
cM

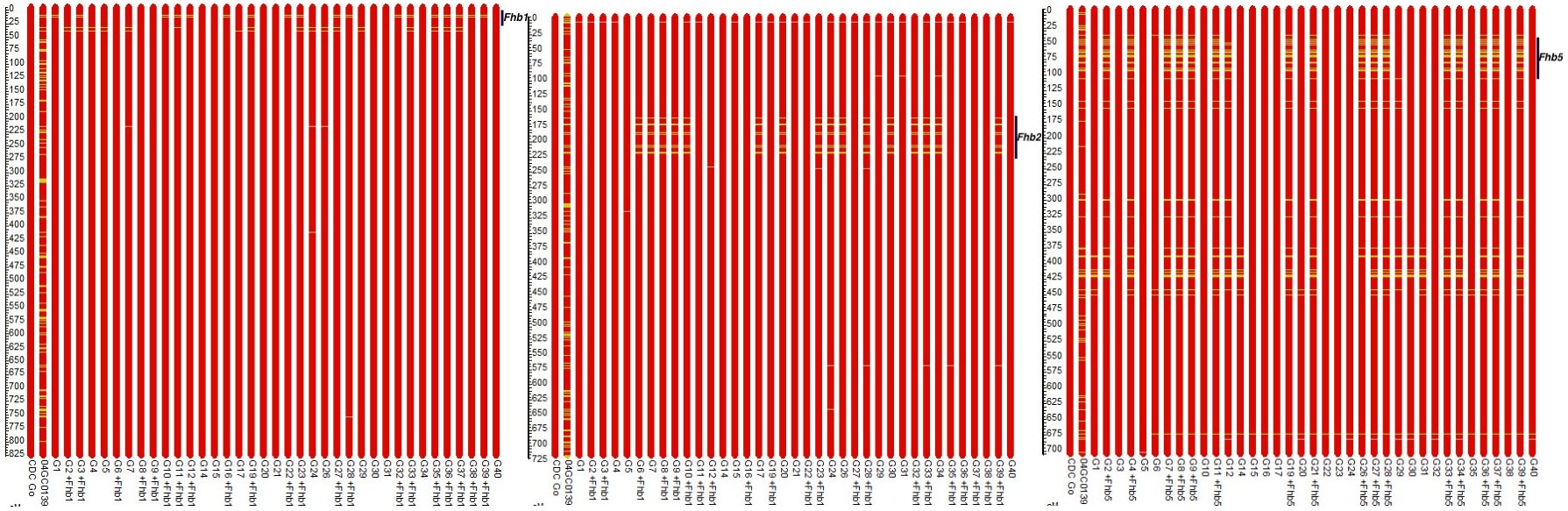

Figure 3.2. Graphical presentation of physical position of introgressed segments on chromosomes 3B (carrying *Fhb1*), 6B (carrying *Fhb2*), 5A (carrying *Fhb5*) and other chromosomes from 04GC0139 (resistance donor parent, yellow segments) into CDC Alsask (upper panel) and CDC Go (lower panel) (red segments) near-isogenic lines. The scale bar on left hand side indicates physical position (Mb) and the black bar on the right indicates haplotype segment carrying *Fhb1*, *Fhb2* or *Fhb5* gene. Each bar represents a genotype. The grey and blue segments indicate unknown and heterozygous alleles, respectively.

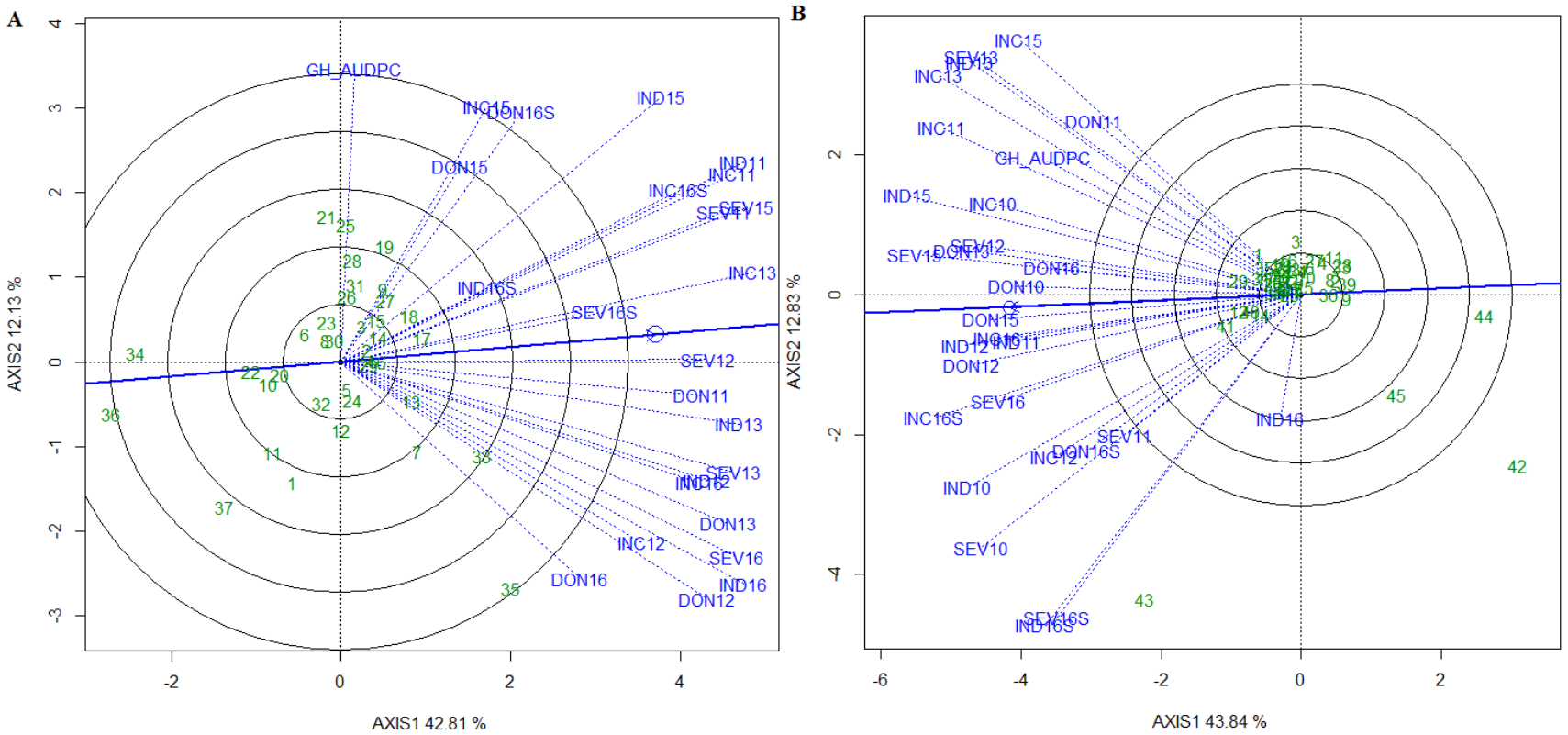

Figure 3.3. Genotype and genotype by environment (GGE) interaction plot showing the relationship among genotypes, environments and their interaction for: (A) CDC Alsask, and (B) CDC Go near-isogenic lines (NILs). Numbers in the green indicate NIL entries and vectors (dotted blue lines) are unique to given environment (blue labels for vectors). The solid blue line passing through the origin of the plot is the 'Average Environment Axis' indicating the most ideal and discriminating environment. The axes of the plot indicate standard deviation for phenotype (proportional to length of environment vector). The phenotypic variation explained by both axes is indicated next to the axes labels.

In the field evaluation of the CDC Alsask population, only gene combinations of *Fhb2+Fhb5* and *Fhb1+Fhb2+Fhb5* reduced FHB incidence and all three genes or their combinations reduced severity and FHB index compared to the recurrent parent (Table 3.3). The DON toxin was reduced only by *Fhb1+Fhb5*, *Fhb2+Fhb5* and *Fhb1+Fhb2+Fhb5*. For CDC Go, only the combination of all three genes reduced incidence and index, whereas all other gene classes were comparable to CDC Go. The DON accumulation was reduced by *Fhb5* and combinations of *Fbh5* with *Fhb1* and *Fhb2*, as did *Fhb1+Fhb2+Fhb5*. The combination of these three genes reduced FLD_INC, FLD_SEV, FLD_IND, and FLD_DON by 9, 32, 37, and 49% in the CDC Alsask background, and by 14, 20, 26, 40% in the CDC Go background, respectively.

Table 3.1. Analysis of variance (*F*-values) for near-isogenic lines (NILs) in CDC Go and CDC Alsask backgrounds, carrying all combinations of three Fusarium head blight (FHB) resistance genes: *Fhb1*, *Fhb2*, and *Fhb5*. Fixed effects of FHB resistance genes and entry (nested within gene) are provided for FHB severity assessed in the greenhouse at 14 days post inoculation (GH14), 21 days post inoculation (GH21), area under disease progress curve (GH_AUDPC), field incidence (FLD_INC), field severity (FLD_SEV), field FHB index (FLD_IND), deoxynivalenol (FLD_DON) accumulation, and broad-sense heritability (H^2). For greenhouse data, the effect of chemotype (3ADON or 15ADON), and chemotype by gene interaction is also presented.

Effect	df[a]	GH14	GH21	GH_AUDPC	FLD_INC	FLD_SEV	FLD_IND	FLD_DON
				CDC Alsask				
Gene (G)	12	82.47***	364.28*	178.70***	9.60***	16.82***	13.25***	5.20***
Gene (entry)	29	2.29^{ns}	3.42^{ns}	3.90***	1.86^{ns}	1.21^{ns}	0.98^{ns}	1.04^{ns}
Chemotype (C)	1	11.38**	1.41^{ns}	19.80***	-	-	-	-
C*G	12	0.99^{ns}	1.01^{ns}	2.17*	-	-	-	-
H^2 (%)	-	87.5	92.4	90.6	77.3	52.3	59.6	21.4
				CDC Go				
Gene (G)	12	19.71***	25.19***	25.60***	11.47***	9.74***	10.92***	7.39***
Gene (entry)	30	2.03**	1.65*	2.04**	1.07^{ns}	1.03^{ns}	0.95^{ns}	1.13^{ns}
Chemotype (C)	1	8.03*	3.02^{ns}	7.38*	-	-	-	-
C*G	12	0.99^{ns}	1.15^{ns}	1.12^{ns}	-	-	-	-
H^2 (%)	-	80.9	90.4	86.3	58.0	56.3	45.0	15.4

Note: *, **, ***: significant at $P<0.05$, $P<0.001$, $P<0.0001$, respectively; ns – not significant.
[a]Degree of freedom.

Table 3.2. Means and standard errors for FHB severity in the greenhouse at 14 days post inoculation (GH14), 21 days post inoculation (GH21), and area under disease progress curve (GH_AUDPC) in gene classes and check lines for CDC Alsask and CDC Go near-isogenic lines. Means within each column for each population followed by the same letter are not statistically significantly different according to Fisher's least significant difference (LSD) at $P = 0.05$.

Gene/genotype	GH14 (%)			GH21 (%)			GH_AUDPC		
	Mean[a]	SEM[b]	PDR[c]	Mean	SEM	PDR	Mean	SEM	PDR
CDC Alsask									
CDC Teal (susceptible check)	72.7 a	2.3	-	98.6 a	1.1	-	977.3 a	26.9	-
CDC Alsask (recurrent parent)	59.1 bc	1.8	-	97.2 a	1.5	-	862.0 b	21.6	-
AC Barrie (moderately resistant/intermediate check)	49.1 d-g	3.3	-	83.3 b	2.0	-	676.3 de	32.1	-
ND2710 (resistant check)	7.4 i	1.6	-	15.4 d	4.1	-	124.2 g	24.1	-
04GC0139 (resistance donor parent)	6.1 i	1.4	89.7	7.6 d	1.3	92.2	87.9 g	14.7	89.8
Null (n=4)	55.3 bcd	1.6	6.4	91.3 ab	1.9	6.1	749.3 c	18.1	13.1
Fhb1 (n= 6)	42.2 gh	2.0	28.6	82.4 b	2.5	15.2	607.2 ef	22.8	29.6
Fhb2 (n= 4)	47.6 c-g	2.0	19.5	88.0 b	2.5	9.5	673.3 d	22.1	21.9
Fhb5 (n= 2)	44.8 e-h	3.0	24.2	80.1 bc	3.9	17.6	613.9 def	33.4	28.8
Fhb1+Fhb2 (n= 2)	48.4 b-h	4.5	18.1	86.6 bc	4.1	10.9	685.5 cde	50.1	20.5
Fhb1+Fhb5 (n= 4)	50.0 b-e	2.4	15.4	82.1 bc	2.0	15.5	666.9 de	22.9	22.6
Fhb2+Fhb5 (n= 6)	47.2 d-f	1.4	20.1	81.1 bc	1.7	16.6	640.9 de	14.1	25.6
Fhb1+Fhb2+Fhb5 (n= 4)	37.0 h	3.5	37.4	70.9 c	4.7	27.1	529.8 f	39.2	38.5
CDC Go									
CDC Teal (susceptible check)	72.7 a	7.1	-	98.7 a-d	7.2	-	977.6 a	68.9	-
CDC Go (recurrent parent)	78.0 a	7.1	-	100.0 a-d	7.2	-	917.8 ab	68.9	-
AC Barrie (moderately resistant/intermediate check)	49.1 bc	7.1	-	83.3 bcd	7.2	-	676.6 cd	68.9	-
ND2710 (resistant check)	7.4 e	7.1	-	15.5 f	7.1	-	124.5 f	68.9	-
04GC0139 (resistance donor parent)	5.9 e	7.1	92.4	7.9 f	7.1	92.1	87.6 f	68.9	90.5
Null (n=7)	67.9 a	2.9	12.9	99.0 a	2.7	1.0	844.5 ab	27.5	8.0
Fhb1 (n= 6)	63.4 b	3.1	18.7	95.8 abc	3.0	4.2	805.6 bc	29.5	11.1
Fhb2 (n= 4)	68.2 a	3.7	12.6	97.5 ab	3.6	2.5	848.6 ab	35.4	7.5
Fhb5 (n= 2)	53.1 bc	5.1	31.9	83.2 d	5.1	16.8	686.6 d	49.2	25.2
Fhb1+Fhb2 (n= 4)	45.8 c	3.7	41.3	88.6 bcd	3.6	11.4	653.8 d	35.5	28.8
Fhb1+Fhb5 (n= 6)	47.2 c	3.1	39.5	87.0 d	3.0	13.0	657.4 d	29.5	28.4
Fhb2+Fhb5 (n= 4)	52.4 c	3.8	32.8	87.1 cd	3.7	12.9	693.9 d	36.0	24.4
Fhb1+Fhb2+Fhb5 (n= 5)	29.8 d	3.4	61.8	67.1 e	3.2	32.9	464.8 e	32.0	49.4

[a]Least squares mean; [b]Standard error of the mean; [c]Percent disease reduction.

Table 3.3. Means and standard errors for field incidence (FLD_INC), field severity (FLD_SEV), field FHB index (FLD_IND), and deoxynivalenol (FLD_DON) accumulation in gene classes and check lines for CDC Alsask and CDC Go near-isogenic lines. The data is combined over six environments. Means within each column for each population followed by same letter are not statistically significantly different according to Fisher's least significant difference (LSD) at $P = 0.05$.

Gene/genotype	FLD_INC (%)			FLD_SEV (%)			FLD_IND (%)			FLD_DON (ppm)		
	Mean[a]	SEM[b]	PDR[c]	Mean	SEM	PDR	Mean	SEM	PDR	Mean	SEM	PDR
CDC Alsask												
CDC Teal (susceptible check)	78.7 a	4.3	-	61.7 a	8.4	-	51.1 a	6.9	-	43.6 a	8.7	-
CDC Alsask (recurrent parent)	76.0 ab	4.4	-	62.7 a	8.4	-	48.8 a	7.0	-	34.8 ab	8.7	-
AC Barrie (moderately resistant/intermediate check)	58.6 d	4.7	-	37.1 f	8.4	-	22.1 d	7.0	-	18.4 cd	6.4	-
ND2710 (resistant check)	50.2 de	4.7	-	18.8 g	7.0	-	10.0 e	4.0	-	9.5 d	4.0	-
04GC0139 (resistance donor parent)	48.4 e	4.3	36.3	25.7 g	7.1	59.0	12.2 e	4.1	75.0	9.5 d	4.0	72.7
Null (n=4)	74.0 abc	3.7	2.6	49.8 bc	7.9	20.6	37.8 b	6.8	22.5	27.4 bc	8.4	21.3
Fhb1 (n= 6)	75.6 ab	3.6	0.5	47.0 cd	7.8	25.0	36.5 bc	6.7	25.2	26.2 bc	8.3	24.7
Fhb2 (n= 4)	74.2 abc	3.7	2.4	51.3 b	7.9	18.2	39.8 b	6.8	18.4	30.4 b	8.4	12.6
Fhb5 (n= 2)	74.8 abc	3.8	1.6	48.3 bcd	7.9	23.0	36.7 bc	6.8	24.8	23.6 bc	8.4	32.2
Fhb1+Fhb2 (n= 2)	74.6 abc	3.9	1.8	46.1 cde	8.0	26.5	35.2 bc	6.8	27.9	26.4 bc	8.5	24.1
Fhb1+Fhb5 (n= 4)	72.7 abc	3.7	4.3	47.4 bcd	7.9	24.4	36.2 bc	6.8	25.8	19.9 cd	8.1	42.8
Fhb2+Fhb5 (n= 6)	68.3 c	3.6	10.1	44.6 de	7.8	28.9	31.3 c	6.8	35.9	19.9 cd	8.0	42.8
Fhb1+Fhb2+Fhb5 (n= 4)	69.1 c	3.6	9.1	42.8 ef	7.9	31.7	30.6 cd	6.7	37.3	17.6 cd	8.0	49.4
CDC Go												
CDC Teal (susceptible check)	76.7 a	8.0	-	67.7 a	7.4	-	51.7 a	7.9	-	32.2 a	6.8	-
CDC Go (recurrent parent)	75.6 ab	8.0	-	46.6 b	7.4	-	37.2 b	7.9	-	30.6 a	6.7	-
AC Barrie (moderately resistant/intermediate check)	55.1 d	8.1	-	35.7 b	7.6	-	21.1 d	8.0	-	17.4 de	6.8	-
ND2710 (resistant check)	39.1 e	8.1	-	19.4 c	7.6	-	9.7 e	8.0	-	5.3 f	6.9	-
04GC0139 (resistance donor parent)	37.5 e	8.0	50.4	19.1 c	7.4	59.0	7.8 e	7.9	79.0	8.1 f	6.6	73.5
Null (n=7)	72.9 abc	7.7	3.6	45.4 b	7.1	2.6	35.9 b	7.7	3.5	29.2 a	6.2	4.6
Fhb1 (n= 6)	70.8 abc	7.7	6.4	43.6 b	7.1	6.4	33.9 bc	7.7	8.9	25.5 abc	6.3	16.1
Fhb2 (n= 4)	71.2 abc	7.7	5.8	43.0 b	7.2	7.7	33.4 bc	7.7	10.2	28.7 ab	6.3	6.0
Fhb5 (n= 2)	67.1 abc	7.8	11.2	43.4 b	7.3	7.3	32.8 bc	7.8	11.8	21.4 cde	6.5	30.1
Fhb1+Fhb2 (n= 4)	70.3 abc	7.7	7.0	40.7 b	7.2	12.7	31.4 bc	7.7	15.6	24.6 a-d	6.3	19.6
Fhb1+Fhb5 (n= 6)	66.5 bc	7.7	12.0	40.8 b	7.1	12.4	30.6 bc	7.7	17.7	20.3 cde	6.3	33.7
Fhb2+Fhb5 (n= 4)	69.6 abc	7.7	7.9	42.3 b	7.2	7.9	32.8 bc	7.7	11.8	22.8 b-e	6.3	25.5
Fhb1+Fhb2+Fhb5 (n= 5)	65.0 cd	7.7	14.0	37.4 b	7.2	19.7	27.4 cd	7.7	26.3	18.3 e	6.3	40.2

[a]Least squares mean; [b]Standard error of the mean; [c]Percent disease reduction.

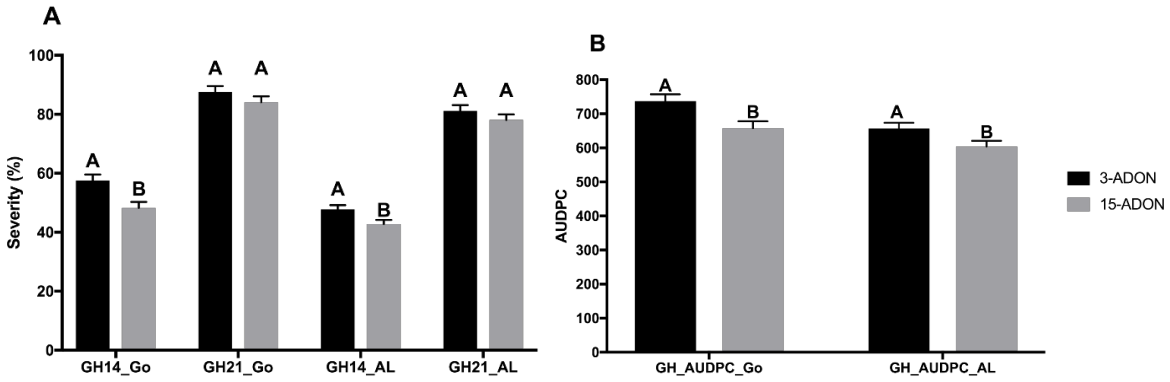

Figure 3.4. Fusarium head blight severity in CDC Go and CDC Alsask near-isogenic lines (NILs) following point inoculation with 3-ADON and 15-ADON chemotypes of Fusarium graminearum (50,000 macroconidia/ml) (A) in the greenhouse at 14 and 21 days post inoculation (dpi) (B) Area under disease progress curve (AUDPC) was calculated from three ratings: 7, 14, and 21 dpi. Bars with the same letter code are not statistically significantly different according to Fisher's least significant differences at $P = 0.05$. The LSmeans were calculated from all NILs (excluding parents and checks) in each population.

3.5.3. Marker main effects and epistatic interactions

Epistatic interaction analyses were carried out between marker pairs for all marker loci and multiple genome-wide interactions were identified that influenced FHB parameters (Table 3.4). Statistically significant epistatic interactions ($P < 0.001$) among other marker loci and *Fhb1*, *Fhb2*, and *Fhb5* were identified; interactions with *Fhb5* were the most common among the three genes, however, the nature of the epistatic interactions (additive/additive-dominant) could not be defined. In the CDC Alsask population, epistatic interactions explained up to 18.1% of the variation for FLD_INC, 24.4% for FLD_SEV, 25.9% for FLD_IND, and 16.4% for FLD_DON accumulation (Table 3.4). Similarly, for CDC Go, up to 16.6% of the phenotypic variation was explained for GH_AUDPC, 18.7% for FLD_INC, 10.7% for FLD_SEV, 18.9% for FLD_IND, and 22.2% for FLD_DON accumulation. In addition to *Fhb1*, *Fhb2*, and *Fhb5*, four stable alleles (stable alleles in this paper are those identified in multiple environments) in CDC Alsask NILs and five in CDC Go NILs were identified that conferred resistance against FHB (Tables 3.5 and 3.6). Of the resistance improving alleles, one of the four in CDC Alsask and three of the five in CDC Go were contributed by the susceptible recurrent parent. One of the four alleles identified in CDC Alsask on chromosome 6A overlapped with QTL *Qfhb.ndwp-6A* reported by Zhao et al. (2018); they mapped the QTL from ND2710, an advanced breeding line from North Dakota, USA and derivative of Sumai 3. The favourable alleles at 1DS, 6AS, *Qfhb.ndwp-6A*, 7BS loci in CDC Alsask reduced FHB index up to 23.4, 15.7, 17.2, and 17.2% and and DON accumulation by

as much as 26.0, 13.7, 37.8, and 14.8%, respectively (Table 3.5). In CDC Go, the favourable alleles at 1DL, 2AL, 2DL, 6DS, 7AL loci reduced FHB index up to 19.0, 23.2, 16.7, 22.3%, and 5.6% and DON accumulation up to 24.5, 19.4, 15.1, 18.8, and 18.8%, respectively (Table 3.6).

3.5.4. Physical mapping and functional annotation

To determine the physical location of all genes/loci associated with FHB resistance, the corresponding SNP marker sequences were used. As expected, *Fhb1* was located on the distal end of the Chromosome 3B between 8 – 21 Mb; *Fhb2* between 159 – 234 Mb; *Fhb5* in region between 46 – 111 Mb (Fig. 3.2). Other than FHB major genes, all other regions were physically located in a narrow interval with the exception of 6DS and 7AL in the CDC Go population (Table 3.6). Although expressed genes were retrieved for all FHB resistance governing regions, we have reported only the annotated genes for regions other than *Fhb1*, *Fhb2*, and *Fhb5* (Table 3.7; data not shown, available from author upon request). For functional annotation of expressed genes in *Fhb1*, *Fhb2*, and *Fhb5* regions, readers are directed to studies by Dhokane et al. (2016), Rawat et al. (2016), Samad-Zamini et al. (2017), and Schweiger et al. (2013 and 2016). Of the 33 expressed genes in the *Fhb1* region, reported by Schweiger et al. (2016), only six were found in the Chinese Spring database through POTAGE; whereas all six candidates for *Fhb2* reported by Dhokane et al. (2016) were retrieved from POTAGE (data not shown). Using POTAGE and POSEQ recombination bin carrying SNP markers associated with the Chromosome regions 1DS, *Qfhb.ndwp-6A*, 1DL, 2AL, 2DL, 6DS, and 7AL, a total of 70, 147, 3, 85, 515, 416, and 161 expressed genes were retrieved (data not shown); however, in Table 7 we present only those expressed genes that were directly associated with the 90K SNP marker sequences. The most important annotated genes, which could be the potential candidates for FHB resistance governing regions were disease resistance proteins, protein kinases (including mitogen-activated protein kinases), disease resistance nucleotide binding sites and leucine rich repeats (NBS-LRR), glutathione syntetase, dihydroflavonol 4-reductase (involved in flavonoid biosynthesis), glycosyl transferases, NAC domain containing protein and F-box domain containing proteins (Table 3.7) as these have been reported to play a role in disease resistance (FHB and diseases of other crops) (reviewed in Bent and Mackay 2007; Schweiger et al. 2013, 2016; Dhokane et al. 2016; Brar et al. 2018a).

Table 3.4. Significant ($P = 0.001$) of epistatic marker-marker interactions and percent phenotypic variation explained (R^2) by the interaction in CDC Alsask and CDC Go near-isogenic lines (NILs). Here AA and BB alleles are from recurrent parents CDC Go/CDC Alsask and resistance donor parent 04GC0139, respectively.

Trait	Chromosome-Marker/loci and alleles (in parentheses) involved	R^2
	CDC Alsask	
INC	6A-Ku_c1976_663 (AA), 5B-wsnp_Ku_c12464_20125626 (AA)	18.1
	6A-Excalibur_c18333_175 (AA), 5D-IACX6288 (AA)	16.6
	6A-Ku_c1976_663 (AA), 5B-Excalibur_c29304_176 (AA), 5B-tplb0027f13_1493 (AA)	10.6
	5B-wsnp_Ku_c12464_20125626 (AA), 5B-BobWhite_c13340_412 (AA)	5.8
SEV	5D-Excalibur_c34793_1260 (AA), 6A-RAC875_c13610_822 (BB), 6A-BS00071571_51(AA)	24.4
	Fhb1-3B-CAP7_c1576_371 (AA), 2D-Excalibur_c73791_215 (AA), 2D-IAAV8570 (AA), 2D-RAC875_c319_1776 (AA)	17.4
	3D-Kukri_rep_c96809_457 (AA), 2D-Excalibur_c73791_215 (AA), 2D-IAAV8570 (AA), 2D-RAC875_c319_1776 (AA)	6.8
IND	***Fhb5***-5A-BS00077990_51 (BB), ***Fhb5***-5A-Tdurum_contig10128_593 (BB), ***Fhb5***-5A-BS00071087_51 (BB), ***Fhb5***-5A-BS00045284_51 (BB), 5A-BS00078572_51 (BB), 5A-BS00078573_51 (BB), 5B-tplb0027f13_1493 (AA), 5B-Excalibur_c29304_176 (AA), 5A-wsnp_Ex_c11309_18272248 (BB)	24.8-25.9
	4B-BS00022582_51 (BB), 4B-BS00022582_51 (BB), 1D-RAC875_c10387_685 (AA), 1D-Kukri_c26168_713 (AA), 1D-BobWhite_c1715_887 (AA), 1D-Excalibur_c15692_532 (AA), Un-BS00064204_51 (AA), 1A-Kukri_c29150_143 (AA)	20.7
	5B-Ex_c5594_2630 (AA), ***Fhb5***-5A-BS00077990_51(BB), ***Fhb5***-5A-Tdurum_contig10128_593(BB), ***Fhb5***-5A-BS00071087_51(BB), ***Fhb5***-5A-BS00045284_51 (BB), 5A-BS00078573_51 (BB), 5A-Ra_c322_1259 (BB), 5A-BS00078572_51 (BB), 5A-GENE-3218_77 (BB), 5A-wsnp_Ex_c11309_18272248 (BB)	7.8-19.7
	4A-wsnp_Ku_c4342_7887834 (BB), 2B-wsnp_Ex_c17576_26303707 (BB), 7B-CAP11_c8077_69 (AA)	6.8-12.6
	6B-Tdurum_contig81911_179 (BB), 1A-Kukri_c23985_166 (BB), 1A-Excalibur_c75270_566 (BB), 1A-Tdurum_contig43646_147 (BB)	12.4
DON	7A-Excalibur_c52972_213 (AA), ***Fhb5***-5A-BS00077990_51 (AA), ***Fhb5***-5A-BS00071087_51 (AA), 5A-wsnp_Ex_c11309_18272248 (AA), 6B-Tdurum_contig42203_3670 (AA)	3.3-16.4
	5B-Ex_c5594_2630 (AA), 1B-Tdurum_contig893_53 (BB), 1A-Tdurum_contig5560_193 (BB), 1B-Tdurum_contig42558_134 (BB)	15.5
	5A-BS00078572_51 (AB), 6B-Tdurum_contig81911_179 (AA)	15.2
	Fhb5-5A-BS00077990_51 (AA), ***Fhb5***-5A-Tdurum_contig10128_593 (AA), ***Fhb5***-5A-BS00071087_51 (AA), ***Fhb5***-5A-BS00045284_51 (AA), ***Fhb1***-3B-BS00063445_51 (AA), ***Fhb2***-6B-wsnp_Ex_c5058_8981554 (BB), ***Fhb2***-6B-Kukri_c66290_127, 5A-wsnp_Ex_c11309_18272248 (AA), 2B-BobWhite_rep_c49523_266 (BB), 3B-BS00001335_51 (AA), 6D-Excalibur_c17241_388 (BB), 3A-BS00036089_51 (AA), 3D-Kukri_rep_c111139_338 (BB)	5.7-8.4
	7B-BS00063852_51 (AA), 1D-BS00015317_51 (BB), 1D-Excalibur_c15692_53 (BB), 1D-RAC875_c10387_685 (BB)	6.5
	Fhb5-5A-BS00077990_51 (AA), ***Fhb5***-5A-Tdurum_contig10128_593 (AA), ***Fhb5***-5A-BS00071087_51 (AA), ***Fhb5***-5A-BS00045284_51 (AA), ***Fhb1***-3B-BS00063445_51 (AA), Un-BS00064204_51 (AA), 1A-Kukri_c29150_143 (AA), 1D-Kukri_c26168_713 (AA), 1D-BobWhite_c1715_887 (AA), 1D-Excalibur_c15692_532 (AA)	3.2-6.2
	Fhb2-6B-wsnp_Ex_c5058_8981554 (BB), 6D-Excalibur_c17241_388 (BB), 6B-Tdurum_contig42203_3670 (AA)	6.1
	CDC Go	

GH_AUDPC	***Fhb5***-5A-wsnp_Ra_rep_c69221_66574148 (AA), 2A-Tdurum_contig21786_270 (AA), 2D-IACX8602 (AA), 7D-RAC875_c11969_384 (AA), 4D-wsnp_JD_rep_c51623_35119179 (AA), 7A-RAC875_c22592_2255 (AA), 7D-tplb0041e14_1096 (AA)	8.8-16.6
	Fhb5-5A-wsnp_Ra_rep_c69221_66574148 (BB), ***Fhb5***-5A-BS00045284_51 (BB), 7D-RAC875_c11969_384 (AA), 4D-wsnp_JD_rep_c51623_35119179 (AA), 7D-tplb0041e14_1096 (AA)	16.6
INC	***Fhb5***-5A-BS00045284_51 (BB), ***Fhb5***-5A-barc186 (BB), ***Fhb5***-5A-BS00041219_51 (BB), ***Fhb5***-5A-barc117 (BB), ***Fhb5***-5A-wsnp_Ra_rep_c69221_66574148 (BB), 2A-wsnp_Ex_c36481_44425685 (AA), 2D-Excalibur_c65796_394 (AA)	11.0-18.7
	Fhb5-5A-BS00045284_51 (AA), ***Fhb5***-5A-barc186 (AA), ***Fhb5***-5A-wmc705 (AA), ***Fhb5***-5A-barc117 (AA), ***Fhb5***-5A-wsnp_Ra_rep_c69221_66574148 (AA), ***Fhb1***-3B-RAC875_c4389_1412 (BB), 7A-Excalibur_c61603_1052 (AA)	11.9-16.6
	Fhb5-5A-BS00041219_51 (AA), ***Fhb5***-5A-barc117 (AA)	12.6
	Fhb5-5A-BS00041219_51 (BB), ***Fhb5***-5A-wsnp_Ra_rep_c69221_66574148 (BB), 1A-IAAV4238 (AA), 1B-Excalibur_c35289_64 (AA), 1D-Excalibur_c26495_84 (AA), 5B-Kukri_c6176_1400 (AA)	9.2-12.7
	Fhb2-6B-Ra_c3381_1027 (AA), 2A-wsnp_Ex_c36481_44425685 (BB), 6D-BS00110365_51 (AA)	9.4
SEV	***Fhb1***-RAC875_c4389_1412 (BB), ***Fhb2***-6B-Ra_c3381_1027 (AA), 6D-BS00110365_51 (AA)	9.3-10.1
	Fhb2-6B-Ra_c3381_1027 (AA), 3B-wsnp_JD_c222_352320 (BB), 6D-BS00110365_51 (AA)	10.1
	2A-wsnp_Ex_c36481_44425685 (BB), 7B-GENE-4981_53 (BB), ***Fhb2***-6B-Ra_c3381_1027 (AA)	10.2
	7A-wsnp_Ex_c39221_46569987 (AA), ***Fhb5***-5A-barc186 (AA), ***Fhb5***-5A-BS00041219_51 (AA)	8.2-10.7
IND	***Fhb5***-5A-wsnp_Ra_rep_c69221_66574148 (BB), ***Fhb5***-5A-BS00045284_51 (BB), ***Fhb5***-5A-barc117 (AA), ***Fhb5***-5A-wmc705 (AA), ***Fhb2***-6B-Ra_c3381_1027 (AA), 2A-wsnp_Ex_c36481_44425685 (BB), 6A-Kukri_c56494_585 (BB), 2A-Tdurum_contig21786_270 (AA), 2D-IACX8602 (AA), 6D-BS00110365_51 (AA)	17.0-18.9
	1A-IAAV4238 (BB), 1B-Excalibur_c35289_64 (BB), 2D-Excalibur_c65796_394 (BB), 5B-BobWhite_c11038_605 (BB)	15.5
	Fhb1-RAC875_c4389_1412 (BB), 5B-Kukri_c6176_1400 (BB)	10.1
DON	***Fhb5***-5A-BS00045284_51 (AA), ***Fhb5***-5A-barc186 (AA), 7A-Excalibur_c7897_600 (AA)	5.0-22.2
	Fhb5-5A-BS00041219_51 (BB), ***Fhb5***-5A-wsnp_Ra_rep_c69221_66574148 (BB), ***Fhb5***-5A-BS00045284_51 (BB), 7A-Excalibur_c7897_600 (AA), 4D-wsnp_JD_rep_c51623_35119179 (AA), 7D-tplb0041e14_1096 (AA)	10.1-21.3
	Fhb1-RAC875_c4389_1412 (AA), ***Fhb2***-6B-Ra_c3381_1027 (AA), ***Fhb5***-5A-BS00041219_51 (AA), 6D-BS00110365_51 (AA), 3B-wsnp_JD_c222_352320 (AA)	8.1-20.3
	Fhb5-5A-wsnp_Ra_rep_c69221_66574148 (AA), 1A-IAAV4238 (BB)	14.8
	Fhb5-5A-wsnp_Ra_rep_c69221_66574148 (AA), ***Fhb5***-5A-barc186 (AA), ***Fhb1***-RAC875_c4389_1412 (AA), 3B-wsnp_JD_c222_352320 (AA)	5.6-9.9

Table 3.5. Single nucleotide polymorphism (SNP) markers (other than *Fhb1*, *Fhb2*, and *Fhb5*) associated ($P < 0.05$) with Fusarium head blight index (FLD_IND), severity (FLD_SEV), incidence (FLD_INC), deoxynivalenol accumulation (FLD_DON), and area under disease progress curve from greenhouse evaluation (GH_AUDPC) in CDC Alsask near-isogenic lines. The numbers not in parentheses represent differences (in units for the traits) in LSmeans and the number in parentheses indicate percent disease reduction relative to susceptible allele.

Chr./Locus (allele)[a]	Physical interval (Mb)	2011[b]	2012	2013	2015	2016	2016S	Average	GH_AUDPC
				FLD_IND					
1DS (BB)	10.39 – 26.18	-	3.2 (7.2)	6.9 (23.4)	-	3.6 (23.2)	-	2.0 (5.6)	105.1 (15.9)
6AS (BB)	3.35	5.3 (8.0)	3.8 (11.2)	4.0 (13.6)	7.8 (15.7)	-	-	3.3 (9.1)	-
Qfhb.ndwp-6A[b] (BB)	602.5 – 611. 8	-	-	3.7 (11.8)		3.0 (17.2)	-	-	-
7BS (AA)	170.52	4.3 (6.4)	3.5 (11.6)	-	9.1 (17.2)	-	3.2 (12.2)	3.5 (9.3)	68.9 (10.0)
				FLD_SEV					-
1DS (BB)	10.39 – 26.18	-	2.9 (6.7)	7.9 (17.6)	2.4 (3.7)	5.7 (23.3)	-	3.2 (6.7)	-
6AS (BB)	3.35	-	9.3 (20.1)	-	4.4 (6.8)	-	-	-	-
Qfhb.ndwp-6A (BB)	602.5 – 611. 8	-	-	9.4 (18.3)	-	-	3.3 (12.5)	-	-
7BS (AA)	170.52	-	4.9 (10.5)	-	4.9 (7.3)	-	2.8 (8.4)	2.6 (5.4)	-
				FLD_INC					
1DS (BB)	10.39 – 26.18	-	3.8 (5.0)	3.5 (5.5)	-	-	-	-	-
6AS (BB)	3.35	5.2 (6.1)	-	8.3 (12.6)	7.7 (10.2)	-	-	-	-
Qfhb.ndwp-6A (BB)	602.5 – 611. 8	-	5.9 (7.4)	-	-	-	-	-	-
7BS (AA)	170.52	4.1 (4.7)	-	7.9 (11.6)	8.8 (11.2)	-	-	-	-
				FLD_DON					
1DS (BB)	10.39 – 26.18	12.8 (23.8)	9.8 (24.3)	5.1 (23.6)	2.6 (9.9)	-	1.3 (26.0)	4.5 (18.1)	-
6AS (BB)	3.35	-	5.5 (13.7)	-	3.7 (13.7)	-	-	-	-
Qfhb.ndwp-6A (BB)	602.5 – 611. 8	10.4 (17.3)	11.4 (23.8)	2.3 (10.1)	-	-	1.4 (37.8)		-
7BS (AA)	170.52	-	4.2 (10.1)	3.4 (14.8)	2.8 (10.1)	-	-	-	-

[a]Here AA and BB in parentheses indicates the CDC Alsask (recurrent susceptible parent) or 04GC0139 (resistance donor parent) alleles, respectively, that contribute resistance.
[b]Refer to Zhao et al. (2018).

Table 3.6. Single nucleotide polymorphism (SNP) markers (other than *Fhb1*, *Fhb2*, and *Fhb5*) significantly associated ($P < 0.05$) with Fusarium head blight index (FLD_IND), severity (FLD_SEV), incidence (FLD_INC), deoxynivalenol accumulation (FLD_DON), and area under disease progress curve from greenhouse evaluation (GH_AUDPC) in CDC Go near-isogenic lines. The numbers not in parentheses represent differences (in units for the traits) in LSmeans and the number in parentheses indicates percent disease reduction relative to susceptible allele.

Chr./Locus (allele)[a]	Position (Mb)	2010[b]	2011	2012	2013	2015	2016	2016S	Average	GH_AUDPC
				FLD_IND						
1DL (AA)	492.17 – 495.11	3.3 (19.0)	-	-	4.1 (6.6)	3.6 (5.7)	-	-	-	80.1 (10.5)
2AL (AA)	717.8 – 718.73	4.1 (23.2)	6.1 (13.5)	4.9 (16.1)	-	3.4 (5.4)	-	-	3.1 (9.2)	100.4 (13.0)
2DL (AA)	293.13	2.8 (16.7)	2.4 (5.6)	4.5 (15.2)	-	3.9 (6.2)	2.1 (15.2)	-	2.2 (6.6)	95.3 (12.5)
6DS (BB)	72.01 – 136.12	-	-	6.8 (22.3)	4.6 (7.5)	4.0 (6.3)	-	-	2.6 (7.8)	116.7 (15.3)
7AL (BB)	519.96 – 619.15	-	-	-	3.4 (5.6)	-	-	-	-	-
				FLD_SEV						
1DL (AA)	492.17 – 495.11	3.8 (13.9)	-	-	-	-	-	-	-	-
2AL (AA)	717.8 – 718.73	5.4 (19.3)	5.0 (9.3)	3.8 (8.1)	-	-	-	-	2.6 (6.0)	-
2DL (AA)	293.13	4.4 (16.1)	3.5 (6.5)	2.8 (6.2)	-	-	-	-	-	-
6DS (BB)	72.01 – 136.12	-	-	6.7 (14.1)	4.4 (6.2)	4.3 (6.7)	4.0 (19.5)	-	3.0 (6.9)	-
				FLD_INC						
1DL (AA)	492.17 – 495.11	4.4 (7.2)	-	-	-	-	-	-	-	-
2AL (AA)	717.8 – 718.73	-	4.2 (5.0)	6.7 (10.4)	-	-	4.8 (6.9)	2.4 (6.7)	3.2 (4.5)	-
2DL (AA)	293.13	-	-	5.1 (8.1)	-	-	5.4 (7.8)	-	-	-
6DS (BB)	72.01 – 136.12	-	4.6 (7.3)	-	-	-	4.5 (6.6)	-	-	-
7AL (BB)	519.96 – 619.15	5.0 (8.3)	-	-	-	-	-	-	-	-
				FLD_DON						
1DL (AA)	492.17 – 495.11	4.4 (18.3)	8.5 (14.0)	1.5 (5.3)	-	4.0 (13.8)	-	1.2 (24.5)	3.0 (11.5)	-
2AL (AA)	717.8 – 718.73	2.6 (11.6)	5.6 (9.5)	4.2 (14.1)	6.3 (19.4)	-	-	-	2.6 (10.1)	-
2DL (AA)	293.13	-	-	4.1 (13.9)	4.7 (15.1)	1.5 (5.5)	-	0.7 (11.4)	-	-
6DS (BB)	72.01 – 136.12	-	7.3 (12.4)	-	-	-	1.2 (18.8)	0.8 (17.8)	-	-
7AL (BB)	519.96 – 619.15	2.6 (11.7)	11.2 (18.8)	-	-	2.1 (7.7)	-	-	2.4 (9.6)	-

[a]Here AA and BB in parentheses indicates the CDC Go (recurrent susceptible parent) or 04GC0139 (resistance donor parent) alleles, respectively, that contribute resistance.

Table 3.7. List of genes (gene ID and name) annotated for single nucleotide polymorphism (SNP) loci conferring resistance to Fusarium head blight (FHB). For each annotated gene, Munich Information Center for Protein Sequences (MIPS) annotation hit ID is provided.

Locus associated with FHB resistance	Gene ID	Gene name	MIPS annotation hit ID	Comments[c]
1DS	Traes_1DS_BDACE1560	Disease resistance protein	sp|Q9T048|DRL27_ARATH	Expressed in all plant parts
	Traes_1DS_F3F17A72C	Protein kinase superfamily protein	AT5G28080.2	High expression in stem and spike (Z32, Z39, Z65)
	Traes_1DS_205D3AC8B	Disease resistance protein CC-NBS-LRR class family	AT5G63020.1	Highly expressed in spike (Z39)
	Traes_1DS_4E3A925B9	Leucine-rich repeat receptor-like protein kinase family protein	AT4G08850.1	Expressed in all plant parts
6AS	Traes_6AS_318DA417A	Protein kinase	AT3G25490.1	Only expressed in leaf (Z23, Z71), stem (Z65), and spike (Z65)
Qfhb.ndwp-6A[a]	Traes_6AL_90B062F76	F-box/RNI-like superfamily protein	AT3G26922.1	Highly expressed in spike (all stages)
	Traes_6AL_8A5E06C77	LRR receptor-like serine/threonine-protein kinase	UniRef90_M8CZR7	Expressed in all plant parts except root
	Traes_6AL_1B43FE620	Lysine-specific histone demethylase 1 homolog 3	sp|Q9CAE3|LDL3_ARATH	Highest expression in spike (Z32 and Z65)
	Traes_6AL_8BA1FF8B2	NAC domain containing protein 2	AT5G04410.1	Expressed in all plant parts
	Traes_6AL_F759812CF	Acyl-CoA-binding domain-containing protein 4	sp|Q9MA55|ACBP4_ARATH	Expressed in all plant parts
7BS	-[b]	-	-	-
1DL	Traes_1DL_63D5C4C8E	Histone deacetylase	AT5G22650.1	Highly expressed in root, stem, and spike (Z65)
2AL	Traes_2AL_57CC2BFDD	dihydroflavonol 4-reductase	AT5G42800.1	Only expressed in grain (Z71)
	Traes_2AL_3341560A9	ATP binding protein	UniRef90_UPI0002BC9F6D	Highly expressed in grain (Z85)
	Traes_2AL_D4EED56CE	histone-lysine N-methyltransferase	AT3G21820.1	Highly expressed in grain (Z85)
	Traes_2AL_B01F4C113	polymerase delta 4	AT1G09815.1	Highly expressed in grain (Z75)
2DL	Traes_2DL_2249C5E82	Regulator of chromosome condensation RCC1 family protein	AT5G63860.1	Highest expression in spike (Z65)
6DS	Traes_6DS_352313CDF	glutathione synthetase 2	AT5G27380.1	Expressed in all parts
	Traes_6DS_A9E719CC8	Pentatricopeptide repeat-containing protein	sp|Q9SVH0|PP329_ARATH	Highly expressed in spike (Z32)
	Traes_6DS_E0FD61378	Unknown	UniRef90_UPI000234F957	Highly expressed in spike (Z32)

	Traes_6DS_C9398DB9C	Synaptotagmin-5	sp|O00445|SYT5_HUMAN	Only expressed in spike (Z65)
	Traes_6DS_78871A7EA	26S protease regulatory subunit 7 homolog A	sp|Q9SSB5|PRS7A_ARATH	Expressed in all parts
	Traes_6DS_762984823	S-adenosylmethionine synthase 4	sp|Q4LB21|METK4_HORVU	Highly expressed in grain (Z85)
7AL	Traes_7AL_13DE4FF55	Lipase 1	sp|P17573|LIP1_GEOCN	Highly expressed in leaf and spike (Z65)
	Traes_7AL_677F233CE	F-box domain containing protein	UniRef90_Q7G5F5	Highly expressed in spike and grain (all stages)
	Traes_7AL_F60FF74CA	Rer1 family protein	AT4G39220.1	Expressed in all plant parts
	Traes_7AL_89E0BA362	Peptidyl-prolyl cis-trans isomerase B	sp|Q9TW32|PPIB_DICDI	Expressed in all plant parts
	Traes_7AL_C501CCF17	Similar to RCD (ribose catalytic domain) one 1	AT2G35510.1	Highly expressed in spike and grain (all stages)
	Traes_7AL_530CAE15B	mitogen-activated protein kinase	AT5G19010.1	Expressed in all plant parts
	Traes_7AL_99483DCCC	Mitochondrial substrate carrier family protein	AT2G46320.1	Highly expressed in grain (Z85)
	Traes_7AL_6599B5B49	Disease resistance protein	sp|Q9T048|DRL27_ARATH	Expressed in all plant parts and spike (Z65)
	Traes_7AL_52779A5E2	nodulin MtN21 /EamA-like transporter family protein	AT3G45870.1	Expressed in all plant parts
	Traes_7AL_D45376F32	myb-like transcription factor family protein	AT3G25790.1	Highly expressed in stem and spike (all stages)
	Traes_7AL_2279551BA	putative type 1 membrane protein	AT3G24160.1	Expressed in all plant parts
	Traes_7AL_8895EDF48	Glycosyltransferase family 61 protein	AT3G18180.1	Expressed in all plant parts
	Traes_7AL_8CDD7A174	UDP-sugar pyrophosphorylase	AT5G52560.1	Expressed in all plant parts
	Traes_7AL_F45599D0D	histone acetyltransferase of the CBP family 12	AT1G16710.1	Expressed in all plant parts
	Traes_7AL_432085C4D1	exocyst subunit exo70 family protein G1	AT4G31540.1	Highest expression in spike (Z65)
	Traes_7AL_8783C1471	Zinc finger protein	sp|Q9C9A9|COL7_ARATH	Highly expressed in spike (Z65) and grain
	Traes_7AL_7B680A58E	Leucine-rich repeat receptor-like protein kinase	AT2G33170.1	Expressed in all parts

[a]Refer to Zhao et al. (2018).
[b]No annotation obtained.
[c]Here Z32, Z39, Z65, Z71, Z79, Z85 indicates the cereal growth stages. For more information on cereal growth stages, please refer to Lancashire et al. (1991).

3.6. Discussion

In this study, we successfully introgressed Sumai 3 derived *Fhb1*, *Fhb2*, and *Fhb5* genes in two elite hard red spring wheat cultivars (CDC Go and CDC Alsask) using microsatellite markers. Although studies by Miedaner et al. (2006), McCartney et al. (2007), Pumphrey et al. (2007), Xue et al. (2010), and Salameh et al. (2011) have also reported successful introgression and evaluation of Sumai 3 derived genes in elite wheat cultivars; our study has several advantages. Firstly, many of these studies did not perform repeated backcrossing and rather derived recombinant inbred lines involving multiple parents, which are expected to carry relatively larger proportion of the resistant donor, whereas we performed repeated backcrossing with implementation of markers at each BC cycle. Secondly, all the studies cited evaluated only *Fhb1* and *Fhb5* and ignored *Fhb2*, another well-characterized gene for FHB Type-II resistance (Cuthbert et al. 2006; Dhokane et al. 2016). Lastly, we genotyped our NILs with a large number of SNP markers in addition to microstaellite markers and were able to evaluate polymorphism on all chromosomes and the marker-marker interactions based on phenotypic assessment in 8-9 environments. By repeated backcrossing, we were able to reduce the proportion of donor parent alleles to a large extent, which was even lower than the theoretically expected value of 6.25%. Similar results for introgression of four FHB resistance QTL were reported in Xue et al. (2010b) although their results could be biased as they used only 150 microsatellite markers. The results from our study and Xue et al. (2010b) indicated that the MAS is not only helpful in foreground selection of resistance genes or QTL, but to retain a major portion of the recurrent parent's chromatin. As NILs in both populations, particularly CDC Go, carried <3% of the donor parent's genome, we can reliably quantify the allelic effects of *Fhb1*, *Fhb2*, and *Fhb5* in our populations.

Theoretically, the variation in allelic composition of NILs is expected only for the chromosome carrying the gene of interest, but that is practically impossible, especially when microsatellites are used for selection that targets multiple sites in the genome of allopolyploids such as wheat. Therefore, allelic variation on all chromosomes for given SNP markers was expected. The SNP markers from the wheat 90K assay provided very useful information as they represented polymorphisms on all 21 wheat chromosomes and were uniformly distributed over all chromosomes (Wang et al. 2014). A number of SNPs on 3BS (carrying *Fhb1*), 5AS (*Fhb2*), and 6BS (*Fhb2*), including those mapped in gene/QTL intervals were located together (physically) on the chromosome arms and inherited together as a haplotype block (Fig. 3), which could be attributed to strong linkage disequilibrium among markers. In particular, *Fhb1* and *Fhb5* were relatively large haplotype blocks with

suppressed recombination; *Fhb1* is a diverse haplotype from susceptible spring wheat lines including Chinese Spring (Schweiger et al. 2016; Buerstmayr et al. 2017). The *Fhb5* gene was fine-mapped to the low recombination peri-centromeric region of chromosome 5A and the SNPs in the gene interval were all mapped to the same region in our populations; polymorphism was absent for most of the chromosome region validating results of successful introgression of *Fhb5*. Low recombination frequencies in *Fhb1* and *Fhb5* regions could be another reason for the relatively large physical segments carrying exactly the same marker haplotypes on 3BS and 5AS.

Unlike most other studies where NIL/entry nested within gene/QTL class had significant variance estimates, our study indicated insignificant variation among NILs within the same QTL class (Table 3.1). Alternatively, all NILs carrying the same QTL behaved similarly in our populations. These results indicated that there was no or negligible recombination between the markers used for foreground selection and the gene under selection. Loss of target QTL/genes on successful backcrossing is quite possible (because of double crossover events), however, all three genes were recovered in both backgrounds, possibly by using multiple microsatellites flanking the genes at each BC cycle. Also, repeated backcrossing and a very small proportion of the resistant donor could have resulted in less confounding effects from other alleles inherited along with the three major genes under selection. Moderate to high heritability estimates for all FHB parameters suggested that a large proportion of the differences observed among the NILs has a genetic basis. Heritability estimates in GH evaluations were particularly strong, which was not surprising as the environmental variation was minimal in these cases. As expected, the 3-ADON chemotype of *Fg* resulted in higher FHB severity as compared to the 15-ADON chemotype in GH evaluations in both populations because the 3-ADON chemotype is known to be more aggressive and produces more DON than the 15-ADON chemotype (Ward et al. 2008; Gilbert et al. 2010, 2014). Despite the fact that the 3-ADON chemotype resulted in higher disease severity, the difference between 3-ADON and 15-ADON chemotypes was not significant 21 days post inoculation because resistance to FHB in wheat was not complete and the Sumai 3 genes only slow fungal progression. With time (by 21 days after inoculation), both resistant and susceptible spikes will exhibit FHB symptoms, particularly under conducive conditions coupled with artificial inoculations.

Despite the tendency towards reduced FHB symptoms (incidence, severity, and/or index) and DON accumulation in NILs carrying Sumai 3 derived genes, it was not significant for most of the gene classes in the CDC Go population. This may have been due to the relatively higher level of resistance in recurrent parent CDC Go as compared to CDC Alsask

(Anonymous 2015a). Some level of resistance in CDC Go compared to CDC Alsask was also evident from the fact that CDC Go has three resistance improving alleles, whereas CDC Alsask has only one (Tables 3.5 and 3.6). Similar results on insignificant improvement in FHB resistance in winter wheat cultivar 'Apache' (MR) were reported on introgression of *Fhb1* and *Fhb5* (Salameh et al. 2011) and by Pumphrey et al. (2007) with introgression of *Fhb1* in recipient lines carrying good Type-I resistance. Also, Pumphrey et al. (2007) did not detect significant differences for FHB disease severity or the proportion of FDK in half of the families contrasting for *Fhb1*. In practice, it is hard to combine all favourable alleles in one genetic background, particularly when both parents carry favourable alleles; there was no NIL entry in either the CDC Go or the CDC Alsask populations that carried all favourable alleles from each parent. Similar to the results reported by Salameh et al. (2011), NILs carrying none of three major FHB genes (classified as 'null') in our study tended to improve resistance compared to the recurrent parents and the differences were actually significant in the CDC Alsask NILs. The improved resistance of such NILs could be attributed to some other minor favourable loci derived from either parent (Tables 3.5 and 3.6). Our study and all studies cited in our paper, report that even after pyramiding *Fhb1*, *Fhb2*, and *Fhb5* in the same background, the improvement did not lead to development of any NIL or RIL as resistant as the donor parent or the resistant check. This indicates that Sumai 3 and its immediate derivatives include multiple other loci conferring FHB resistance. In our study, we identified 2-3 additional loci, derived from the resistant donor parent, but none of the loci were overlapping in both populations, which in part could explain the additional resistance in the NILs. In addition to the Sumai 3 derived chromosome regions/loci identified in our study, Anderon et al. (2001) reported QTL (in addition to *Fhb1*, *Fhb2*, *Fhb5*) on 3AL and 6AS, and Zhou et al. (2002) on 2B and 7A.

The genes expressed in the chromosome regions associated with resistance include a wide variety of proteins including disease resistance proteins, protein kinases and nucleotide-binding and leucine rich repeat type proteins, which are most commonly associated with resistance to plant pathogens (Table 3.7; Bent and Mackey 2007; data not shown). The prediction of disease resistance proteins and kinases (highly expressed in spikes) in resistance conferring regions further validated our results and indicated their potential involvement in FHB suppression. Although genes listed in Table 3.7 are mostly expressed in spikes and/or grain, and are directly associated with marker sequences, these should be considered in future studies with caution because there were many other genes predicted in the regions (data not shown). The absence of genes that were predicted in the *Fhb1* region were also absent from

our POTAGE analyses, which could be attributed to the fact that this region was very diverse in susceptible lines in terms of gene content and size (Schweiger et al. 2016).

Another important observation from our results was that Sumai 3 genes did not show additive responses for field resistance, particularly in the CDC Go population (Table 3.3). The expression of *Fhb5*, which is considered to confer mainly Type-I resistance, was as strong as *Fhb1* (Type-II resistance) in both populations, indicating that *Fhb5* may also confers some level of Type-II resistance. The non-additive response of Sumai 3 derived genes or non-significant reduction even upon introgression of major genes such as *Fhb1* or *Fhb5* suggests epistatic or gene-gene interactions, which are often speculated, but overlooked in such studies. With the given marker density and good sample size in both populations, we were able to underpin the markers/genes involved in significant epistatic interactions in both populations that explained >20% of the phenotypic variation of all FHB parameters. Epistatic marker-marker interactions were previously reported for some other diseases of wheat particularly for stem rust Ug99 resistance (Yu et al. 2011, 2012); however, it is worth mentioning that interactions reported by Yu et al. (2011) explained less than 9% of the phenotypic variation which could be attributed to the nature of resistance in rusts (vertical/qualitative) vs FHB (horizontal/quantitative). Additionally, the role of environment in epistatic interactions and complex traits such as FHB was also significant, which is why epistatic interactions in our study accounted for a relatively large part of the total phenotypic variation (Bernardo 2008; Buerstmayr et al. 2009). Frequent involvement of Sumai 3 derived genes, particularly *Fhb5*, in epistatic interactions also suggests their critical role in FHB resistance. Although the nature of epistasis could not be determined in our study, the significant involvement of *Fhb1*, *Fhb2*, and *Fhb5* in interactions along with other loci (from both the recurrent and the donor parent) could explain the non-additive phenotypic expression in our populations and possibly other studies.

Before breeders can utilize any identified/mapped QTL or gene in their breeding program, validation using MAS is usually warranted because the effect is not always similar in all genetic backgrounds. NILs with improved resistance and phenological similarity to more advanced elite lines can easily be used for MAS in wheat breeding programs. However, the allelic effect on FHB resistance could differ depending on genetic background and complex epistatic interactions, thus affecting expression and penetrance of the genes in the recipient lines. Although our study suggested that improved resistance in lines carrying so-called 'native' resistance may not be as much as in S or MS lines, rare transgressive segregants can also be obtained from such cultivars/lines, which in turn again depends on their genetic background. In fact, Sumai 3 itself was a transgressive segregant from its

parents Funo and Taiwan-Xiomai wheats (Bai et al. 2018). The importance of 'native' resistance in local elite cultivars should not be ignored while breeding for FHB resistance in wheat.

CHAPTER 4

Evaluation of Fusarium head blight resistance genes *Fhb1*, *Fhb2*, and *Fhb5* introgressed into elite Canadian hard red spring wheats: Part II. Effect on agronomic and end-use quality traits and implications for breeding*

*The content of this Chapter is published as a full-length research article in 'Molecular Breeding' journal (See Brar et al. 2019b).

4.1. Preface

The previous chapter examined the effect of Sumai 3 derived genes (*Fhb1*, *Fhb2*, and *Fhb5*) on reducing Fusarium head blight (FHB) severity and deoxynivalenol accumulation. Also, it is evident from the results presented in Chapter 3 that how genetic background of the recipient parent, proportion of alleles from exotic donor and allelic interactions can influence gene expression. As the genes for FHB resistance are originally derived from exotic parent i.e. Chinese cultivar Sumai 3, it becomes important from breeder's perspective to investigate linkage drag that might result from these introgressions. This Chapter will present detailed results on the effects of Sumai 3 derived alleles on agronomic and end-use quality traits in the near-isogenic lines discussed in Chapter 3.

4.2. Abstract

Utilizing exotic sources of genes (from lines originating in China and Brazil) to develop resistance to Fusarium head blight (FHB) in common wheat is an established practice in North America due to lack of comparable resistance (smaller phenotypic effect) in local germplasm and/or associated markers for ease of selection. This study evaluated the effects of three major Sumai 3 derived FHB resistance genes *Fhb1*, *Fhb2*, and *Fhb5*, and other minor alleles inherited during crossing, on agronomic and end-use quality traits in hard red spring wheats from Canada. The BC_3 derived near-isogenic lines in CDC Go (n = 38) and CDC Alsask (n = 32) backgrounds carrying all possible combinations of these three major genes were tested in six site-years. Among agronomic traits, introgressions resulted in lower thousand kernel weight and increased plant height with *Fhb5*. Among end-use quality traits, SDS-sedimentation volume and grain protein content were affected. In addition to *Fhb1*, *Fhb2*, and *Fhb5*, we identified 10 loci in CDC Alsask NILs and 9 in CDC Go near-isogenic lines (NILs) that affected the traits measured. We found that none of these additional loci were common in both populations, indicating the presence of many alleles in exotic sources that can result in linkage drag. Linkage drag is largely dependent on the genetic background

and the proportion of resistance alleles. Therefore, we observed more adverse effects in CDC Alsask NILs than in CDC Go. Improvements in FHB resistance can still be made by introgressing these major genes using marker-assisted selection and selecting rare segregants with improved agronomic and end-use quality.

4.3. Introduction

Wheat (*Triticum* spp. L.) is one of the few widely grown field crops in Canada that is classified into various milling/market classes based on growth habit, quality and seed coat color (McCallum and DePauw 2008). Breeders are challenged to bring together favourable traits for end-use quality, disease resistance, agronomic and yield components, which is not always possible, particularly when there is little segregation in elite germplasm for a given trait. Among disease resistance traits, an intermediate level of resistance to Fusarium head blight (FHB) is required, at a minimum, for commercial cultivar registration in western Canada (Anonymous 2015b). FHB mainly caused by the hemi-biotroph *Fusarium graminearum* Schw. (teleomorph: *Gibberella zeae* (Schw.) Petch) is one of five priority-one diseases that wheat breeders must achieve an intermediate level of resistance to register new cultivars. Among the five priority-one diseases, leaf and stem rust are generally well managed due to long term breeding efforts. Stripe rust is a sporadic problem and cultivars carrying slow-rusting adult plant resistance genes are sufficient to meet the standard for registration (McCallum et al. 2016; Brar et al. 2018b). Resistance to FHB is relatively more challenging in that the trait is quantitative, highly influenced by environment and has a relatively narrow genetic base for variation in the primary gene pool (Buerstmayr et al. 2009).

Wheat breeding programs in Canada, and elsewhere, focus on the development of FHB resistant wheat cultivars, along with the development of high yields and improved overall grain quality (Gilbert and Haber 2013). The first step breeders take to introduce resistance genes into their material for FHB is to identify potential resistant donor parents and cross these with their elite material; however, in the absence of local resistance sources, they rely on exotic sources. Chinese landraces and cultivars, including Sumai 3 and some Brazilian wheat lines, are among the most commonly utilized exotic sources of FHB resistance by breeders in North America (Bai et al. 2018). One point of discussion among wheat breeders regards the use of exotic resistance quantitative trait loci (QTL) such as *Fhb1*, *Fhb2*, *Fhb4* and *Fhb5*, as opposed to so-called 'native' resistance found in local breeding lines, due to the concern arising from the lack of well-dedicated studies on linkage drag. There are a few studies (McCartney et al. 2007; Xue et al. 2010b; Salameh et al. 2011; Baksh et al. 2013; Balut et al. 2013; Clark et al. 2016) that have reported the effect of some major

exotic FHB QTL, or genes, on agronomic and end-use quality traits, but the results do not always hold true for all wheat classes or backgrounds. Additionally, most of these studies focussed on *Fhb1* and/or *Fhb5*. It has previously been shown that FHB resistance genes, or QTL, exhibit distinct behaviours in different genetic backgrounds (Verges et al. 2006; Pumphrey et al. 2007; Clark et al. 2016). With years of breeding efforts, new wheat varieties tend to show yield improvements over predecessors. This then presents a challenge for breeders making selections from their advanced lines, which eventually results in a loss of advanced material carrying exotic FHB resistance, as most of the time they out-yield as compared to other material. The majority of the native/local lines carrying FHB resistance remain uncharacterized and/or carry minor effect QTL that are not easy to select for using molecular markers, unlike the exotic major effect QTL (Bokore et al. 2017). The challenge is increased for breeders when environmental factors and genetic backgrounds affecting gene expression are considered.

As described in Chapter-3; in an effort to utilize exotic FHB resistance QTL in a more efficient manner, the bread wheat breeding program at the Crop Development Centre, University of Saskatchewan, Canada used a Sumai 3 derivative line (04GC0139) carrying three major well-characterized genes (*Fhb1*, *Fhb2*, and *Fhb5*) crossed repeatedly with hard red spring wheat cultivars to develop near-isogenic lines (NILs) so as to study the effect on disease suppression, agronomic and end-use quality traits. Chapter-3 of this dissertation entitled "**Evaluation of Fusarium head blight resistance genes *Fhb1*, *Fhb2*, and *Fhb5* introgressed into elite Canadian hard red spring wheats: Part I. Effect on disease severity and deoxynivalenol accumulation as affected by genetic background and epistatic interactions"** presented results on disease evaluation and this Chapter discusses findings on linkage drag resulting from the introgression of Sumai 3 derived FHB resistance genes into elite Canadian hard red spring wheats. The objectives were to evaluate near-isogenic lines (NILs) in CDC Go and CDC Alsask backgrounds, carrying all possible combinations of *Fhb1*, *Fhb2*, and *Fhb5*, for agronomic and end-use quality traits. In addition to characterizing the effects of the 3 aforementioned, well-characterized genes, we also evaluated the potential effect of other minor alleles on agronomy and end-use quality derived from the resistant donor parent.

4.4. Materials and methods

4.4.1. Plant material and marker analyses

The same set of NILs, described in Chapter-3, was used for the linkage drag analyses for agronomic and end-use quality traits. Single nucleotide polymorphism (SNP) data was analyzed in similar way as described in Chapter-3.

4.4.2. Yield and quality performance trials

All 32 NILs in the CDC Alsask and all 38 NILs in the CDC Go backgrounds were evaluated along with their parents over six site-years in Saskatchewan in 2016 and 2017 (Table 4.1). The sites were established at the University of Saskatchewan Goodale, Kernen, and Skarsgard Research Farms. At all three sites, the lines were seeded in 4.46 m^2 field plots in a randomized complete block design with four replicates. Crop husbandry followed the standard measures for yield performance trials. For weed control, the herbicide Velocity m3 [with three active ingredients: thiencarbazone-methyl (Group 2), pyrasulfotole (Group 27), and bromoxynil (Group 6); Bayer Crop Science] @ 1 L/ha was sprayed. No other herbicide, fungicide or insecticide was used. Plots were harvested using a plot combine harvester. The harvested grain was forced-air dried at (35°C) for 24 hrs.

Table 4.1. Description of study sites, seeding, herbicide application and harvesting dates.

	Kernen Research Farm	**Goodale Research Farm**	**Skarsgaard Research Farm**
Latitude and Longitude	52.24°N 106.67°W	52.03°N 106.29°W	52.02°N 106.25°W
Soil type			
Seeding dates	May 4, 2016	May 6, 2016	May 6, 2016
	May 22, 2017	May 12, 2017	May 13, 2017
Herbicide application[a]	June 1, 2016	June 2, 2016	June 2, 2016
	June 20, 2017	June 7, 2017	June 7, 2017
Harvest dates	August 26,2016	September 3, 2016	September 9, 2016
	September 7, 2017	August 30, 2017	August 29, 2017

[a]Velocity m3 @ 1L/ha [combines three active ingredients: thiencarbazone-methyl (Group 2), pyrasulfotole (Group 27), and bromoxynil (Group 6); Bayer Crop Science].

4.4.3. Agronomic measurements

Heading dates (HD) and physiological maturity (MT) dates were recorded when approximately 50% of the spikes were extruded (BBCH #58-59) or 50% of spikes were mature (BBCH #89). Plant height (HT) was measured at physiological maturity from both ends of the plot and averaged. Height was measured from soil surface to the tip of the spike, excluding awns. Lodging was assessed using the Belgian lodging scale as follows: Belgian

lodging score = area x intensity x 0.2 (Oplinger et al. 1985). The lodged area was rated on a scale of 1 (plot unaffected) to 10 (entire plot affected) and intensity was rated on a scale from 1 (plants standing upright) to 5 (plants lying totally flat). Grain yield (YLD) was measured from dried grain samples after harvest. A sub-sample from the yield samples for each line was cleaned to remove chaff and used for measure test weight (TW, kg/hl) and thousand-kernel weight (TKW). Test weight was measured using a 600 ml chondrometer and TKW was measured from the weight of 250 random seeds (multiplied by 4).

4.4.4. End-use quality assessment

Grain samples were cleaned of Fusarium damaged kernels (FDKs) and small seeds before quality assessment. Samples were ground to obtain wholemeal flour using a Cyclone Sample Mill (UDY Corporation, Fort Collins, CO) equipped with 1.0 mm sieve. For end-use quality assessment, grain protein concentration (GP) (%), Hagberg falling-number (FN) and SDS – sedimentation volume (cc) (SDS) were measured. Grain protein concentration was measured from total nitrogen (multiplied by 5.7) as determined using a LECO FP-528 CNA analyzer calibrated with ethylenediaminetetraacetic acid (LECO Corp., Saint Joesph, MI, USA) [American Association of Cereal Chemists (AACC) Method 46-30]. Sedimentation volumes were obtained using the method described by AACC Method 56-60.01. The falling number test was performed using AACC Method 56-81B.

4.4.5. Statistical analyses

The data collected from agronomic and end-use quality evaluations was subjected to correlation and analysis of variance (ANOVA). Before conducting the ANOVA, assumptions of the independence, normal distribution and homogeneity of the residuals for all class variables were verified using Shapiro-Wilk and Levene's Tests implemented in procedure UNIVARIATE using SAS (Statistical Analytical Software) ver. 9.4 (SAS Institute, Inc., Cary, NC). Heterogeneous variances, if any, were modeled using 'repeated/group=effect' statement in procedure MIXED (Littell et al. 2006). Variance component estimates and corresponding *F*-values were calculated using procedure MIXED in SAS ver. 9.4 with the 'ddfm= kenwardroger' option to approximate degrees of freedom. Smaller differences in means of gene classes were expected for the traits measured, therefore to reduce the chances of committing Type-I errors, mean separation was conducted using the Tukey's honest significant difference (HSD) test. All tests used a nominal alpha level of 0.05. For multiple means comparison, only recurrent parent and NILs were used as the resistant parent 04GC0139 was not expected to behave similarly. Moreover, the goal was to compare NILs with the elite recurrent parent and not the resistance donor. Pearson's correlation coefficients between various parameters were calculated using procedure CORR

in SAS. Associations among environments, genotypes, and the genotype by environment interaction were also analyzed and visualized using biplot analyses (Yan and Tinker 2006) in the R environment using the GGEBiplotGUI package (Frutos et al. 2014; the R Core Team 2016). For biplot analyses, the following settings were used: singular value portioning, environment-metric preserving; and genotype by environment scaling, according to standard deviation; centered by environment (G+G*E). Broad-sense heritability (H^2) was estimated as described in Brar et al. (2018).

4.5. Results

The *F*-values were significant among and within gene classes for all traits for the CDC Alsask population in 2016 and 2017, with the exceptions of YLD and FN in 2016, and HD, HT, YLD, and FN in 2017 (Table 4.2). For the CDC Go population, there were no significant differences among, or within gene classes for HD, FN and lodging in either year, as indicated by insignificant *F*-values. For the CDC Go population in 2016 and 2017, *F*-values were significant for MT, HT, TKW among and within gene classes. In the CDC Go population, *F*-values for gene class and entry nested within gene class for SDS volume and GP were significant only in 2016. Broad-sense heritability for all traits, except lodging, were moderate to high, depending on the year. The moderate and high H^2 estimates further indicated a strong genetic basis for variation among lines. The two biplot axes for the CDC Alsask population explained 57% of the phenotypic variation in 2016 and 42% in 2017; for the CDC Go population, the biplot axes explained 36% of the variation in 2016, and 26% in 2017 (Fig. 4.1). The positive (acute angle between trait vectors) and negative correlations (obtuse angle between traits vectors) among different traits corroborates the Pearson's correlation coefficients (Appendices E and F). The majority of the NIL entries were removed from the origin of the biplot indicating significant genotype by environment interaction, which was also evident from ANOVA results (Fig. 4.1; data not shown). There was sufficient variation among NIL entries in all environments for the traits measured, indicated by long environment vectors in biplots.

For HD in CDC Alsask in 2016, NILs carrying *Fhb1+Fhb5* headed earlier than the recurrent parent and *Fhb5* tended to shorter HD, which was favourable from a breeder's viewpoint (Table 4.3). For the CDC Go population, all NILs were comparable and only the resistant donor parent headed five days later relative to the recurrent parent CDC Go (Table 4.4). For MT, all NILs were comparable to their recurrent parents in both populations in both years (Tables 4.3 and 4.4). Plant height of CDC Alsask NILs were all comparable to the recurrent parent in both years (Table 4.3). For the CDC Go population, NILs carrying

Fhb1+*Fhb5*, *Fhb2*+*Fhb5* and *Fhb1*+*Fhb2*+*Fhb5* tended to increase PH in both years and the effect was significant for *Fhb5* in 2016 and *Fhb1*+*Fhb5* in 2017 (Table 4.4). It is hard to evaluate the effect of Sumai 3 alleles for HT in CDC Alsask NILs as the recurrent parent is significantly taller than the resistant donor (Table 4.3). The NILs were more prone to lodging in 2016, as compared to CDC Alsask, particularly those carrying *Fhb5*, *Fhb1*+*Fhb5*, *Fhb2*+*5*, and *Fhb1*+*Fhb2*+*Fhb5* (Table 4.3). In 2017, all NIL entries were comparable to CDC Alsask. The correlation between HT and lodging was positive and significant for both NIL populations in both years (Fig. 4.1; Appendices E and F).

All NIL entries in both populations were comparable to their recurrent parent for YLD; however, in the CDC Alsask population, the introgression of Sumai 3 alleles tended to increase YLD (Tables 4.3 and 4.4). For TKW in CDC Alsask, NILs in both 2016 and 2017, except for those carrying *Fhb2, Fhb2*+*Fhb5*, and *Fhb1*+*Fhb2*+*Fhb5*, all other gene combinations were comparable to recurrent parent CDC Alsask (Table 4.3). Similarly, for the CDC Go NILs, *Fhb5* and *Fhb2*+*Fhb5* in 2016 and *Fhb1*, *Fhb5*, and *Fhb1*+*Fhb2*+*Fhb5* gene classes in 2017 had lower TKW (Table 4.4). Notably, for TKW, even the NIL entries carrying none of the three genes (Null) had lower means as compared to the recurrent parents in both populations (Tables 4.3 and 4.4). For TW, CDC Go NILs did not differ from their recurrent parent in either 2016 or 2017 (data not shown). Similarly, in the CDC Alsask population, NILs were comparable for TW to their recurrent parent in both years (Table 4.5).

Among end-use quality traits, CDC Go NILs were not different from either of the parents for FN or GP (Table 4.6). For SDS-sedimentation volume, introgression of FHB resistant alleles improved the trait in CDC Alsask NILs. However, the results were the opposite for CDC Go NILs in 2016 (Tables 4.5 and 4.6). In the CDC Go population, *Fhb2*+*Fhb5* and *Fhb1*+*Fhb2*+*Fhb5* lowered the SDS-sedimentation volume values compared to the recurrent parent in 2016 (Table 4.6). In CDC Alsask NILs, the effect of Sumai 3 alleles was positive on FN and negative on GP with the exception of *Fhb5*, which lowered FN as compared to CDC Alsask (Table 4.5). For GP in the CDC Alsask population, except for *Fhb1*, all other gene classes had lower GP than the recurrent parent in both years. The lower protein values could be attributed to increased yield as yield and GP were negatively correlated (Appendices E and F).

The marker data analyses (as described in Chapter-3) revealed loci other than *Fhb1*, *Fhb2* and *Fhb5,* that were associated with agronomic and end-use quality traits in both NIL populations (Table 4.7). None of the loci were common between CDC Go and CDC Alsask NILs. Of the 10 loci in the CDC Alsask NILs, four affected more than one trait and of the

nine loci in the CDC Go NILs, only the locus on 1A affected two traits. Favourable alleles were present in both the recurrent and the donor parent for the traits under study.

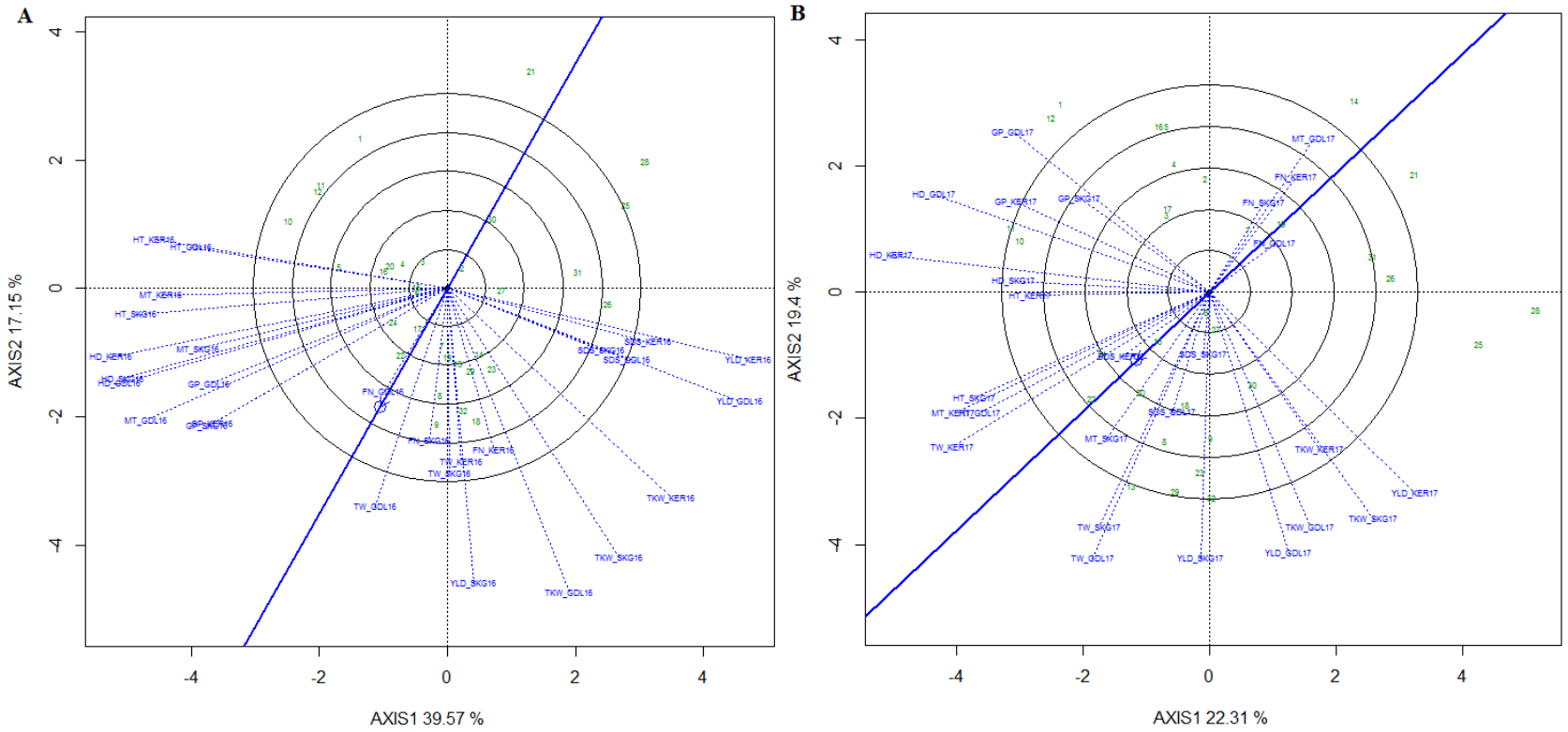
A
AXIS2 17.15 %
AXIS1 39.57 %
HT_KER16
HT_GDL16
MT_KER16
HT_SKG16
HD_KER16
MT_SKG16
HD_SKG16
HD_GDL16
GP_GDL16
MT_GDL16
GP_KER16
FN_GDL16
FN_SKG16
FN_KER16
TW_KER16
TW_SKG16
TW_GDL16
YLD_SKG16
TKW_GDL16
TKW_SKG16
TKW_KER16
SDS_SKG16
SDS_GDL16
SDS_KER16
YLD_KER16
YLD_GDL16
B
AXIS2 19.4 %
AXIS1 22.31 %
GP_GDL17
MT_GDL17
FN_KER17
HD_GDL17
GP_KER17
GP_SKG17
FN_SKG17
FN_GDL17
HD_KER17
HD_SKG17
HT_KER17
HT_SKG17
MT_KER17
MT_GDL17
SDS_KER17
SDS_SKG17
SDS_GDL17
TW_KER17
MT_SKG17
TKW_KER17
YLD_KER17
TKW_SKG17
TKW_GDL17
TW_SKG17
TW_GDL17
YLD_SKG17
YLD_GDL17

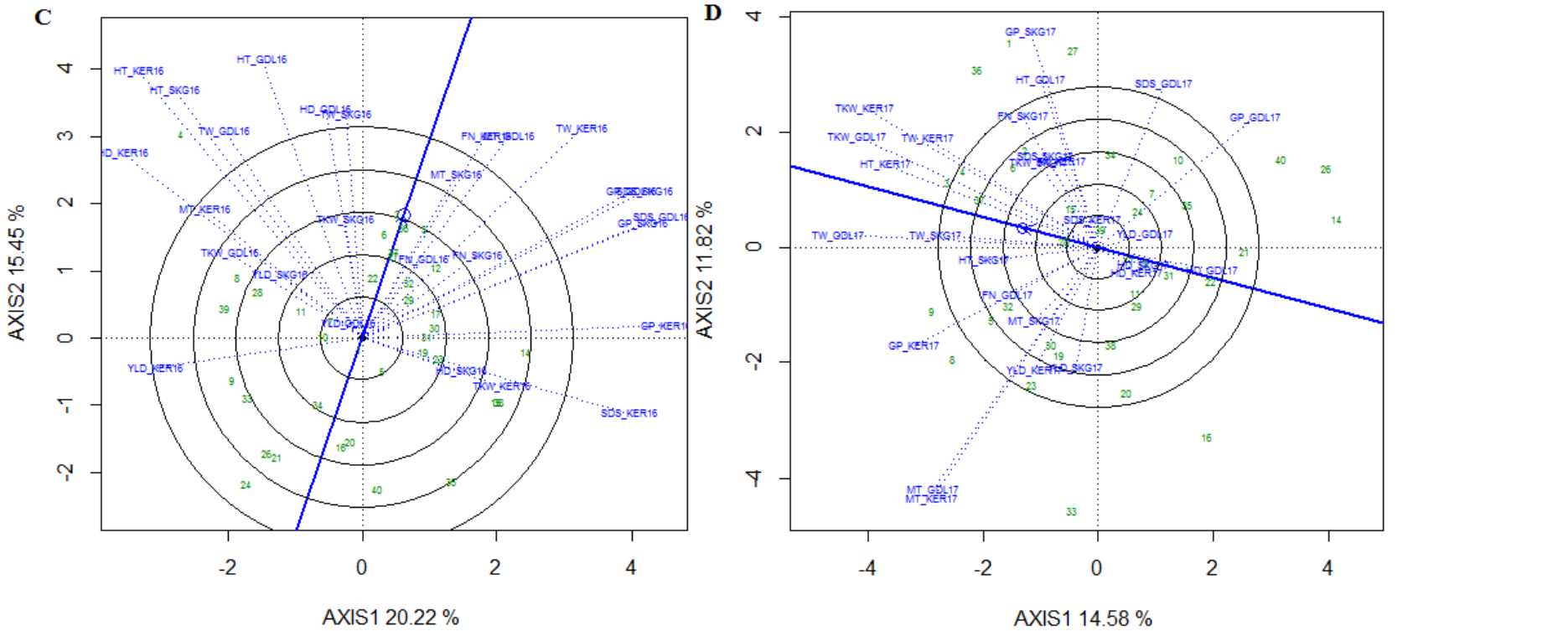

Figure 4.1. Genotype and genotype by environment (GGE) interaction plot showing relationship among genotypes, environments and their interaction for (A-B) CDC Alsask and (C-D) CDC Go near-isogenic lines (NILs) for 2016 (A and C) and 2017 (B and D). Numbers in the green indicates NIL entries and blue labels and vectors represents environment. The solid blue line passing through the origin of the plot is the 'Average Environment Axis' indicating the most ideal and discriminating environment. The axes of the plot indicate standard deviation for phenotype (proportional to length of environment vector). The phenotypic variation explained by both axes is indicated next to the labels. Here: HD= days to heading, MT= days to maturity, HT= plant height at physiological maturity, YLD=yield, TW=test weight, TKW= thousand kernel weight, SDS= SDS sedimentation volume, FN= Hagberg falling number, GP=grain protein.

Table 4.2. *F*-values and broad-sense heritability (H^2) estimates of near-isogenic lines (NILs) in CDC Go and CDC Alsask backgrounds, carrying all combinations of three Fusarium head blight (FHB) resistance genes: *Fhb1*, *Fhb2*, and *Fhb5*. The table presents the fixed effects of FHB resistance gene and entry (nested within gene) on agronomic and end-use quality traits. Grain yield, test weight, thousand kernel weight, and grain protein content are based on 14.5% moisture basis.

Effect	df[a]	Heading (days)	Maturity (days)	Plant height (cm)	Grain yield (kg/ha)	Test weight (kg/hl)	Thousand kernel-weight (g)	SDS-sedimentation (cc)	Hagberg falling number	Grain protein (%)	Lodging (Belgian scale)
						2016					
CDC Alsask NILs											
Gene	9	17.35***	3.55*	4.59**	0.98^{ns}	4.74*	43.34***	6.40***	3.22*	42.77***	6.48***
Gene (entry)	24	72.66***	12.34***	9.30***	3.44*	14.33***	20.68***	22.70***	1.95^{ns}	36.29***	2.47**
H^2	-	0.85	0.78	0.58	0.35	0.54	0.83	0.87	0.67	0.91	0.25
CDC Go NILs											
Gene	9	0.68^{ns}	2.29*	10.79***	2.68^{ns}	0.37^{ns}	3.94*	8.97***	1.53^{ns}	13.33***	1.00^{ns}
Gene (entry)	32	1.09^{ns}	2.18**	3.36***	1.75*	1.07^{ns}	3.15**	3.86***	1.24^{ns}	2.84**	1.40^{ns}
H^2	-	0.58	0.64	0.43	0.40	0.51	0.62	0.61	0.69	0.76	0.29
						2017					
CDC Alsask NILs											
Gene	9	1.85^{ns}	3.77**	0.51^{ns}	2.20^{ns}	4.41**	40.00***	3.34**	1.51^{ns}	9.89**	2.01*
Gene (entry)	24	7.09***	2.51*	4.77**	3.95**	10.32***	12.22***	5.09***	3.30***	8.97***	2.04**
H^2	-	0.39	0.42	0.38	0.42	0.44	0.93	0.61	0.63	0.77	0.32
CDC Go NILs											
Gene	9	0.47^{ns}	7.30***	9.84***	1.95^{ns}	0.53^{ns}	3.67*	2.19^{ns}	0.51^{ns}	0.92^{ns}	1.58^{ns}
Gene (entry)	32	1.24^{ns}	4.73***	3.35***	2.04^{ns}	4.15*	3.50**	1.41^{ns}	1.56^{ns}	0.82^{ns}	1.37^{ns}
H^2	-	0.49	0.76	0.41	0.42	0.43	0.78	0.67	0.66	0.71	0.23

Note: *, **, ***: significant at $P<0.05$, $P<0.001$, $P<0.0001$, respectively; [a]Degree of freedom.

Table 4.3. Least square means and standard error of mean for agronomic traits in gene classes and parents for CDC Alsask near-isogenic lines (NILs) for 2016 and 2017 growing seasons. The data in each year was combined over three sites. Means followed by same letter are not statistically significantly different according to Tukey's honest significant difference (HSD) at $P = 0.05$. All traits are reported at a constant 14.5% moisture basis.

Genotype/gene class	Heading (days)		Maturity (days)		Plant height (cm)		Grain yield (kg/ha)		TKW[a] (g)		Lodging[b]	
	Mean[c]	SEM[d]	Mean	SEM	Mean	SEM	Mean	SEM	Mean	SEM	Mean	SEM
2016												
04GC0139 (RD)[e]	55.4	0.54	98.6	0.61	91.8	2.27	4007	287.0	33.3	0.86	1.05	0.58
CDC Alsask (RP)[f]	55.2 ab	0.53	90.8 ab	0.61	98.4 ab	2.34	4289[d]	270.7	37.4 a	0.90	2.13 c	0.58
Null (n= 4)[e]	54.9 b	0.50	91.0 ab	0.52	99.7 a	2.24	4570	239.2	35.6 c	0.74	4.61 ab	0.29
Fhb1 (n= 6)	54.8 b	0.50	90.8 ab	0.51	97.6 b	2.21	4535	237.4	36.9 a	0.73	3.85 bc	0.24
Fhb2 (n= 4)	55.0 ab	0.50	91.3 ab	0.52	97.2 b	2.23	4617	241.1	36.0 bc	0.73	3.58 c	0.29
Fhb5 (n= 2)	54.5 b	0.52	90.7 ab	0.55	98.2 ab	2.27	4628	247.2	36.6 abc	0.78	4.75 ab	0.41
Fhb1+Fhb2 (n= 2)	55.6 a	0.51	91.6 ab	0.55	96.8 b	2.27	4622	247.6	37.5 a	0.76	3.31 c	0.41
Fhb1+Fhb5 (n= 4)	53.8 c	0.50	90.5 b	0.52	97.4 b	2.23	4578	240.4	36.7 ab	0.74	5.20 a	0.29
Fhb2+Fhb5 (n= 6)	54.7 b	0.50	91.6 a	0.51	99.5 a	2.22	4435	238.0	33.7 d	0.74	4.99 a	0.24
Fhb1+Fhb2+Fhb5 (n= 4)	54.7 b	0.50	91.4 ab	0.52	98.4 ab	2.24	4461	237.6	34.5 d	0.74	4.84 ab	0.29
2017												
04GC0139 (RD)	58.5	1.57	95.0	1.30	92.0	1.70	5067	212.2	33.9	0.28	0.09	0.55
CDC Alsask (RP)	56.2[d]	1.57	89.6 ab	1.36	100.5[d]	1.69	4816[d]	209.9	36.9 abc	0.41	5.95 a	0.55
Null (n= 4)	55.7	1.38	89.3 b	1.24	98.0	1.54	4846	181.6	35.0 d	0.22	4.86 ab	0.33
Fhb1 (n= 6)	55.6	1.36	90.0 ab	1.22	98.4	1.52	4982	178.1	36.8 ab	0.21	5.36 a	0.30
Fhb2 (n= 4)	55.6	1.37	90.3 ab	1.25	98.3	1.54	5032	181.4	35.3 d	0.22	4.33 b	0.33
Fhb5 (n= 2)	55.0	1.42	89.5 ab	1.28	97.7	1.59	4988	191.4	36.1 c	0.23	5.38 ab	0.42
Fhb1+Fhb2 (n= 2)	55.9	1.42	91.5 a	1.32	97.8	1.59	5178	191.4	37.1 a	0.23	4.73 ab	0.42
Fhb1+Fhb5 (n= 4)	55.1	1.38	89.8 ab	1.23	97.9	1.54	4906	182.3	36.1 bc	0.24	5.52 a	0.33
Fhb2+Fhb5 (n= 6)	55.7	1.36	90.7 a	1.23	98.8	1.52	4994	178.2	34.1 e	0.21	5.23 ab	0.30
Fhb1+Fhb2+Fhb5 (n= 4)	55.5	1.38	91.4 a	1.25	98.7	1.54	5003	181.7	34.7 de	0.26	5.18 ab	0.33

[a]Thousand kernel weight; [b]Measured using Belgian scale as follows: Area affected (1-9) x Intensity of lodging (1-5) x 0.2; [c]Least squares' mean; [d]Standard error of mean; [e]Number of NILs; [d]Means are not statistically different among gene classes; [e]Resistance donor; [f]Recurrent parent.

Table 4.4. Least square means and standard error of mean for agronomic traits in gene classes and parents for CDC Go near-isogenic lines (NILs) for 2016 and 2017 growing seasons. The data in each year was combined over three sites. Means followed by same letter are not statistically significantly different according to Tukey's honest significant difference (HSD) at $P = 0.05$. All traits are reported at a constant 14.5% moisture basis.

Genotype/gene class	Heading (days)		Maturity (days)		Plant height (cm)		Grain yield (kg/ha)		TKW[a] (g)	
	Mean[c]	SEM[d]	Mean	SEM	Mean	SEM	Mean	SEM	Mean	SEM
2016										
04GC0139 (resistance donor)	54.7	0.69	98.6	0.63	90.3	1.79	3889	282.9	33.3	1.25
CDC Go (recurrent parent)	50.3[f]	0.69	91.0 ab	0.54	81.7 bcd	1.79	5017[f]	282.9	41.6 a	1.37
Null (n= 7)[e]	50.0	0.65	91.1 ab	0.45	81.2 d	1.63	5003	274.0	40.3 ab	1.34
Fhb1 (n= 6)	50.0	0.67	91.1 ab	0.46	82.2 cd	1.63	5055	274.3	40.2 ab	1.34
Fhb2 (n= 4)	50.1	0.67	91.2 ab	0.47	81.8 cd	1.65	5095	275.2	40.3 ab	1.35
Fhb5 (n= 2)	50.3	0.67	91.2 ab	0.50	85.2 a	1.70	5192	277.8	39.9 b	1.35
Fhb1+Fhb2 (n= 4)	50.2	0.67	91.5 a	0.46	82.7 bcd	1.65	5103	275.2	40.3 ab	1.35
Fhb1+Fhb5 (n= 6)	50.1	0.67	90.9 b	0.46	84.1 ab	1.64	4989	274.3	40.7 ab	1.35
Fhb2+Fhb5 (n= 4)	49.8	0.67	90.7 b	0.48	83.0 bc	1.65	4975	275.2	40.1 b	1.35
Fhb1+Fhb2+Fhb5 (n= 5)	50.2	0.67	91.1 ab	0.46	83.9 ab	1.64	5079	274.6	40.6 ab	1.35
2017										
04GC0139 (resistance donor)	55.3	0.95	97.2	0.40	89.0	4.38	4452	746.8	35.0	0.95
CDC Go (recurrent parent)	50.7[f]	0.95	90.3 abc	0.36	84.6 bc	4.37	5208[f]	744.6	42.8 a	0.93
Null (n= 7)	50.8	0.94	89.6 c	0.24	84.8 c	4.32	5340	734.0	41.3 bc	0.85
Fhb1 (n= 6)	50.9	0.94	90.7 a	0.25	84.8 c	4.32	5334	734.3	41.1 bc	0.85
Fhb2 (n= 4)	51.0	0.94	90.6 ab	0.26	84.5 c	4.33	5418	735.4	41.5 abc	0.87
Fhb5 (n= 2)	50.9	0.95	89.9 abc	0.32	86.6 ab	4.34	5268	738.8	41.3 bc	0.88
Fhb1+Fhb2 (n= 4)	50.9	0.94	90.5 ab	0.27	84.7 c	4.33	5382	735.4	41.9 ab	0.86
Fhb1+Fhb5 (n= 6)	50.9	0.94	90.3 ab	0.25	86.9 a	4.32	5346	734.2	41.7 abc	0.85
Fhb2+Fhb5 (n= 4)	50.9	0.94	89.8 bc	0.27	86.0 abc	4.33	5438	735.4	40.8 c	0.85
Fhb1+Fhb2+Fhb5 (n= 5)	50.9	0.94	90.9 b	0.25	86.6 ab	4.33	5441	734.8	41.4 abc	0.85

[a]Thousand kernel weight; [b]Measured using Belgian scale as follows: Area affected (1-9) x Intensity of lodging (1-5) x 0.2; [c]Least squares' mean; [d]Standard error of mean; [e]Number of NILs; [f]Differences not significant.

Table 4.5. Least square means and standard error of mean for test weight and end-use quality traits in gene classes and parents for CDC Alsask near-isogenic lines (NILs) in 2016 and 2017 growing seasons. The data in each year was combined over three sites. Means followed by same letter are not statistically significantly different according to Tukey's honest significant difference (HSD) at $P = 0.05$. All traits are reported at constant 14.5% moisture basis.

Genotype/gene class	Test weight (kg/hl)		SDS-sedimentation volume (cc)		Hagberg falling number		Grain protein (%)	
	Mean[a]	SEM[b]	Mean	SEM	Mean	SEM	Mean	SEM
			2016					
04GC0139 (resistance donor)	81.2	0.31	52.6	1.46	331	24.7	14.5	0.26
CDC Alsask (recurrent parent)	79.2 ab	1.01	78.3 c	1.44	455 c	23.8	16.6 a	0.27
Null (n= 4)[c]	79.4 b	0.21	81.3 abc	1.08	474 bc	20.5	16.1 a	0.25
Fhb1 (n= 6)	79.1 b	0.20	81.2 bc	1.05	477 bc	20.1	16.2 a	0.25
Fhb2 (n= 4)	79.4 b	0.20	80.2 c	1.09	490 ab	20.2	15.7 b	0.25
Fhb5 (n= 2)	79.4 b	0.23	79.8 bc	1.14	460 c	20.9	15.6 bc	0.25
Fhb1+Fhb2 (n= 2)	80.1 a	0.22	79.9 bc	1.19	501 a	20.5	15.8 b	0.25
Fhb1+Fhb5 (n= 4)	79.6 ab	0.20	83.2 a	1.08	474 bc	20.2	15.4 cd	0.25
Fhb2+Fhb5 (n= 6)	79.5 b	0.20	80.1 c	1.05	474 bc	20.1	15.2 d	0.25
Fhb1+Fhb2+Fhb5 (n= 4)	78.8 b	0.52	82.2 ab	1.09	470 bc	20.3	15.2 d	0.25
			2017					
04GC0139 (resistance donor)	86.5	0.68	52.4	5.47	354	7.84	14.9	0.79
CDC Alsask (recurrent parent)	84.4 b	0.68	75.8 c	5.45	408 a	7.72	16.8 a	0.78
Null (n= 4)	84.5 b	0.66	80.5 a	5.30	402 ab	6.73	16.3 ab	0.76
Fhb1 (n= 6)	84.3 b	0.65	80.6 a	5.28	401 ab	6.61	16.3 ab	0.76
Fhb2 (n= 4)	84.3 b	0.66	79.7 a	5.30	405 a	6.72	16.1 bc	0.76
Fhb5 (n= 2)	84.2 b	0.66	78.3 abc	5.35	390 b	7.07	15.7 cd	0.77
Fhb1+Fhb2 (n= 2)	85.1 a	0.66	80.0 a	5.35	410 a	7.07	15.8 bcd	0.77
Fhb1+Fhb5 (n= 4)	84.6 ab	0.66	80.3 a	5.30	403 ab	6.75	15.7 cd	0.76
Fhb2+Fhb5 (n= 6)	84.2 b	0.65	77.5 bc	5.28	400 ab	6.61	15.6 cd	0.76
Fhb1+Fhb2+Fhb5 (n= 4)	84.3 b	0.66	79.2 ab	5.30	401 ab	6.73	15.5 d	0.76

[a]Least squares mean; [b]Standard error of mean; [c]Number of NILs.

Table 4.6. Least square means and standard error of mean for end-use quality traits in gene classes and parents for CDC Go near-isogenic lines (NILs) in 2016 and 2017 growing seasons. The data in each year was combined over three sites. Means followed by the same letter are not statistically significantly different according to Tukey's honest significant difference (HSD) at $P = 0.05$. All traits are reported at constant 14.5% moisture basis.

Genotype/gene class	SDS-sedimentation volume (cc)		Hagberg falling number		Grain protein (%)	
	Mean	SEM	Mean	SEM	Mean	SEM
		2016				
04GC0139 (resistance donor)	51.8	2.19	308	10.98	15.0	0.20
CDC Go (recurrent parent)	80.1 a	2.12	408[d]	11.61	15.2 abc	0.23
Null (n= 7)[c]	79.0 a	1.99	407	7.28	15.3 a	0.21
Fhb1 (n= 6)	79.0 a	1.99	405	7.43	15.3 a	0.21
Fhb2 (n= 4)	77.9 a	2.10	404	7.95	15.1 abc	0.21
Fhb5 (n= 2)	77.5 a	2.10	410	9.33	14.7 d	0.22
Fhb1+*Fhb2* (n= 4)	78.7 a	2.01	409	7.95	15.3 a	0.21
Fhb1+*Fhb5* (n= 6)	78.9 a	2.00	415	7.43	15.1 ab	0.21
Fhb2+*Fhb5* (n= 4)	77.2 b	2.01	403	7.95	14.9 cd	0.21
Fhb1+*Fhb2*+*Fhb5* (n= 5)	74.5 c	2.00	397	7.64	14.9 bcd	0.22
		2017				
04GC0139 (resistance donor)	50.2	4.02	340	8.17	14.0	0.35
CDC Go (recurrent parent)	79.4[d]	4.04	359[d]	7.38	14.6[d]	0.34
Null (n= 7)	78.6	3.89	356	5.47	14.6	0.26
Fhb1 (n= 6)	77.9	3.89	358	5.54	14.5	0.27
Fhb2 (n= 4)	76.2	3.90	357	5.80	14.5	0.27
Fhb5 (n= 2)	77.5	4.09	357	6.63	14.3	0.31
Fhb1+*Fhb2* (n= 4)	78.6	3.91	362	5.78	14.5	0.27
Fhb1+*Fhb5* (n= 6)	78.5	3.89	361	5.55	14.5	0.27
Fhb2+*Fhb5* (n= 4)	76.7	3.91	353	5.76	14.5	0.27
Fhb1+*Fhb2*+*Fhb5* (n= 5)	75.1	3.90	359	5.64	14.3	0.27

[a]Least squares mean; [b]Standard error of mean; [c]Number of NILs; [d]means are not statistically different among gene classes.

Table 4.7. Single nucleotide polymorphism (SNP) markers alleles (other than *Fhb1*, *Fhb2*, *Fhb5*) associated (significant at $P = 0.001$ for coefficient of determination) with agronomic and end-use quality traits in CDC Alsask and CDC Go near-isogenic lines (NILs).

Chromosome - Marker name	Physical location (Mb)[a]	Associated trait(s) and favourable allele[b]
	CDC Alsask NILs	
1A - *TA001286-0611-w*	3.78	SDS-sedimentation (BB)
1B - *TA002086-0901*	1.52	Days to heading (BB), plant height (BB), grain protein (AA)
2A - *RAC875_c19328_198*	400.98	Hagberg falling number (BB)
2B - *Excalibur_rep_c68899_1400*	91.03 – 92.99	Plant height (BB)
3B - *Kukri_c21818_519, BS00022122_51*	547.45 – 556.05	Plant height (AA), Thousand kernel weight (AA)
5B - *wsnp_CAP11_c948_571287*	475.58	Test weight (AA)
5B - *IACX9261, IAAV2426, IAAV1148, IAAV2219*	545.40 – 577.30	Plant height (BB), grain protein (AA)
7B - *BS00063852_51*	170.52	Days to maturity (BB), test weight (AA)
7D - *Kukri_c58234_519, Ex_c8238_637*	413.24 – 461.20	Grain protein (AA)
7D - *Excalibur_c4508_1007, wsnp_Ex_c145_285194*	518.78 – 530.67	Grain protein (AA)
	CDC Go NILs	
1A - *TA001450-1081*	513.12	Days to heading (BB)
1A - *IAAV5567*	571.27	Yield (BB), SDS-sedimentation (AA)
1A - *IAAV4238, RAC875_c62550_470*	582.86 – 583.89	Days to maturity (BB)
1D - *RAC875_c68124_167*	474.01	SDS-sedimentation (AA)
2D - *RAC875_c4267_1269*	293.13	Plant height (AA)
2A - *wsnp_Ex_rep_c69014_67914888*	675.07 – 676.98	Thousand kernel weight (AA)
2A - *Kukri_c29170_680*	692.93 – 693.29	Thousand kernel weight (AA)
7A - *BS00038787_51, IAAV4340, IAAV4831*	112.26 – 124.79	Days to maturity (BB)
7A - *Excalibur_c113078_320*	688.96 – 689.26	SDS-sedimentation (AA)

[a]Refer to whole-genome shotgun assembly of Chinese Spring common wheat (https://urgi.versailles.inra.fr/).

[b]AA – CDC Go or CDC Alsask, BB – 04GC0139 (resistance donor).

4.6. Discussion

As a continuation of Chapter-3, this study further investigated potential linkage drag associated with the NILs segregating for Sumai 3 derived FHB major genes. The yield trials in our study were established in 2016 and 2017. It was ensured that the grain harvest from test plots were not affected by FHB so that the allelic effects could be measured reliably. The earlier heading with introgression of *Fhb5* and *Fhb1+Fhb5*, in addition to no adverse effects shown by *Fhb1* in this study, support similar results reported by McCartney et al. (2007), Salameh et al. (2011) and Tamburic-Ilincic (2012). Suzuki et al. (2012) reported delayed anthesis/heading due to the introgression of *Fhb2* from Sumai 3 in Japanese spring wheat, which was not confirmed by any other study, nor ours. Salameh et al. (2011), Suzuki et al. (2012) and Tamburic-Ilincic (2012) reported a significant increase in HT from the introgression of the *Fhb5* allele, which supports our findings. McCartney et al. (2007) reported reduced HT from the introgression of the 3BS allele from Nyubai, which is flanked by *gwm493* and *gwm533* spanning the *Fhb1* region and the QTL is considered to be the same as *Fhb1* (Liu et al. 2006). We did not detect any negative effect from *Fhb1* on agronomy, which agrees with all other studies (Salameh et al. 2011; Suzuki et al. 2012), except for McCartney et al. (2007). The negative effect of Sumai 3 alleles on TKW was reported by McCartney et al. (2007) and von der Ohe et al. (2010), similar to our findings, whereas no effect was reported by Salameh et al. (2011) and Suzuki et al. (2012). McCartney et al. (2007) also reported a 0.3-0.4% decrease in GP with the introgression of *Fhb5*, which corroborate our findings on decreased GP from *Fhb1* and *Fhb2* introgressions, or from stacking of two or more FHB genes together.

We successfully identified loci, other than the three major genes under investigation, that influenced trait values in both populations. More than one locus was identified for traits showing greater differences in least square means, such as TKW and SDS-sedimentation volumes in the CDC Go and GP in the CDC Alsask populations. None of these loci were in common for the CDC Alsask or the CDC Go populations, which implies that there could be many uncharacterized loci in exotic FHB resistance donors that can result in linkage drag. NILs carrying FHB resistance genes in both populations had lower TKW, which could be attributed not only to *Fhb1*, *Fhb2* and *Fhb5,* but also to two additional polymorphic loci in CDC Go and to one in the CDC Alsask population resulting in the mean difference. All favourable alleles for TKW were derived from recurrent parents suggesting that any additional allele in linkage phase with favourable resistance improving alleles from the resistant donor parents could result in linkage drag affecting TKW or other traits. Although

the resistant donor parent had late maturity, the NILs in the CDC Go population tended to have a lower MT, which could be attributed to two additional favourable marker alleles from the resistant donor. For MT, Baksh et al. (2013) reported that *Fhb1* caused early maturity in hard red winter wheat in the USA. Our study did not corroborate this association. CDC Alsask NILs tended to have higher SDS-sedimentation volumes, whereas CDC Go NILs behaved oppositely (Tables 5 and 6). The discrepancy could be attributed to the CDC Alsask NILs segregating for the locus where the resistant donor allele also favoured the trait, whereas in the CDC Go population, three loci were segregating for which only the recurrent parent allele was favourable. Additionally, CDC Alsask carried the *Glu-B1* locus which encodes for the overexpressed Bx7OE glutenin-subunit (Hucl et al. 2016). Similarly, the lower GP in CDC Alsask NILs could be attributed to the addition of major FHB genes, where three other segregating loci affect the trait, with the favourable allele derived from the recurrent parent.

In conclusion, our results, together with those of the other studies reviewed, support the conclusion that agronomic and end-use quality trait values vary depending on the genetic background of the recipient parent and the proportion of donor parent alleles. As the proportion of the alleles derived from the non-adapted resistant donor parent is greater in CDC Alsask NILs as compared to CDC Go, we observed more linkage drag in CDC Alsask NILs. In addition, there appears to be a trade-off between linkage drag and resistance improvement when breeders utilize exotic resistance donors. In summary, there were no negative effects on agronomic traits except for TKW and a small increase in HT with the introgression of *Fhb5*. For end-use quality traits, there were small negative effects in SDS-sedimentation volume and GP. However, these small effects were largely dependent on the genetic background of the recurrent parent. Repeated backcrossing can minimize deleterious impacts of the introgressed segments and marker-assisted selection can speed resistance breeding effort by selection for genes with major effects such as *Fhb1*, *Fhb2*, *Fhb4*, and *Fhb5* even in the absence of disease. Although a total absence of linkage drag is not possible, breeders should use the best NILs developed in their program to cross with susceptible elite backgrounds to eventually select rare segregants that have reported desirable levels of disease resistance, agronomic and end-use quality traits.

CHAPTER 5

Fusarium head blight (FHB) resistance genes *Fhb1* and *Fhb5* in hard red spring wheat do not interact with metconazole fungicide*

*The content of this Chapter is published as a full-length research article in 'Plant Disease' journal (See Brar et al. 2019c).

5.1. Preface

Chapter 3 has a detailed description of near-isogenic lines (NILs) in CDC Go and CDC Alsask backgrounds and their allelic proportions from resistant donor parent. In Chapters 3 and 4, we have precisely evaluated the effects (on disease, agronomy and end-use quality) of Sumai 3 derived Fusarium head blight (FHB) resistance genes, *Fhb1*, *Fhb2*, and *Fhb5*. As described in Chapters 1 and 2, an integrated approach is recommended for management of FHB in wheat and fungicide application and genetic resistance are two integral parts of such strategy. The experiment discussed in the present Chapter was designed to study if *Fhb1* and *Fhb5* have any interaction with the fungicide application. Interaction of genes and fungicides is reported in other wheat pathosystems, however, there is no such study on interaction of triazoles and FHB resistance genes. Triazole chemistry-based fungicide with active ingredient metconazole was chosen as it is recommended for FHB in Canada.

5.2. Abstract

Fusarium head blight (FHB) (caused by *Fusarium graminearum* Schwabe) is one of the most important diseases of wheat in Canada and can cause significant economic loss. Although plenty of research has been published on integrated control of FHB and some of these studies have reported cultivar by fungicide interactions, the interaction of specific Sumai 3 derived major FHB QTL with triazole fungicides has not been reported. In our study, near-isogenic lines (NILs; <1.0% genome/alleles from the resistance donor), carrying *Fhb1* and *Fhb5* in a hard red spring wheat cultivar CDC Go background, were used to study the interaction of the genes with the triazole fungicide Caramba® (metconazole). Field experiments were conducted in five site-years in Saskatchewan, Canada between 2016 and 2017. There was an additive effect between the NILs and metconazole in suppressing FHB and deoxynivalenol (DON) accumulation in the grain. Fungicide efficacy (FE) on FHB in wheat is often inconsistent in the literature. In our study, FHB severity was generally lower and FE was higher on the moderately susceptible (MS) CDC Go than on the moderately resistant (MR) NILs carrying *Fhb1* and *Fhb5*, relative to respective untreated controls. In spite of higher FE,

the MS cultivar still showed greater FHB severity as compared to MR NILs. This shows the importance of using cultivar resistance in FHB management. Under moderate or high FHB disease pressure, fungicides may be warranted even on MR cultivars to reduce the FHB index and DON accumulation.

5.3. Introduction

Fusarium head blight (FHB), commonly known as scab, is a fungal disease of small grain cereal crops such as wheat, barley, oats, rye, and annual canarygrass (Cholango-Martinez et al. 2016; McMullen et al. 2012). The disease can be caused by several *Fusarium* spp., but is most acute when these crops are infected by *Fusarium graminearum* Schwabe (syn: *Gibberella zeae* Schw. [Petch]), at least in Canada and the United States and most wheat growing regions worldwide. *Fusarium graminearum* has been referred to as a species complex (FGSC) that includes at least 16 biogeographically structured lineages (Shen et al. 2012). The disease is not new to North America, and its importance can be realized from severe epidemics in 1993 and 1996, which resulted in the establishment of the United States Wheat and Barley Scab Initiative (USWBSI) to advocate specific federal funding for FHB research. The economic impact of those epidemics is discussed in great detail in a feature article by McMullen et al. (1997). This spike disease of small grain cereals results in yield as well as quality loss and causes seedling blight if infected seed is sown the next year (Gilbert and Haber 2013). The quality loss is mainly associated with the production of shrivelled, light-weight and chalky white kernels contaminated with mycotoxins, including deoxynivalenol (DON) and nivalenol (NIV) that have detrimental effects on human and animal health (Gilbert and Haber 2013; McMullen et al. 2012). Due to the concerns over toxin accumulation in the grain, countries have imposed limits on toxin levels present in food and feed items which makes it a more practical problem associated with FHB (Gilbert and Haber 2013). In spite of massive research, FHB remains an important disease of wheat in Canada and world-wide, and the resulting toxins are the most dangerous consequence of FHB epidemics.

Effective management of FHB disease is imperative to prevent yield and quality losses in small-grain cereals. Several studies support the integration of cultural, chemical and host resistance to manage FHB in wheat (Amarasinghe et al. 2013; Blandino et al. 2012; Scala et al. 2016; Wegulo et al. 2011; Willyerd et al. 2012). However, until recently there was a limited choice/availability of moderately resistant (MR) cultivars, and even today, the majority of the cultivars in western Canada (and elsewhere) are only moderately susceptible (MS) or Intermediate (I) in resistance (Anonymous 2018). Cultivars with differential

resistance are mainly in hexaploid wheat, whereas all durum cultivars in North America are susceptible to MS. A crop species diverse (e.g. four-year crop) rotation has become a less common practice by growers because of limited choices of non-host crops, large farm size, and economic reasons (Beres et al. 2018). Use of fungicides has been adopted by wheat growers, and the triazole fungicides are one of the most important classes that have been used since the 1980s to control plant pathogenic fungi (Cools et al. 2013). Among fungicides, demethylation inhibitor (DMI) triazole fungicides are preferred for control of FHB and for reducing DON accumulation (Boyacioglu et al. 1992; McMullen et al. 2012; Paul et al. 2008). Compared to single site-specific fungicides that can be rendered ineffective due to single point mutations in the pathogen, the efficacy of DMIs has decreased relatively slowly as they target multiple sites (Cools et al. 2013). Triazoles are preferred over quinone outside inhibitor (QoI) fungicides as the latter tend to increase DON contamination of the grain (Amarasinghe et al. 2013; Bissonnette et al. 2018; Paul et al. 2018; Ye et al. 2017). Evaluation of commonly used DMI inhibitors indicated that metconazole (Caramba®; BASF Corporation, Ludwigshafen, Germany), prothioconazole (Proline®; Bayer CropScience, Leverkusen, Germany), and tebuconazole + prothioconazole (Prosaro®; Bayer CropScience) would offer the most effective FHB and DON reduction (Paul et al. 2008). The greater efficacy of metconazole and prothioconazole + tebuconazole in reducing FHB index and DON was also demonstrated in a recent network meta-analyses of 19 years of fungicide trials in the United States (Paul et al. 2018).

Few studies have determined the effect of integrating multiple strategies to manage FHB in wheat, particularly the combination of host resistance and fungicide application (Amarasinghe et al. 2013; McMullen et al. 2012; Mesterhazy et al. 2003; Scala et al. 2016; Wegulo et al. 2011; Willyerd et al. 2012; Ye et al. 2017). Significant cultivar by fungicide interaction was reported in some of the above-mentioned studies; however, only very few of the studies used cultivars carrying any known resistance gene/QTL. FHB resistant cultivars with identified QTLs or genes were only available in the last 5-6 years; most studies looked at fungicide efficacy on single or multiple cultivars with only small differences in FHB resistance/tolerance. Some of the MR cultivars in North America derive their resistance from Sumai 3 or its derivatives and carry *Fhb1*, *Fhb2*, *Fhb5* and/or minor QTL and the use of Sumai 3 derived resistance in modern cultivars is increasing (reviewed in Bai et al. 2018; Gilbert and Haber 2013; McMullen et al. 2012). The availability of breeder-friendly and robust molecular markers for *Fhb1* has helped to introgress this gene into elite wheat germplasm (Liu et al. 2008; Rawat et al. 2016). Recently, *Fhb1* was introgressed into 16 locally adapted hard winter wheat cultivars and breeding lines from five states in the USA

(Bai et al. 2018). Some of the prior studies looked at combining fungicide application with MR cultivars to mitigate the damage by FHB, but the results were not consistent and the resistance genes/QTLs in these cultivars were unknown. The objective of the present study was to investigate potential interactions of well-characterized FHB resistance genes with a triazole fungicide in FHB control. Near-isogenic lines (NILs) carrying *Fhb1*, *Fhb2*, and *Fhb5* in the same genetic background were used in order to account for the effects resulting from these introgressed genes. The fungicide Caramba (metconazole) was chosen based on prior information and its recommended use in western Canada.

5.4. Materials and methods

5.4.1. Plant material

Six wheat lines were included in the present study that consisted of CDC Go (recurrent parent of NILs and a MS check), Carberry (*Fhb1*+*Fhb5*+ unknown QTL; MR check), CDC Go NIL-2 (*Fhb1*+*Fhb5*), CDC Go NIL-21 (*Fhb5*), CDC Go NIL-28 (*Fhb1*+*Fhb2*+*Fhb5*), and CDC Go NIL-38 (*Fhb1*). CDC Go (pedigree: Grandin/SD3055) and Carberry (pedigree: Alsen/Superb) are hard red spring wheat cultivars, registered for cultivation in western Canada (DePauw et al. 2011; P. J. Hucl, unpublished data). The NILs were developed from the crosses CDC Go*4/04GC0139 by the single-seed decent method. Line 04GC0139 (pedigree: ND2710/RL4851//BW278), was provided by Dr. Julian Thomas (retired, Cereal Research Centre, Agriculture and Agri-Food Canada, Winnipeg, MB), and carries *Fhb1*, *Fhb2*, and *Fhb5* genes (J. Thomas; G.S. Brar, unpublished data). During NIL development, F_1 donor for each BC cycle was screened with microsatellite markers for marker-assisted selection, i.e. *umn10* for *Fhb1* (Liu et al. 2008), *gwm133* and *gwm644* for *Fhb2* (Cuthbert et al. 2007), and *gwm304*, *gwm293*, *barc117*, *wmc705* for *Fhb5* (Xue et al. 2011).

5.4.2. NIL genotyping

The original crosses were made to develop NILs carrying combinations of *Fhb1*, *Fhb2* and *Fhb5* in the CDC Go background, and microsatellite markers flanking these QTL regions were utilized for marker-assisted selection. To confirm the presence of these QTL regions, NILs were genotyped further with the following molecular markers: *umn10*, *gwm493* and *gwm533*, functional markers for the pore-forming toxin (PFT) protein associated with *Fhb1* (Liu et al. 2008; Rawat et al. 2016), as well as single nucleotide polymorphism (SNP) markers from Zhao et al. (2018); *gwm304*, *barc117*, *wmc705*, *gwm415*, *gwm293*, *barc180*, *barc186* and SNPs from Buerstmayr et al. (2017) for *Fhb5*; and *gwm644*, CAPS3 and SNPs from Zhao et al. (2018) for *Fhb2*. Additionally, NILs were also genotyped using a wheat 90K iSelect SNP genotyping assay (90K, hereafter) following the protocol described by

Wang et al. (2014). Briefly, SNP alleles were called using GenomeStudio (Illumina Inc., San Diego, CA, USA) and filtered based on polymorphisms between parents. All SNP markers from the wheat 90K assay were physically positioned on the Chinese Spring wheat reference genome sequence. The SNP-bearing sequences were probed to the entire bread wheat NRGene genome assembly RefSeq ver. 1.0 (International Wheat Genome Sequencing Consortium, https://wheat-urgi.versailles.inra.fr/Seq-Repository/Assemblies) using an *in-house* BLAST portal.

5.4.3. Study sites, experimental design, disease inoculation and fungicide application

The experiment was conducted in field plots near Saskatoon and Outlook (2016), and Saskatoon, Melfort and Outlook (2017) for a total of five site-years. However, the Saskatoon site (2017) was abandoned due to negligible disease pressure of FHB. Details on seeding, inoculation, fungicide application, disease assessment and harvest dates are provided in Table 1. Sprinkler irrigation was provided at Saskatoon for four weeks starting from early flowering to foster a conducive environment for disease development, whereas the Melfort trial was not irrigated. At the Outlook site, irrigation was applied through an overhead low-pressure system to keep the available soil moisture above 50%. In 2016, due to above normal (155% of normal) precipitation, only a single application of 12.5 mm was applied on June 8. In 2017, irrigation was applied six times (June 27, 28, July 6, 10, 18, and 31) targeting at 12.5 mm for single application and 75 mm for the whole growing season. The experiment was a randomized complete block design with four replications. The experiment had 12 treatment combinations consisting of six genotypes and two fungicide application treatments (applied or not applied). Corn (*Zea mays* L.) spawn inoculum (colonized by *F. graminearum*) was applied to the surface of all plots at all sites about 12-14 days prior to flowering at 5 g/m^2. Two isolates of *F. graminearum*, M9-07-1, a 3-ADON chemotype (NRRL 52068) and M1-07-2, a 15-ADON chemotype (NRRL 47847), were used for preparing corn spawn inoculum (Gilbert et al., 2014). The corn spawn inoculum was prepared using PDA plate method described in Gilbert and Woods (2006). Natural rainfall and irrigation re-hydrated the corn inoculum and initiated fungal growth and sporulation. The triazole fungicide metconazole was applied at the recommended 50% anthesis crop growth stage (BBCH #65; Lancashire et al. 1991) at 1000 ml/ha with a tractor-mounted sprayer (manufacturer) at 110 liters/ha carrier volume.

5.4.4. Disease assessment, DON quantification, measurement of agronomic traits and grain protein content

Disease assessment was done 21 to 23 days after the 50% anthesis, crop stage BBCH#65. Disease incidence was measured by counting infected spikes from a total of 50 spikes

collected from five random spots in the plot. Disease incidence was expressed in percentage from 0 (no spike infected) to 100% (all spikes examined infected). For disease severity, the proportion of each of the infected spikes was assessed using the FHB visual rating scale of Stack and McMullen (1998). Fusarium head blight index for each plot was calculated using the following formula: FHB Index= (percent disease incidence x percent disease severity)/100. A random sub-sample of approximately 10 g of seed from hand harvested samples was ground to meal for DON assessment. Analysis of DON was carried out using Thermo Fisher's Gallery Analyzer® based on the enzyme linked immunosorbent assay (ELISA) described by Sinha et al. (1995). DON measurements were carried out in two technical replications for each sample, which were averaged and expressed as the average in parts per million (ppm). Yield was determined from combine-harvested dried grain samples. A sub-sample of the grain samples was cleaned to remove chaff and used to measure test weight (TW) (kg/hl) and thousand-kernel weight (TKW) (g). Test weight was measured using a 600 ml chondrometer and TKW was determined by weighing 250 random seeds multiplied by four. To standardize the yield traits in each plot, grain yield, TW, and TKW data were adjusted to 14.5% moisture basis. Grain protein (GP) concentration (%) was measured using LECO FP-528 according to the American Association of Cereal Chemists (AACC) Method 46-30. Grain protein concentration was also adjusted to a 14.5% moisture basis.

5.4.5. Statistical analyses

Data were analyzed separately for all site-years using procedure MIXED in Statistical Analysis Software (SAS) ver. 9.4. (SAS Institute Inc., Cary, NC). Error variances of the data from all site-years, for all class variables, were tested for normality using the Shapiro-Wilk test and homogeneity of variance using the Levene's test. Heterogeneous variances were modeled using the 'repeated /group=effect' statement (Littell et al. 2006). Analysis of variance (ANOVA) was conducted to partition variance among treatments and investigate the effect of resistance genes on FHB phenotypic traits as well as agronomic traits and grain protein content. The resistance genes and fungicide treatment were considered fixed factors, and all other factors were considered random. The interaction of random factors with fixed factors was also considered random. Mean comparisons were performed using Fisher's protected least significant difference (LSD) procedure to protect against Type-II error. All site-years were analyzed separately (due to only four site-years of data) as well as a combined site-years analyses was performed. The significance level of $P = 0.05$ was used for all tests. Fungicide efficacy (FE) for FHB incidence, severity, index, DON, and grain yield was calculated as: [(Check – fungicide treated)/check] × 100. To calculate FE, all four NILs

(MR) carrying specific FHB resistance genes were compared against CDC Go (MS) using raw phenotypic data. The raw data for all site-years was combined and used to generate least squares means for calculation of FE. In addition, least squares means were calculated for all measured traits for MS (CDC Go) vs MR (all NILs) for both treatments to evaluate the effects of resistance level combination with fungicide application. Pearson's correlation coefficients were calculated using procedure CORR in SAS. Except for the correlation analyses, all other analyses were performed by excluding Carberry, as the purpose of the study was to examine the effects and interactions under a similar genetic background; Carberry was not expected to behave similarly in terms of agronomic and yield/quality traits.

5.5. Result

5.5.1. Genomic composition of NILs

The NILs were backcross three (*4) derived lines from the resistance donor parent '04GC0139' and theoretically should possess 3% of their alleles from the donor parent. Genotyping with the wheat 90K assay allowed us to thoroughly investigate allelic composition and the proportion of alleles derived from each parent. The proportion of the genome in the NILs derived from the donor and the recurrent parents is presented in Table 5.2. The four NILs selected carried 0.6-0.8% of the alleles of the resistant donor and approximately 99.0% of the alleles of the recurrent parent. Line NIL-21 does not carry *Fhb1*, which is evident from the results as it carried only 0.03% of the alleles on Chromosome 3B from the donor parent, whereas other NILs carrying *Fhb1* carried 0.9-1.3% of the alleles from the donor parent (Table 5.2). Although NIL-2 carries *Fhb1* and it has smaller proportion of 3B alleles from recurrent parent, the line possesses PFT gene, the candidate for *Fhb1*. Except for NIL-21, which carried *Fhb2*, the NILs did not carry >0.1% alleles on Chromosome 6B from the donor parent. Similarly, the lower proportion of alleles on Chromosome 5A from the donor parent suggests that NIL-38 does not carry *Fhb5*. Genotyping with molecular markers that flanked the gene interval further confirmed these results.

5.5.2. Treatment and interaction effects

The data for each site-year was analyzed separately as well as combined analyses of all site-years; the random effects of replication (plot), interactions of replication by treatment and genotype (NILs) were insignificant (data not presented). In general, *F*-value estimates were greater for fungicide treatments than genotypes in 2016 and the reverse was observed in 2017. For FHB scores (incidence, severity, index and DON accumulation), *F*-values for genotype and fungicide treatments were significant for each of the aspects with the exception of DON accumulation in Outlook 2017 and Melfort 2017, and severity in Saskatoon 2016

(Table 3). Among agronomic traits, fungicide treatments improved each of the aspects only in 2016 trials and genotype differences for yield in Saskatoon 2016, TW in Outlook 2016 and Outlook 2017, and TKW in Melfort 2017 trials. For GP, *F*-values were significant for genotype only in 2017. The genotype (gene) by fungicide interaction was significant for following parameters: severity in Outlook 2016, and DON, TW, and GP in Outlook 2017. Variance estimates for interactions were higher (greater *F*-values) for Outlook 2017 than other site-years whereas it was marginal for disease severity, especially with Outlook 2016. For combined site-years analyses, *F*-values were significant for genotypes for all traits except TW and yield and for fungicide treatment for all traits except GP. Interaction of genotype by treatment was not significant for any trait in the combined analyses.

All NILs performed better than their recurrent parent CDC Go for all disease symptom parameters. In terms of FHB incidence, none of the NILs differed from each other in Saskatoon 2016 or Outlook 2017, whereas NIL-28 performed better than NIL-21 in Outlook 2016 and NIL-38 in Melfort 2017, respectively. In 2016, the FHB severity of NIL-28 was lower than that of the other three NILs. In Outlook 2017, FHB severity of NIL-2, NIL-21, and NIL-28 were comparable to each other and better than NIL-38, whereas in Melfort 2017, NIL-28 was less severely affected as compared to NIL-21 and NIL-38. The FHB index of NIL-28 was lower than other NILs, although NIL-21 and NIL-2 were comparable in Outlook 2017. In Saskatoon 2016, NIL-38 and NIL-2 were comparable for DON accumulation, whereas NIL-21 and NIL-28 had significantly lower DON. In Outlook 2016, DON accumulation of NIL-38 was not different from CDC Go while all other NILs were similar to each other. In 2016, when genotypes differed for DON accumulation, irrespective of resistance level or fungicide treatment, all genotypes had more than 1 ppm DON (data not presented). DON measurements in 2017 were lower than 2016 which could be attributed to relatively lower incidence (Table 4; data not shown). Wherever genotype by fungicide interactions were significant, it was generally the result of superior performance (lower disease, increased yield) of NIL-38 relative to the unsprayed control.

The NILs did not differ for agronomic traits in most of the environments (Table 4). For TW, NIL-2 and NIL-28 were similar in Outlook 2016 and Outlook 2017, the only two site-years where the NILs differed for the trait. The TW of NIL-38 was consistently lower than NIL-2 in both site-years. For TKW, NILs differed only in Melfort 2017; NIL-21 had lower TKW than the other three NILs or the recurrent parent CDC Go. Similarly, for grain yield, the NILs differed only in Saskatoon 2016; The yield of NIL-28 was higher than CDC Go and NIL-21. Grain yield was lowest for NIL-21, although it differed significantly only from NIL-2 and NIL-28. Differences among NILs for GP were observed in 2017, where

NIL-21 had the lowest GP content in both site-years. In Outlook 2017, GP of CDC Go was comparable to that of the NILs, except for NIL-21 which showed slightly lower GP relative to others. In Melfort 2017, NIL-38 had the highest GP content than that of CDC Go, NIL-21, and NIL-28. In addition to GP, significant differences were observed for fungicide treatment in at least two of the four site-years (Table 5). Wherever significant, lines receiving fungicide treatment showed lower disease measurements and higher TW, TKW and yield. For combined site-years analyses, results were mostly concordant with individual site-year analyses.

Least squares means were calculated for MR NILs vs the MS recurrent parent CDC Go (Fig. 1) for all measured traits. For all disease traits: FHB incidence, severity, index and DON accumulation, both resistance levels (MR vs MS) were significantly different as were the fungicide application treatments. For the agronomic traits (TW, TKW, Yield) only fungicide treatments differed significantly. There was no difference between MR vs MS or sprayed vs unsprayed treatments for GP.

5.5.3. Correlation coefficients and fungicide efficacy

Strong positive correlations (R >0.60, P = 0.001) were observed among FHB incidence, severity and index, whereas the disease estimates showed positive but only moderate correlation with DON (R = 0.35 - 0.59, P = 0.05) (Table 6). FHB incidence, severity, index and DON accumulation were negatively correlated with the agronomic traits TW, TKW and grain yield, while the agronomic traits were sometimes positively correlated among themselves, but in other instances they were not significant, for example for Outlook 2016, yield with TW and TKW, and in Outlook 2017, yield with TW. Fungicide efficacy was higher on CDC Go (MS) than that on the MR NILs for all the parameters measured, except the FHB incidence (Fig. 2). Among the genotypes, FE was generally not significant, irrespective of the FHB incidence, severity and index, DON or grain yield.

Table 5.1. Description of study sites, soil type, seeding, inoculation, fungicide application, and disease rating dates, average monthly temperature, and precipitation[a].

	Saskatoon, SK	**Outlook, SK**	**Melfort, SK**
Latitude and longitude	52.24°N 106.67°W	51.28°N 107.03°W	52.51°N 104.36°W
Soil zone/series/texture	Black Chernozemic loam	Dark Brown	Moist Black
Seeding date (2016/2017)	May 19	May 17/May 18	May 25
Inoculation date (2016/2017)	June 30	June 28/July 7	July 10
Anthesis/fungicide application (2016/2017)	July 10	July 5/July 10	July 17
Disease rating (2016/2017)	August 2	July 28/August 3	August 12

Table 5.2. Proportion of the genome of each near-isogenic line from the recurrent parent CDC Go (A) and the resistant donor parent, 04GC0139 (B) used in the study, based on genome-wide single nucleotide polymorphisms markers (90,000 illumina iSelect assay). H and U represent heterozygous or unknown alleles.

	Whole genome			**Chromosome 3B (carrying *Fhb1*)**			**Chromosome 5A (carrying *Fhb5*)**			**Chromosome 6B (carrying *Fhb2*)**		
Line	**A (%)**	**B (%)**	**H/U (%)**	**A (%)**	**B (%)**	**H/U (%)**	**A (%)**	**B (%)**	**H/U (%)**	**A (%)**	**B (%)**	**H/U (%)**
NIL-2 (*Fhb1*+*Fhb5*)	99.3	0.68	0.03	99.1	0.86	0.05	94.0	5.93	0.06	99.8	0.08	0.11
NIL-21 (*Fhb5*)	99.2	0.73	0.03	100	0.03	0	93.1	6.86	0.03	99.8	0.11	0.08
NIL-28 (*Fhb1*+*Fhb2*+*Fhb5*)	99.1	0.78	0.11	98.4	1.28	0.26	91.8	6.61	0.12	98.1	1.58	0.28
NIL-38 (*Fhb1*)	99.4	0.58	0.04	98.7	1.28	0.05	99.5	0.53	0	99.9	0.05	0.05

Table 5.3. Analysis of variance (*F*-values and corresponding *P*-values; significant *P*-values are in boldface) for the experiments conducted in four site-years in Saskatchewan, Canada to study the interaction of Fusarium head blight (FHB) resistance genes with the metconazole (Caramba®) fungicide applied at 50% anthesis. The table shows the variance components along with statistical significance of genotypes fungicide and their interaction in each site-year on FHB incidence, severity, index, deoxynivalenol (DON) accumulation, test weight (TW), thousand-kernel weight (TKW), yield and grain protein (GP).

Source of variation	Incidence[a] (%)	Severity[b] (%)	Index[c] (%)	DON (ppm)	TW (kg/hl)	TKW (g)	Yield (kg/ha)	GP (%)
	***F*-value (*P*-value)[d]**	***F*-value (*P*-value)**	***F*-value (*P*-value)**	***F*-value (*P*-value)**	***F*-value (*P*-value)**	***F*-value (*P*-value)**	***F*-value (*P*-value)**	***F*-value (*P*-value)**
Saskatoon 2016								
Genotype (G)	7.19 **(0.0003)**	13.73 **(<.0001)**	40.45 **(<.0001)**	6.35 **(0.0010)**	1.48 (0.2140)	2.10 (0.1058)	3.91 **(0.0125)**	1.30 (0.2932)
Fungicide (F)	33.83 **(<.0001)**	0.14 (0.7130)	10.66 **(0.0055)**	6.95 **(0.0148)**	88.17 **(<.0001)**	71.23 **(<.0001)**	52.24 **(<.0001)**	2.21 (0.1480)
G*F	1.31 (0.2882)	0.51 (0.7258)	1.01 (0.4455)	1.73 (0.1733)	1.03 (0.3843)	0.41 (0.7934)	1.16 (0.3482)	1.08 (0.3852)
Outlook 2016								
G	14.12 **(<.0001)**	8.55 **(0.0001)**	13.13 **(0.0024)**	4.40 **(0.0075)**	6.18 **(0.0011)**	2.04 (0.1140)	1.11 (0.3703)	1.25 (0.3114)
F	27.60 **(<.0001)**	15.69 **(0.0005)**	29.94 **(0.0003)**	8.54 **(0.0428)**	64.50 **(<.0001)**	15.35 **(0.0005)**	14.59 **(0.0007)**	2.91 (0.0983)
G*F	2.50 (0.0660)	3.17 **(0.0292)**	3.04 (0.0961)	0.38 (0.8179)	1.01 (0.4182)	0.96 (0.4417)	1.26 (0.3082)	0.17 (0.9511)
Outlook 2017								
G	4.62 **(0.0098)**	13.05 **(<.0001)**	14.32 **(<.0001)**	3.41 (0.0525)	3.50 **(0.0200)**	0.99 (0.4258)	1.32 (0.2866)	13.56 **(<.0001)**
F	13.21 **(0.0019)**	7.77 **(0.0096)**	15.44 **(0.0005)**	3.25 (0.1017)	3.32 (0.0795)	0.10 (0.7524)	0.16 (0.6880)	0.32 (0.5775)
G*F	1.37 (0.5877)	1.65 (0.1901)	2.51 (0.0654)	6.90 **(0.0062)**	6.31 **(0.0010)**	1.39 (0.2614)	1.51 (0.2264)	5.98 **(0.0014)**
Melfort 2017								
G	12.39 **(<.0001)**	10.52 **(0.0009)**	10.88 **(<.0001)**	1.49 (0.2453)	-[e]	3.16 **(0.0278)**	0.24 (0.9135)	5.78 **(0.0234)**
F	7.63 **(0.0102)**	9.47 **(0.0059)**	7.98 **(0.0088)**	0.24 (0.6312)	-	0.58 (0.4541)	0.49 (0.4893)	0.04 (0.8421)
G*F	0.76 (0.5627)	1.52 (0.2628)	0.50 (0.7340)	0.40 (0.8087)	-	0.80 (0.5344)	0.53 (0.7140)	0.88 (0.5218)
Combined site-years								
G	15.71 **(<.0001)**	24.63 **(<.0001)**	23.34 **(<.0001)**	9.08 **(<.0001)**	2.38 (0.0560)	2.49 **(0.0456)**	0.89 (0.4699)	4.28 **(0.0027)**
F	80.02 **(<.0001)**	14.71 **(0.0002)**	67.24 **(<.0001)**	8.47 **(0.0044)**	73.27 **(<.0001)**	18.97 **(<.0001)**	17.22 **(<.0001)**	3.48 (0.0642)
G*F	1.01 (0.4037)	0.38 (0.8196)	2.07 (0.0945)	1.18 (0.3252)	0.82 (0.5148)	0.99 (0.4127)	0.45 (0.7747)	0.060 (0.6665)

[a]Percentage of spikes infected from total spikes.

[b]Percent of the florets of each spike infected with FHB.

[c]FHB index = (percent disease incidence x percent disease severity)/100.

[d]Fisher's statistics. Here *, **, ***, [ns] represent significant at $P = 0.5, 0.001, 0.0001$, and not significant respectively; [e]-: Not measured.

Table 5.4. Least squares means (sprayed+unsprayed) of Fusarium head blight (FHB) incidence, severity, index, deoxynivalenol accumulation (DON), test weight (TW), thousand kernel weight (TKW), yield and grain protein for the near-isogenic lines (NILs) carrying FHB resistance genes in four site-year field trials. Test weight, TKW, Yield and grain protein estimates are based on constant moisture content. Means comparison was performed without inclusion of Carberry.

Genotype/NIL (gene)	Incidence[a] (%)	Severity[b] (%)	Index[c] (%)	DON (ppm)	TW (kg/hl)	TKW (g)	Yield (kg/ha)	Protein (%)
Saskatoon 2016								
Carberry (moderately resistant)	22.3	19.0	4.2	2.6	80.4	34.4	3286	16.1
CDC Go (moderately susceptible NILs parent)	38.8 a	46.6 a	18.0 a	5.6 a	77.4 a	37.7 a	3040 bc	15.8 a
NIL-38 (*Fhb1*)	31.1 b	31.3 b	9.8 b	4.2 b	77.4 a	37.1 a	3103 abc	15.6 a
NIL-21 (*Fhb5*)	31.4 b	31.3 b	9.7 b	2.6 c	77.1 a	36.0 a	2886 c	15.4 a
NIL-2 (*Fhb1+5*)	28.9 b	29.9 b	8.5 b	3.3 bc	77.8 a	36.4 a	3261 ab	15.5 a
NIL-28 (*Fhb1+Fhb2+Fhb5*)	27.3 b	24.1 c	6.6 c	2.1 c	77.5 a	36.3 a	3344 a	15.3 a
Outlook 2016								
Carberry	34.3	9.8	4.5	2.2	79.5	36.1	2882	17.2
CDC Go	51.3 a	17.3 a	9.1 a	4.6 a	76.3 b	39.5 a	3161 a	16.0 a
NIL-38 (*Fhb1*)	38.1 bc	11.1 b	4.2 b	3.6 ab	76.3 b	39.0 a	3610 a	15.8 a
NIL-21 (*Fhb5*)	40.0 b	13.3 b	5.6 b	2.4 bc	76.9 a	39.0 a	3224 a	15.3 a
NIL-2 (*Fhb1+5*)	36.3 bc	13.1 b	4.7 b	2.1 c	77.0 a	40.6 a	2978 a	16.2 a
NIL-28 (*Fhb1+Fhb2+Fhb5*)	31.3 c	10.5 c	3.3 c	2.4 bc	76.7 ab	39.7 a	3206 a	16.0 a
Outlook 2017								
Carberry	15.0	8.0	1.2	0.68 a	79.0	38.3 a	5570 a	15.4
CDC Go	39.4 a	19.0 a	7.8 a	0.66 a	77.3 a	41.8 a	5640 a	16.0 a
NIL-38 (*Fhb1*)	28.1 b	14.4 b	4.1 b	0.93 a	76.6 b	38.8 a	5889 a	16.0 a
NIL-21 (*Fhb5*)	28.1 b	10.4 cd	2.9 bc	0.24 a	76.7 b	39.7 a	5760 a	15.5 b
NIL-2 (*Fhb1+5*)	24.4 b	12.4 bc	3.1 bc	0.50 a	77.1 a	41.3 a	6162 a	16.0 a
NIL-28 (*Fhb1+Fhb2+Fhb5*)	23.8 b	9.1 cd	2.2 c	0.87 a	76.9 ab	40.5 a	5877 a	15.9 a
Melfort 2017								
Carberry	6.0	9.5	0.6	0.32	-[d]	38.8	4368	15.1
CDC Go	21.3 a	22.7 a	5.0 a	0.58 a	-	41.7 a	4545 a	14.3 b
NIL-38 (*Fhb1*)	13.1 b	17.3 b	2.3 b	0.95 a	-	41.9 a	4447 a	15.1 a
NIL-21 (*Fhb5*)	11.9 bc	18.0 b	2.3 b	0.35 a	-	40.0 b	4370 a	13.9 c
NIL-2 (*Fhb1+5*)	11.1 bc	15.5 bc	1.8 b	0.43 a	-	41.7 a	4380 a	14.7 ab
NIL-28 (*Fhb1+Fhb2+Fhb5*)	9.7 c	12.0 c	1.2 b	0.37 a	-	41.3 a	4443 a	14.2 b
Combined site-years								
Carberry								
CDC Go	37.7 a	23.8 a	9.1 a	2.9 a	77.0 a	40.2 a	4769 a	15.5 a
NIL-38 (*Fhb1*)	27.7 b	17.2 b	5.0 b	2.4 a	76.8 a	39.2 ab	4938 a	15.7 a
NIL-21 (*Fhb5*)	27.4 bc	16.2 b	4.6 bc	1.3 b	76.9 a	38.7 b	4724 a	15.2 b
NIL-2 (*Fhb1+5*)	22.9 d	16.5 b	3.7 cd	1.5 b	77.3 a	40.0 a	2861 a	15.6 a
NIL-28 (*Fhb1+Fhb2+Fhb5*)	23.3 cd	11.7 c	2.8 d	1.2 b	77.1 a	39.4 ab	4893 a	15.4 ab

Note: Means followed by the same letter within columns are not significantly different (LSD, $P<0.05$). Carberry was not included in the mean comparisons because it was not expected to behave similarly to CDC Go and NILs because of different genetic background; [a]Percentage of spikes infected by FHB; [b]Percent of infected florets on each spike; [c]FHB index = (percent disease incidence x percent disease severity)/100; [d]NM: Not measured.

Table 5.5. Means of Fusarium head blight (FHB) incidence, severity, index, deoxynivalenol accumulation (DON), test weight (TW), thousand kernel weight (TKW), yield, and grain protein for fungicide treatment (Caramba®, metconazole, Group 3, BASF Canada)- in four site-years in Saskatchewan. Test weight, TKW, yield, and grain protein estimates were based on moisture content of 14.5%. Means comparison was performed after excluding Carberry.

Fungicide treatment	Incidence[a] (%)	Severity[b] (%)	Index[c] (%)	DON (ppm)	TW (kg/hl)	TKW (g)	Yield (kg/ha)	Protein (%)
Saskatoon 2016								
Sprayed	27.2 b	32.2 a	9.2 b	2.9 b	78.4 a	38.5 a	3423 a	15.6 a
Unsprayed	35.8 a	33.0 a	11.9 a	4.2 a	76.5 b	34.8 b	2831 b	15.4 a
Outlook 2016								
Sprayed	34.8 b	11.5 b	4.1 b	2.2 b	77.5 a	40.4 a	3610 a	16.1 a
Unsprayed	44.0 a	14.7 a	6.7 a	3.5 a	76.7 b	38.7 b	2862 b	15.6 a
Outlook 2017								
Sprayed	24.0 a	11.7 b	3.0 a	0.52 a	77.4 a	40.6 a	5896 a	15.9 a
Unsprayed	33.5 b	14.4 a	5.1 a	0.76 a	77.0 b	40.2 a	5834 a	15.9 a
Melfort 2017								
Sprayed	11.6 b	14.5 b	1.4 b	0.47 a	-[d]	41.5 a	4480 a	14.5 a
Unsprayed	14.7 a	18.6 a	2.8 a	0.56 a	-	41.1 a	4393 a	14.4 a
Combined site-years								
Sprayed	21.8 b	15.7 b	3.5 b	1.5 b	77.5 a	40.2 a	4352 a	15.6 a
Unsprayed	33.8 a	18.5 a	6.6 a	2.2 a	76.5 b	38.7 b	4004 b	15.4 a

Note: Means followed by the same letter within columns are not based on Fisher's least significant differences (LSD) at $P<0.05$.

[a]Percentage of spikes infected from total spikes.

[b]Percent of the florets of each spike infected with FHB.

[c]FHB index = (percent disease incidence x percent disease severity)/100.

[d]-: Not measured.

Table 5.6. Pearson's correlation coefficients between Fusarium head blight (FHB) incidence, severity, index, deoxynivalenol (DON) accumulation, test weight (TW), thousand kernel weight (TKW) and yield. Test weight was not measured for Melfort 2017. Correlations were not significant among grain protein and any of the other traits.

	Incidence[a]	Severity[b]	Index[c]	DON	TW	TKW	Yield
Saskatoon 2016							
Incidence	-						
Severity	0.12 ns	-					
Index	0.78***	0.67***	-				
DON	0.54**	0.23 ns	0.51**	-			
TW	-0.65***	-0.31*	-0.62***	-0.21 ns	-		
TKW	-0.43**	0.17 ns	-0.23 ns	-0.05 ns	0.35*	-	
Yield	-0.67***	-0.41*	-0.58***	-0.36*	0.65***	0.57***	-
Outlook 2016							
Incidence	-						
Severity	0.66***	-					
Index	0.90***	0.86***	-				
DON	0.53**	0.38*	0.53**	-			
TW	-0.46**	-0.55***	-0.39**	0.24 ns	-		
TKW	-0.26 ns	-0.30*	-0.32*	-0.39**	0.33*	-	
Yield	-0.23 ns	-0.36*	-0.51**	0.08 ns	0.25 ns	0.08 ns	-
Outlook 2017							
Incidence	-						
Severity	0.56**	-					
Index	0.85***	0.86***	-				
DON	0.11 ns	0.09 ns	0.16 ns	-			
TW	-0.34*	-0.33*	-0.30*	-0.01 ns	-		
TKW	0.23 ns	0.16 ns	0.21 ns	-0.30*	0.10 ns	-	
Yield	-0.05 ns	-0.06 ns	-0.09 ns	-0.16 ns	0.08 ns	0.32*	-
Melfort 2017							
Incidence	-						
Severity	0.74***	-					
Index	0.95***	0.86***	-				
DON	0.37*	0.10 ns	0.25*	-			
TW	-	-	-	-	-		
TKW	-0.08 ns	-0.06 ns	-0.11 ns	0.13 ns	-	-	
Yield	0.03 ns	-0.06 ns	-0.05 ns	-0.08 ns	-	0.50**	-

Note: *, **, ***: Correlation coefficients significant at $P<0.05$, $P<0.001$, $P<0.0001$, respectively; ns- not significant; [a]Percentage of spikes infected from total spikes; [b]Percent area of spikes infected with FHB out of infected spikes; [c]FHB index = (percent disease incidence x percent disease severity)/100.

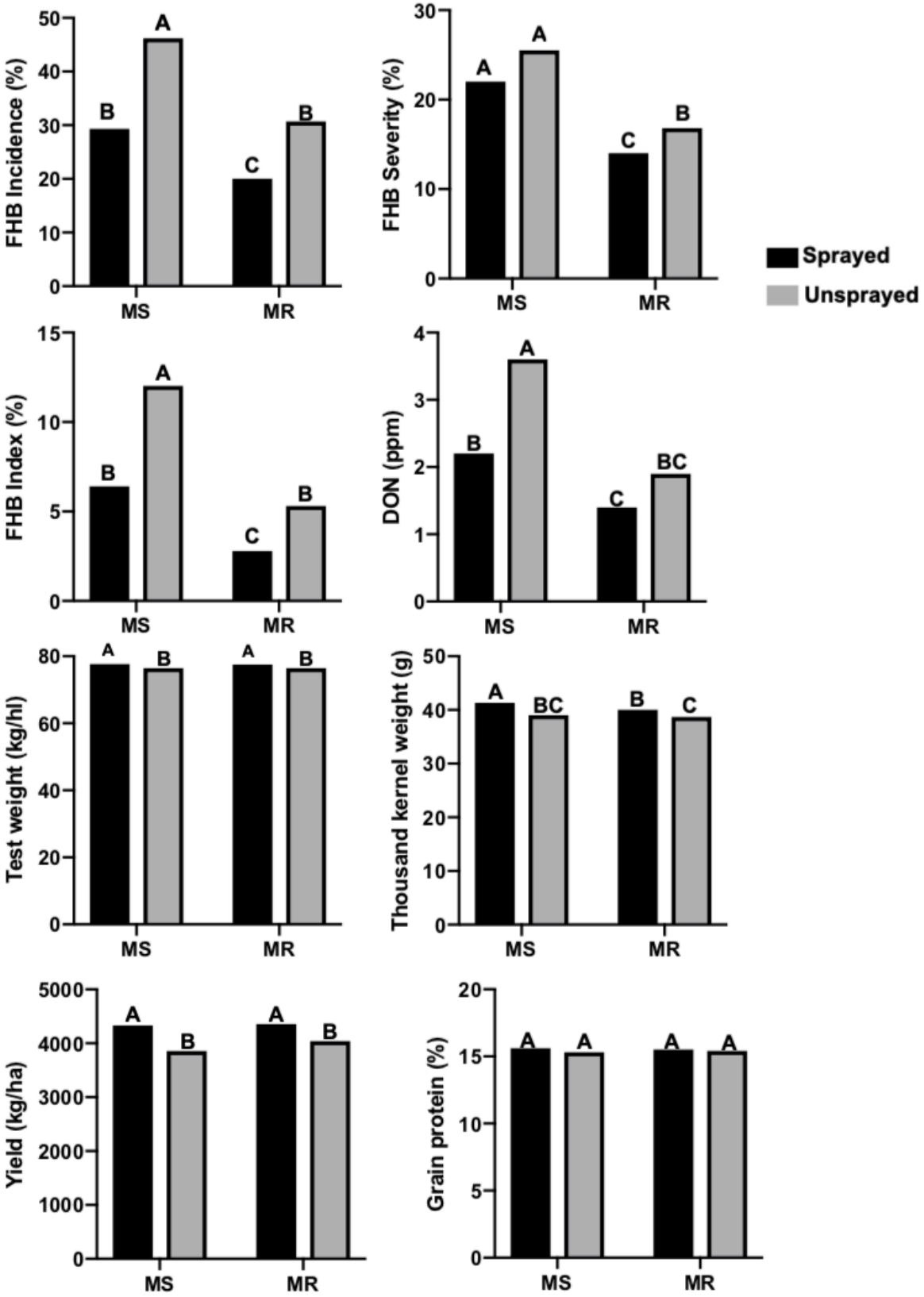

Figure 5.1. Least squares means for Fusarium head blight (FHB) incidence, severity, index, deoxynivalenol (DON), test weight, thousand kernel weight, grain yield, and grain protein in moderately susceptible (MS; CDC Go) and moderately resistant (MR; NIL-2, NIL-21, NIL-28, NIL-38) hard red spring wheat lines. Bars with the same letter are not significantly different according to Fisher's Least Significant Difference at $P = 0.05$.

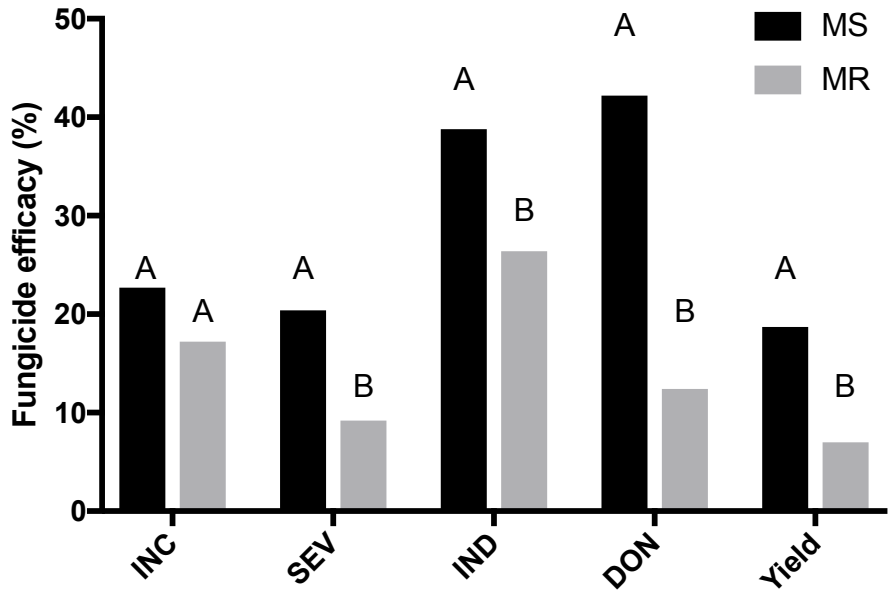

Figure 5.2. Fungicide efficacy (%) for Fusarium head blight incidence (INC), severity (SEV), index (IND), deoxynivelanol (DON), and grain yield in moderately susceptible (MS) and moderately resistant (MR) hard red spring wheat lines. Bars with the same letter are not significantly different according to Fisher's least significant difference (LSD) test at $P = 0.05$.

5.6. Discussion

This research was conducted to investigate the potential interaction of Sumai 3 derived genes (*Fhb1, Fhb5* and/or *Fhb2*) with a recommended metconazole fungicide in control of FHB on wheat. To our knowledge this is the first study on the effect of individual and combinations of Sumai 3 genes in a near-isogenic backgrounds. Carberry was not used for the mean comparisons due to difference in genetic background and it possibly carrying minor QTL for FHB resistance in addition to *Fhb1* and *Fhb5*. Although CDC Go is an MS cultivar and also carries three very minor FHB resistance loci (on Chromosomes 1DL, 2AL, and 2DL), these three loci are equally distributed in the NILs (G. S. Brar, unpublished data), thus their presence is not expected to influence the overall results and conclusions of this study. We used only one triazole fungicide in our study to avoid potentially more complex genotype by fungicide interactions as reported previously (Amarasinghe et al. 2013; Mesterhazy et al. 2003). Metconazole was among the best fungicide active ingredients to reduce FHB and DON, according to a meta-analysis comprising >100 uniform fungicide trials conducted in the United States (Paul et al. 2008). It is also on the recommended list of fungicides for suppressing FHB and DON in western Canada (Anonymous 2018). We utilized NILs carrying less than 1.0% of the alleles from the resistant donor parent to estimate gene by fungicide interactions with minimized interference caused by different genetic background.

Host resistance and fungicide treatment both elicited responses to yield and disease measurements and most agronomic/end-use quality traits (TW, TKW, and GP) in this study. The positive correlations among FHB index and DON and negative correlations of FHB index with yield traits are consistent with previous studies (McMullen et al. 2012; Gilbert and Haber 2013). Insignificant genotype by fungicide interactions for disease parameters suggest an additive response of Sumai 3 derived genes to metconazole (Table 3 and Fig. 1). We observed an interaction of *Fhb1* with the fungicide for FHB severity and DON, respectively, in only one site-year each, which could be attributed to environmental or unknown factors. FHB affects yield and related traits by causing bleaching of infected spikes and affecting the vascular system, which result in overall lower TW and TKW. Resistant wheat genotypes are able to reduce such losses as compared to susceptible ones (McMullen et al. 2012). In our study, in spite of carrying *Fhb5*, NIL-21 performed poorly (tended to have lower TW, TKW, yield and GP) than the recurrent parent CDC Go or other NILs, which in part could be due to the level of disease, but these traits may also be affected by linkage drag by other alleles from the resistance donor. This was evident in separate yield trials without FHB where NIL-21 showed poorer yield or quality traits when compared to NIL-28 or CDC Go (G.S. Brar, unpublished data).

Inconsistent findings of FE on cultivars/lines that differ for FHB resistance (more likely tolerance in old cultivars) and variable efficacy of different triazole fungicide active ingredients in previous studies have been attributed to environmental and pathogen factors (Amarasinghe et al. 2013; Blandino et al. 2012; Boyacioglu et al. 1992; D'Angelo et al. 2014; Hollingsworth et al. 2008; Mesterhazy et al. 2003, 2018; Paul et al. 2008; Wegulo et al. 2011, Willyerd et al. 2012). Our study demonstrated generally greater FE for the MS cultivar CDC Go and lower efficacy on the MR NILs. This is contrary to Mesterhazy et al. (2003 and 2018), and Wegulo et al. (2011) as they reported higher FE on MR cultivars. Similar to our study, Willyerd et al. (2012) and Ye et al. (2017) also reported higher FE on MS or S cultivars. The important factor to consider among these results is the FHB pressure; in trials with moderate to high disease pressure, greater FE is expected for MR genotypes because the fungicide alone would likely be insufficient on a susceptible cultivar. Under low disease pressure, however, FE can be relatively greater for MS/S genotypes because the infection level on a resistant cultivar would be too low to warrant a fungicide spray. The disease pressure reported by Mesterhazy et al. (2003 and 2018) and Wegulo et al. (2011) were much higher as compared to Willyerd et al. (2012) and Ye et al. (2017). Hollingsworth et al. (2008) drew similar conclusions in their study; the level of FHB was much higher on MS/S cultivars than that on untreated MR, and thus a fixed absolute reduction in MR cultivars

would translate into greater efficacy. However, this would not hold true in trials under low disease pressure, such as ours. Under the low disease pressure, the actual reduction (not a relative change) in FHB and DON was less dramatic on the MR than on MS, thus resulting in higher relative FE for CDC Go, despite the fact that the ultimate disease measurements were lower on NILs. The other reason for higher FE on MR under high disease pressure may be that genetic resistance can be in several mechanisms, including Type-I, Type-II or even Type-III forms over the lifetime of the plant.

The FE results in our study imply that in years with low disease pressure, such as 2017, resistance alone is generally enough to prevent much of the yield loss caused by FHB. As a result, we did not detect yield benefits for fungicide treatments (Table 5). In years with moderate to high disease pressure (2016 in our study), however, the application of triazoles suppressed FHB and reduced the yield loss. However, it is worth mentioning that in spite of the improved efficacy on CDC Go relative to untreated controls, higher levels of disease were still observed on this MS cultivar relative to those on NILs (Table 4; Fig. 1). These results indicate that application of metconazole to a MR cultivar can be beneficial under moderate to high disease pressure (Fig. 1). DON accumulation was >1 ppm in both the NILs and CDC Go for 2016 trials, which meant that even under moderate disease pressure, moderate resistance plus fungicide application may still result in a low level of DON accumulation in harvested grains. Since the FHB resistance genes are only partially effective under high disease pressure, it is not uncommon to observe little to no difference in DON accumulation or FHB index between MS and MR (Blandino et al. 2012; G.S. Brar, personal observation).

Our study demonstrated the additive nature of Sumai 3 derived FHB resistance genes with metconazole in suppressing FHB and DON accumulation in the grain (Table 3; Fig. 1). Introgression of *Fhb1* and/or *Fhb5* into hard red spring wheat should improve FHB control in Saskatchewan. Under moderate to heavy disease pressure, adding a fungicide application to MR cultivars can further enhance the effectiveness of FHB control, often increasing the grain yield (Fig. 1). However, this strategy alone may not reduce DON accumulation to an acceptable level and thus additional options should also be considered for the integrated FHB management. In western Canada, extended crop rotation may be warranted in the eastern prairies (Manitoba and eastern Saskatchewan) due to more severe FHB than in the western prairies including Alberta and western Saskatchewan (Beres et al. 2018). This cultural practice should be combined with cultivar resistance and, under high disease pressure, also with fungicides. The efficacy of triazole fungicides can vary depending largely on disease pressure, but also on host resistance, environmental conditions and application methods (D'Angelo et al. 2014; McMullen et al. 2012; Paul et al. 2008). In context of Canadian hard

red spring wheat cultivation, the integration of host resistance and fungicide application in the eastern prairies is unavoidable as FHB has been a problem in that region for many years; however, wheat growers in the western prairies, particularly the province of Alberta, may not yet benefit from fungicide application if FHB is not usually severe. In fact, the adoption of FHB resistant cultivars has been higher in Manitoba than Alberta, which reflects the experience of wheat growers with FHB (Beres et al. 2018). Although preventing DON accumulation is very important from international trade and market viewpoint, in the end, DON is an economic issue when present. Wheat growers should consider all possible strategies to manage FHB under moderate or higher disease pressure. To bring DON levels down to an acceptable limit, growers should not just rely on host resistance and fungicide application but consider cultural practices and most importantly a minimum of four-year crop rotation.

CHAPTER 6

High-density mapping and annotation of novel quantitative trait loci (QTL) for resistance to Fusarium head blight (FHB) in durum and emmer wheat

6.1. Preface

Chapters 3-5 were focussed on studying the effects of Sumai 3 derived Fusarium head blight (FHB) resistance genes in common wheat. This Chapter is part of host resistance study, however, in durum wheat. As described in Chapter 2, there are not many sources of resistance in tetraploid wheat which are comparable to Sumai 3, researchers have identified some emmer wheat accessions with good level of Type-II resistance to FHB. A part of this PhD dissertation was to re-map the resistance conferring loci in a mapping population, developed at the Crop Development Centre, from an emmer wheat accession and an elite durum wheat line. The Chapter presented results on resistance gene mapping in emmer and durum wheat.

6.2. Abstract

Fusarium head blight (FHB), mainly caused by *Fusarium graminearum (Fg)*, threatens durum wheat (*Triticum turgidum* L. subsp. *durum*) production worldwide. Moderately resistant or resistant durum wheat cultivars registered for commercial cultivation do not exist in North America, although some emmer wheat accessions are reported to carry heritable resistance to FHB. In our study, an emmer wheat accession BGRC3487 (*Triticum turgidum* L. subsp. *dicoccum*; moderately resistant) and an advanced durum wheat line DT735 (intermediate in resistance) were used to identify novel quantitative trait loci (QTL) for FHB field resistance and resistance to the 3-ADON chemotype of *Fg*. Backcross recombinant inbred lines (n = 160) were evaluated for FHB field resistance (Type-I + Type-II) in five field site-years, for Type-II resistance in two greenhouse experiments, and genotyped using 81,587 single nucleotide polymorphism (SNP) markers. Fifteen QTL (derived from both parents) for FHB resistance were identified on 11 of the 14 wheat chromosomes using saturated linkage maps. Majority of the QTL were consistently detected in multiple environments. The combination of four relatively large-effect and promising QTL reduced field FHB index, severity, incidence and visual rating index by 59%, 48%, 30%, and 29%, respectively. Epistatic interactions among the four QTL for resistance to the 3-ADON chemotype were identified, thus resulting in 77-80% disease reduction by combining two non-interacting QTL and up to a 59% reduction by combining all four QTL. Majority of the QTL reported in the

study are novel and represent narrow intervals between the flanking markers; therefore, this resistance could be amenable to marker-assisted selection in breeding FHB resistant durum wheat cultivars.

6.3. Introduction

Durum wheat (*Triticum turgidum* L. subsp. *durum* Desf.) accounts for approximately 10% of global wheat cultivation and production of approximately 37 million tons (Kabbaj et al. 2017). Among wheat classes in Canada, Canada Western Amber Durum (CWAD) is the second most important class after Canada Western Red Spring (CWRS) (Clarke et al. 2010). Fusarium head blight (FHB), commonly known as scab, is one of the most devastating diseases of small-grain cereals in North America and other warmer regions worldwide (McMullen et al. 2012; Gilbert and Haber 2013). It was assumed that durum wheat would not be affected by FHB as it is cultivated in relatively drier habitats (Somers et al. 2006). The disease, which can be caused by several Ascomycete species of the genus *Fusarium*, but mainly *Fusarium graminearum* Schwabe [teleomorph: *Gibberella zeae* (Schw.) Petch.], has affected durum wheat production in North America with several epidemics in the past; 2016 being the most recent in Saskatchewan (Randy Kutcher, unpublished data). The disease causes yield and quality losses resulting from shriveled light-weight kernels (called Fusarium damaged kernels) and the accumulation of mycotoxins, particularly deoxynivalenol and its acetylated forms (McMullen et al. 2012; Bai et al. 2018). A 50-70% loss of marketable grain in epidemic years in not uncommon (Brewer and Hammond-Kosack 2015) and therefore it is important to invest resources and effort in breeding for FHB resistance in durum wheat to sustain productivity and quality.

An integrated disease management approach is recommended to prevent yield and quality loss, and host resistance is considered one of the most important strategies (Bai et al. 2018). Unfortunately, none of the commercially grown durum wheat cultivars in North America are even moderately resistant (MR); all known cultivars are either susceptible (S) or moderately susceptible (MS) (Clarke et al. 2010; Zhang et al. 2014; Anonymous 2018a). Durum wheat cultivars released recently in the upper Great Plains carry some tolerance to the disease; however, not comparable to the resistance level in bread wheat cultivars. Improving FHB resistance in durum wheat breeding lines is a challenging task as the trait is quantitative, and strongly influenced by environmental factors (Buerstmayr et al. 2009). The lack of elevated levels of resistance in the cultivated gene pool presents an additional challenge for durum wheat breeders (Prat et al. 2014). Efforts to identify resistance in durum wheat have not been successful, and only a very few accessions with a low level of resistance (not

comparable to hexaploid wheat) are reported (Elias et al. 2005; Talas et al. 2011; Huhn et al. 2012; Miedaner and Longin, 2014). Although there is no clear reason for the susceptibility of durum wheat to FHB, studies have reported the presence of susceptibility factors and/or suppressor genes in the genome that compromise resistance alleles (Stack et al. 2002; Kishii et al. 2005; Garvin et al. 2009; Ghavami et al. 2011). Unsuccessful attempts to transfer FHB resistance associated with QTL from hexaploid wheat to durum wheat were challenged by differences in ploidy level and the absence of the D-genome, which may play a role in enhancing or complementing resistance from the A- and/or B-genomes (Fakhfakh et al. 2011). Despite this difficulty, Prat et al. (2017) reported successful introgression of *Fhb1* into cultivated European durum wheat backgrounds resulting in improvement in FHB resistance. Introgression of another well-characterized QTL (*Fhb5*) from Sumai 3 is reported to affect spike fertility in durum wheat (Prat et al. 2014). Thus, introgression of FHB genes from bread wheat into durum wheat may be possible, but definitely challenging and there maybe linkage-drag.

More than 250 QTL for FHB resistance in hexaploid are reported, whereas <40 are reported in tetraploid wheat (Buerstmayr et al. 2009; Prat et al. 2014; Bai et al. 2018; Jia et al. 2018). Lack of resistance in elite durum wheat led researchers to explore resistance in related tetraploid species and fortunately genetic variation exists in subspecies of the primary gene pool in durum wheat (Somers et al. 2006; Gladysz et al. 2007; Prat et al. 2014). Moderately resistant emmer wheats have been identified, i.e. *T. turgidum* subsp. *dicoccoides*, *T. turgidum* subsp. *dicoccum*, Schrank ex Schübl. and *T. turgidum* subsp. *carthlicum*, which subsequently led to their utilization in molecular mapping (Miller et al. 1998; Buerstmayr et al. 2003; Somers et al. 2006; Oliver et al. 2007; Buerstmayr et al. 2013). The majority of the FHB resistance QTL mapped in tetraploid wheat are derived from the aforementioned emmer wheat accessions (reviewed in Prat et al. 2014). Because the ploidy level and genome constitution is the same as elite durum wheat, the emmer wheat accessions are very useful for FHB resistance breeding efforts in durum wheat breeding programs. Other than breeding for FHB resistance, grain quality traits are also important because durum wheat semolina is used to produce pasta worldwide (Soresi et al. 2017). The hard grain texture, amber color, and other grain quality traits related to endosperm protein are responsible desirable qualities for durum semolina. Thus, it is important for breeders to select for FHB resistance, but against other traits that might influence end-use quality.

The first step for any resistance breeding effort starts with identification and mapping of loci or quantitative trait loci (QTL) conferring FHB resistance that can be easily utilized in plant breeding (Buerstmayr et al. 2009). For QTL mapping studies, genetic maps are one of

the most important tools, and precise, well-ordered ultra-dense maps are very useful to identify all QTL controlling a quantitative trait (Avni et al. 2014). Unfortunately, most previous FHB QTL mapping studies in tetraploid wheat utilized low throughput marker systems such as simple sequence repeats (SSRs), sequence tagged site (STS), target region amplification polymorphism (TRAP) plus relatively lower numbers of markers, which resulted in large intervals between the flanking markers for the majority of the QTL regions mapped (reviewed in Prat et al. 2014). Given the complexity of the wheat genome, large numbers of markers are required to accurately represent each chromosome. Recent advances in genotyping technologies have led to increased numbers of single nucleotide polymorphism (SNP) markers that fulfill the conditions for whole-genome representation and the wheat 90K iSelect assay is one of the few SNP arrays that has 81,587 SNP markers representing all wheat chromosomes (Wang et al. 2014). The large number of SNPs from the wheat 90K iSelect assay are particularly useful for generating ultra-dense maps for QTL mapping studies and thus are potentially helpful in narrowing down the QTL interval.

In an effort to enhance FHB resistance in durum wheat breeding material at the Crop Development Centre, University of Saskatchewan, a tetraploid emmer wheat landrace with a high level of Type-II resistance was identified and used to develop a mapping population. The goal of this research was to map FHB resistance QTL from a population derived from an emmer wheat landrace and an advanced durum breeding line from Canada. The same population was previously used to map QTL using diversity array technology (DArT) and SSR markers; however, with limited markers (Ruan et al. 2012). The specific objectives of our study were: (i) to develop a dense genetic map using 81,587 SNP markers from the 90K wheat iSelect assay (Wang et al. 2014), (ii) to map QTL for FHB field resistance, and in the greenhouse to Type-II resistance to the 3-ADON chemotype of *F. graminearum*, and seed coat color, and (iii) to determine the physical positions of the resistance loci and search for annotated genes in the QTL regions.

6.4. Materials and methods

6.4.1. Plant material

A backcross recombinant inbred population (BCRIL) consisting of 160 lines ($BC_1F_{6:10}$) was developed from a cross of BGRC3487/2*DT735 using single-seed descent at the Crop Development Centre, University of Saskatchewan, Canada (Ruan et al. 2012). The *T. turgidum* L. subsp. *dicoccum* line BGRC3487 is a domesticated tetraploid wheat landrace that was obtained from Braunschweig Genetic Resources Centre, Germany and has a high level of Type-II resistance to FHB. The advanced durum breeding line DT735 (derived from

DT696/AC Avonlea) developed at the Swift Current Research and Development Center of the Agriculture & Agri-Food Canada has an intermediate level of FHB resistance (Clarke et al. 2010).

6.4.2. FHB evaluations

FHB field evaluations were performed on 160 RILs along with their parents and check cultivars in irrigated FHB nurseries in Canada at Carman, Manitoba; Sainte-Foy, Quebec; and Saskatoon, Saskatchewan between 2008–2018 comprising a total of five site-years. The population was also evaluated for resistance to the 3-ADON chemotype of *F. graminearum* (isolate M9-04-6) in 2009 in the greenhouse (GH-SEV). Except for Sainte-Foy, where visual rating index (FLD-VRI) data was collected, data from all other locations included incidence (FLD-INC), severity (FLD-SEV), and index (FLD-IND). The detailed field and greenhouse phenotypic evaluation procedures for 2008-2010 are described in Ruan et al. (2012). In addition to 2008-2010, the population was phenotyped in 2016 in the FHB Nursery at Saskatoon; in 2017 in CIMMYT's International FHB screening nursery and greenhouse. In the Saskatoon irrigated nursery, lines were seeded in three replications in hills and inoculation was performed by spreading *F. graminearum* colonized corn spawn. FLD-INC and FLD-SEV were assessed 22-23 days post inoculation using the visual rating scale from Stack and McMullen (1998) to calculate FLD-IND as previously described (Ruan et al. 2012). At CIMMYT, for greenhouse evaluation (GH-CIM), six seeds were sown in one pot for each line and at 50% anthesis, the mainstem spike for each plant was point inoculated by injecting 10 µl of macroconidial spore suspension (50,000 spores/ml) in a single floret in the middle of the spike. Disease rating was performed 21 days post inoculation by counting the number of infected spikelets over the total number of spikelets in the spike.

6.4.3. High-throughput genotyping

The population was previously genotyped using 103 SSR markers and 837 DArT markers (Ruan et al. 2012). In 2016, the population was genotyped along with its parents, using the wheat 90,000 iSelect assay (90K hereafter) comprised of 81,587 SNPs (Wang et al. 2014), to enrich and confirm the genomic regions carrying resistance QTL mapped by Ruan et al. (2012). SNP alleles were called using Genome Studio (Illumina Inc., San Diego, CA, USA) and filtered based on polymorphisms between parents.

6.4.4. Seed color assay

BGRC3487 expressed red seed coat color, whereas amber colored grain (due to yellow carotenoid pigments) is preferred in durum wheat cultivars, which is expressed in DT735. Thus, the BCRILs were assayed for seed coat color segregation using a method described

previously (Matus-Cádiz et al. 2003; Ruan et al. 2012) and the phenotypic data from Ruan et al. (2012) was used for QTL mapping in combination with the 90K genotypic data.

6.4.5. Phenotypic data analyses

Previously generated phenotypic data on the population was obtained from Ruan et al. (2012). For 2016 and 2017 data, least square means were calculated using procedure MIXED in SAS ver. 9.4 (Littell et al. 2006). Homogeneity and normality of residuals for all class variables was tested using Levene's and Shapiro-Wilk's tests using procedure UNIVARIATE in SAS ver. 9.4. Heterogenous variances, if any, for class variables were modeled using repeated /group=effect statement with procedure MIXED. For calculating broad-sense heritability (H^2), variance components were estimated using procedure VARCOMP in SAS ver. 9.4. Correlation coefficients among all traits were also calculated using procedure CORR in SAS ver. 9.4. Associations among environments, genotypes, and genotype by environment interaction were also analyzed and visualized using biplot analyses (Yan and Tinker 2006) in the R environment using GGEBiplotGUI package (Frutos et al. 2014). For biplot analyses, following setting were used: singular value portioning- environment-metric preserving; genotype by environment scaling- according to standard deviation; centered by environment (G+G*E).

6.5.6. Marker analyses, linkage and QTL mapping

Prior to linkage mapping, SNP loci with missing genotype in more than 25% of the population were discarded. Also, the loci deviating from expected 3:1 ratio were discarded. Genetic linkage maps were constructed using JoinMap ver. 4.0 (Van Ooijen 2006) at the LOD score of 4.0 or above using 'Haldane' mapping function. Linkage groups were assigned chromosome names by comparing markers and their order to the published consensus maps (Wang et al. 2014; Macferri et al. 2015). Least square means for all phenotypic traits were used for QTL mapping and analyses using MapQTL ver. 6.0 (Van Ooijen 2006). Firstly, a simple interval mapping (IM) approach was used to identify the chromosome regions and the markers associated with the traits. Final QTL mapping and analyses were performed by using the peak marker (with LOD >2.0) for each QTL region as cofactor with a multiple QTL model (MQM) approach. QTL for plant height were also mapped, and where coincided with FHB resistance traits, plant height was used as a cofactor to account for dependence or independence. Threshold of each chromosome was computed using permutation test implemented in the software with 1,000 iterations (Van Ooijen 2006). QTLs identified with MQM were also validated/confirmed using composite interval mapping (CIM) algorithm in WinQTL Cartographer (Wang et al. 2012). For CIM mapping, cofactor selection was performed using forward and backward regression at 1.0 cM walk speed at $P = 0.1$ as

significance threshold. All QTL reported in the present study are designated as *QFhb.usw* or *QCl.usw* following the recommended rules for Gene Symbolization in wheat (http://wheat.pw.usda.gov), where '*QFhb*' and '*QCl*' indicates QTL for FHB and seed coat color, respectively, and '*usw*' is the laboratory designation for Dr. Curtis Pozniak's lab at the University of Saskatchewan.

6.4.7. Physical mapping, annotation and comparison with previously mapped QTL

All SNP markers flanking or in the QTL intervals were physically positioned on the Chinese Spring wheat genome sequence available through International Wheat Genome Sequencing Consortium. The SNP-bearing sequences were probed to the entire bread wheat NRGene genome assembly ver. 1.0 (International Wheat Genome Sequencing Consortium, https://wheat-urgi.versailles.inra.fr/Seq-Repository/Assemblies) using an in-house BLAST portal and to wild emmer wheat (*T. dicoccoides* cv. Zavitan) whole-genome assembly WEWSeq v.1 (https://wheat.pw.usda.gov/cgi-bin/seqserve/blast.cgi). The best hits, based on sequence similarity and cumulative alignment length percentage of matches, were considered. For annotation, the flanking marker sequences were used to find expressed genes on the scaffolds using POTAGE (PopSeq Ordered *Triticum aestivum* Gene Expression) (Suchecki et al. 2017). POTAGE integrates map location with gene expression and inferred functional annotation and visualizes these data through a web browser interface. In order to compare QTL mapped in our study with others, the flanking marker sequences (if available) were used for BLAST to determine physical position or SNP markers tightly linked to the SSR/DArT markers were used for comparison.

6.5. Results

6.5.1. Phenotypic evaluations and heritability estimates

The BCRILs had a continuous distribution for FHB related-traits in all environments with a very small proportion of transgressive segregants in some environments (Fig. 6.1; Table 6.1). In all the environments, the resistant donor parent BGRC3487 was less diseased than the susceptible parent DT735 (Fig. 6.1; Table 6.1). Analysis of variance showed significant genetic variation among RILs (P <0.001) or significant genotype by environment interaction (P <0.001) for FLD-IND, FLD-SEV, FLD-INC, or FLD-VRI (data not shown). Broad-sense heritabilities (H^2) ranged from 24 to 84% and were highest for greenhouse evaluations (Table 6.1). Except for FLD-INC, heritability estimates of all other traits were moderate to high. The high heritability detected under controlled greenhouse conditions could be attributed to lower residual variance, which accounted for the minimal variation. A low to moderate positive correlation was observed in most environments, indicated by the acute angle among

environmental vectors in biplot analyses and Pearson's correlation coefficient values (Fig. 6.2; Appendix G). Correlation coefficients between 2008 and 2010 site-years were higher than with 2009 indicating more similarity in 2008 and 2010 site-years, in terms of disease pressure. The low to moderate correlations among FHB traits in different environments could be attributed to difference in FHB resistance expression which was evident from check data, for example, the resistant check FHB37 had FLD-SEV of 2.3-12.5% and FLD-INC of 6.6-40.0%, and the susceptible check AC Morse had FLD-SEV of 39.1-70.0% and FLD-INC of 78.9-86.1% (data not shown). The two principal components explained approximately 61% of the phenotypic variation of the population. Long environmental vectors for all environments, except GH-CIM, indicated that genotypes could be differentiated in all environments. The phenotypic data for seed coat color showed a bi-modal distribution indicating qualitative nature of the trait and thus a few major genes involved.

Table 6.1. Mean and range of Fusarium head blight (FHB) traits (%) in the BGRC3487/2*DT735 population, parental mean values, broad-sense heritability (H^2) for field (FLD) and greenhouse (GH) disease evaluations.

Trait[a]	Population			Parents		H^2
	Mean	Range	SD[b]	BGRC3487	DT735	
FLD-IND	24.1	6.3 – 60.9	9.4	7.7	32.6	-
FLD-SEV	31.0	13.1 – 66.2	9.8	13.3	40.8	55.2
FLD-INC	68.3	42.7 – 92.8	9.7	44.4	74.3	23.5
FLD-VRI	60.2	19.3 – 89.1	11.2	2.8	53.6	56.9
FLD-INC16	57.9	15.0 – 96.7	14.1	20.0	76.6	65.0
FLD-SEV16	23.6	9.0 – 58.3	7.9	15.0	32.0	55.2
FLD-IND16	14.3	1.6 – 46.7	7.5	4.0	24.3	67.0
GH-SEV	44.0	6.8 – 95.9	22.8	12.4	56.8	83.6
GH-CIM	22.1	1.4 – 74.8	13.1	11.5	49.2	-

[a]Here: FLD-IND: field FHB index; FLD-SEV: field FHB severity; FLD-INC: field FHB incidence; FLD-VRI: field FHB visual rating index; GH-SEV: greenhouse severity for 3-ADON chemotype; GH-CIM: greenhouse severity measured in 2017.

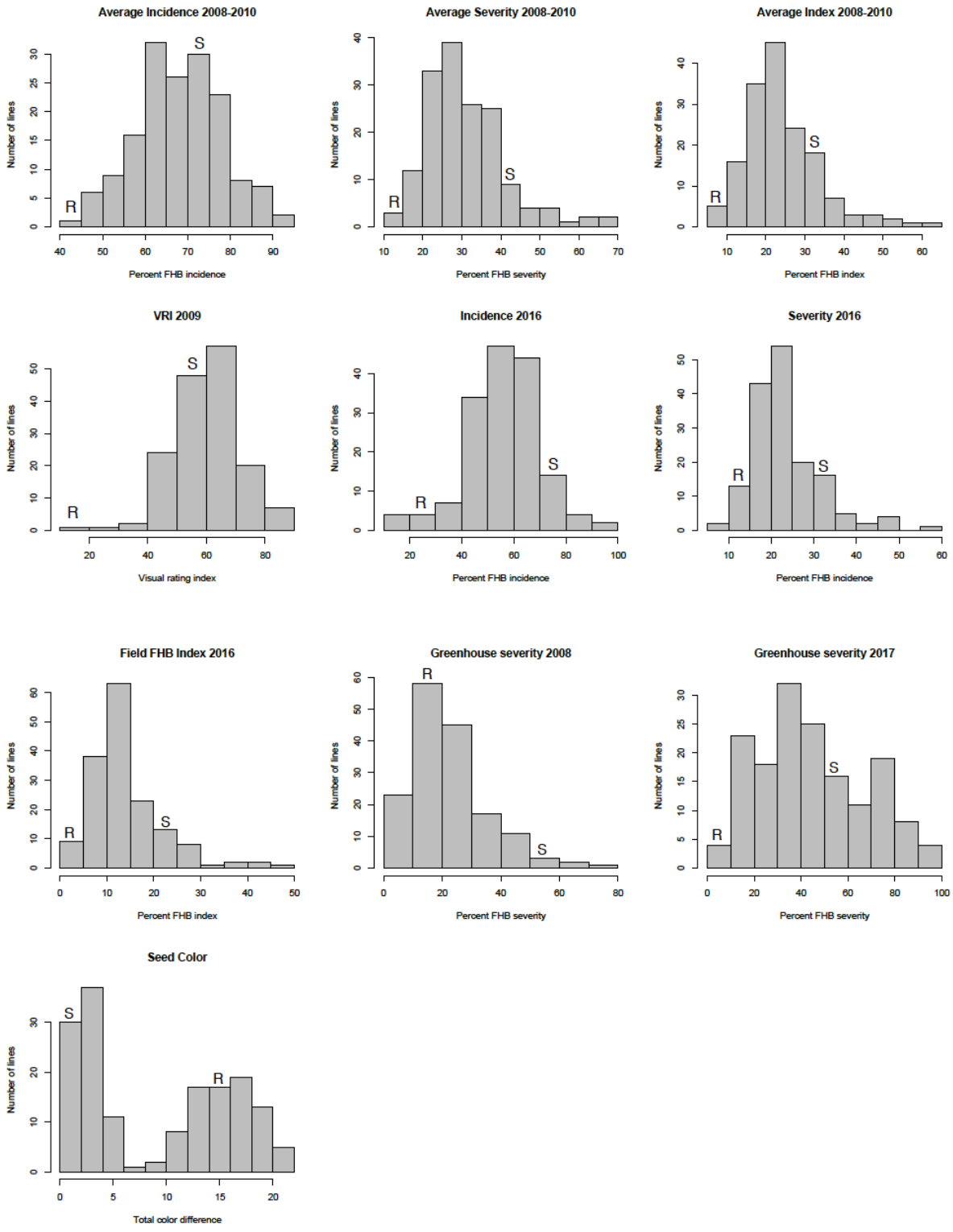

Figure 6.1. Frequency distribution of 160 backcross recombinant inbred lines from BGRC3487/2*DT735 cross for Fusarium head blight (FHB) traits and seed coat color. Here 'R' and 'S' represents resistance donor parent (BGRC3487) and recurrent susceptible parent (DT735), respectively.

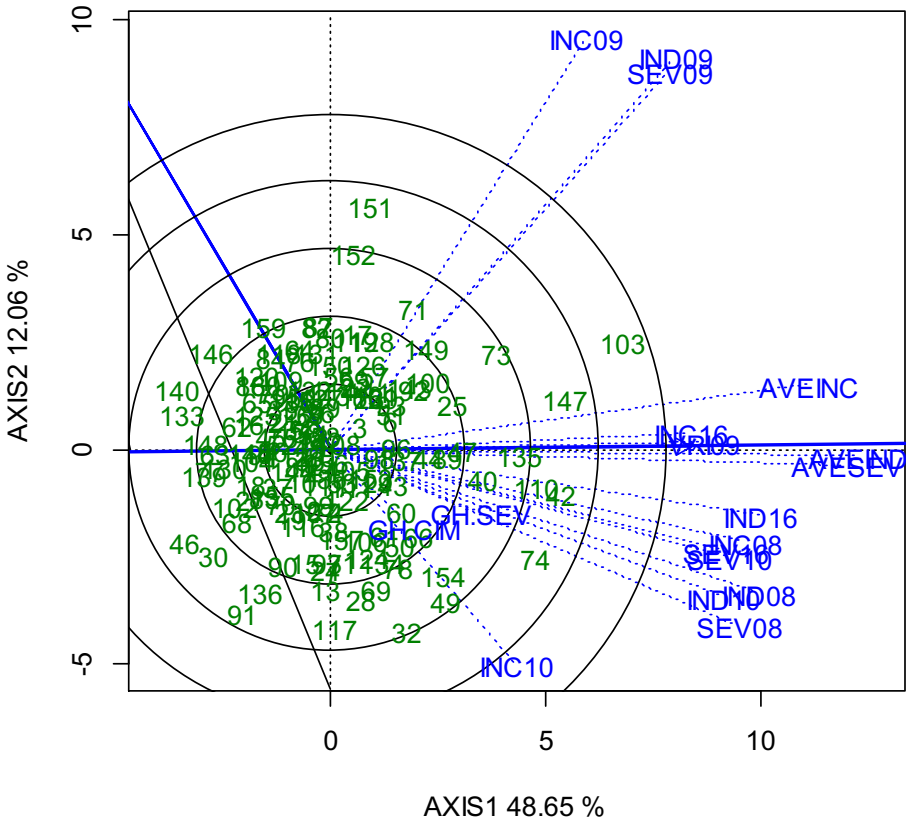

Figure 6.2. Genotype and genotype by environment (GGE) interaction plot showing relationship among genotypes, environments and their interaction. Numbers in the green indicates recombinant inbred lines entries from BGRC3487/2*DT735 population and blue labels and vectors are unique to every environment. The solid blue line passing through the origin of the plot is 'Average Environment Axis' indicating the most ideal and discriminating environment. The axes of the plot indicate standard deviation for phenotype (proportional to length of environment vector). The phenotypic variation explained by both axes is indicated next to the labels. Here: INC: incidence, SEV: severity, IND: index, GH-SEV: greenhouse severity.

6.5.2. High-density linkage mapping

Of the 81,587 SNPs from the 90K iSelect genotyping assay, 55,038 were assigned to the A and B genomes, which are relevant to tetraploid wheat (Wang et al. 2014). After quality filtering of the 55,038 SNPs, 5,650 were used for linkage mapping. Strong signals for both parental alleles indicated that 5,645 of these SNPs could be used as co-dominant markers. In the remaining five SNPs, only one of the parental alleles was amplified in the infinium reaction. A total of 29 linkage groups were obtained with a minimum LOD threshold of 3.0 (Table 6.2). Correspondence of mapped markers with those on consensus maps (Wang et al. 2014; Macferri et al. 2015) was used to assign each linkage group and orient to the short (S) or long (L) chromosome arms. All 5,650 markers comprised 1,777 groups/skeleton markers that were used for QTL mapping. The total length of the genetic map was 1822.5 cM, with

an average distance of 1.03 cM between adjacent skeleton markers, but some markers had a distance of >10 cM as well (Table 6.2; Fig. 6.3). The number of skeletal markers ranged between 55 and 280 for each of the 14 chromosomes and average number of attached markers per skeleton marker was 3.2. In general, skeleton markers in centromeric regions had the largest group of attached markers (data not shown). In total, more markers were mapped to the B genome (66%, 688.6 cM) than to the A genome (34%; 1133.9 cM). The expected heterozygosity per locus in an F_{10} population is 0.195%; the average heterozygosity per locus in our population was 0.167% and 831 markers had >0.167% heterozygous genotypes (range 0.625-12.5) (data not shown). Of 831 heterozygous markers, only 32 had >2.0% heterozygosity. The highly heterozygous markers were distributed all over the chromosomes. Out of 2,240 RIL x chromosome combinations (160 RILs x 14 chromosomes = 2,240), 374 chromosomes (16.7%) remained non-recombinant (parental, BGRC3487 = 12, DT735 = 362) (Appendix H). Parental chromosomes were identified in all 14 chromosomes with 3/4 in the A genome. The highest number of parental chromosomes were present in 2A (67) and the lowest in 2B (7). Notably, the number of parental chromosomes per chromosome was correlated with the chromosome's genetic length (ρ = -0.64, P = 0.01) and to the number of skeleton markers (ρ = -0.76, P = 0.01) (Appendix I).

Table 6.2. Summary of the genetic map constructed with 160 BCRILs from BGRC3487/2*DT735 cross.

Chromosome	All markers	Skeleton markers	Length (cM)	cM/Locus
1AS	102	41	21.2	0.52
1AL	95	28	31.1	1.11
1BS	372	110	84.0	0.76
1BL1	138	59	44.2	0.75
1BL2	62	25	7.5	0.30
2AS	74	10	9.5	0.95
2AL	160	45	36.3	0.81
2B	981	280	288.6	1.03
3AS	112	30	35.3	1.18
3AL	156	63	113.8	1.81
3BS	129	50	42.3	0.85
3BL1	162	51	22.8	0.45
3BL2	209	34	49.6	1.46
3BL3	132	49	27.9	0.57
4AS	32	8	7.7	0.96
4AL1	108	34	20.4	0.60
4AL2	44	24	51.7	2.15
4B	339	84	110.4	1.31
5A	321	90	134.2	1.49
5AL	28	16	23.7	1.48
5BS	63	23	19.6	0.85
5BL	201	75	145.3	1.94
6A	337	116	85.5	0.74
6B	480	129	108.6	0.84
6BL	47	14	45.6	3.26
7AS	145	84	72.8	0.87
7AL	209	48	45.5	0.95
7BS	127	54	53.0	0.98
7BL	285	103	84.6	0.82
Group 1	769	263	188.0	0.71
Group 2	1,215	335	334.5	1.00
Group 3	900	277	291.6	1.05
Group 4	523	150	190.1	1.27
Group 5	613	204	322.8	1.58
Group 6	864	259	239.7	0.93
Group 7	766	289	255.8	0.89
A genome	1,923	637	688.6	1.08
B genome	3,727	1,140	1133.9	0.99
Total	5,650	1,777	1822.5	1.03

6.5.3. QTL mapping

Several QTL on all chromosomes except 1B, 2A, and 3A were identified that conferred resistance to FHB (Table 6.3, Fig. 6.3). Fifteen QTL were identified for FHB field resistance (FLD-IND, FLD-INC, FLD-SEV) and 11 of these QTL were derived from the moderately susceptible/intermediate parent DT735 (Table 6.3). Of these 15 QTL, three were also identified for GH-CIM and explained 5.7-6.4% of the phenotypic variation. For FLD-VRI, 14 QTL were identified, of which 11 were the same as FLD-IND, FLD-SEV, or FLD-INC. Of the three QTL unique to FLD-VRI, one was contributed by the resistant parent BGRC3487. Two of the 15 QTLs, *QFhb.usw-2BL* and *QFhb.usw-7BS*, were associated with increased plant height where the DT735 allele increased plant height by six to nine cm (Table 6.3; data not shown). Except for a few QTL, most were identified in multiple environments (Table 6.3). Four QTL, all derived from the resistant parent BGRC3487, were identified for resistance to the 3-ADON chemotype of *F. graminearum* in the greenhouse and explained 10.1-11.7% of the phenotypic variation (Table 6.3). Prior to this work, Ruan et al. (2012) mapped 11 QTL for FHB field resistance (on 2A, 3B, 5A, 5B, 7A, 7B) and two for resistance to the 3-ADON chemotype (on 1B and 4B) of *F. graminearum* using SSR and DArT markers. Among QTL for FHB field resistance, *QFhb.usw-7AS1* was the same as *QFhb.usw-7A1,* and *QFhb.usw-7AS2* the same as *QFhb.usw-7A2* from Ruan et al. (2012). For resistance to the 3-ADON chemotype, no significant QTL on 1B were mapped in the present study, whereas *QFhb.usw-4BL2* in our study was the same as *QFhb.usw-4B* in their study with the only discrepancy that in our study the QTL was derived from the resistant parent. Surprisingly, none of three QTL on 3B in our study overlapped with *QFhb.usw-3B* in their study. However, *QFhb.usw-3BLc* is relatively close to *gwm566*, which lies in the 3B interval of the Nyubai allele that was speculated to coincide with the 3B QTL of Ruan et al. (2012).

One of the disadvantages associated with BGRC3487 as a parent is that it has a red seed coat, unlike DT735 which has an amber colored seed coat (favoured in durum wheat). Based on the NaOH test, the lines had a bimodal distribution with an amber seed coat for 79 of the BCRILs and a red seed coat for 81 (Fig. 6.1). The classification fit a 9 (amber): 7 (red) ratio (chi-square statistic = 2.80; $P = 0.10$) and a 29 (amber): 35 (red) ratio (chi-square = 1.23, $P = 0.26$), indicating that two or three genes may control seed coat color. Three QTL were mapped (Table 6.4) for seed coat color, and all were the same as reported by Ruan et al. (2012), determined from physical position of the SNP markers linked to the flanking markers from the consensus maps (Macferri et al. 2015).

Table 6.3. Summary of quantitative trait loci (QTL) associated with Fusarium head blight (FHB) traits and Fusarium graminearum 3-ADON chemotype severity from the greenhouse in BGRC3487/2*DT735 population. The QTL with asterisk mark confer resistance dependent on increased plant height (6-9 cm increase) from the favourable allele.

Trait	QTL	Chr.	Source of Resistance allele	2008		2009		2010		Mean (2008-2010)		2016	
				LOD[a]	PVE[b]	LOD	PVE	LOD	PVE	LOD	PVE	LOD	PVE
FLD-IND	*QFhb.usw-1AL*	1AL	BGRC3487	2.4	6.5	-	-	-	-	2.2	6.1	-	-
	*QFhb.usw-2BL**	2BL	DT735	4.2	11.3	-	-	3.0	8.3	3.6	9.9	-	-
	QFhb.usw-3BS	3BS	DT735	-	-	-	-	2.0	5.6	-	-	3.9	10.6
	QFhb.usw-3BLc	3BL	DT735	4.4	11.9	-	-	-	-	2.6	7.3	-	-
	QFhb.usw-3BL	3BL	BGRC3487	-	-	3.5	9.6	-	-	1.9	5.2	3.5	9.5
	QFhb.usw-4BS1	4BS	DT735	-	-	3.2	8.7	2.8	7.8	3.3	8.9	2.4	6.6
	QFhb.usw-4BS2	4BS	DT735	1.9 ns	5.4	-	-	3.4	9.3	3.5	9.6	2.1	5.4
	QFhb.usw-4BL1	4BL	DT735	3.4	9.2	2.0	5.4	2.4	6.6	4.5	12.1	2.3	6.3
	QFhb.usw-5AS	5AS	DT735	2.1	5.7	-	-	1.9 ns	5.2	2.1	5.7	3.2	8.8
	QFhb.usw-5AL	5AL	DT735	1.8 ns	4.9	4.7	12.7	-	-	3.9	10.7	-	-
	QFhb.usw-5BL	5BL	BGRC3487	-	-	3.1	8.5	-	-	2.3	6.4	4.6	12.2
	QFhb.usw-6BS1	6BS	DT735	-	-	-	-	2.0	5.6	2.1	5.9	2.8	7.8
	QFhb.usw-7AS1	7AS	BGRC3487	-	-	2.0	5.7	-	-	2.0	5.6	2.4	6.6
	QFhb.usw-7AS2	7AS	DT735	3.0	8.2	-	-	2.9	7.9	2.8	7.8	-	-
	*QFhb.usw-7BS**	7BS	DT735	2.9	8.0	-	-	3.7	10.1	3.2	8.7	2.1	5.9
FLD-SEV	*QFhb.usw-1AL*	1AL	BGRC3487	2.6	7.2	-	-	-	-	2.3	6.3	-	-
	*QFhb.usw-2BL**	2BL	DT735	4.1	11.1	-	-	2.3	6.4	3.3	9.1	-	-
	QFhb.usw-3BS	3BS	DT735	-	-	-	-	1.9	5.2	-	-	2.9	7.9
	QFhb.usw-3BLc	3BL	DT735	5.3	14.2	-	-	-	-	3.4	9.2	-	-
	QFhb.usw-3BL	3BL	BGRC3487	-	-	4.0	10.8	-	-	1.8	5.0	3.5	9.5
	QFhb.usw-4BS1	4BS	DT735	-	-	3.2	8.7	2.7	7.6	2.8	7.7	2.1	5.8
	QFhb.usw-4BS2	4BS	DT735	-	-	-	-	3.3	9.1	3.3	9.0	2.3	6.3
	QFhb.usw-4BL1	4BL	DT735	2.8	7.6	1.7 ns	4.7	3.4	9.3	4.6	12.2	2.2	6.1
	QFhb.usw-5AS	5AS	DT735	2.4	6.6	-	-	-	-	2.1	5.7	2.5	7.0
	QFhb.usw-5BL	5BL	BGRC3487	-	-	3.2	8.9	-	-	2.1	5.7	2.8	7.8
	QFhb.usw-6BS1	6BS	DT735	-	-	-	-	1.8	5.0	2.1	5.9	2.5	6.8
	QFhb.usw-7AS1	7AS	BGRC3487	-	-	2.0	5.6	-	-	1.8	5.0	2.9	8.1
	QFhb.usw-7AS2	7AS	DT735	3.7	10.1	-	-	3.5	9.6	3.0	8.4	-	-
	*QFhb.usw-7BS**	7BS	DT735	3.3	9.1	-	-	3.1	8.6	3.4	9.3	2.3	6.5
FLD-INC	*QFhb.usw-2BL**	2BL	DT735	2.5	6.8	-	-	2.2	6.1	-	-	-	-
	QFhb.usw-3BS	3BS	DT735	-	-	-	-	-	-	-	-	3.1	8.5
	QFhb.usw-3BLc	3BL	DT735	2.4	6.7	-	-	-	-	-	-	-	-

	QFhb.usw-3BL	3BL	BGRC3487	2.4	6.7	1.7	5.0	-	-	2.8	7.6	3.5	9.5
	QFhb.usw-4BS1	4BS	DT735	3.0	8.1	-	-	-	-	4.0	11.0	2.0	5.6
	QFhb.usw-4BS2	4BS	DT735	3.3	8.9	-	-	-	-	2.4	6.5	1.9	5.3
	QFhb.usw-5AS	5AS	DT735	2.7	7.4	-	-	2.6	7.3	2.6	7.2	4.6	12.4
	QFhb.usw-5AL	5AL	DT735	-	-	2.7	7.4	-	-	3.5	9.5	-	-
	QFhb.usw-5BL	5BL	BGRC3487	3.0	8.1	2.1	5.6	-	-	3.2	8.9	6.7	17.5
	QFhb.usw-7AS1	7AS	BGRC3487	1.9	5.3	1.8	5.1	-	-	3.5	9.5	-	-
	*QFhb.usw-7BS**	7BS	DT735	1.9	5.2	-	-	-	-	-	-	-	-
FLD-VRI	*QFhb.usw-2BL**	2BL	DT735	-	-	2.2	6.1	-	-	-	-	-	-
	QFhb.usw-3BS	3BS	DT735	-	-	2.9	8.1	-	-	-	-	-	-
	QFhb.usw-3BLc	3BL	DT735	-	-	2.0	5.6	-	-	-	-	-	-
	QFhb.usw-3BL	3BL	BGRC3487	-	-	3.2	8.9	-	-	-	-	-	-
	QFhb.usw-4BL1	4BL	DT735	-	-	2.5	7.1	-	-	-	-	-	-
	QFhb.usw-5BS	5BS	DT735	-	-	2.7	7.6	-	-	-	-	-	-
	QFhb.usw-5BL	5BL	BGRC3487	-	-	3.8	10.5	-	-	-	-	-	-
	QFhb.usw-6BS1	6BS	DT735	-	-	3.2	8.8	-	-	-	-	-	-
	QFhb.usw-7AS1	7AS	BGRC3487	-	-	2.2	6.1	-	-	-	-	-	-
	*QFhb.usw-7BS**	7BS	DT735	-	-	4.1	11.1	-	-	-	-	-	-
GH-SEV	*QFhb.usw-1AL*	1AL	BGRC3487	-	-	3.7	10.1	-	-	-	-	-	-
	QFhb.usw-4AL	4AL	BGRC3487	-	-	3.8	10.3	-	-	-	-	-	-
	QFhb.usw-4BL2	4BL	BGRC3487	-	-	4.3	11.7	-	-	-	-	-	-
	QFhb.usw-6BS2	6BL	BGRC3487	-	-	4.1	11.1	-	-	-	-	-	-
GH-CIM	*QFhb.usw-3BL*	3BL	BGRC3487	-	-	2.1	5.9	-	-	-	-	-	-
	QFhb.usw-5BL	5BL	BGRC3487	-	-	2.0	5.7	-	-	-	-	-	-
	QFhb.usw-5AS	5AS	DT735	-	-	2.3	6.4	-	-	-	-	-	-

[a]Logarithm of odds score.

[b]Percent phenotypic variance explained.

Table 6.4. Summary of quantitative trait loci (QTL) associated with seed coat color in the BGRC3487/2*DT735 population.

QTL	Chromosome	LOD[a]	PVE[b]
QCl.usw-3BL	3BL	23.8	49.8%
QCl.usw-3AL	3AL	7.1	18.6%
QCl.usw-5AS	5AS	4.9	13.4%

[a]Logarithm of odds score; [b]Percent phenotypic variance explained.

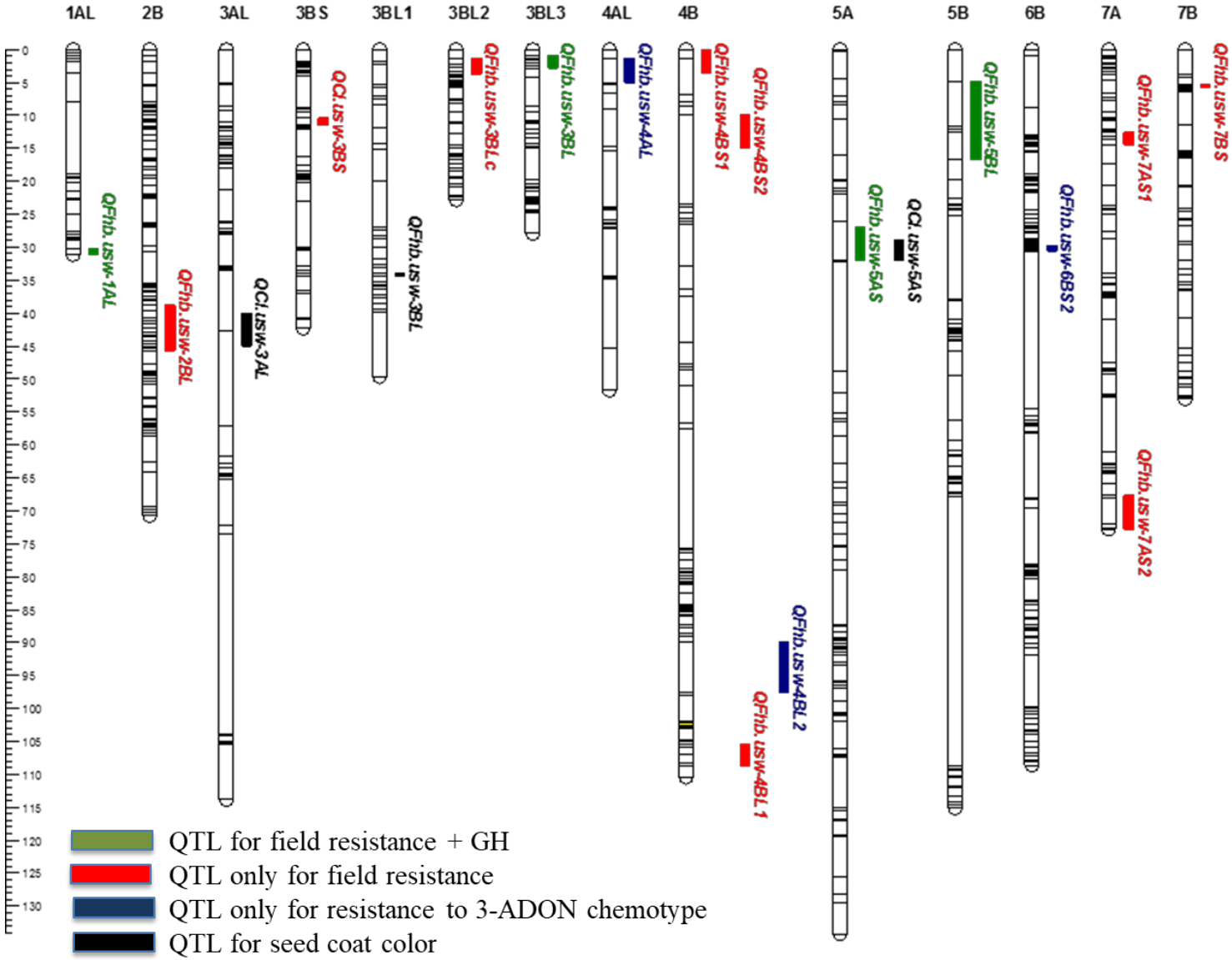

Figure 6.3. Portions of genetic linkage maps with quantitative trait loci (QTL) associated with Fusarium head blight (FHB) resistance and seed coat color in the BGRC3487/2*DT735 population (F_{10}). The scale on the left indicate genetic distance (cM) between single nucleotide polymorphism (SNP) markers.

6.5.4. Effect of pyramiding QTL and epistatic interactions

Among 15 QTL for FHB field resistance, the four best (in terms of percent variation explained) and most stable (in terms of detection in multiple environments) QTL (*QFhb.usw-3BL*, *QFhb.usw-4BL1*, *QFhb.usw-5BL*, and *QFhb.usw-7BS*) were selected to examine epistatic interactions and effect of combining of FHB resistance alleles. The QTL on 3BL, 4BL1, 5BL, and 7BS explained up to 9.6, 12.1, 12.2, and 10.1% of the variation for FLD-IND; 10.8, 12.2, 8.9, and 9.3% of the variation for FLD-SEV; 9.5, -, 17.5, and 5.2% of the variation for FLD-INC; 8.9, 7.1, 10.5, and 11.1% of the variation for FLD-VRI, respectively (Table 6.3). Additionally, QTL on 3BL and 5BL, derived from BGRC3487, were also detected in GH-CIM. The effects of the individual QTL and their combinations on FHB severity was further investigated by grouping RILs according to genotypes of the closest marker loci. When present individually, all four QTL reduced FHB compared to lines carrying none of these QTL (Table 6.5). An interaction ($P < 0.05$) among QTLs was observed between *QFhb.usw-3BL* and *QFhb.usw-4BL1*; and an interaction between 3BL and *QFhb.usw-5BL* was detected (Table 6.5) although it could not be examined as none of the NILs carried the 5BL QTL singly (data not shown). Combining two QTL did not reduce FHB more than a single QTL, and again this could be attributed to an epistatic interaction among QTL, not just the four QTL, but also among others. Taken together, QTL 3BL, 3BL+7BS, 5BL+4BL1, 3BL+4BL1+5BL+7BS were equally effective and reduced FLD-IND, FLD-SEV, FLD-INC, and FLD-VRI by up to 59-60, 47-53, 17-30, and 28-44%, respectively (Table 6.5). The QTL *QFhb.usw-3BL* alone was as effective as the combination of all four QTL in reducing FHB. In addition to examining the effect of all four stable QTL combined, Fig. 6.4 shows the effect of combining all QTL identified for FHB reduction. Among the 160 BCRILs, all lines carried between 2-14 resistance QTL and in general, pyramiding multiple resistance alleles was effective, but the RILs carrying just two QTL were equally effective as pyramiding seven or eight QTL. It is noteworthy that the combination of 3BL, 4BL1, 5BL, and 7BS was as effective as combining 14 QTL (Table 6.5 and Fig. 6.4). Among the four QTL for resistance to the 3-ADON chemotype, significant QTL-QTL interactions ($P < 0.05$) were also observed for *QFhb.usw-1AL* x *QFhb.usw-6BS2*, and *QFhb.usw-4AL* x *QFhb.usw-4BL2* (Table 6.6). The 1AL+4BL2 and 4BL2+6BL combinations were the most effective, reducing GH-SEV by 77-80%.

Table 6.5. Effects of combinations of favorable alleles at stable quantitative trait loci (QTL) on Fusarium head blight (FHB) traits in BGRC3487/2*DT735 population. The values in parentheses depicts percent disease reduction compared to lines carrying no resistance alleles (Null).

QTL combinations	Number of RILs	FLD-IND[a]			FLD-SEV[b]			FLD-INC[c]			FLD-VRI[d]		
		Mean[e]	SEM[f]	PDR[g]	Mean	SEM	PDR	Mean	SEM	PDR	Mean	SEM	PDR
Null	14	33.5 a	2.0	-	41.0 a	2.0	-	74.5 a	2.3	-	73.0 a	2.6	-
QFhb.usw-3BL (Q1)	1	13.7 bcd	7.4	59.1	19.2 b-e	7.5	53.2	61.6 abc	8.6	17.3	40.8 fg	9.8	44.1
QFhb.usw-5BL (Q2)	0	-	-	-	-	-	-	-	-	-	-	-	-
QFhb.usw-4BL1 (Q3)	18	22.3 bc	1.7	33.4	30.1 bcd	1.8	26.6	65.9 b	2.0	11.5	63.3 ce	2.3	13.3
QFhb.usw-7BS (Q4)	12	25.2 b	2.1	24.8	33.4 b	2.2	18.5	67.7 b	2.5	9.1	63.8 bc	2.8	12.6
Q1+Q2	1	20.2 a-d	7.4	39.7	28.3 a-e	7.5	31.0	64.2 abc	8.6	13.8	46.3 cdf	9.8	36.6
Q1+Q3	4	25.4 abc	3.7	24.2	34.5 abc	3.8	15.9	69.1 ab	4.3	7.2	75.0 ab	4.9	0.0
Q1+Q4	2	13.9 cd	5.2	58.6	20.3 de	5.3	50.5	56.1 bc	6.1	24.7	49.1 def	6.9	32.7
Q2+Q3	2	13.4 cd	5.2	60.0	21.6 de	5.3	47.3	54.9 bc	6.1	26.3	52.3 cdf	6.9	28.4
Q2+Q4	1	27.1 a-d	7.4	19.1	33.2 a-e	7.5	19.0	72.0 ab	8.6	3.4	56.5 a-f	9.8	22.6
Q3+Q4	66	21.1 bc	0.9	37.0	28.2 cd	0.9	31.2	67.1 b	1.1	9.9	59.4 cef	1.2	18.6
Q1+Q2+Q3	1	16.8 bcd	7.4	49.9	25.0 b-e	7.5	39.0	66.5 abc	8.6	10.7	60.8 a-f	9.8	16.7
Q1+Q3+Q4	8	19.9 bcd	2.6	40.6	26.7 b-e	2.7	34.9	64.4 b	3.1	13.6	58.4 cdf	3.5	20.0
Q1+Q2+Q4	1	23.4 a-d	7.4	30.2	30.4 a-e	7.5	25.9	68.6 abc	8.6	7.9	70.1 a-d	9.8	4.0
Q2+Q3+Q4	15	19.6 bc	1.9	41.5	27.4 cd	1.9	33.2	64.0 b	2.2	14.1	53.8 dg	2.5	26.3
Q1+Q2+Q3+Q4	14	13.9 d	2.0	58.6	21.5 e	2.0	47.6	52.3 c	2.3	29.8	51.9 d-g	2.6	28.9

[a]Field FHB index (%) = (percent incidence x percent severity)/100.
[b]Field FHB severity (percent of spikelets infected in infected spikes).
[c]Field FHB incidence (percent of spikes infected in the plot).
[d]Visual rating index.
[e]least squares mean.
[f]Standard error of mean.
[g]Percent disease reduction.

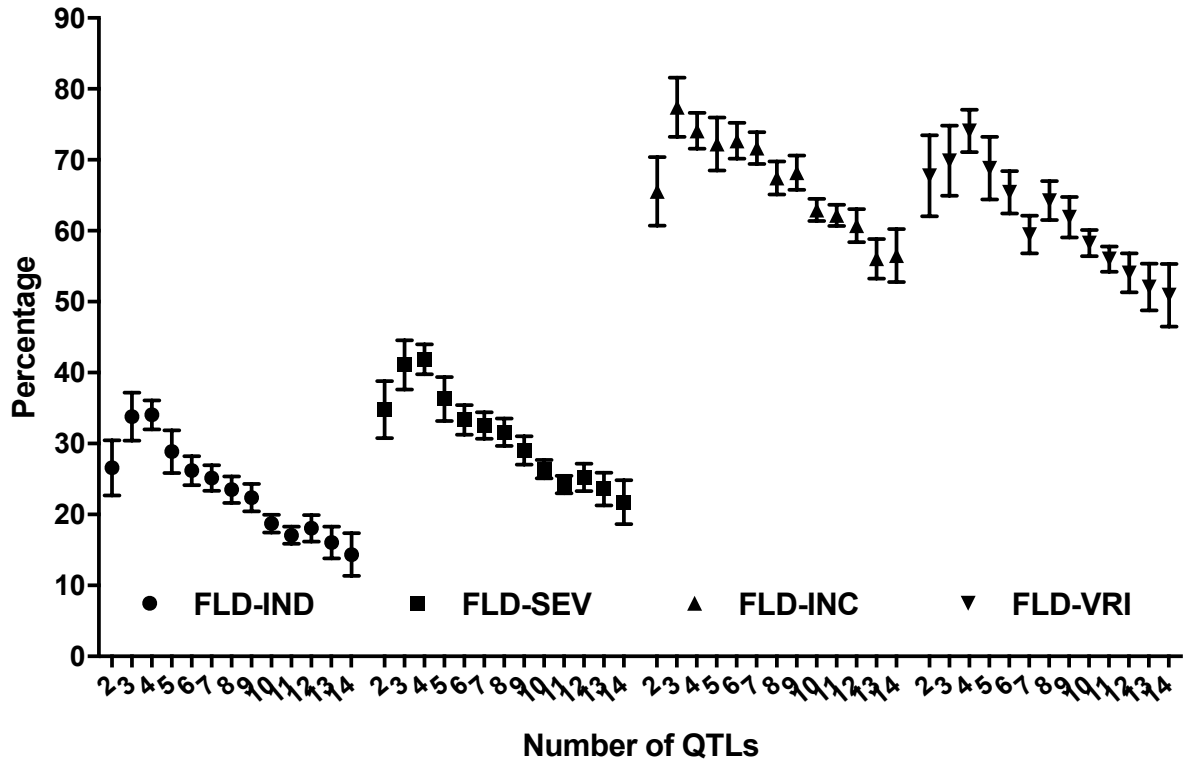

Figure 6.4. Fusarium head blight index (FLD-IND), severity (FLD-SEV), incidence (FLD-INC), and visual rating index (FLD-VRI) estimates from field evaluations as affected by number of pyramided QTL.

Table 6.6. Effects of various combinations of quantitative trait loci (QTL) associated with alleles conferring resistance to the Fusarium graminearum 3-ADON chemotype in the greenhouse evaluation of the BGRC3487/2*DT735 population.

QTL(s)	Number of RILs	LSmean[a]	SEM[b]	PDR[c]
Null	79	54.3 cd	2.2	-
QFhb.usw-1AL (Q1)	15	40.4 cd	5.0	25.6
QFhb.usw-4AL (Q2)	5	35.4 b-f	8.7	34.1
QFhb.usw-4BL2 (Q3)	7	43.4 bcd	7.4	20.1
QFhb.usw-6BL (Q4)	12	35.7 c-f	5.6	34.3
Q1+Q2	4	32.7 c-f	9.7	39.8
Q1+Q3	3	12.5 ef	10.0	77.0
Q1+Q4	1	87.2 a	19.5	0.0
Q2+Q3	6	39.0 b-e	8.0	28.2
Q2+Q4	2	21.6 def	13.8	60.2
Q3+Q4	3	10.9 f	10.0	79.9
Q1+Q2+Q3	7	23.5 def	7.4	56.7
Q1+Q3+Q4	0	-	-	-
Q1+Q2+Q4	10	26.9 def	6.2	50.5
Q2+Q3+Q4	4	26.5 def	9.7	51.2
Q1+Q2+Q3+Q4	2	22.1 def	13.8	59.3

[a]Least squares mean.

[b]Standard error of mean.

[c]Percent disease reduction.

6.5.5. Physical mapping and annotation

The physical positions of SNP markers, in hexaploid wheat (Chinese Spring) and tetraploid wheat (Zavitan), flanking the mapped QTL were in accordance with their genetic map positions, except for *QFhb.usw-3BS* which was physically located on Chromosome 3AS (Table 6.7). A few QTL with large genetic map intervals between flanking markers i.e. *QFhb.usw-2BL*, *QFhb.usw-3BLc*, *QFhb.usw-4BL2*, *QFhb.usw-5BL*, also covered a large physical area of the chromosome. The majority of the QTL were represented by narrow genetic/physical interval. Except for QTL *QFhb.usw-5AS*, which coincided with *QCl.usw-5AS*, all other QTL corresponded to the physical intervals with functionally annotated genes (data not shown; available on request). Among QTL for FHB resistance, the number of annotated genes ranged from nine (for *QFhb.usw-6BS1*) to 933 (for *QFhb.usw-3BLc*) (data not shown; available on request). For *QCl.usw-3AL* and *QCL.usw-3BL*, 308 and 69 annotated genes were obtained, respectively. A wide variety of predicted genes were annotated in the QTL interval for FHB. However, many of the genes can easily be eliminated based on their zero expression values in spike, particularly Zadoks growth stage Z65, which represent 50% anthesis stage. Similarly, genes for seed coat color are expected to have higher expression level at the seed stage.

Table 6.7. Genetic and physical positions of QTL for Fusarium head blight (FHB) resistance and seed coat color in BGRC3487/2*DT735 population.

QTL	Genetic interval (cM)	Physical interval - CS (Mb)[a]	Physical interval - Zavitan (Mb)[b]
		QTL for FHB resistance	
QFhb.usw-1AL	30.23 – 31.08	490.08 – 492.13	492.52 – 494.65
QFhb.usw-2BL	238.79 – 245.69	706.73 – 759.82	702.03 – 758.01
QFhb.usw-3BS	10.38 – 11.54	9.99 – 14.76 (on 3A)	0.87 – 5.32 (on 3A)
QFhb.usw-3BLc	1.30 – 5.54	159.57 – 257.32	56.67 – 264.87
QFhb.usw-3BL	0.89 – 2.82	795.33 – 796.46	808.34 – 811.72
QFhb.usw-4BS1	0.00 – 1.30	0.62 – 0.64	4.54
QFhb.usw-4BS2	9.76 – 9.89	5.78	1.52
QFhb.usw-4BL1	105.39 – 108.61	595.27 – 602.40	600.13 – 608.57
QFhb.usw-4BL2	89.86 – 97.57	428.70 – 499.85	435.54 – 505.89
QFhb.usw-5AS	31.903	35.26 – 36.02	36.58 – 37.38
QFhb.usw-5AL	62.90 – 66.46	439.56 – 442.35	437.05 – 439.84
QFhb.usw-5BL	4.79 – 16.66	488.10 – 507.87	494.21 – 513.09
QFhb.usw-6BS1	56.33 – 56.67	37.25 – 38.76	36.23 – 37.76
QFhb.usw-6BS2	29.71 – 30.56	20.68 – 22.10	19.97 – 22.44
QFhb.usw-7AS1	13.07 – 17.39	34.54 – 37.72	28.66 – 31.94
QFhb.usw-7AS2	67.73 – 72.78	88.99 – 92.43	86.46 – 90.27
QFhb.usw-7BS	5.43 – 5.64	46.99 – 59.61	50.85 – 178.99
		QTL for seed coat color	
QCl.usw-3AL	42.652	689.75	449.97
QCl.usw-3BL	33.89 – 34.31	741.86 – 750.86	755.36 – 771.12
QCl.usw-5AS	31.903	35.26 – 36.02	36.58 – 37.38

[a]Refer to whole-genome shotgun assembly of Chinese Spring common wheat (https://urgi.versailles.inra.fr/).
[b]Refer to whole-genome shotgun assembly of Zavitan emmer wheat.

6.6. Discussion

The genetic map developed in our study provided good coverage of the tetraploid wheat genome, since the size of the gaps in the chromosome arms were small in most cases. Although the average interval length is 1.03 cM, there are some areas with large gaps in the linkage groups (Appendix J). The large gaps in some genomic regions could be the introgressions, non-recombinant segments from BGRC3487, which were identical by descent to the parent or the regions with a lack of polymorphism between the parents. Relatively low recombination rates in our population were also evident from the large proportion of parental chromosomes. A lower recombination rate is observed around the centromere due to the tight physical arrangement of chromatin in the region; the less condensed telomeric regions are recombination 'hot-spots' (Faris et al. 2000). The centromeric regions tend to be 'SNP rich' in terms of genetic distances, due to their lower recombination rates (Poland et al.

2012). In most cases, the largest number of markers attached to any given skeleton markers were located around the centromere (data not shown). In a RIL mapping population, recombination occurs in F_1 and then in subsequent generations with half of the effect compared to the previous generation. In our population, we reported 16.7% of the BCRIL x chromosome combinations were parental types; Of these 16.7% parental combinations, only 0.5% were identical to BGRC3487, which is expected because the F_1 was backcrossed to DT735, which contributed to large proportion of the genome in the BCRILs. The large number of parental chromosome types results in lower recombination in hybrids and our data support this hypothesis (Appendix I). Genetic maps with fewer or small number of markers, as reported in most of the previously published FHB QTL mapping studies, could be vulnerable to mistakes due to under-representation of the genome and presented large gaps between markers. In contrast, even though our map contains large number of SNP markers, it covers only 1822.5 cM, whereas the previously published maps varied between 1272 – 3600 cM (reviewed in Avni et al. 2014).

Breeding for FHB resistance in durum wheat is one of the top priorities in the breeding programs in upper Great Plains of North America. Lack of resistance in cultivated durum make it imperative to search for resistance in other related species. In this study, we have identified stable and consistent QTL for FHB field resistance as well as resistance to 3-ADON chemotype, from elite durum wheat line DT735 and emmer wheat landrace BGRC3487 using high-density genetic linkage maps. The QTL identified in the present study were compared to previously published studies, particularly in tetraploid wheat (Somers et al. 2006; Kumar et al. 2007; Gladysz et al. 2007; Garvin et al. 2009; Ghavami et al. 2011; Buerstmayr et al. 2012; Lu et al. 2013; Zhang et al. 2014; Giancaspro et al. 2016; Zhu et al. 2016; Sari et al. 2018). All QTL reported in our study, except *QFhb.usw-1AL* and *QFhb.usw-5AS*, were novel and did not overlap with any previously reported genomic region/QTL. The *QFhb.usw-1AL* QTL in our study was in the same genomic region as the 1AL QTL in Giancaspro et al. (2016), indicating that the two QTL could either be the same or tightly linked. In our study, the 1AL QTL was derived from the resistant parent BGRC3487 and in Giancaspro et al. (2016), it originated from bread wheat accession 02-5B-318 (carrying alleles from Sumai 3). The genomic region carrying *QFhb.usw-5AS* (derived from DT735) in our study overlapped with the 5AS QTL derived from a susceptible bread wheat cultivar 'Naxos' reported in Lu et al. (2013). The 5AS QTL of Lu et al. (2013) was responsible for fewer Fusarium damaged kernels and lower DON accumulation, however, in our study it governed FHB field resistance. Our population was not tested for DON accumulation, so it is speculated that this QTL might also reduce kernel infection and lower

toxin accumulation. Ruan et al. (2012) mapped a QTL on 5A, the same as Singh et al. (2008) and Sari et al. (2018), who identified the 5A QTL from DT696 (a parent of DT735); however, Ruan et al. (2012) mapped it from the resistant parent BGRC3487. In our study, both the 5A QTL were derived from DT735 and one of the QTL could be the same as 5A from DT696. None of the QTL mapped on 3B, 5A, and 6B in our study overlap with well-characterized *Fhb1* (on 3BS), *Fhb2* (on 6BS), and *Fhb5* (on 5AS) genes in hexaploid wheat.

The *F. graminearum* population in North America is classified into chemotypes based on type of mycotoxin produced i.e. 3-ADON or 15-ADON. Until 1998, 15-ADON producing population of *F. graminearum* was predominant in western Canada, however, an exotic introduction (from Italy) of more toxigenic 3-ADON producing population of the pathogen replaced much of 15-ADON chemotype producing population (Ward et al. 2008; Gilbert et al. 2010). Between 1998 to 2004, the proportion of 3-ADON chemotype increased by 14-fold making ratio of two chemotype producing populations 1:1 in western Canada. That resulted in increased interest among researchers to test their material with 3-ADON chemotype. In fact, >80% of the most recent *F. graminearum* population from Saskatchewan was 3-ADON producing (Randy Kutcher, unpublished data). The four QTL identified from BGRC3487 in our study can serve as good targets by breeders to combat this aggressive and more toxin producing chemotype of *F. graminearum*.

It is well-established fact that FHB is a quantitative trait and the disease development is highly affected by environmental factors (Buerstmayr et al. 2009; Zhang et al. 2014). Because of higher susceptibility of durum wheat than common wheat, the disease expression is even more variable and thus it is not uncommon to have overwhelming disease in some site-years that eventually mask the small effect QTL. The disease pressure in 2008 and 2010 site-years was more similar than 2009 and that could be the reason why most of the QTL detected in 2008 or 2010 were not detected in 2009 and vice-versa. Despite environmental variation, majority of QTL in our study were detected in more than three site-years indicating their significance and stable nature although percent variation explained was not high. The lower contribution of majority of QTL in percent variation explained could be attributed to the fact that the recurrent parent DT735 also carried good level of resistance, which is evident from the results. The introgression of QTL mapped in our study could improve resistance to FHB in susceptible and moderately susceptible backgrounds. A large number of annotated genes were identified in the mapped QTL regions although majority of the genes could be eliminated based on their zero expression values in spike stages, particularly Z65. Of the predicted genes in our study, protein kinases, Glutathione S-transferases, methyltransferase proteins, zinc-finger protein, ubiquitin-protein ligase, 4-coumarate CoA ligases, leucine rich

repeats, ABC transporter are some of the potential ones as they have been reported to play a role in disease resistance, including FHB, in crop plants (Bent and Mackey 2007; Krattinger et al. 2009; Dhokane et al. 2016; Schweiger et al. 2016). However, having one of these as candidates for FHB resistance should be considered with caution because there are many other predicted proteins in the QTL regions and it need more dedicated studies to identify the reliable potential candidates.

Red seed coat color as expressed in BGRC3487 is not desirable because durum wheat cultivars must have Amber colored grain and thus a part of this study was to re-map QTL for seed coat color. All three QTL on 3BL, 3AL, and 5AS for the trait matched the results from Ruan et al. (2012). In hexaploid wheat, three recessive homeologus alleles at 3A, 3B, and 3D chromosomes are required to produce colorless seed coat and 3AL and 3BL QTL mapped in our study are likely associated with red seed coat color genes R-A1 (on 3A) and R-B1 (on 3B) (Mcintosh and Cusick 1987; McIntosh et al. 1998). The QTL on 5AS may not be associated with seed coat color *per se* and in fact could be associated with the yellow endosperm color of the grain overlapping with a QTL on 5A for yellow pigment mapped by Hessler et al. (2002). Ruan et al. (2012) reported and concluded that except for 2009, the BCRILs expressing red and amber seed coat were not statistically different in FHB expression. Phenotypic data collected in 2016 Saskatoon FHB Nursery as well as greenhouse data from CIMMYT corroborate this conclusion. Moreover, the major seed coat color QTL on 3BL did not overlap with FHB resistance QTL (Table 6.7). Thus, the seed coat color in our BCRIL population is not associated with FHB expression.

Several published studies have reported the correlation of plant height with FHB resistance (reviewed in- Buerstmayr et al. 2009; Gilbert and Haber 2013). Our study has identified two QTL (*QFhb.usw-2BL*, *QFhb.usw-7BS*) derived from DT735 where favorable allele increased plant height by six to nine cm and resistance is largely governed by plant height at these loci (Table 6.3). As these QTL are associated with increased plant height and a large proportion of resistance expression is due to increased height which is not preferred as taller cultivars tend to lodge. Therefore, such QTL may not be desirable to select for and relationship of plant height and FHB resistance should be determined in mapping studies, where possible, before implementing a marker-assisted selection strategy.

In conclusion, the tetraploid wheat lines BGRC3487 and DT735 are good sources of FHB resistance and both carry novel QTL. The consistent nature of the QTL accompanied by narrow physical interval makes them good candidates for marker assisted selection in durum wheat breeding programs. Our study and previously published studies have shown the

promise in pyramiding multiple FHB resistance QTL and flanking SNP marker from the most promising QTL can be a good target and starting point for resistance breeding efforts.

CHAPTER 7

Showcasing the application of synchrotron-based X-ray computed tomography in host-pathogen interactions: the role of wheat rachilla & rachis nodes in Type-II resistance to *Fusarium graminearum**

*The content of this Chapter is published as a full-length research article in 'Plant, Cell & Environment' journal (See Brar et al. 2019d).

7.1. Preface

In present day, many new technologies are introduced in the field of plant science and plant biology including techniques for plant imaging and spectroscopy. Despite the availability of state-of-art imaging technologies, there are very few studies on imaging host-pathogen interactions and none on *Fusarium*-wheat interaction. Synchrotrons present an excellent source of beamlines that can be utilized in imaging plants, and University of Saskatchewan is fortunate to have Canada's only third-generation synchrotron on its campus. There were some plant imaging studies published from my committee member Dr. Karunakaran's group before starting this PhD program. The curiosity coupled with availability of the facility led us to develop a study to image *Fusarium*-wheat interactions using X-ray computed tomography. After reviewing the literature, we developed a hypothesis to re-confirm the role of wheat rachilla + rachis nodes in Type-II resistance to *Fusarium graminearum*. This Chapter is a proof-of-concept to image *Fusarium*-wheat interactions and present results on that. With a learning experience, future studies can be performed with more accuracy and precision to test hypotheses related to wheat pathosystems that cause in structural changes in tissues.

7.2. Abstract

Fusarium head blight (FHB), caused primarily by *Fusarium graminearum* (*Fg*), is one of the most devastating diseases of wheat. Host resistance in wheat is classified into five types (Type-I to Type-V) and a majority of moderately resistant genotypes carry Type-II resistance (resistance to pathogen spread in the rachis) alleles, mainly from the Chinese cultivar Sumai 3. Histopathological studies in the past failed to identify the key tissue in the spike conferring resistance to pathogen spread and most of the studies used destructive techniques, potentially damaging the tissue(s) under study. In the present study, non-destructive synchrotron-based phase contrast X-ray imaging and computed tomography techniques were

used to confirm the part of the wheat spike conferring Type-II resistance to *Fg* spread thus showcasing the application of synchrotron-based techniques to image host-pathogen interactions. Seven wheat genotypes of moderate resistance to FHB were studied for changes in the void space volume fraction and grayscale/voxel intensity following *Fg* inoculation. Cell-wall biopolymeric compounds were quantified using Fourier-transform mid-infrared spectroscopy for all genotype-treatment combinations. The study revealed that the rachilla and rachis nodes together are structurally important in conferring Type-II resistance. The structural reinforcement was not necessarily observed from lignin deposition, but rather from an unknown mechanism.

7.3. Introduction

Wheat (*Triticum aestivum* L.) serves as a staple food for over 50 million people, yet productivity is limited by a number of biotic and abiotic stresses. Among biotic stresses, *Fusarium graminearum* Schwabe (*Fg*) (teleomorph: *Gibberealla zeae* (Schweinitz) Petch) has emerged as a global pathogen of wheat causing head blight (syn. scab), which results in yield and quality losses (McMullen et al. 2012). *Fusarium culmorum* W.G. Smith is another species responsible for FHB in wheat but it is prevalent only in temperate climates. Grain quality loss is caused by the accumulation of trichothecene mycotoxins such as deoxynivalenol and its acetylated forms, which pose serious health risks above a threshold of ~1 ppm. Breeding for host resistance is considered an environmentally safe and cost-effective approach to manage this disease. Five types (Type-I to V) of host resistance mechanisms have been identified in wheat (reviewed in Gilbert and Haber 2013). Among these, selection for Type-II (resistance to pathogen spread in the spike) is relatively easy for plant breeders. Only a few sources of resistance, mainly originating from east Asia (cv. Sumai 3 and its derivatives) and Brazil (cvs. Maringa, Frontana and their derivatives) are extensively used in breeding programs worldwide (McCartney et al. 2004; Buerstmayr et al. 2009).

Field epidemics of FHB result when warm and humid environmental conditions coincide with the onset of anthesis (McMullen et al. 2012). The susceptibility of wheat florets at anthesis and the general progression of Fusarium head blight has been recognized for over a century (Arthur 1891; Atanasoff 1920; Pugh et al. 1933; Anderson 1948). The histology of spike infection has been studied extensively in the last decade, revealing the infection route of the two main species responsible for FHB, i.e. *Fg* and *F. culmorum* (Kang and Buchenauer 2000; Ribichich et al. 2000; Miller et al. 2004; Jansen et al. 2005; Brown et al. 2010). Post-floral invasion, these pathogens spread throughout the spikelet inter- and

intra-cellularly down the rachis through the rachis node. Although ample information is available on the infection pattern and the mode of infection of *Fusarium* spp., the majority of studies did not include wheat genotypes with differential resistance/susceptibility to FHB. Thus, the conclusions were limited to infection patterns of *Fusarium* spp. in various parts of the wheat spike. It is a well-established fact that the *Fusarium* spp. causing FHB produce a cocktail of cell-wall degrading enzymes that interfere with the first line of defense by hydrolyzing plant cell-wall barriers (Walter et al. 2010). In anatomical and histological studies published between 2000 and 2010, the authors concluded that spikelet to spikelet spread of the fungus was inhibited by cultivars with Type-II resistance. The limited number of studies that included cultivars with differential susceptibility to FHB, indicated that the cellular changes in those cultivars are generally similar and the only difference is in the rate of disease progression (Kang and Buchenauer 2000; Ribichich et al. 2000). Cultivars with Type-II resistance, resist pathogen spread in the rachis thus slowing disease development or progression.

Anatomical features associated with Type-II resistance include: spike traits such as dense vascular bundles in the rachis, small diameter vessels, strong and thick cortical sclerenchyma cell-walls, and short internodes in the upper part of the rachis (Zhang and Ye 1993; Yu et al. 1996). None of these studies could identify the actual tissue or part of the wheat spike conferring resistance to pathogen spread. However, later studies by Jansen et al. (2005) and Zhang et al. (2008) pointed to the rachis node as an important part of the spike resisting fungal spread. Earlier, histopathology studies were mostly aimed at understanding the host-pathogen interaction and pathogen infection processes (Arthur 1891; Atanasoff 1920; Pugh et al. 1933; Anderson 1948; Kang and Buchenauer 2000; Ribichich et al. 2000; Miller et al. 2004; Jansen et al. 2005; Brown et al. 2010). More recent studies have focussed on metabolomics, proteome or gene expression profiling of the host-pathogen interaction (Gunnaiah and Kushalappa 2014; Atanasova-Penichon et al. 2016; reviewed in Kazan et al. 2012; Shah et al. 2017). A large number of candidate genes in resistant cultivars are associated with the phenotypic expression and temporal and spatial profiling of the genes. Thus, histological studies can provide information on pathogen spread or colonization of each part of the spike making it easier to associate candidate genes with structural changes.

Imaging technologies have advanced the field of plant biology by making non-destructive analyses of plants organs and biological phenomena possible (Tanino et al. 2017). The non-destructive analyses of plant parts can be achieved by X-ray phase contrast imaging (PCI) and computed tomography (CT) from either conventional lab-based or synchrotron sources. So far, only two studies (from co-author Dr. Karunakaran's group) used

synchrotron-based techniques to study the *Fg*-wheat interaction. These studies used Fourier-transform mid infrared (FTIR) spectroscopy to focus mainly on the biochemical changes occurring in the cultivars with differential resistance responses (Lahlali et al. 2015, 2016). Our study utilized synchrotron X-ray imaging to elucidate structural changes resulting from *Fg* infection in near-isogenic lines segregating for Sumai 3 derived resistance genes (*Fhb1*, *Fhb2*, and *Fhb5*) that carried less than 4% donor alleles. Reviewing information available in the literature, we hypothesized that the rachilla and/or rachis nodes provide resistance to *Fg* spread in resistant wheat genotypes. The pathogen causes the plant cell-wall deterioration following colonization; these structural changes likely create measurable changes in X-ray attenuation so as to be amenable to more direct quantification of void space and plant tissue. Our study essentially combined information on *Fg* infection processes causing changes in tissue structure and use of the X-ray imaging system to non-destructively analyze and quantify changes in specific regions of interest (ROIs) around the rachis nodes to test the hypothesis. As the pathogen degrades the tissue, the tissue volume is decreased, which in turn increases porosity, thus causing differences in X-ray attenuation. By measuring those parameters, we attempted to demonstrate and confirm the role of the rachilla and the rachis nodes in Type-II resistance to *Fg* in wheat. Although the role of the rachis node in Type-II resistance has previously been demonstrated by Jansen et al. (2005) and Zhang et al. (2008), our study took a very different approach and focussed on the application of 3D imaging technologies, thus showcasing the application of imaging technologies to study host-pathogen interactions.

7.4. Theory behind X-ray phase contrast imaging

When X-rays pass through an object, they are attenuated and phase-shifted based on the density and composition of the material (Als-Nielsen and McMorrow 2011). X-rays are electromagnetic waves and the refractive index of an object can be defined as: $n = 1 - \delta + i\beta$, where δ is the decrement in part of the refractive index, i.e. a phase shift term, and β is the attenuation term for absorption. In physical theory (with simplification), the total phase shift $\emptyset$ can be related to δ as, $\emptyset = \delta kz$ and the absorption term β can be related to k and z as, $\mu' = \mu z = 2\beta kz$, where μ is the absorption coefficient, k is the wavenumber, and z is the object thickness (Liu et al. 2013b). Thick materials cause more attenuation in the hard X-ray region and thus provide sufficient contrast based on absorption alone. In soft materials such as plant tissues, the phase shift term δ can be up to three times higher than the attenuation term, β. Acquisition of the phase shift $\emptyset$ is advantageous over absorption, μ' for better image

contrast with lower dose of the X-ray beam. In an X-ray imaging system, the sample-to-detector distance (*d*) is often set in such a way that *d* is less than *L*, where '*L*' is the distance between source and sample (Westneat et al. 2008). When X-rays pass through the sample, interference occurs between the diffracted components of the beam and the non-diffracted portion, creating an edge-enhanced image of the sample on the detector. Fresnel diffraction, resulting from adjustment of *d*, allows for control of the edge enhancement effect, which is the key feature of synchrotron-based PCI (Karunakaran et al. 2015). The same principle applies to CT, which is a three-dimensional extension of 2D-PCI.

7.5. Materials and methods

7.5.1. Plant material

Seven wheat genotypes were selected for the study: CDC Alsask (a hard red spring wheat cultivar), 04GC0139 (a resistant donor of *Fhb1*, *Fhb2*, and *Fhb5* QTLs/genes), four near-isogenic lines (carrying less than 4% alleles from the resistance donor) in a CDC Alsask background (Alsask2, Alsask8, Alsask22, Alsask25) segregating for *Fhb1*, *Fhb2*, and *Fhb5*, and a putative intergeneric spring wheat line 00Ar134-1 (Table 7.1). The presence of genes was confirmed using molecular markers: *umn10*, *gwm493*, *gwm533*, functional markers for the pore-forming toxin (PFT) protein in *Fhb1* and single nucleotide polymorphisms (SNPs) markers from Zhao et al. (2018) in *Fhb1* region; *wmc105*, *wmc152*, *wmc397*, *wmc398*, and *gwm644* flanking *Fhb2*; and *wmc705*, *barc117*, *gwm293*, *gwm304*, *gwm415, barc180, barc186,* and *Ra_c23129_348* (SNP marker), flanking *Fhb5* (McCartney et al. 2004; Rawat et al. 2016; Buerstmayr et al. 2017; Zhao et al. 2018). The line 00Ar134-1 is derived from a cross of wheat and *Elymus repens* L. (wheatgrass), and was included as it has a good level of resistance to FHB (Brar and Hucl 2017). Genes *Fhb1* and *Fhb2* govern Type-II resistance to FHB, whereas *Fhb5* mainly governs Type-I resistance (resistance to initial infection) plus some Type-II resistance (Buerstmayr et al. 2009). Three plants were grown in one gallon pots (~13 cm diameter) under controlled conditions of 18 h, 21 °C days and 6h, 17°C nights. Plants were watered every 3 days and fertilized with 10 g of slow-release N-P-K (14-14-14) fertilizer 4 weeks after seeding. Three wheat plants sown per gallon pot resulted in good growth with sufficient tillers, similar to field grown plants under rainfed conditions (personal observation). Each genotype was seeded in six pots with three plants per pot, each pot representing an independent biological replication. Three pots were used for *Fg* inoculations and the remaining three for procedural controls.

Table 7.1. Wheat genotypes used to assess biopolymeric and structural changes in the rachilla and rachis resulting from wheat-Fusarium graminearum interaction.

Genotype	Resistance gene/QTL	Proportion of alleles from resistance donor in NILs[a]	Description
CDC Alsask	None	-	Susceptible parent for CDC Alsask Near-isogenic lines (NILs)
04GC0139	*Fhb1, Fhb2, Fhb5*	-	Resistant parent for NILs
Alsask2	*Fhb1*	3.0%	NIL
Alsask8	*Fhb1, Fhb2*	2.8%	NIL
Alsask22	*Fhb1, Fhb2, Fhb5*	3.8%	NIL
Alsask25	*Fhb2, Fhb5*	3.5%	NIL
00Ar134-1	Unknown	-	-

[a]Determined from genotypic data generated from wheat 90,000 iSelect assay with 81,587 single nucleotide polymorphism markers (Wang et al. 2014; Brar et al. 2019a, 2019b).

7.5.2. Fungal isolates, inoculum preparation, procedure, and disease assessment

Two isolates of *Fg*, M9-07-1, a 3-ADON chemotype (NRRL 52068) and M1-07-2, a 15-ADON chemotype (NRRL 47847), were used for inoculations (Gilbert et al. 2014). The isolates were cultured individually on potato dextrose agar (PDA) and mixed in a 1:1 ratio after attaining the working concentration of 10^5 macroconidia/ml in distilled water. At about 50% anthesis (50% of the anthers are extruded), four spikelets in the center of a main stem spike on each plant were point inoculated with 10 µl of spore suspension per spikelet. The spore suspension was placed between the lemma and palea of a basal floret. Alsask25 was also spray inoculated with 1 ml spore suspension per spike as it carries *Fhb5*, the gene for Type I resistance. The inoculated spikes were then covered with clear plastic bags for 48 h to maintain humidity. Prior to covering the spikes, the plastic bags were misted with distilled water. An equal number of procedural controls with distilled water inoculations were included in the experiment. For each replication, six spikes were inoculated for each treatment, and a total of 18 spikes per genotype for each of the two treatments: procedural control and *Fg* inoculated spikes. The inoculated spikes were assessed at 12 and 20 days post inoculation (dpi) for disease severity based on the scale of Stack and McMullen (1998).

7.5.3. X-ray phase contrast imaging (PCI) and computed tomography (CT)

The phase contrast X-ray images of wheat spikes were collected from the Biomedical Imaging and Therapy beamline (BMIT-BM, 05B1-1) at the Canadian Light Source. The overall experimental workflow for X-ray imaging is depicted in Appendx 11. The beamline uses a bending magnet and multi-layer monochromator to produce high-brightness

monochromatic X-rays. The beamline was set up in PCI mode with the sample to detector distance at 20 cm, in which phase contrast effects were optimized for the spike samples. The X-ray energy of the incident beam was set to 20 keV, and a 0.5 mm thick aluminum filter was used before the monochromator to reduce the heat load on the monochromator crystals. Although the accessible energy range of the BMIT-BM is 15-40 keV, the beam energy was set to 20 keV based on previous results from Karunakaran et al. (2015), which suggested this to be optimum for imaging above-ground plant parts. The transmitted X-ray images were recorded by converting the X-ray intensities into visible images using a scintillator (comprised of Gd_2O_2S:Tb) combined with a visible-light camera (which together comprise an X-ray detector). A camera (ORCA-Flash 4.0) with the effective pixel dimensions of 13.123 µm was used in this study. A total of 1800 projections were collected in a field of view of over 180° rotation. The voxel size of the resulting dataset had an effective pixel size of 13.123 microns (pixel length and width) with this detector. The dark current of the detector was recorded (dark image) when there was no incident X-ray beam.

Spikes at 12 dpi were used for X-ray imaging. Freshly excised spikes of the samples were kept in an enclosed Falcon tube and brought to the beamline for imaging. The spikes were imaged within 2 h of being excised. For CT, the control and *Fg*-inoculated spike of each sample were put together in an opaque 50 ml plastic tube so that for downstream analyses comparison of control vs. inoculated spike was easier. This also allowed us to image a greater number of samples in the time-frame available. Three biological replications of each genotype-treatment combinations were imaged. The imperfection of the incoming X-ray beam and inhomogeneity of the scintillator screen was captured by recording an image when there was no sample in front of the detector (flat image). For phase CT, 10 dark field and 10 flat field images, with a maximum exposure time of 600-800 ms depending on the beam intensity, were recorded before and after collecting CT images and the average of the flat and dark images were used for normalization using PITRE (phase-sensitive X-ray image processing and tomography reconstruction) software (Chen et al. 2012).

7.5.4. Image processing

The 2D projection PCI images were normalized using flat and dark images and the X-ray intensity images were converted into optical densities using the Beer-Lambert law. Data analyses for background correction and normalization of all projections were carried out using custom scripts written by BMIT staff and implemented in ImageJ software (ImageJ 1.44p, National Institutes of Health, USA). A final image was produced as: (bright average – image dark field) / (flat average – image dark field). In order to image the entire specimen,

multiple CT scans (typically two or three) were appended together after reconstruction and this 'stitched' scan was analyzed. The images collected for CT data were processed using PITRE software (Chen et al. 2012). For 3D reconstruction of images and processing, various tools implemented in NRecon software (ver. 1.6.9.4, Skyscan) and Avizo standard software (ver. 7.1.1, FEI Visualization Sciences Group) were employed. Each reconstructed scan was saved as a sequence of 16-bit TIFF files, each of which represented a 1-pixel cross-section through the imaged area. Ring artifacts were removed during reconstruction (to remove errors arising from variance in detector pixel sensitivity), but no further manipulation of images was done. In order to ensure that grayscale values were comparable for all datasets, the same grayscale output range was used for all reconstructions. A grayscale is one in which the value of each pixel is a single sample representing the amount of light expressed as intensity information (Burger and Burge 2013). For CT, grayscale values represent the X-ray absorption values, where higher (brighter) grayscale values indicate higher absorption and lower (darker) indicate lower absorption. X-ray absorption in turn depends on the density of tissues (plant tissue in our case) in the samples, which depends on the physical density of the material (heavier/denser absorbs more). In the case of plant tissues, the lowest grayscale value is of air, which in our case was measured to be an average of 24,700 (on a 16-bit scale of 0 – 65,535). Grayscale values are synonymous with voxel intensity and both terms are used interchangeably in literature. For all quantitative analyses, ROIs from the spike were chosen (Fig. 7.1) based on infection pattern and the route of the pathogen as described in the literature.

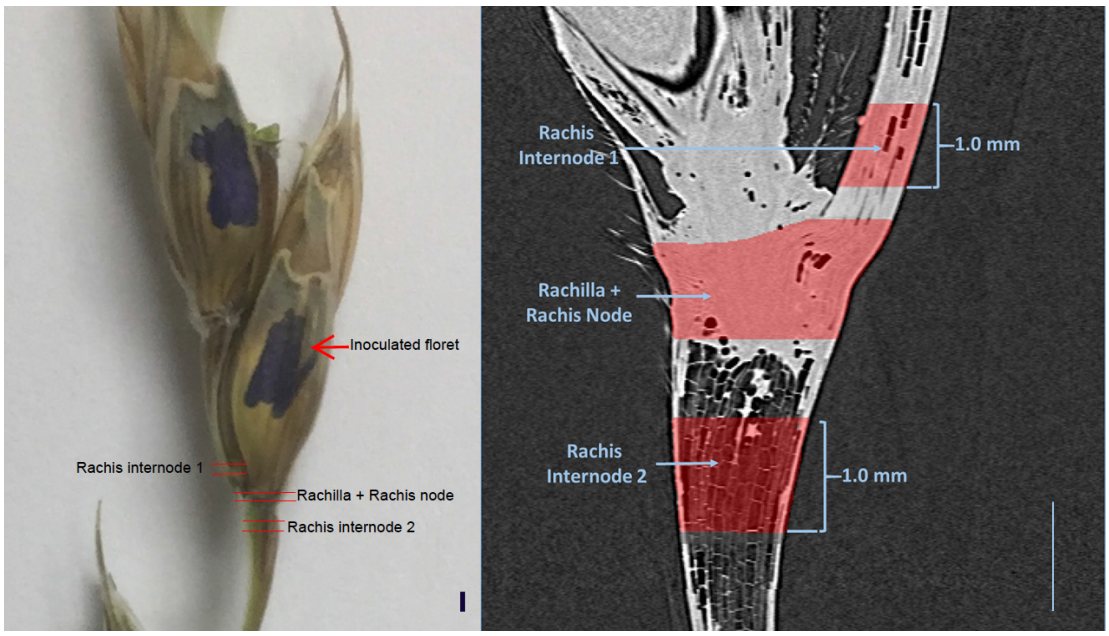

Figure 7.1. Components of the wheat spike comprising regions of interest (ROI) used for Fourier transformed infrared (FTIR) analyses and X-ray image analyses for void space/tissue

volume fraction and grayscale intensity (voxel intensity): (a) illustrates ROIs in the inoculated biological sample, and (b) in the 2D X-ray phase contrast image. Scale bar: 1 mm.

7.5.4.1. Image segmentation, in silico evaluation of volume fraction and grayscale measurements

Prior to image segmentation, each dataset was divided into control and infected biological samples by cropping each of these separately from the same scan. The seed sections of the samples were removed by positioning a cylindrical volume around the base of the floret in a manner that followed the natural curvature of the rachis (Appendix L). The 3D volumes reconstructed using NRecon software and TIFF stacks exported using Avizo software ver. 7.1.1 were used to generate a 3D rendering and analyses of 1 mm ROIs (Fig. 7.1). The purpose of *in silico* evaluation of volume fraction and grayscale measurements was to quantify the extent of tissue damage or pathogen spread in ROIs in wheat spikes. This was achieved by isolating these ROIs as sub-volumes and then measuring the volume fraction of void space within the ROIs (Fig. 7.2). Segmentation of the volume contained within the plant tissue boundaries was then carried out by applying a threshold filter (where all pixels containing a grayscale value above or below a certain threshold were selected) in order to select the plant tissue. This was followed by a 'fill holes' algorithm to fill in any bounded areas in the cross-sectional planes of the dataset (Fig. 7.2). All segmented volumes were manually inspected to ensure that they were representative of the desired ROIs (Fig. 7.2). Segmentation of the void spaces within the ROIs was carried out using a simple threshold filter, with the threshold value determined by the maximum grayscale value of air, i.e. 28,000 (which was measured using the space present outside the biological samples in the dataset) (Appendix M). In order to select only void space inside the ROIs, the total plant tissue sub-volume was used as a mask. The absolute volumes (in μm^3) of ROIs for plant tissue volume and internal void space were measured. The volume fractions were calculated (applying normalization to account for differences in tissue anatomy and morphology affecting measurements) by simply dividing the void space volume by the respective total plant volumes in each ROI. Similarly, voxel intensity/grayscale measurements were done on all ROIs and 16-bit grayscale histograms with a range of 0 – 65,535 grayscale values (representing voxel intensity) were plotted.

It should be noted that the voxel volume of 13.123 μm^3 was very small compared to the size of the structures measured. The smallest segmented structures were void spaces inside the rachis, which yielded an average volume of 5.7×10^7 μm^3 (with the smallest volume in the entire dataset 2.1×10^6 μm^3). However, some of these structures do contain

smaller substructures with higher surface-area-to-volume ratios, which would in principle lead to increased quantization error and partial volume effects compared to larger, more contiguous geometry. This may have introduced a slight negative bias for small structures compared to larger structures, but manual review of the geometry of these small substructures indicated that this error was likely to be very small and that the features appeared to be well-resolved qualitatively. In order to remove very small structures that may simply be the result of noise, any contiguous segmented volume with fewer than 9 pixels (representing a 3 x 3 x 3 pixel cube) were removed from the segmented volume of all structures before calculating volume fractions.

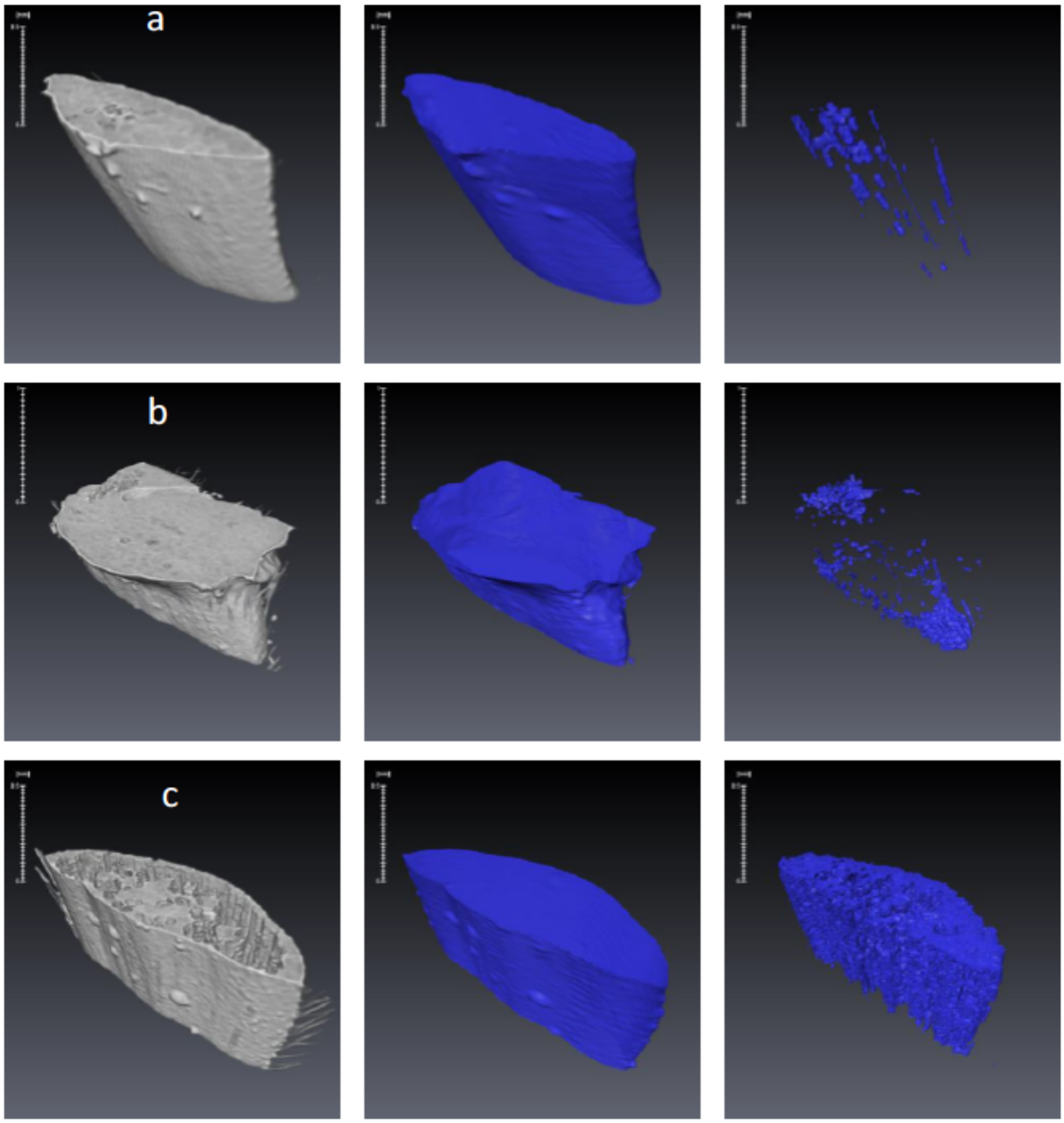

Figure 7.2. Illustrations of segmentation output for: (a) rachis internode 1, (b) rachilla + rachis node, and (c) and rachis internode 2 region of interest (ROI) sub-volumes. For each ROI, the original ROI grayscale volume is in the column on the left, the total plant tissue volume is in the center column, and the void space volume in the column on the right.

7.5.5. Bulk Fourier transform mid infrared (FTIR) spectroscopy

Spikes collected at 12 dpi were used for FTIR analyses. All FTIR spectroscopy data were collected at the mid-infrared beamline (01B1-1) at the Canadian Light Source using a globar source (silicon carbide). A Bruker-IFS 66 V/S spectrophotometer (Bruker Optics, Ettlingen, Germany) with a mercury16 cadmium-telluride (MCT) detector was used for the FTIR measurements. The Bruker system was controlled using OPUS software (Bruker Optik GmbH, Germany). The tissue near the rachis internode, consisting of the rachilla and rachis

node, was excised from three spikes per genotype per treatment (from three biological replications) and pooled (Fig. 7.1). The pooled samples were freeze dried and then ground to fine powder. Approximately 1-2 mg of the powder was homogenized with ~94-96 mg of dry potassium bromide (KBr) using a pestle and mortar, and the mixture compressed to make a pellet. Three pellets as three technical replications were made for each genotype. Thus, FTIR data was collected on three technical replications (not biological replications). Transmission infrared spectra were obtained from technical replicated pellets. Each spectrum was collected in the range of 4000 - 800 cm^{-1} wavenumbers representing the mid-infrared. Each spectrum was an average of 64 scanned spectra and pure KBr spectra (background to normalize all spectra for samples) with 128 scans. The spectra obtained for each pellet was first corrected for pellet weight, sample weight and KBr weight and then corrected using the multiplicative scattering correction (MSC) algorithm. To determine the small spectral changes in the fingerprint region (1800 - 600 cm^{-1}), a second derivative spectroscopy technique was employed using the Savitzky-Golay algorithm (9 smoothing points). The FTIR peaks for the various bipolymeric compounds (Table 7.2) were assigned using the Quick Peaks routine in OriginPro software ver. 9.1 (OriginLab Coorporation, MA, USA) using the settings described in Lahlali et al. (2016). Quantitative data were measured for important biopolymers such as lignin, pectin, cellulose, and xylan by integrating the area under the specific bands using OriginPro software (Table 7.2).

Table 7.2. Assignment of bands in the bulk Fourier transform mid infrared (FTIR) spectra of the rachilla and rachis node tissue of the wheat spike for two treatments. Treatments consisted of inoculations of the central four spikelets in the main-stem spike, with a Fusarium graminearum spore suspension (10^5 spores/ml); procedural control mock-inoculated with distilled water[a].

FTIR wavenumber (cm^{-1})	Corresponding biopolymeric compound
1720-1750 (strong)	Pectin/Polygalactouronic acid (PGA), ester, carbonyl C=O stretching, saturated aliphatics
1590-1615 (strong)	Lignin, Aromatic C=C stretching
1515-1505 (strong)	Lignin, Aromatic C=C stretching
1025-1005 (strong)	Cellulose
1070-1050 (strong)	C-O vibrations in the cellulose group
900-880 (strong)	Xylan
847-827 (medium)	Lignin, Aromatic C-H ring vibrations

[a]For assignment of FTIR peaks to different compounds, refer to: Segneanu et al. (2012); Lahlali et al. (2015).

7.5.6. Statistical analyses

For analyses of phenotypic and quantitative data (volume fraction and grayscale intensity), normality and homogeneity of error variance for all class variables were estimated using Shapiro-Wilk's and Levene's tests, respectively, implemented in procedure UNIVARIATE in the Statistical Analysis Software (SAS) ver. 9.4. Heterogeneous variances in class variables, if any, were modeled using repeated/group=effect statement in procedure MIXED (Littell et al. 2006). Analysis of variance (ANOVA) was performed, to partition variance among manipulated factors, using procedure MIXED in SAS ver. 9.4 (Littell, Milliken, Stroup, Wolfinger, & Schabenberger, 2006). The least significance difference (LSD) was calculated according to Fisher's method with the DDFM = kenwardroger option for approximating the degrees of freedom. All tests used a nominal alpha level of $P \leq 0.05$. Principal component analysis (PCA) for FTIR dataset was conducted using the MATLAB program.

7.6. Results

7.6.1. FHB resistance evaluation

Differences among wheat genotypes were evident from macroscopic observations of *Fg*-inoculated spikes (Fig. 7.3). By 4 dpi, inoculated florets of all genotypes had started to turn brown (data not shown). Clear differences among genotypes were evident at 12 dpi, i.e. all NILs and 00Ar134-1 were significantly different from the susceptible cultivar CDC Alsask (Figs. 7.3 and 7.4). Generally, disease progression was faster down the rachis node of inoculated spikelets compared to upward progression (Fig. 7.3B); however, the NILs and 00Ar134-1 had similar phenotypes for FHB progression and were not statistically different from each other for disease severity at 12 dpi (Figs. 7.3A and 7.4). At 12 dpi, except for CDC Alsask, including the inoculated spikelets, disease symptoms were not observed on more than four spikelets of any genotype (Fig. 7.3A). Interestingly, the symptoms were observed in three to four rachis internodes around inoculated florets, even though spikelets on these internodes were intact (Fig. 7.3). The disease severity at 12 dpi was less than 20% for all NILs and 00Ar134-1 and 70% for CDC Alsask. Similarly, at 20 dpi, CDC Alsask disease severity was greater than for other genotypes (Fig. 7.4). At 20 dpi, 04GC0139 had the lowest disease severity (<20%) approximately the same as 00Ar134-1, Alsask2, and Alsask25 (spray inoculated). Disease severity of the NILs Alsask8, Alsask22, and Alsask25 (point inoculated) were statistically similar to each other, but lower than CDC Alsask and higher than 04GC0139 (Fig. 7.4). On average, the NILs performed better than the recurrent parent CDC Alsask although 1/3 to 1/4 of the spike was infected with *Fg* at 20 dpi (Figs. 7.3 and 7.4).

7.6.2. X-ray imaging and computed tomography

Reconstruction of CT scans from each genotype-treatment-replication combination were made following generation of ~1800 (5 Mb) images for each. These images were then stacked and rendered into a 3D volume where the spike was reproduced *in silico* down to a voxel (pixel in 3D) representing an *in planta* linear resolution of ~13 microns (Figs. 7.5A and 7.5B). Clear differences in X-ray attenuation were observed for different parts of wheat spike ROIs, particularly rachis internode 2 (Fig. 7.5C). The areas corresponding to increased X-ray attenuation (high voxel intensity) appeared brighter than areas with low X-ray attenuation.

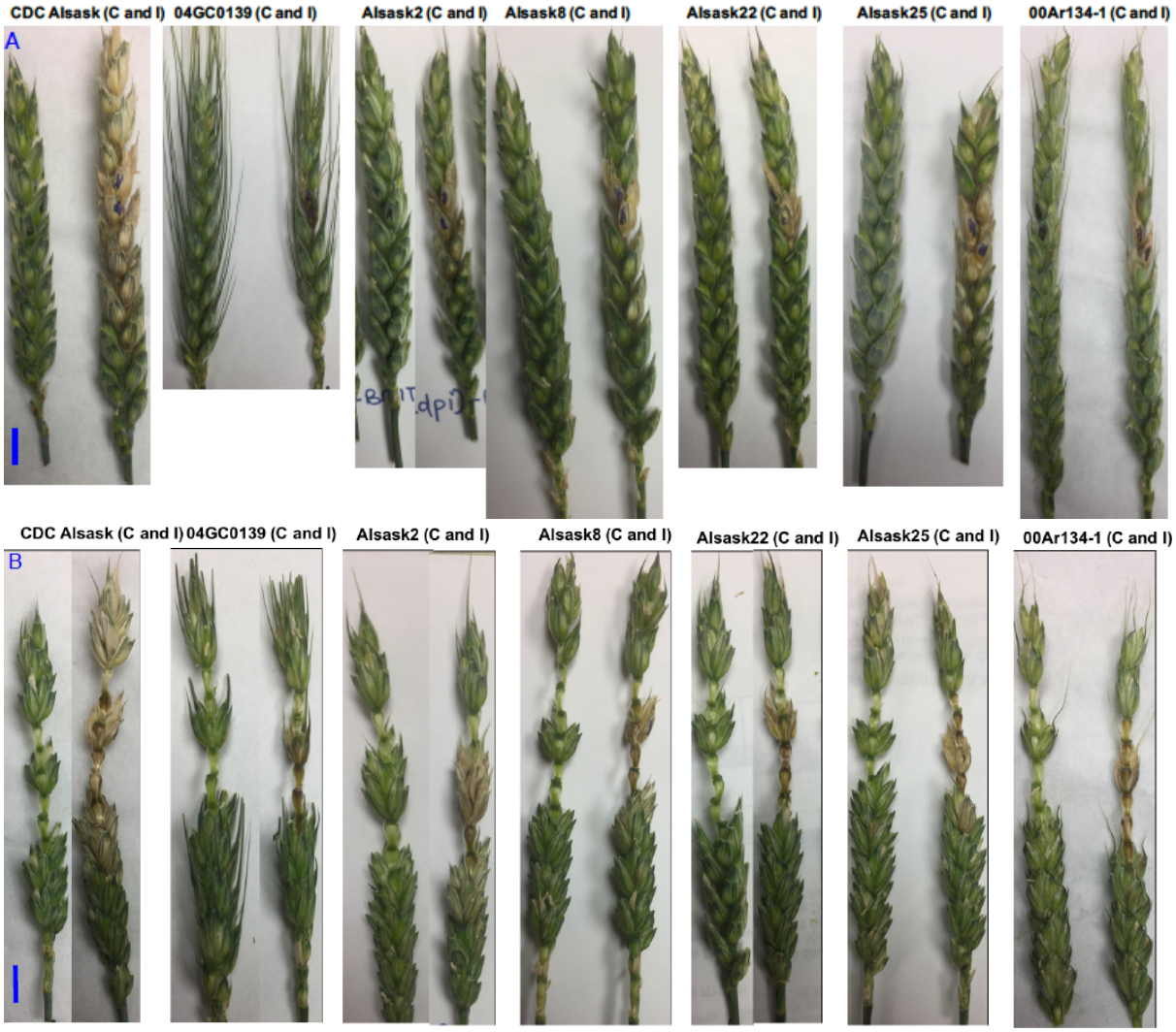

Figure 7.3. Symptoms of Fusarium head blight on: (A) the spike, and (B) the rachis (spikelets removed) following *Fusarium graminearum* (*Fg*) point-inoculation (10^5 spores/ml) in seven wheat genotypes at 12 days post inoculation. Genotypes were either infected (I) with *Fg* (I) or mock-infected with distilled water as a procedural control (C). Figs. A and B are from the same spikes of all genotypes. Genotypes carry the following genes: CDC Alsask (null), 04GC0139 (*Fhb1*+*Fhb2*+*Fhb5*+), Alsask2 (*Fhb1*), Alsask8 (*Fhb1*+*Fhb2*), Alsask22 (*Fhb1*+*Fhb2*+*Fhb5*), Alsask25 (*Fhb2*+*Fhb5*), 00Ar134-1 (unknown). Scale bar: 1 cm.

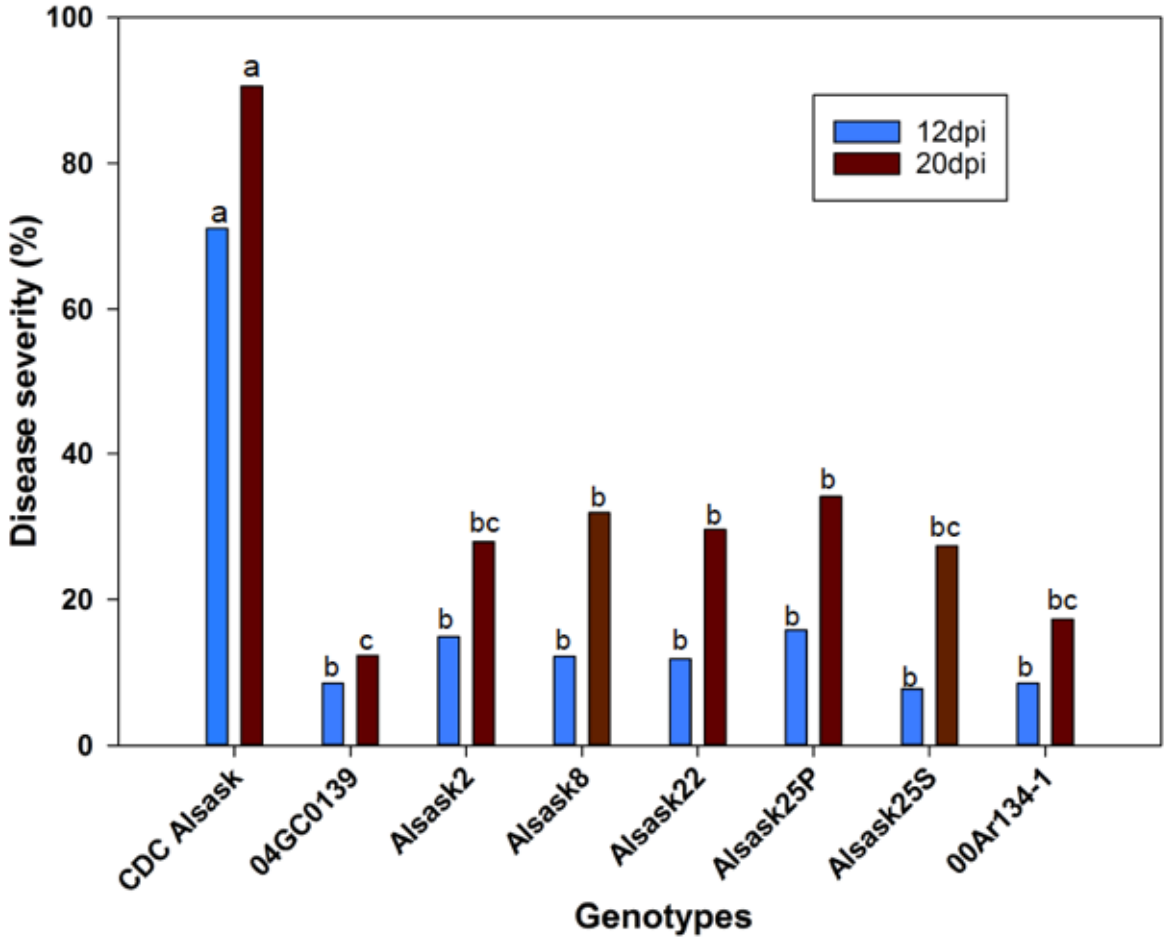

Figure 7.4. Fusarium head blight (FHB) severity of wheat genotypes in response to point inoculation by *Fusarium graminearum* (10^5 spores/ml) at 12 and 20 days post inoculation (dpi). Alsask25 was both point (P) and spray (S) inoculated. Genotypes with same letter codes are not statistically different according to Fisher's least significant differences (LSD) at $P = 0.05$. Genotypes carry the following genes: CDC Alsask (null), 04GC0139 (*Fhb1*+*Fhb2*+*Fhb5*+), Alsask2 (*Fhb1*), Alsask8 (*Fhb1*+*Fhb2*), Alsask22 (*Fhb1*+*Fhb2*+*Fhb5*), Alsask25 (*Fhb2*+*Fhb5*), 00Ar134-1 (unknown).

7.6.3. Tissue and void space volumes in ROIs

From the ANOVA of void space volume fraction, genotypes had a significant influence on the trait in the rachilla + rachis node and in rachis internode 2, whereas the treatment effect was significant for all three ROIs (Table 7.3). Genotype and treatment interaction was significant only for the rachilla + rachis node. For the rachilla + rachis node, CDC Alsask had a higher void space volume than 04GC0139 and all other lines were comparable to the susceptible parent (Table 7.4). Although the NILs were not statistically different from their recurrent parent in void space volume fraction, a trend for the trait was evident: Alsask2>Alsask8>Alsask25>Alsask22>00Ar134-1. Only Alsask22 and 00Ar134-1 were comparable to the resistant parent 04GC0139. For rachis internode 2, except Alsask22, all

other NILs and CDC Alsask were statistically similar with higher void space volume than 04GC0139.

A significant treatment effect was observed as control samples had lower void space volume in all three ROIs as compared to *Fg*-treated samples (Table 7.4). The significant genotype by treatment interaction for the rachilla + rachis node resulted from lowered void space volume for 04GC0139 following *Fg*-inoculation, although the means did not differ statistically (Table 7.4). It is noteworthy to mention that treatment resulted in a significant change in void space volume for all genotypes following *Fg*-inoculation, except 04GC0139 and 00Ar134-1.

Table 7.3. Two-way analysis of variance for volume fraction (ratio of porosity and tissue volume) and Grayscale[a] intensity calculated from computed tomography data for wheat spike samples. Samples consisted of rachilla + rachis node, internodes above (rachis internode 1) and below (rachis internode 2) of the inoculated florets in the middle of main-stem spike. The two-way component tested effects of genotype and *F. graminearum* point-inoculation treatment (10^5 spores/ml injected in middle florets). Here, *F* = Fisher's F-statistic value, *P* = probability.

For volume fraction	**Genotype**		**Treatment**		**Genotype*Treatment**	
	F	***P***	***F***	***P***	***F***	***P***
Rachis internode 1 (ROI-1)	1.41	0.28	29.11	<0.001	2.35	0.09
Rachis internode 2 (ROI-3)	3.82	<0.05	5.34	<0.05	1.86	0.13
Rachilla + rachis node (ROI-2)	3.13	<0.05	84.99	0.0001	3.50	<0.05
For Grayscale intensity						
Rachis internode 1 (ROI-1)	6.10	0.30	23.04	<0.001	6.2	0.30
Rachis internode 2 (ROI-3)	4.29	<0.05	6.9	<0.05	1.86	0.16
Rachilla + rachis node (ROI-2)	4.52	<0.05	65.86	0.0001	3.94	<0.05

[a]A grayscale is one in which the value of each voxel is a single sample representing the amount of light expressed as intensity information.

Table 7.4. Mean values (LSmeans) for void space volume fraction and grayscale/voxel intensity data for wheat spike samples. Genotypes carry the following genes: CDC Alsask (null), 04GC0139 (*Fhb1*+*Fhb2*+*Fhb5*+), Alsask2 (*Fhb1*), Alsask8 (*Fhb1*+*Fhb2*), Alsask22 (*Fhb1*+*Fhb2*+*Fhb5*), Alsask25 (*Fhb2*+*Fhb5*), 00Ar134-1 (unknown). Samples consisted of rachilla + rachis node of the *Fusarium graminearum* (*Fg*)-inoculated (I) and procedural control (C) florets in the middle of main-stem spike. The measurements were done on three regions of interest (ROIs): rachis internode 1 (ROI-1) i.e. internode just above inoculated floret, rachilla + rachis node (ROI-2), and rachis internode 2 (ROI-3), the internode just below the inoculated floret. Means followed by the same letter are not statistically significantly different according to Fisher's least significant differences (LSD) at $P = 0.05$. Here: '-' means not significant.

	Void space volume fraction			Grayscale/voxel intensity		
Effect	**ROI-1**	**ROI-2**	**ROI-3**	**ROI-1**	**ROI-2**	**ROI-3**
Genotype (G)						
CDC Alsask	0.134 a	0.185 a	0.612 a	32632 a	31848 b	27081 b
04GC0139	0.027 a	0.026 c	0.219 b	35494 a	35593 a	33381 a
Alsask2	0.103 a	0.153 ab	0.446 a	35003 a	34308 ab	29695 ab
Alsask8	0.126 a	0.153 ab	0.507 a	33589 a	33174 ab	29583 ab
Alsask22	0.071 a	0.111 bc	0.537 a	34567 a	34247 ab	29407 ab
Alsask25	0.100 a	0.150 ab	0.481 a	33929 a	33205 ab	29203 ab
00Ar134-1	0.046 a	0.089 bc	0.462 a	34797 a	34284 ab	30088 ab
Treatment (T)						
Control (C)	0.026 b	0.026 b	0.413 b	35364 a	35410 a	30242 a
Fg-inoculated (I)	0.147 a	0.221 a	0.519 a	33211 b	32207 b	29311 b
G*T						
CDC Alsask-C	-	0.020 d	-	-	34810 abc	-
CDC Alsask-I	-	0.351 a	-	-	28886 d	-
04GC0139-C	-	0.027 cd	-	-	35372 abc	-
04GC0139-I	-	0.025 cd	-	-	35814 ab	-
Alsask2-C	-	0.032 cd	-	-	35579 ab	-
Alsask2-I	-	0.274 ab	-	-	33037 abcd	-
Alsask8-C	-	0.030 cd	-	-	35309 abc	-
Alsask8-I	-	0.276 ab	-	-	31039 bcd	-
Alsask22-C	-	0.024 d	-	-	35529 ab	-
Alsask22-I	-	0.199 b	-	-	32964 abcd	-
Alsask25-C	-	0.025 d	-	-	35868 a	-
Alsask25-I	-	0.274 ab	-	-	30542 cd	-
00Ar134-1-C	-	0.026 cd	-	-	35403 abc	-
00Ar134-1-I	-	0.151 bc	-	-	33166 abcd	-

7.6.4. Grayscale (voxel intensity) measurements and distributions in ROIs

The ANOVA for grayscale values were the same as void space volume fraction for all three ROIs (Table 7.3). For rachis internode 1, the grayscale was similar for all genotypes. For the rachilla + rachis node ROI, 04GC0139 was greater than CDC Alsask; however, none of the NILs or 00Ar134-1, differed from either parent or each other. A trend in numerical grayscale value was observed as follows for the NILs and 00Ar134-1: Alsask2>00Ar134-1>Alsask22>Alsask25>Alsask8. For rachis internode 2, results were the same as for the

rachilla + rachis node ROI, except for a slight difference in the trend for values: 00Ar134-1>Alsask2>Alsask8>Alsask22>Alsask25.

A significant treatment effect was observed as control samples had higher grayscale values for all three ROIs as compared to *Fg*-treated samples (Table 7.4). The significant genotype by treatment interaction for the rachilla + rachis node resulted from increased grayscale value for 04GC0139 following *Fg*-inoculation, although the means did not differ significantly (Table 7.4). Interestingly, only CDC Alsask and Alsask25 were statistically different for both treatments. Also, for both void space volume fraction and grayscale values, only the rachilla + rachis node results were consistently similar. Although, the other two ROIs were also somewhat similar, a clear difference among genotypes representing macroscopic phenotype was not observed.

The structural changes in X-ray CT sections after *Fg* inoculation in all genotypes were evident (Fig. 7.5C). Distortion and disintegration of host tissue following infection, and failure of the ovary to develop in the inoculated floret were clearly observed. Using customized Python based scripts, histograms of the voxel intensity for each ROI were plotted (voxels ranging between 99 to 145 million). The distribution of voxels was mono-modal for rachis internode 1 and the rachis + rachilla node, and bi-modal for rachis internode 2. The bi-modal distribution resulted from differences in X-ray attenuation between tissue regions of the ROI. In rachis internode 2, the material covering the greatest area or voxel count was the air in cell lumens and vascular bundles, which formed the tall peaks on the histograms (Fig. 7.5C). The histogram showed that the mean of the peak had a grayscale value of approximately 24,000, which also made it clear that the peak was for void space, or air, in the tissue. The small peak in the histogram represented the actual plant tissue in that ROI. The only exception was for genotype 04GC0139, where tissue volume for rachis internode 2 was greater than the air volume as represented by a smaller peak for air. Also, the peak was comparable for both material types in 00Ar134-1, as histogram height was the same for air and tissue. The histograms and 2D X-ray CT sections clearly reflected the measurements in Table 7.4.

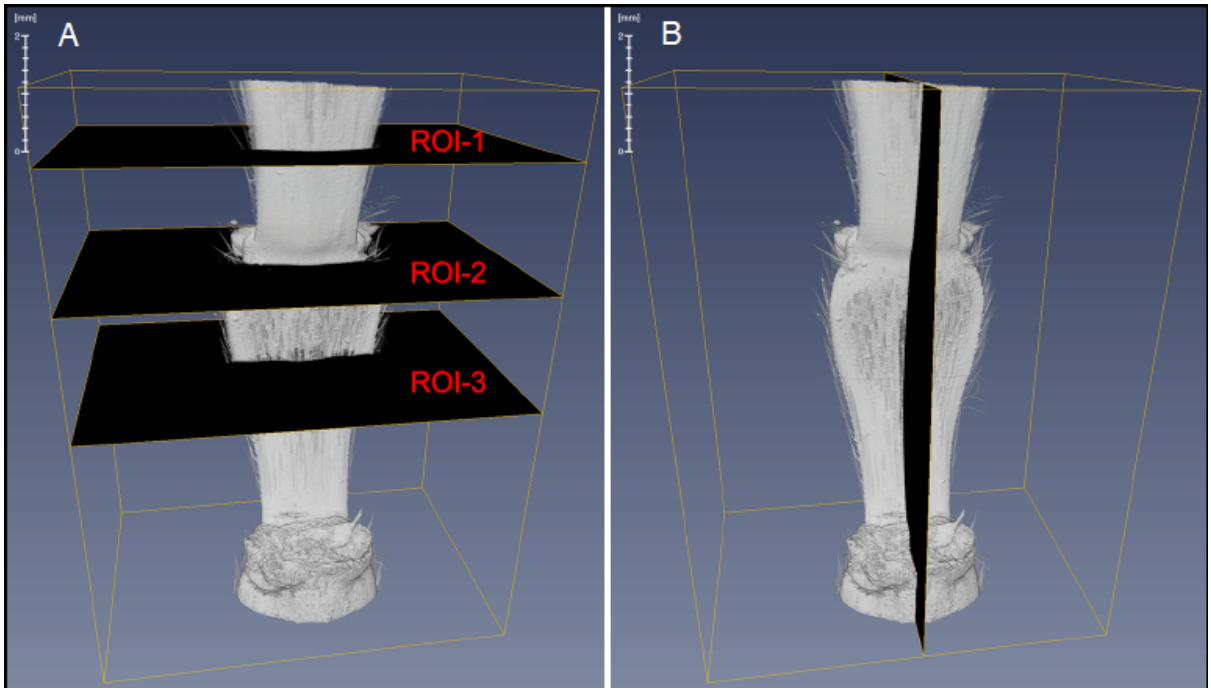
A
ROI-1
ROI-2
ROI-3
B

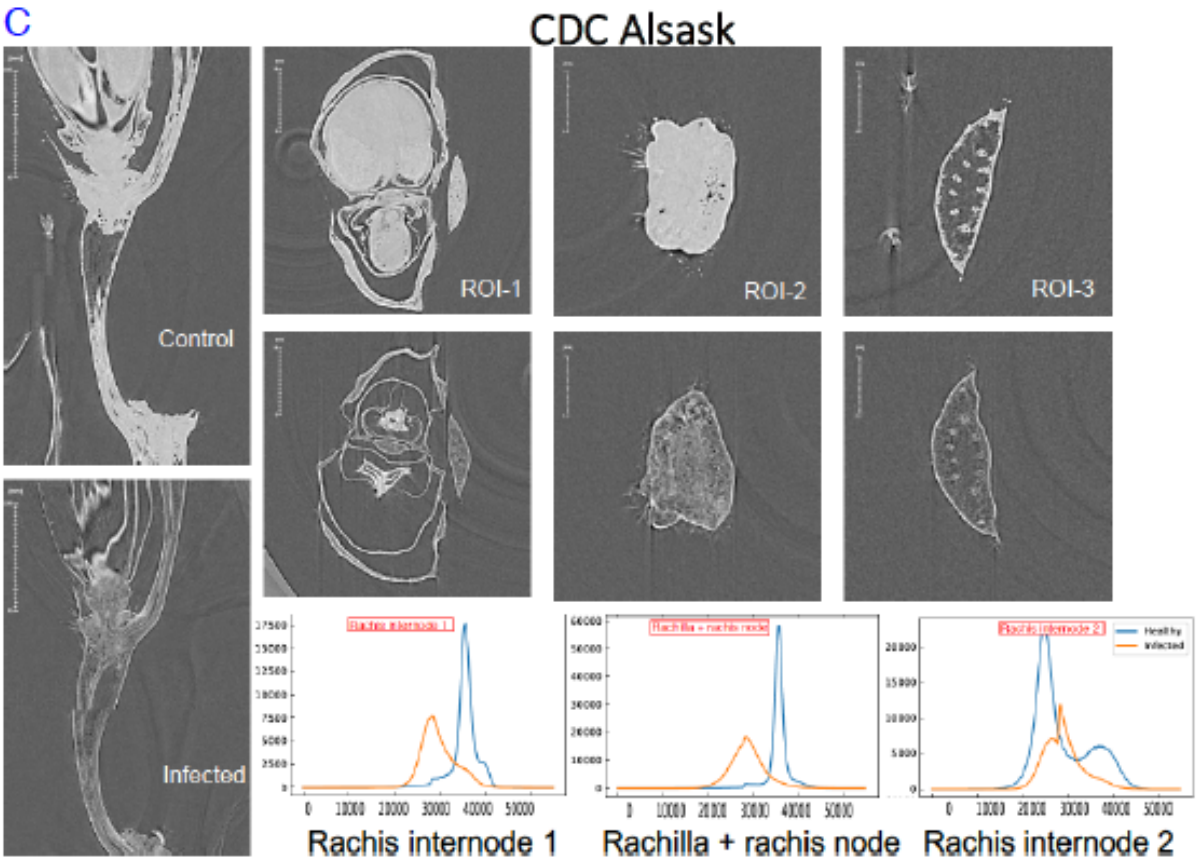
C
CDC Alsask
Control
Infected
ROI-1
ROI-2
ROI-3
Rachis internode 1
Rachilla + rachis node
Rachis internode 2

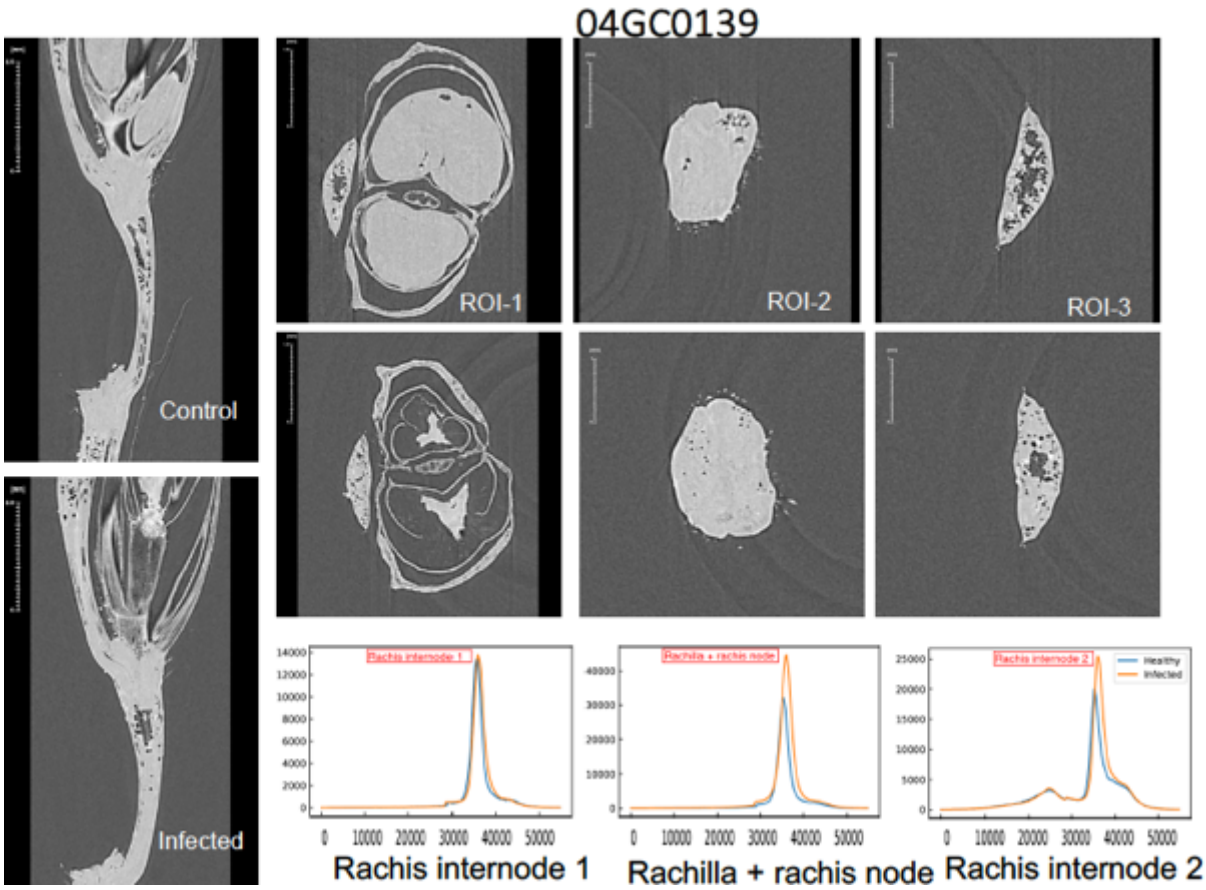
04GC0139
Control
Infected
ROI-1
ROI-2
ROI-3
Rachis internode 1
Rachilla + rachis node
Rachis internode 2
Healthy
Infected

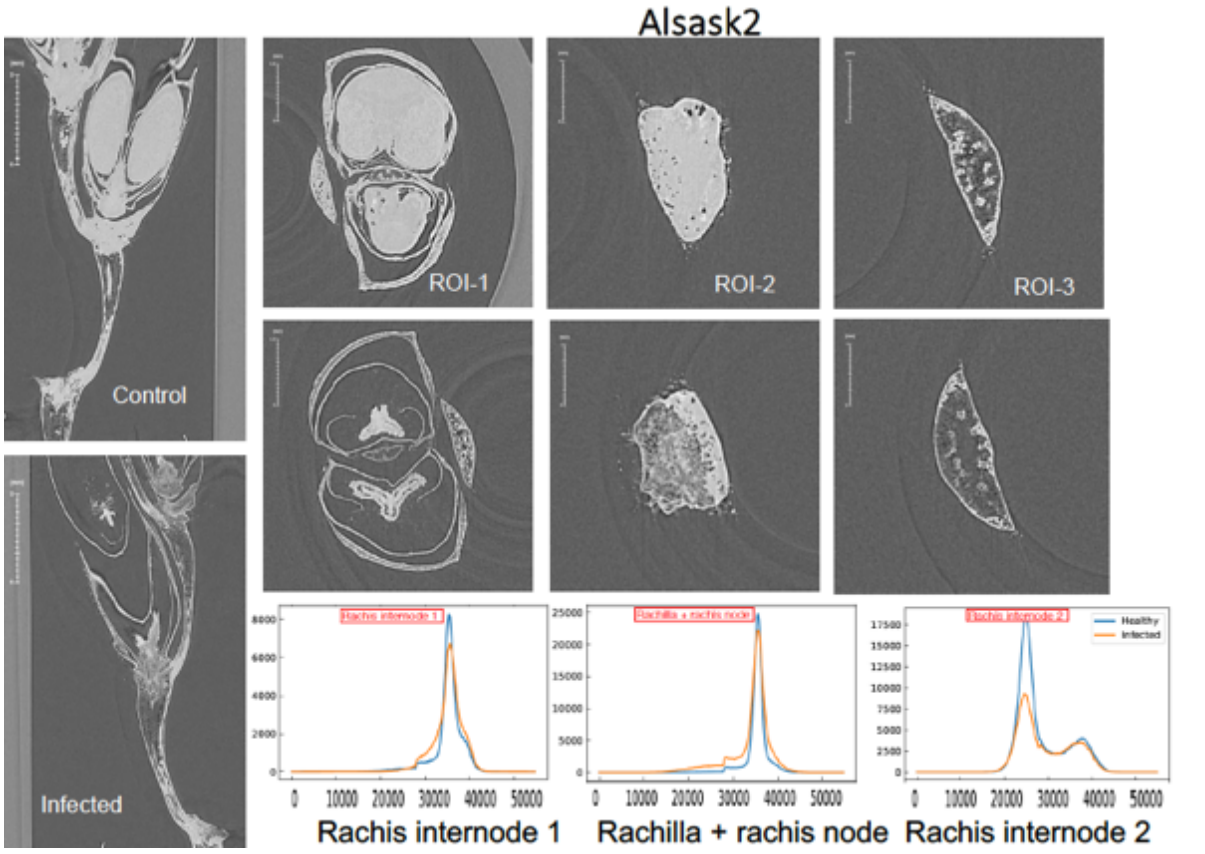
Alsask2
Control
Infected
ROI-1
ROI-2
ROI-3
Rachis internode 1
Rachilla + rachis node
Rachis internode 2
Healthy
Infected

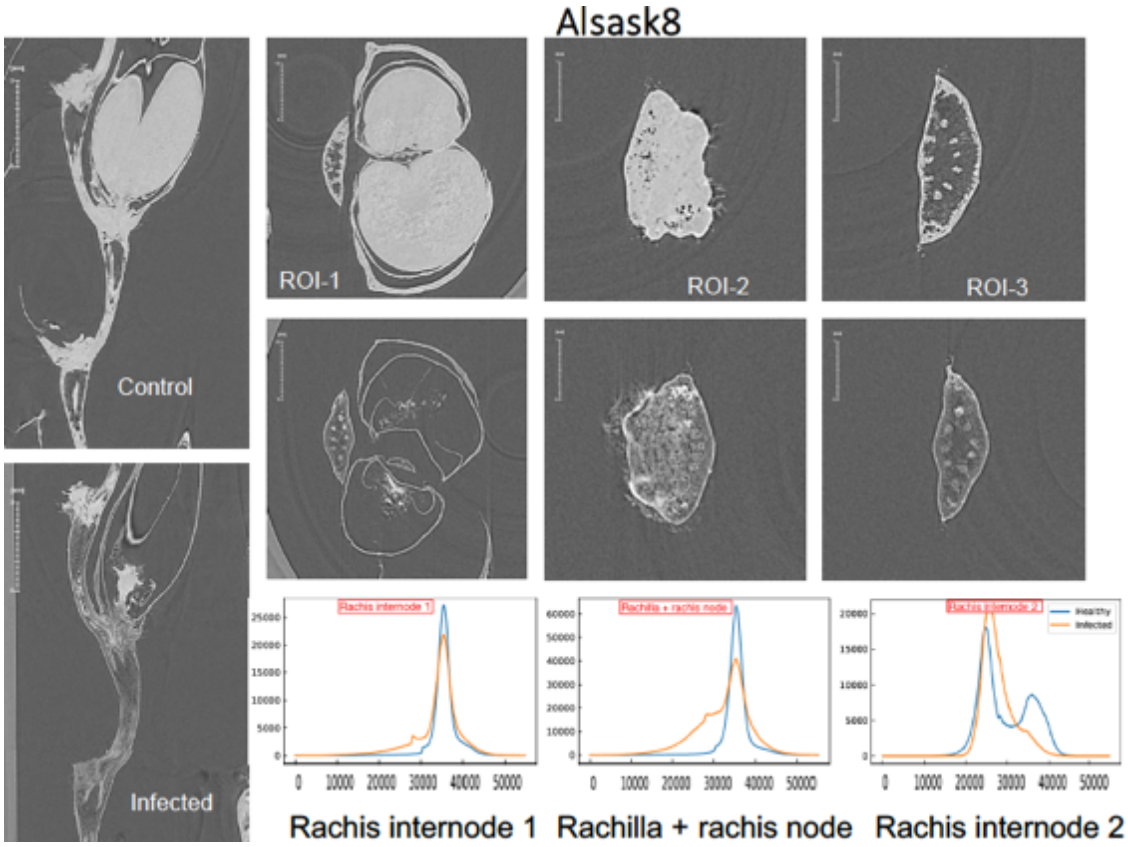
Alsask8
Control
Infected
ROI-1
ROI-2
ROI-3
Rachis internode 1
Rachilla + rachis node
Rachis internode 2
Rachis internode 1
Rachilla + rachis node
Rachis internode 2

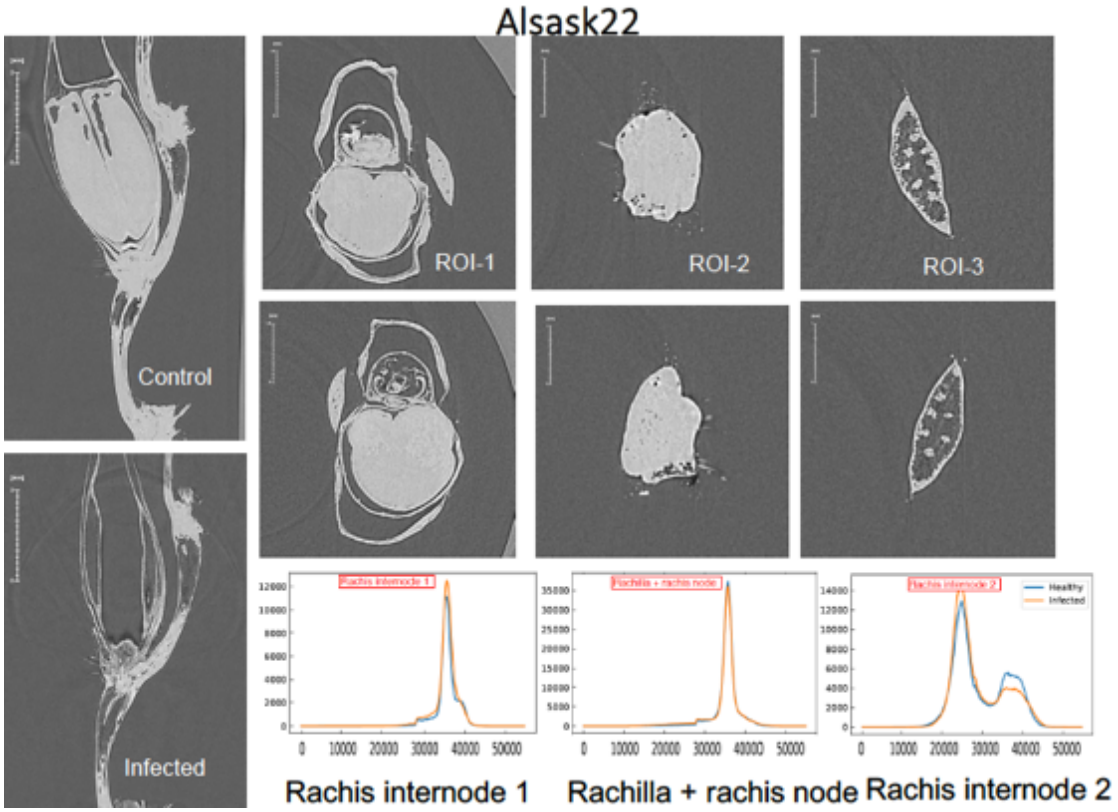
Alsask22
Control
Infected
ROI-1
ROI-2
ROI-3
Rachis internode 1
Rachilla + rachis node
Rachis internode 2
Rachis internode 1
Rachilla + rachis node
Rachis internode 2

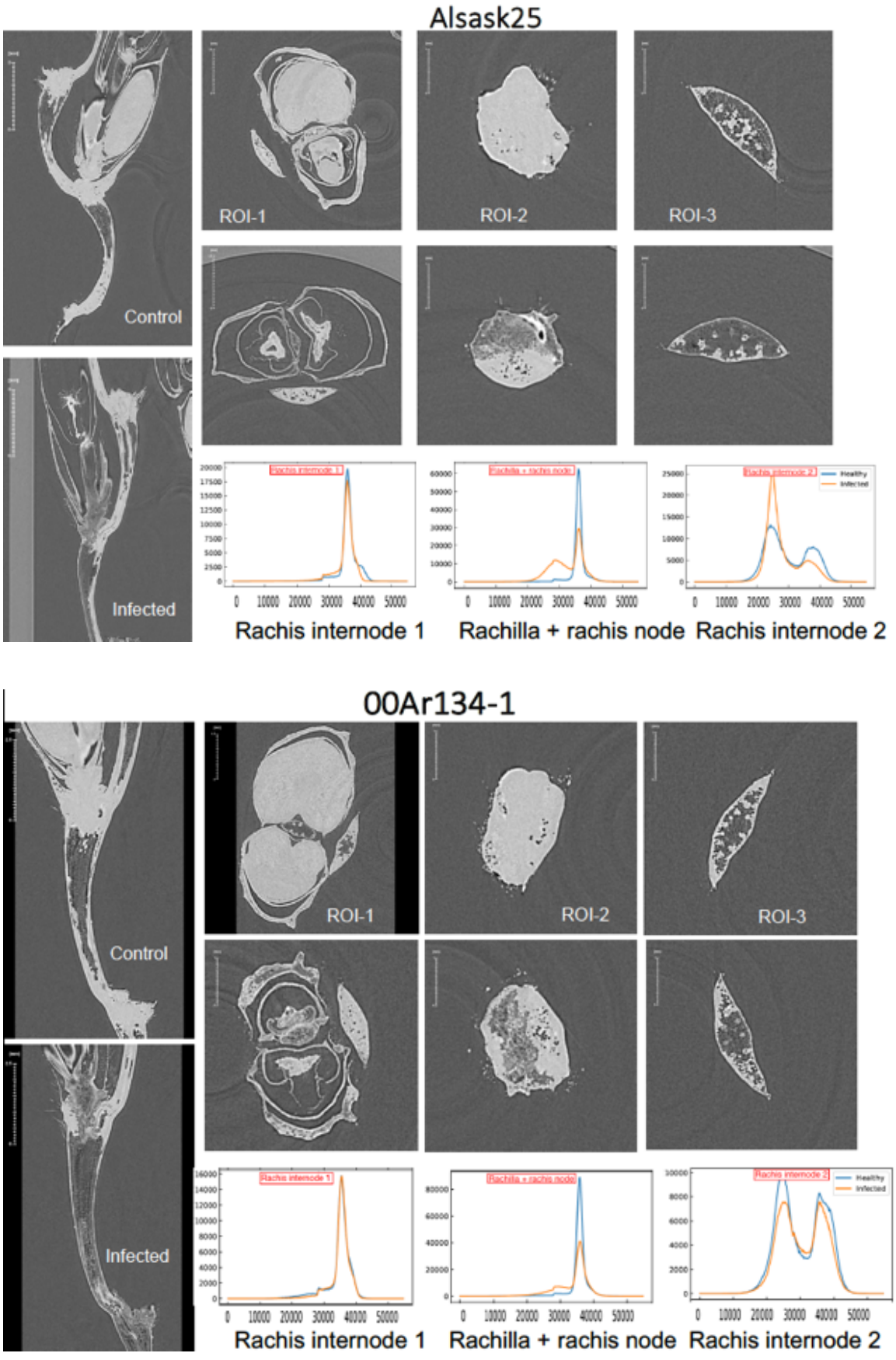

Figure 7.5. Full 3D rendering of a single specimen (00Ar134-1 Control) with black 2D planes indicating the positions at three regions of interest (ROIs) for which cross sections (A)

as well as the longitudinal section (B) were generated. (C) Voxel/grayscale distribution among three ROIs in wheat genotypes differing in Fusarium head blight resistance alleles used in the study. The genotypes were subjected to two treatments: procedural control (point inoculated with distilled water) and *Fusarium graminearum* point-inoculated (Infected). The three ROIs are: rachis internode 1 (ROI-1), rachilla + rachis node (ROI-2), and rachis internode 2 (ROI-3). Genotypes carry the following genes: CDC Alsask (null), 04GC0139 (*Fhb1*+*Fhb2*+*Fhb5*+), Alsask2 (*Fhb1*), Alsask8 (*Fhb1*+*Fhb2*), Alsask22 (*Fhb1*+*Fhb2*+*Fhb5*), Alsask25 (*Fhb2*+*Fhb5*), 00Ar134-1 (unknown). Histograms of voxel/grayscale intensity distribution for each ROI are provided below the 2D X-ray image sections. X-axes and Y-axes of histograms represent grayscale/voxel intensity (ranges between 0 - 65,535) and voxel frequency, respectively. Scale bars = 2 mm (A & B) and 1.5 mm (C).

7.6.5. FTIR analyses

Principal component analysis of wavenumbers from the fingerprint region (1800-800 cm^{-1}) differentiated genotype-treatment combinations, indicating that there were differences in biochemical composition of genotypes and changes in composition resulting from *Fg*-inoculation (Fig. 7.6). Principal component 1 explained 48% of the total variation, and principle component 2, 11%. The integrated area under FTIR peaks (in the fingerprint region) corresponding to plant cell wall compounds was measured for rachilla + rachis node tissue (Tables 7.2 and 7.5). The extent of the biopolymeric compounds measured differed among genotypes. The treatment effect was significant only for lignin, while the genotype by treatment interaction was significant for all compounds. Following *Fg* inoculation, the lignin content increased and a significant genotype by treatment interaction for lignin resulted from lower (although not significantly) lignin content in Alsask8, Alsask22, and 00Ar134-1. Following infection, results for cellulose, pectin, and xylan were inconsistent among genotypes, but not statistically significant. The changes in FTIR bands corresponding to these compounds were also reflected in the second-derivative FTIR spectra of the genotypes (Appendix N).

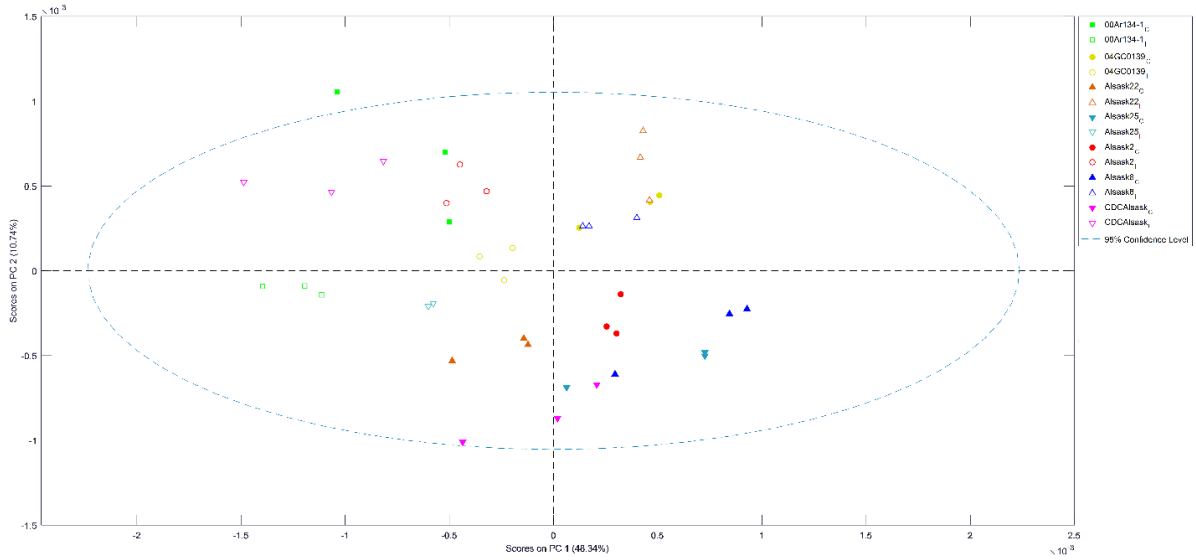

Figure 7.6. Principal component analysis of seven wheat genotypes differing in resistance alleles for Fusarium head blight resistance for wavenumbers in the fingerprint region (800-1800 cm^{-1}) of Fourier transform infrared (FTIR) spectra. The genotypes were subjected to two treatments: procedural control (point inoculated with distilled water) (C) and Fusarium graminearum point-inoculated (I).

7.7. Discussion

Fusarium head blight is one of the five top priority diseases of wheat in Canada, which not only reduces yield, but destroys protein and results in toxin accumulation in grain. After floral infection, hyphae can enter the rachis through rachilla and rachis nodes in susceptible cultivars and spread inter- and intra-cellularly in the rachis (Kang & Buchnenauer, 2000; Brown et al., 2010). Histopathological studies have used traditional microscopy or immuno-labelling techniques that do not always represent the normal source-sink relationship. Our study was the first to incorporate synchrotron-based imaging techniques combined with near-isogenic lines with a similar genetic background to elucidate changes in wheat spikes following *Fg* infection. Other studies did not focus on the specific tissues of the spike that confer resistance to pathogen spread. We attempted to test and re-confirm whether the rachilla and rachis nodes are important in terms of Type-II resistance or if all spike parts behave similarly in resisting pathogen spread in the rachis. Thus, three regions of interest close to inoculated florets were studied for structural traits affected by *Fg* infection.

Table 7.5. Two-way analysis of variance for pectin, lignin, cellulose, and xylan from Fourier transform mid infrared (FTIR) data for wheat spike samples. Genotypes carry the following genes: CDC Alsask (null), 04GC0139 (*Fhb1*+*Fhb2*+*Fhb5*+), Alsask2 (*Fhb1*), Alsask8 (*Fhb1*+*Fhb2*), Alsask22 (*Fhb1*+*Fhb2*+*Fhb5*), Alsask25 (*Fhb2*+*Fhb5*), 00Ar134-1 (unknown). Samples consisted of the rachilla + rachis node of the inoculated florets in the middle of the main-stem spike. The two-way component tested effects of genotype and *Fusarium graminearum* (*Fg*) point-inoculation treatment (10^5 spores/ml injected in middle florets). Here, *F* = Fisher's F-statistic value, *P* = probability value. Mean values (LSmeans) for pectin, lignin, cellulose, and xylan from Fourier transform infrared (FTIR) data for wheat spike samples are presented for genotype*treatment. Samples consisted of the rachilla + rachis node of the *Fg*-inoculated (I) and procedural control (C) florets in the middle of the main-stem spike. Means followed by same letter code are not statistically significantly different according to Fisher's least significant differences (LSD) at P = 0.05.

	Lignin		**Lignin (ring)**		**1365-1386**		**Cellulose**		**Pectin**		**Xylan**	
	F	***P***	***F***	***P***	***F***	***P***	***F***	***P***	***F***	***P***	***F***	***P***
Genotype (G)	97.0	0.0001	37.4	0.0001	17.0	<0.001	10.0	<.001	11.97	0.0001	4.97	<0.05
Treatment (T)	551.0	0.0001	384.8	<0.05	37.2	<0.05	9.56	0.06	1.15	0.30	0.04	0.85
G*T	117.5	0.0001	25.15	0.0001	30.7	0.0001	8.56	<0.05	32.18	0.0001	5.73	<0.05
G*T												
CDC Alsask-C	0.023 de		0.058 bcd		0.039 cde		0.089 abc		0.083 ab		0.128 ab	
CDC Alsask-I	0.044 a		0.093 a		0.059 ab		0.107 ab		0.086 ab		0.117 ab	
04GC0139-C	0.023 de		0.046 de		0.046 bcde		0.078 bc		0.071 bcd		0.093 ab	
04GC0139-I	0.030 c		0.063 bc		0.051 bc		0.085 bc		0.072 bcd		0.104 ab	
Alsask2-C	0.025 cd		0.054 cde		0.050 bcd		0.088 abc		0.078 ab		0.121 ab	
Alsask2-I	0.039 ab		0.073 b		0.051 bcd		0.092 abc		0.079 ab		0.088 ab	
Alsask8-C	0.018 ef		0.039 e		0.038 cde		0.072 c		0.074 abc		0.094 ab	
Alsask8-I	0.015 fg		0.054 cde		0.038 de		0.079 bc		0.053 d		0.082 b	
Alsask22-C	0.029 c		0.059 bcd		0.050 bcd		0.088 abc		0.084 ab		0.093 ab	
Alsask22-I	0.030 c		0.059 bcd		0.035 e		0.068 c		0.054 cd		0.079 b	
Alsask25-C	0.012 g		0.039 ef		0.035 e		0.094 abc		0.053 d		0.083 ab	
Alsask25-I	0.038 ab		0.068 bc		0.059 ab		0.107 ab		0.082 ab		0.122 ab	
00Ar134-1-C	0.039 ab		0.075 b		0.055 ab		0.096 abc		0.086 ab		0.106 ab	
00Ar134-1-I	0.037 b		0.091 a		0.066 a		0.116 a		0.094 a		0.133 a	

Most histological studies of the wheat-*Fg* interaction have used only a single cultivar/genotype, or at most two cultivars, and evident differences in their histology could not necessarily be attributed directly to known FHB resistance alleles (Kang and Buchenauer 2000; Ribichich et al. 2000; Miller et al. 2004; Jansen et al. 2005; Brown et al. 2010). To actually examine the phenotypic variation associated with Sumai 3 derived alleles, our study incorporated NILs in a CDC Alsask (an FHB susceptible hard red spring wheat cultivar from Canada) background carrying either singly or combination *Fhb1*, *Fhb2*, and *Fhb5*. The phenotypic characterization of these genotypes under controlled conditions indicated the benefit Sumai 3 genes to improve resistance. Unlike other biotrophic pathogens, where FHB resistance can be complete, resistance is horizontal and the alleles provide partial resistance. Also, in the case of QTL/genes of small effect, as in our study, high disease pressure may mask the moderately resistant or moderately susceptible phenotype of the host. The spore concentration of 10^5 spores/ml accompanied by inoculation of four spikelets (the standard procedure is to inoculate one or two) overwhelmed the effects of these QTL, which may have been why the NILs carrying one or all three QTL expressed the same phenotype, although all the NILs were better than the recurrent parent (Fig. 7.4). Genotype 00Ar134-1 was reported as moderately resistant for field reaction to FHB in multiple environments and our results from indoor phenotyping agree with Brar and Hucl (2017).

Approximately 5 days after inoculation, the pathogen begins to invade rachis internodes by crossing through the rachis node and rachilla section of the spike in susceptible cultivars (Brown et al. 2010). The invasion of the vascular system of the spike results in collapsed cells and disintegration of cell-walls resulting from inter- and intra-cellular growth of the pathogen. Rapid downward spread of pathogen along the rachis was observed in our study, which is in agreement with previously published reports (Miller et al. 2004; Brown et al. 2010). This difference in hyphal spread in the lower and upper part of the spike could be attributed primarily to the lack of a direct connection between vascular bundles of the inoculated spikelet and the rachis above the point of inoculation (Whingwiri et al. 1981; O'Brien et al. 1985). Kang and Buchnenauer (2000) and Zhang et al. (2008) reported that the internode just above the rachis node has compactly arranged cells, whereas in the internode cells are loosely arranged. This may explain the difference in the rate of pathogen spread among wheat genotypes.

Disintegration of tissue in the spike following infection results in structural changes and this change in tissue structure should then result in a change of X-ray attenuation because of the change in density. Thus, our study involved measurements of the proportion of void space to plant tissue volumes in ROIs and grayscale/voxel intensity. Both volume fraction

and grayscale mean measurements were included in this study to provide two closely related, but potentially different quantitative measures of the same phenomenon: the degree of infection/resistance for a given ROI. If a change in grayscale profile is due only to a change the relative number of voxels that denote 'void' and 'plant tissue', and there is no other variation in the mean grayscale value for each type of material, then the volume fraction values and mean grayscale values should have a correlation of 1, and essentially capture the same information. However, if there was an effect that changed the distribution of grayscale values (e.g. a measureable change in plant tissue density), then this would be captured by the mean grayscale value method, but not necessarily by the volume fraction method. In this study, the volume fraction and grayscale mean measures were highly correlated. Both measures were equally valid approaches to quantifying the degree of infection for these datasets under the conditions of this study.

Change in void space and X-ray attenuation following *Fg*-infection was evident in our study and for all three ROIs. Inoculated spikes had higher void space fraction and lower X-ray attenuation compared to procedural controls. These measurements can be successfully employed in future studies where host-pathogen interaction results in structural changes. Somewhat consistent (relatively) differences for void space volume fraction and grayscale values between the two treatments were only observed for the rachilla + rachis node and not for the rachis internodes above or below the inoculation point. Type-II resistance involves structural reinforcement in the rachilla and at the rachis node, resisting pathogen spread from the spikelets to rachis internodes; pathogen spread in internodes appeared to be comparable in susceptible and moderately resistant or resistant genotypes (Fig. 7.3B). The resistance of all the NILs was due to different genes from Sumai 3. This was not only true for Sumai 3 genes, but for all moderately resistant and resistant genotypes because the 00Ar134-1 genotype in our study behaved similarly. This is supported by histological studies of various genotypes by researchers who arrived at the same conclusions on pathogen spread in spikes (Kang and Buchenauer 2000; Ribichich et al. 2000; Miller et al. 2004; Jansen et al. 2005; Brown et al. 2010).

The important structural role of the rachilla and rachis nodes in Type-II resistance are also supported by the fact that pathogen spread in a total of 3 to 4 rachis internodes was observed, whereas florets attached to these internodes were intact (Fig. 7.3). Thus, it appeared that the rachilla and the rachis nodes were important for Type-II resistance and not the internodes. The *Fg* spread was slowed by the rachilla and rachis nodes of the inoculated florets in moderately resistant NILs, and even delayed spread to the internodes did not result in the infection of many florets as rachis nodes of other florets resulted in equal resistance to

spread to the developing ovaries. The rachilla is recognized as a unique structure in the wheat spike, which is connected to the ovary by a central core consisting of a thick layer of thick-walled sclerenchyma cells (Kang and Buchnenauer 2000; Zhang et al. 2008; Ilgen et al. 2009; Brown et al. 2010). Additionally, this attachment region consisting of the rachilla and the rachis node is highly condensed with a very unusual vascular system at the base of the ovary (O'Brien et al. 1985).

Some studies suggest cell-wall lignification to be an important component of FHB resistance in moderately resistant wheat genotypes and have concluded that FTIR based markers can be used to differentiate genotypes (Gunnaiah and Kushalappa 2014; Lahlali et al. 2015; Lahlali et al. 2016; Atanasova-Penichon et al. 2016). In contrast, our study did not find any consistent results for some important bipolymeric compounds such as cellulose, pectin, and xylan. The only significant and consistent results were found for lignin (Table 7.6), but increased lignification was also observed in the susceptible recurrent parent. The role of these cell wall compounds and lignin deposition is a result of basal resistance of plants to most biotic stresses and not necessarily specific to Type-II FHB resistance (Vorwerk et al. 2004; Jansen et al. 2005). However, changes in biopolymeric compounds were significant enough to differentiate genotypes, which could result from the action of cell wall degrading enzymes secreted by *Fg* (Walter et al. 2010).

It should be noted that while synchrotron-based imaging provides an effective way to non-destructively characterize and quantify infected tissue, there are currently no established methods for imaging *Fg* (or any other pathogen) using X-ray-based methods. A goal for future work could be to include other imaging modalities that do allow for tagging and imaging of the pathogen (such as multiphoton laser scanning microscopy) so that the spread of the pathogen can be correlated to the distribution of damaged tissue, ultimately providing a more complete characterization of resistance. The latest imaging technologies are capable of providing 3D volume data to advance understanding of structural changes in plants resulting from pathogen infections, including FHB (Tanino et al. 2017). The fluorescent protein-expressing pathogen isolates can be used in conjunction with multiphoton laser scanning microscopy to generate powerful and informative cell level 3D infection biology imaging. In addition to following fungal spread over time using multiphoton spectroscopy, excitation and emission fingerprinting using auto-fluorescence can be used to image a wide range of host responses to the pathogen, including cell wall thickening, callose deposition, lignification, and other biological responses.

Based on grayscale values and the void space volume fraction, our study re-confirmed that the rachilla + rachis nodes were structurally important parts of the wheat spike that were

associated with Type-II resistance to pathogen spread. Although the rachilla + rachis nodes provide significant resistance to pathogen spread, it is not complete resistance as the pathogen can still invade internodes, however, this structural reinforcement significantly impedes disease progress. The Type-II resistance resulting from the rachilla + rachis node structure was essentially the same in all moderately resistant genotypes, irrespective of the resistance allele haplotype. The structural reinforcement did not necessarily involve lignification of tissue, which was observed even in susceptible genotypes as a part of basal resistance. The spike region where the genotypes differ more consistently was only in the rachilla and rachis node. Direct observation and detailed analyses of anatomical features of wheat spikes following *Fg* inoculation demonstrated the potential of using X-ray imaging as a direct and non-destructive visualization tool for plants that can be implemented in other host-pathogen systems using our study as an example.

CHAPTER 8

Syntheses and conclusions

Cereal crops, particularly wheat, continue to play a major role in satisfying the demand for food by the growing human population (Pena-Bautista et al. 2017). A significant proportion of the global population, mainly in developing countries, depends on cereal-based food for their dietary requirements. Wheat can be cultivated in diverse geopgraphical regions of the world from the equator to temperate regions and can be stored for an indefinite period. In addition, it is a good source of calories and protein. By 2050, the global population is expected to be as much as 10 billion, thus posing a challenge to agricultural researchers. It is currently not possible to increase yields at a rate matching the rate of increase of the global population. To meet the expected increased demand for wheat, there is more pressure on wheat producing countries to increase yield, which could either be done by increasing area under cultivation or achieving greater yields per ha. Area under cultivation can not be increased, and in fact with globalization, it is decreasing every year (Pena-Bautista et al. 2017). To reduce yield loss and sustain productivity, it becomes even more important to manage diseases affecting wheat cultivation.

Fusarium head blight (FHB) is one of the most serious diseases of wheat in North America, China, and Europe, which produce a large portion of the total wheat worldwide. The disease not only reduces yield by affecting the amount and size of seed but affects quality by contamination with harmful mycotoxins. Sometimes, later stage infection of FHB in wheat does not affect yield as the kernels remain plump, but still produces deoxynivalenol rendering it useless for food and/or feed. Breeders rely on data collected from variety performance trials and disease nurseries to select promising lines, however, selecting for FHB resistance or tolerance is more challenging compared to other diseases. The expression of resistance of wheat lines to FHB is influenced by many factors such as environmental conditions, inoculum pressure, pathogen population, and even the person doing the assessment. Not only do environmental conditions result in data variation, it is common that the disease is absence in rainfed environments such as Canada and much of the United States. To reliably select for FHB resistance, breeders test their material in several environments to increase heritability estimates and cull poorly performing lines. Phenotyping wheat for FHB demands a huge input of resources, is very time-consuming, and further complicated by the different types of resistance mechansims.

Resistance in wheat to FHB is not complete and is governed by many genes with minor effect, unlike most other pathogens/diseases. The first most promising QTL/gene (*Fhb1* from Sumai 3) for FHB resistance in wheat was identified and mapped in 1999 (Bai

and Shaner 2004) and it was 17 years before the gene was cloned (Rawat et al. 2016). Among seven formally designated genes, *Fhb1* has the largest effect on FHB Type-II resistance, which has been consistently reported from many independent studies (Bai et al. 1999; Waldron et al. 1999; Zhou et al. 2002; Buerstmayr et al. 2003; Cuthbert et al. 2006; Yu et al. 2008; Schweiger et al. 2016; reviewed in Buerstmayr et al. 2009; and Bai et al. 2018). The gene has also been reported from many wheat landraces not related to Sumai 3 and its origin is reported to be southern China (reviewed in Bai et al. 2018). The gene was subjected to map-based cloning and Rawat et al. (2018) identified a candidate in the *Fhb1* interval, i.e. a chimeric lectin with agglutinin domains and a pore-forming toxin-like domain (*PFT*). They further reported that the resistant allele of *Fhb1* carries a functional *PFT*, whereas genotypes with the susceptible allele carry a malfunctioned allele or complete absence of the allele. However, contrary to these findings, Bai et al. (2018) reported a different candidate (histidine-rich calcium-binding protein) in the *Fhb1* interval (using map-based cloning and EcoTILLING of candidate genes), designated as *TaHRC*. The wild-type allele confers susceptibility, whereas the loss-of-function in the gene results in a resistant reaction. Additionally, they screened a large collection of wheat accessions from China, Japan, and elsewhere and reported the presence of *PFT* in some susceptible accessions, whereas *TaHRC* was present only in resistant accessions. The candidate for *Fhb1* is still debated and some researchers are focusing on more than one candidate to understand the functioning of this important gene.

During the course of this PhD project, the near-isogenic lines (NILs) developed using marker-assisted selection were well-characterized. Originally, the NILs were developed by selecting for microsatellite markers flanking *Fhb1*, *Fhb2*, and *Fhb5*. The introgression of *Fhb2* was not very accurate, as reliable markers in the QTL interval were not available at the time of developing the NILs. In 2017, all NILs were tested with SNP or microsatellite markers suggested from recent publications for all three genes, i.e. *Fhb1*, *Fhb2*, and *Fhb5* (Rawat et al. 2016; Dhokane et al. 2016; Buerstmayr et al. 2017; Zhao et al. 2018). The availability of high-throughput genotyping platforms such as the illumina iSelect SNP assay comprised of 81,587 SNPs allowed us to thoroughly investigate the genomic composition of the NILs. Only with the availability of better markers, could we detect false positive entries that were classified as carriers of any particular gene based on original microsatellite genotyping. It is very important to understand the genetic architecture of NILs or the resistant donor before using it in breeding programs because resistance improvement and potential linkage-drag is largely dependent on the proportion of alleles from the resistant donor and epistatic interactions (which in turn depend on genetic backgrounds of both

parents). Only with the availability of a large numbers of markers and survey sequences of each of the bread wheat chromosomes of Chinese Spring (IWGSC 2014) could we determine the minor effect alleles from both parents that were associated with FHB resistance, agronomic or end-use quality traits.

Utilization of the wheat illumina iSelect 90K assay allowed us to develop saturated genetic linkage maps of backcross derived recombinant inbred lines in the tetraploid wheat population. These high-density maps were particularly useful to map quantitative trait loci (QTL) governing FHB Type-II resistance and seed coat color in durum wheat. The availability of the Chinese Spring genome assembly further allowed determination of the physical positions and the genes annotated in the QTL regions. The QTL flanked by narrow physical/genetic intervals are amendable to marker-assisted selection and the SNP markers for such QTL can be converted into breeder-friendly Kompetitive Allele-Specific PCR (KASP) markers.

For the first time, we successfully utilized synchrotron-based X-ray imaging and computed tomography to study the wheat-*Fusarium* interaction, thus providing a new tool to better understand the structural changes resulting from *Fusarium* infection. The proof-of-concept to image the Wheat-*Fusarium* pathosystem can also be implanted in other pathosystems, thus paving the way for future histopathological studies.

The main conclusions from our studies are: (i) genetic background and epistatic interactions are important factors governing resistance improvement in wheat from introgression of Sumai 3 derived FHB resistance genes. Lines carrying the so called 'native' resistance may not benefit as much as susceptible lines would from the introgression of 'exotic' alleles, (ii) although minimal linkage drag for agronomic and end-use quality traits results from introgression of exotic FHB resistance genes, it is largely governed by the proportion of the resistant donor's genome and/or genetic background, (iii) Sumai 3 derived FHB resistance genes *Fhb1*, *Fhb2*, and *Fhb5* work additively with metconazole to suppress FHB and lower DON accumulation, (iv) novel QTL for FHB resistance are detected in tetraploid wheat using high-density linkage-maps. Resistance is governed by a large number of stable/consistent minor effect QTL in emmer and durum wheat, and (iv) rachilla and rachis nodes are key tissues of the wheat spike, which are structurally important for conferring Type-II resistance to *Fusarium* spp. in wheat.

REFERENCES

Agnes S-H, Szabolcs L-K, Monika V, Laszlo P, Janos P, Csaba L, Akos M (2014) Differential influence of QTL linked to Fusarium head blight, Fusarium-damaged kernel, deoxynivalenol contents and associated morphological traits in a Frontana-derived wheat population. Euphytica 200:9-26.

Als-Nielsen J, McMorrow D (2011) Elements of modern X-ray physics. Wiley-VCH Publishers. ISBN: 978-0-470-97395-0.

Amarasinghe CC, Tamburic-Ilincic L, Gilbert J, Brûlé-Babel A, Fernando WGD (2013) Evaluation of different fungicides for control of Fusarium head blight in wheat inoculated with 3ADON and 15ADON chemotypes of *Fusarium graminearum* in Canada. Can J Plant Pathol 35:200-208.

Anderson AL (1948) The development of *Gibberella zeae* head blight of wheat. Phytopathol 38:595-611.

Anderson JA, Stack RW, Liu S et al. (2001) DNA markers for Fusarium head blight resistance QTLs in two wheat populations. Theor Appl Genet 102:1164-1168.

Anonymous (2001) Introduction to Fourier Transform Infrared Spectrometry. Thermo Nicolet Corporation, Madison, WI, USA.

Anonymous (2015a) Varieties of Grain Crops 2015. In: 2015 Guide. Saskatchewan Seed Growers Association.

Anonymous (2015b) Prairie recommending committee for wheat, rye and triticale, operating procedures. [http://www.pgdc.ca/, accessed in October 2018].

Anonymous (2018a) Varieties of Grain Crops 2018. In: 2018 Guide. Saskatchewan Seed Growers Association.

Anonymous (2018b) Canadian wheat. 2017 Crop Review. [Accessed from https://canadianwheat.ca/review/Canadian%20Wheat%202017%20Crop%20in%20Review_180424.pdf in October 2018].

Arthur JC (1891) Wheat scab. Indiana Agric Exp Station Res Bull 36:129-132.

Atanasoff D (1920) Fusarium-blight (scab) of wheat and other cereals. J Agric Res 20:1-32.

Atanasova-Penichon V, Barreau C, Richard-Forget F (2016) Antioxidant secondary metabolites in cereals: potential involvement in resistance to *Fusarium* and mycotoxin accumulation. Front Microbiol 7:566. doi: 10.3389/fmicb.2016.00566.

Avni R, Nave M, Eilam T, Sela H, Alekperov C, Peleg Z, Dvorak J, Korol A, Distelfeld A (2014) Ultra-dense genetic map of durum wheat x wild emmer wheat developed using the 90K iSelect SNP genotyping assay. Mol BreedING 34:1549-1562.

Bai GH, Shaner G (2004) Management and resistance in wheat and barley to Fusarium head blight. Annu Rev Phytopathol 42:135-161.

Bai G, Su Z, Cai J (2018) Wheat resistance to Fusarium head blight. Can J Plant Pathol [Published online: https://doi.org/10.1080/07060661.2018.1476411]

Baker MJ, Trevisan J, Bassan P, et al. (2014) Using Fourier transform IR spectroscopy to analyze biological materials. Nat Prot 9:1771-1791.

Baksh A, Mengistu N, Baenziger PS, Dweikat I, Wegulo SN, Rose DJ, Bai G, Eskridge KM (2013) Effect of Fusarium head blight resistance gene *Fhb1* on agronomic and end-use quality traits of hard red winter wheat. Crop Sci 53(3):793-801.

Balut AL, Clark AJ, Brown-Guedira G, Souza E, Van Sanford DA (2013) Validation of Fhb1 and QFhs.nau-2DL in several soft red winter wheat populations. Crop Sci 53:934-945. Doi:10.2135/cropsci2012.09.0550.

Ban T (1997) Evaluation of resistance to Fusarium head blight in indigenous Japanese species of *Agropyron* (*Elymus*). Euphytica 97:39-44.

Beavis WD (1998) QTL analyses: power, precision, and accuracy. In: Paterson AH (ed) Molecular dissection of complex traits. CRC Press. Boca Raton, pp 145-162.

Bechtel DB, Kaleiku LA, Gaines RL, Seitz LM (1985) The effects of *Fusarium graminearum* infection on wheat kernels. Cereal Chem 62:191-197.

Bent AF, Mackey D (2007) Elicitors, effectors, and R genes: the new paradigm and a lifetime supply of questions. Annu Rev Phytopathol 45:399-436.

Beres BL, Brule-Babel AL, Ye Z, Graf RJ, Turkington TK, Harding MW, Kutcher HR, Hooker DC (2018) Exploring genotype x environment x management synergies to manage Fusarium head blight in wheat. Can J Plant Pathol 40:179-188.

Bernardo R (2008) Molecular markers and selection for complex traits in plants: learning from the last 20 years. Crop Sci 48:1649-1664.

Bissonnette KM, Kolb FL, Ames KA, Bradley CA (2018) Effect of Fusarium head blight management practices on mycotoxin contamination of wheat straw. Plant Dis. http://dx.doi.org/10.1094/PDIS-09-17-1385-RE.

Blandino M, Haidukowski M, Pascale M, Plizzari L, Scudellari D, Reyneri A (2012) Integrated strategies for the control of Fusarium head blight and deoxynivalenol contamination in winter wheat. Field Crops Res 133:139-149.

Bokore FE, Knox RE, DePauw RM, Clarke F, Cuthbert RD, Campbell HL, Brûlé-Babel A, Gilbert J, Ruan Y (2017) Validation of molecular markers for use with adapted sources of Fusarium head blight resistance in wheat. Plant Dis 101:1292-1299. http://dx.doi.org/10.1094/PDIS-10-16-1421-RE

Booth C (1971) The genus *Fusarium*. Common Mycol. Inst. (CAB) Kew, England. pp.231.

Boyacioglu D, Hettiarachchy NS, Stack RW (1992) Effect of three systemic fungicides on deoxynivalenol (vomitoxin) production by *Fusarium graminearum* in wheat. Can J Plant Sci 72:93-101.

Brar GS, Hucl PJ (2017) 00Ar134-1, a spring wheat line of intergeneric origin. Can J Plant Sci 97:153-156.

Brar GS, Fuentes-Davilla G, He X, Sansaloni CP, Singh RP, Singh PK (2018a) Genetic mapping of resistance in hexaploid wheat for a quarantine disease: Karnal Bunt. Front Plant Sci 9:1497. Doi:10.3389/fpls.2018.01497.

Brar GS, Dhariwal R, Randhawa HS (2018b) Resistance evaluation of differentials and commercial wheat cultivars to natural stripe rust (*Puccinia striiformis*) infection in hot spot regions of Canada. Eur J Plant Pathol 152:493-502.

Brar GS, Brûlé-Babel AL, Ruan Y, Henriquez MA, Pozniak CJ, Kutcher HR, Hucl, PJ (2019a) Genetic factors affecting Fusarium head blight resistance improvement from introgression of exotic Sumai 3 alleles (including *Fhb1*, *Fhb2*, and *Fhb5*) in hard red spring wheat. BMC Plant Biol [Accepted].

Brar GS, Pozniak CJ, Kutcher HR, Hucl PJ (2019b) Evaluation of Fusarium head blight resistance genes *Fhb1*, *Fhb2*, and *Fhb5* introgressed into elite Canadian hard red spring

wheats: effect on agronomic and end-use quality traits and implications for breeding. Mol Breeding 39:44. https://doi.org/10.1007/s11032-019-0957-8

Brar GS, Hnatowich G, Peng G, Hucl PJ, Kutcher HR (2019c) The effect of *Fhb1* and *Fhb5* QTL in hard red spring wheat does not depend on fungicide use for managing Fusarium head blight in wheat. Plant Dis [Published, available online]. https://doi.org/10.1094/PDIS-09-18-1559-RE.

Brar GS, Karunakaran C, Bond T, Stobbs J, Liu N, Hucl PJ, Kutcher HR (2019d) Showcasing the application of synchrotron-based X-ray computed tomography in host-pathogen interactions: The role of wheat rachilla and rachis nodes in Type-II resistance to *Fusarium graminearum*. Plant Cell Environ 42:509-526. doi:10.1111/pce.13431.

Brewer HC, Hammond-Kosack KE (2015) Host to a stranger: *Arabidopsis* and *Fusarium* Ear Blight. Trends Plant Sci 20:651-663.

Brisco EI, Brown LK, Olson EL (2017) Fusarium head blight resistance in *Aegilops tauschii*. Genet Resour Crop Evol 64:2049-2058.

Brown NA, Urban M, Van de Meene AML, Hammond-Kosack KE (2010) The infection biology of *Fusarium graminearum*: Defining the pathways of spikelet to spikelet colonization in wheat ears. Fungal Biol 114:555-571.

Buerstmayr H, Steiner B, Lemmens M, Ruckenbauer P (2000) Resistance to Fusarium head blight in winter wheat: heritability and trait associations. Crop Sci 40:1012-1018. Doi:10.2135/cropsci2000.4041012x.

Buerstmayr H, Stierschneider M, Steiner B, Lemmens M, Griesser M, Nevo E, Fahima T (2003) Variation for resistance to head blight caused by *Fusarium graminearum* in wild emmer (*Triticum dicoccoides*) originating from Israel. Euphytica 130:17-23.

Buerstmayr M, Steiner B, Wagner C, Schwarz P, Brugger K, Barabaschi D, Volante A, Vale G, Cattivelli L, Buerstmayr H (2017) High-resolution mapping of the pericentromeric region on wheat chromosome arm 5AS harbouring the Fusarium head blight resistance QTL *Qfhs.ifa-5A*. Plant Biotechnol J http://doi.org/10.1111/pbi.12850.

Buerstmayr M, Buerstmayr H (2015) Comparative mapping of quantitative trait loci for Fusarium head blight resistance and anther retention in the winter wheat population Capo x Arina. Theor Appl Genet 128:1519-1530.

Buertmayr H, Ban T, Anderson JA (2009) QTL mapping and marker-assisted selection for Fusarium head blight resistance in wheat: a review. Plant Breeding 128:1-26.

Buerstmay M, Lemmens M, Steiner B, Buerstmayr H (2011) Advanced backcross QTL mapping of resistance to Fusarium head blight and morphological traits in a *Triticum macha* x *T. aestivum* population. Theor Appl Genet 123:293-306.

Buerstmayr M, Huber K, Heckmann J, Steiner B, Nelson JC, Buesrtmayr H (2012) Mapping of QTL for Fusarium head blight resistance and morphological and developmental traits in three backcross populations derived from *Triticum dicoccum* x *Triticum durum*. Theor Appl Genet 125:1751-1765.

Buerstmayr M, Alimari A, Steiner B, Buerstmayr H (2013) Genetic mapping of QTL for resistance to Fusarium head blight spread (type 2 resistance) in a *Triticum dicoccoides* x *Triticum durum* backcross-derived population. Theor Appl Genet 126:2825-2834.

Burger W, Burge MJ (2013) Automatic Thresholding. In: Principles of Digital Image Processing (eds W. Burger & MJ Burge) pp. 5-50. Springer.

Burrows M, Thomas C, McRoberts N, Bostock RM, Coop Len, Stack J (2016) Coordination of diagnostic efforts in the Great Plains: wheat virus survey and modeling for disease onset. Plant Dis 100:1037-1045.

Burt C, Steed A, Gosman N et al. (2015) Mapping a Type 1 FHB resistance on chromosome 4AS of *Triticum macha* and deployment in combination with two Type 2 resistances. Theor Appl Genet 128:1725-1738.

Cai X, Chen PD, Xu SS, Oliver RE, Chen X (2005) Utilization of alien genes to enhance Fusarium head blight resistance in wheat: a review. Euphytica 142:309-318.

Cai J, Bai G (2014) Quantitative trait loci for Fusarium head blight resistance in Huangcandou x 'Jagger' wheat population. Crop Sci 54:2520-2528.

Cai J, Wang S, Li T, Zhang G, Bai G (2016) Multiple minor QTLs are responsible for Fusarium head blight resistance in Chinese wheat landrace Haiyangzhong. PLoS One 11(9):e0163292. Doi:10.1371/journal.pone.0163292.

Cainong JC, Bockus WW, Feng Y, Chen P, Qi L, Sehgal SK, Danilova TV, Koo D-H, Friebe B, Gill BS (2015) Chromosome engineering, mapping, and transferring of resistance

to Fusarium head blight disease from *Elymus tsukushiensis* into wheat. Theor Appl Genet 128:1019-1027.

Cativelli M, Lewis S, Appendino ML (2013) A Fusarium head blight resistance quantitative trait locus on chromosome 7D of the spring wheat cultivar Catbird. Crop Sci 53:1464-1471.

Chapman JA, Mascher M, Buluc A et al. (2015) A whole-genome shotgun approach for assembling and anchoring the hexaploid bread wheat genome. Genome Biol 16:26.

Chen PD, Liu DJ (2000) Transfer scab resistance from *Leymus racemosus*, *Roegneria ciliaris*, and *Roegneria kamoji* into common wheat. In: Raupp WJ, Ma Z, Chen PD, Liu DJ (eds.) Proceedings international symposium on wheat improvement for scab resistance, Suzhou and Nanjing. KSU Printing Services, Manhattan pp. 62-67.

Chen P, Liu W, Yuan J, et al. (2005) Development and characterization of wheat-*Leymus racemosus* translocation lines with resistance to Fusarium head blight. Theor Appl Genet 111:941-948.

Chen XF, Faris JD, Hu JG, Stack RW, Adhikari T, Elias EM, Kianian SF, Cai XW (2007) Saturation and comparative mapping of a major Fusarium head blight resistance QTL in tetraploid wheat. Mol Breed 19:113-124.

Chen RC, Dreossi D, Mancini L, Menk R, Rigon L, Xiao TQ, Longo R (2012) PITRE: software for phase-sensitive X-ray image processing and tomography reconstruction. J Synchrotron Rad 19:836-845.

Cholango-Martinez LP, Zhang XM, Hucl PJ, Kutcher HR (2016) First report of Fusarium head blight, caused by *Fusarium graminearum*, on annual canarygrass (*Phalaris canariensis*) in Saskatchewan, Canada. Plant Dis 100:1780.

Chu C, Niu Z, Zhong S, Chao S, Friesen TL, Halley S, Elias EM, Dong Y, Faris JD, Xu SS (2011) Identification and molecular mapping of two QTLs with major effects for resistance to Fusarium head blight in wheat. Theor Appl Genet 123:1107-1119.

Clark AJ, Sarti-Dvorjak D, Brown-Guedira G, Dong Y, Baik B-K, Van Sanford DA (2016) Identifying rare FHB-resistant segregants in intransigent backcross and F_2 winter wheat populations. Front Microbiol. 7:277. Doi: 10.3389/fmicb.2016.00277.

Clarke JM, Clarke FR, Pozniak CJ (2010) Forty-six years of genetic improvement in Canadian durum wheat cultivars. Can J Plant Sci 90(6):791-801.

Cools HJ, Hawkins NJ, Fraaije BA (2013) Constraints on the evolution of azole resistance in plant pathogenic fungi. Plant Pathol 62 (Suppl. 1):36-42.

Cuthbert PA, Somers DJ, Thomas J, Cloutier S, Brûlé-Babel A (2006) Fine mapping *Fhb1*, a major gene controlling fusarium head blight resistance in bread wheat (*Triticum aestivum* L.). Theor Appl Genet 112:1465-1472.

Cuthbert PA, Somers DJ, Brûlé-Babel A (2007) Mapping of *Fhb2* on chromosome 6BS: a gene controlling Fusarium head blight field resistance in bread wheat (*Triticum aestivum* L.). Theor Appl Genet 114:429-437 doi:10.1007/s00122-006-04399-3.

D'Angelo DL, Bradley CA, Ames KA, Willyerd KT, Madden LV, Paul PA (2014) Efficacy of fungicide applications during and after anthesis against Fusarium head blight and deoxynivalenol in soft red winter wheat. Plant Dis 98:1387-1397.

Del Ponte EM, Fernandes JMC, Pavan W, Baethgen WE (2009) A model-based assessment of the impacts of climate variability on Fusarium head blight seasonal risk in southern Brazil. J Phytopathol 157:675-681.

DePauw RM, Knox RE, McCaig TN, Clarke FR, Clarke JM (2011) Carberry hard red spring wheat. Can J Plant Sci 91:529-534.

Dhokane D, Karre S, Kushalappa AC, McCartney C (2016) Integrated metabolon-transcriptomics reveals Fusarium head blight candidate resistance genes in wheat QTL-*Fhb2*. PLoS One 11(5):e0155851.

Dill-Macky R, Salas B (2001) Effect of burning wheat and barley residues on survival of *Fusarium graminearum* and *Cochliobolus sativus*. *In*: Proceedings of 2001 National Fusarium Head Blight Forum, Erlanger, KY, USA. pp. 112.

Dweba CC, Figlan S, Shimelis HA, Motaung TE, Sydenham S, Mwadzingeni L, Tsilo TJ (2017) Fusarium head blight of wheat: pathogenesis and control strategies. Crop Protection 91:114-122.

El Baidouri M, Murat F, Veyssiere M, et al. (2016) Reconciling the evolutionary origin of bread wheat (*Triticum aestivum*). New Phytol doi: 10.1111/nph.14113.

Elias EM, Manthey FA, Stack RW, Kianian SF (2005) Breeding efforts to develop Fusarium head blight resistant durum wheat in North Dakota. In: Canty SM, Boring T,

Wardwell J, Siler L, Ward RW (eds) Proceedings of the 2005 National Fusarium Head Blight Forum, Milwaukee, WI, 11-13 Dec. Michigan State University, East Lansing, pp 25-26.

Engle JS, Lipps PE, Graham TL, Boehm MJ (2004) Effects of choline, betaine and wheat floret extracts on growth of *Fusarium graminearum*. Plant Dis 88(2):175-180.

Erukhimovitch V, Tsror L, Hazanovsky M, Huleihel M (2010) Direct identification of potato's fungal phyto-pathogens by Fourier-transform infrared (FTIR) microscopy. Spectroscopy 24:609-619.

Fakhfakh MM, Yahyaoui A, Rezgui S, Elias EM, Daaloul A (2011) Inheritance of Fusarium head blight resistance in a cross involving local and exotic durum wheat cultivars. Crop Sci 51:2517-2524.

Faris JD, Haen KM, Gill BS (2000) Saturation mapping of a gene-rich recombination hot spot region in wheat. Genetics 154:823-835.

Fedak G, Cao W, Xue A, Savard M, Clarke J, Somers DJ (2007) Enhancement of Fusarium head blight resistance in bread wheat and durum by means of wide crosses. In: Buck HT, Nisi JE, Salomn N (eds.) Wheat production in stressed environments, Springer, Netherlands, pp 91-95.

Feldman M (2001) Origin of cultivated wheat. In: Bonjen AP, Angus WJ, eds. The world of wheat book: a history of wheat breeding. Lavoisier Publishing, Paris, France pp. 3-56.

Frutos E, Purificacion Galindo M, Leiva V (2014) An interactive biplot implementation in R for modeling genotype-by-environment interaction. Stoch Environ Res Risk Assess 28:1629-1641.

Garvin D, Stack R, Hansen J (2009) Quantitative trait locus mapping of increased Fusarium head blight susceptibility associated with a wild emmer wheat chromosome. Phytopathol 99:447-452.

Geravis L, Dedryver F, Morlais JY, et al. (2003) Mapping of quantitative trait loci for field resistance to Fusarium head blight in a European winter wheat. Theor Appl Genet 106:961-970.

Ghavami F, Elias EM, Mamidi S, Ansari O, Sargolzaei M, Adhikari T, Mergoum M, Kianian SF (2011) Mixed model association mapping for Fusarium head blight resistance in Tunisian-derived durum wheat populations. G3:Genes|Genomes|Genetics 1:209-218.

Giancaspro A, Giove S, Zito D, Blanco A, Gadaleta A (2016) Mapping QTLs for Fusarium head blight resistance in an interspecific wheat population. Front Plant Sci 7:1381. Doi:10.3389/fpls.2016.01381.

Gilbert J, Tekauz A, Mueller E, Kromer U (1994) Occurrence of fusarium head blight in Manitoba in 1993. Can Plant Dis Surv 74:77-78.

Gilbert J, Tekauz A (2000) Review: recent developments in research on Fusarium head blight of wheat in Canada. Can J Plant Pathol 22:1-8.

Gilbert J, Woods SM (2006) Strategies and considerations for multi-location FHB screening nurseries. In: T. Ban, J. M. Lewis, and E. E. Phipps (eds.), The Global Fusarium Initiative for International Collaboration: A Strategic Planning Workshop, CIMMYT, El Batan, Mexico. 14-17 March, 2006. pp. 93-102.

Gilbert J, Haber S (2013) Overview of some recent research developments in fusarium head blight of wheat. Can J Plant Pathol 35:149-174.

Gilbert J, Clear RM, Ward TJ, Gaba D, Tekauz A, Turkington TK, Woods SM, Nowicki T, O'Donnell K (2010) Relative aggressiveness and production of 3- or 15-acetyl deoxynivalenol and deoxynivalenol by *Fusarium graminearum* in spring wheat. Can J Plant Pathol 32:146-152.

Gilbert J, Brûlé-Babel A, Guerrieri AT, Clear RM, Patrick S, Slusarenko K, Wolfe C (2014) Ratio of 3-ADON and 15-ADON isolates of *Fusarium graminearum* recovered from wheat kernels in Manitoba from 2008 to 2012. Can J Plant Pathol 36:54-63.

Gilchrist L, Velazquez C, Mujeeb-Kazi A (1999) Resistance to Fusarium head blight in synthetic hexaploid wheats (2n=6x=42, AABBDD). In: P. Hart et al. (eds.) Proceedings of the 1998 FHB Forum, University Printing, East Lansing, MI. pp. 162-164.

Gladysz C, Lemmens M, Steiner B, Buerstmayr H (2007) Evaluation and genetic mapping of resistance to Fusarium head blight in *Triticum dicoccoides*. Israel J Plant Sci 55:263-266.

Guenther, J.C., and Trail, F. 2005. The development and differentiation of *Gibberella zeae* (anamorph: *Fusarium graminearum*) during colonization of wheat. Mycologia. 97:229-237.

Gunnaiah R, Kushalappa AC (2014) Metabolomics deciphers the host resistance mechanisms in wheat cultivar Sumai-3, against trichothecene producing and non-producing isolates of *Fusarium graminearum*. Plant Phyiol Biochem 83:40-50.

Guo J, Zhang X, Hou Y et al. (2015) High-density mapping of the major FHB resistance gene *Fhb7* derived from *Thinopyrum ponticum* and its pyramiding with *Fhb1* by marker-assisted selection. Theor Appl Genet 128:2301-2316.

Haberle J, Holzpfel J, Schweiger G, Hartl L (2009) A major QTL for resistance against Fusarium head blight in European winter wheat. Theor Appl Genet 119:325-332.

He X, Lillemo M, Shi J, Wu J, Bjornstad A, Belova T, Dreisigacker S, Duveiller E, Singh P (2016) QTL Characterization of Fusarium head blight resistance in CIMMYT bread wheat line Soru#1. PLoS One 11(6):e0158052, doi:10.1371/journal.pone.0158052.

Herter CP, Ebmeyer E, Kollers S, Korzun V, Leiser WL, Wurschum T, Miedaner T (2018) *Rht24* reduces plant height in the winter wheat population 'Solitar x Bussard' without adverse effects on Fusarium head blight infection. Theor Appl Genet 131:1263-1272.

Hessler TG, Thomson MJ, Benscher D, Nachit MM, Sorrells ME (2002) Association of a lipoxygenase locus *Lpx-B1*, with variation in lipoxygenase activity in durum wheat seeds. Crop Sci 42(5):1695-1700.

Heun M, Schafer-Pregl R, Klawan D, Castagna R, Accerbi M, Borghi B, Salamini F (1997) Site of einkorn wheat domestication identified by DNA fingerprinting. Science 278:1312-1314.

Hollingsworth CR, Motteberg CD, Wiersma JV, Atkinson LM (2008) Agronomic and economic responses of spring wheat to management of Fusarium head blight. Plant Dis 92:1339-1349.

Huang S, Sirikhachornkit A, Su X, Faris J, Gill B, Haselkorn R, Gornicki P (2002) Genes encoding plastid acetyl-CoA carboxylase and 3-phosphoglycerate kinase of the *Triticum/Aegilops* complex and the evolutionary history of polyploid wheat. Proc Nat Acad Sci USA 99:8133-8138.

Hucl PJ, Pozniak CJ, Chibbar R (2016) Improving hard white wheat to meet changing quality requirements. Agriculture Development Fund Final Report #20100039, Saskatchewan Ministry of Agriculture, Regina, SK. [Accessed from: http://www.agriculture.gov.sk.ca/apps/adf/ADFAdminReport/20100039.pdf, in October 2018].

Huhn M, Elias E, Ghavami F, Kianian S, Chao S, Zhong S, Alamri M, Yahyaoui A, Mergoum M (2012) Tetraploid Tunisian wheat germplasm as a new source of Fusarium head blight resistance. Crop Sci 52:136-145.

Ilgen P, Hadeler B, Maier FJ, Schafer W (2009) Developing kernel and rachis node induce the trichothecene pathway of *Fusarium graminearum* during wheat head infection. Mol Plant-Microbe Interact 22:899-908.

Islam MS, Brown-Guedira G, Van Sanford D, Ohm H, Dong Y, McKendry AL (2016) Novel QTL associated with the Fusarium head blight resistance in Truman soft red winter wheat. Euphytica 207:571-592.

IWGSC (2014) A chromosome-based draft sequence of the hexaploid bread wheat (*Triticum aestivum*) genome. Science 345.

Jansen C, von Wettstein D, Schafer W, Kogel K-H, Felk A, Maier FJ (2005) Infection patterns in barley and wheat spikes inoculated with wild-type and trichodiene synthase gene disrupted *Fusarium graminearum*. Proc Nat Acad Sci USA (PNAS) 102:16892-16897.

Jauhar PP, Peterson TS (1998) Wild relatives of wheat as sources of Fusarium head blight resistance. In: Proceedings of the 1998 National FHB Forum. Michigan State University, East Lansing, MI pp. 77-79.

Jayatilake DV, Bai GH, Dong YH (2011) A novel quantitative trait locus for Fusarium head blight resistance in chromosome 7A of wheat. Theor Appl Genet 122:1189-1198.

Jia H, Zhou J, Xue S et al. (2018) A journey to understand wheat Fusarium head blight resistance in the Chinese wheat landrace Wangshuibai. Crop J 6:48-59.

Jin F, Zhang D, Bockus W, Baenziger PS, Carver B, Bai G (2013) Fusarium head blight resistance in U.S. winter wheat cultivars and elite breeding lines. Crop Sci 53:2006-2013.

Jorgensen LN, Nielsen LK, Nielsen BJ (2012) Control of seedling blight in winter wheat by seed treatments – impact on emergence, crop stand, yield and deoxynivalenol. Acta Agr Scand B-S P. 62:431-440.

Kabbaj H, Sall AT, Al-Abdallat A, Geleta M, Amri A, Filali-Maltouf A, Belkadi B, Ortiz R, Bassi FM (2017) Genetic diversity within a global panel of durum wheat (*Triticum durum*) landraces and modern germplasm reveals the history of alleles exchange. Front Plant Sci 8:1277. Doi:10.3389/fpls.2017.01277.

Kaeppler SM, Phillips RL, Kim TS (1993) Use of near-isogenic lines derived by backcrossing or selfing to map qualitative traits. Theor Appl Genet 87:233-237.

Kang Z, Buchenauer H (2000) Cytology and ultrastructure of the infection of wheat spikes by *Fusarium culmorum*. Mycol Res 104:1083-1093.

Karunakaran C, Lahlali R, Zhu N, et al. (2015) Factors influencing real time internal structure visualization and dynamic process monitoring in plants using synchrotron-based phase contrast X-ray imaging. Sci Rep 5:12119.

Kazan K, Gardiner DM, Manners JM (2012) On the trail of a cereal killer: recent advances in *Fusarium graminearum* pathogenomics and host resistance. Mol Plant Pathol 13:399-413.

Kishii M, Ban T, Ammar K (2005) Improvement of FHB resistance of durum wheat. In: Canty SM, Boring T, Wardwell J, Siler L, Ward RL (eds.) Proceedings of 2005 National Fusarium Head Blight Forum. Milwaukee, WI. Pp. 52.

Krattinger SG, Lagudah ES, Spielmeyer W, Singh RP, Huerta-Espino J, McFadden H, Bossolini E, Selter LL, Keller B (2009) A putative ABC transporter confers durable resistance to multiple fungal pathogens in wheat. Science 323:1360-1363.

Kubo K, Kawada N, Fujita M, Hatta K, Oda S, Nakajima T (2010) Effect of cleistogamy on Fusarium head blight resistance in wheat. Breeding Sci 60(4):405-411.

Kumar S, Stack RW, Friesen TL, Faris JD (2007) Identification of a novel Fusarium head blight resistance quantitative trait locus on Chromosome 7A in tetraploid wheat. Phytopathol 97:592-597.

Lahlali R, Karunakaran C, Wang L, et al. (2015) Synchrotron based phase contrast imaging combined with FTIR spectroscopy reveals structural and biomolecular differences in spikelets play a significant role in resistance to Fusarium in wheat. BMC Plant Biol 15:24, https://doi.org:10.1186/s12870-014-0357-5.

Lahlali R, Kumar S, Wang L, et al. (2016) Cell wall biomolecular composition plays a potential role in the host Type II resistance to Fusarium head blight in wheat. Front Microbiol 7:910. doi:10.3389/fmicb.2016.00910.

Lancashire PD, Bleiholder H, Langeluddecke P, Stauss R, van den Boom T, Weber E, Witzenberger A (1991) A uniform decimal code for growth stages of crops and weeds. Ann Appl Biol 119:561-601.

Leplat J, Friberg H, Abid M, Steinberg C (2013) Survival of *Fusarium graminearum*, the causal agent of Fusarium head blight. A review. Agron Sustain Develop 33:97-111.

Li T, Bai G, Wu S, Gu S (2011) Quantitative trait loci for resistance to fusarium head blight in a Chinese landrace Haiyanzhong. Theor Appl Genet 122:1497-1502.

Li T, Bai G, Wu S, Gu S (2012) Quantitative trait loci for resistance to Fusarium head blight in the Chinese wheat landrace Huangfangzhu. Euphytica 185:93-102.

Li X, Xiang ZP, Chen WQ et al. (2017) Reevaluation of two quantitative trait loci for Type II resistance to Fusarium head blight in wheat germplasm PI 672538. Phytopathol 107:92-99.

Li X, Zhong S, Chen W, Fatima SA, Huang Q, Li Q, Tan F, Luo P (2018) Transcriptome analysis identifies a 140 kb region of chromosome 3B containing genes specific to Fusarium head blight resistance in wheat. Int J Mol Sci 19:852.

Littell RC, Milliken GA, Stroup WW, Wolfinger R, Schabenberger O (2006) SAS for mixed models (2nd Edition). SAS Institute Inc., Cary, NC, USA.

Liu S, Zhang X, Pumphrey MO, Stack RW, Gill BS, Anderson JA (2006) Complex microlinearity among wheat, rice and barley revealed fine mapping of the genomic region harbouring a major QTL for resistance to Fusarium head blight in wheat. Funct Integr Genomics 6:83-89.

Liu S, Pumphrey MO, Gill BS, Trick H, Zhang JX, Dolezel J, Chalhoub B, Anderson, JA (2008) Towards positional cloning of *Fhb1*, a major QTL for Fusarium head blight resistance in wheat. Cereal Res Comm 36:195-201.

Liu S, Christopher MD, Griffey CA, Hall MD, Gundrum PG, Brooks WS (2012) Molecular characterization of resistance to Fusarium head blight in U.S. soft red winter wheat breeding line VA00W-38. Crop Sci 52:2283-2292.

Liu S, Griffey CA, Hall MD, McKendry AL, Chen J, Brooks WS, Brown-Guedira G, Van Sanford D, Schmale DG (2013a) Molecular characterization of field resistance to Fusarium head blight in two US soft red winter wheat cultivars. Theor Appl Genet 126:2485-2498.

Liu Y, Nelson J, Holzner C, Andrews JC, Pianetta P (2013b) Recent advances in synchrotron-based hard x-ray phase contrast imaging. J Phys D: Appl Phys 46:494001.

Lv C, Song Y, Gao L, Yao Q, Zhou R, Xu R, Jia J (2014) Integration of QTL detection and marker assisted selection for improving resistance to Fusarium head blight and important agronomic traits in wheat. Crop J 2:70-78.

Lu Q, Szabo-Hever A, Bjornstad A, Lillemo M, Semagn K, Mesterhazy A, Ji F, Shi J, Skinnes H (2011) Two major resistance quantitative trait loci are required to counteract the increased susceptibility to Fusarium head blight of the *Rht-D1b* dwarfing gene in wheat. Crop Sci 51:2430-2438.

Lu Q, Lillemo M, Skinnes H, He X, Shi J, Ji F, Dong Y, Bjornstad A (2013) Anther extrusion and plant height are associated with Type I resistance to Fusarium head blight in bread wheat line 'Shnaghai-3/Catbird'. Thor Appl Genet 126:317-334.

Macferri M, Ricci A, Salvi S et al. (2015) A high-density, SNP-based consensus map of tetraploid wheat as a bridge to integrate durum and bread wheat genomics and breeding. Plant Biotechnol J 13:648-663.

Mao S-L, Wei Y-M, Cao W, et al. (2010) Confirmation of the relationship between plant height and Fusarium head blight resistance in wheat (*Triticum aestivum* L.) by QTL meta-analysis. Euphytica 174:343-356.

Matus-Cádiz MA, Hucl P, Perron CE, Tyler RT (2003) Genotype x environment interaction for grain color in hard white spring wheat. Crop Sci 43(1):219-226.

McArthur RI, Zhu X, Oliver RE, Klindworth DL, Xu SS, Stack RW, Wang RRC, Cai X (2012) Homoeology of *Thinopyrum junceum* and *Elymus rectisetus* chromosomes to wheat and disease resistance conferred by *Thinopyrum* and *Elymus* chromosomes in wheat. Chromosome Res 20:699-715.

McCallum BD, DePauw RM (2008) A review of wheat cultivars grown in the Canadian prairies. Can J Plant Sci 88:649-677.

McCallum BD, Hiebert CW, Cloutier S et al. (2016) A review of wheat leaf rust research and the development of resistant cultivars in Canada. Can J Plant Pathol 38(1):1-18.

McCartney CA, Somers DJ, Fedak G, Cao W (2004) Haplotype diversity at Fusarium head blight resistance QTLs in wheat. Theor Appl Genet 109:261-271.

McCartney CA, Somers DJ, Fedak G et al. (2007) The evaluation of FHB resistance QTLs introgressed into elite Canadian spring wheat germplasm. Mol Breed 20:209-221. Doi:10.1107/s11032-007-9084-z.

McIntosh RA, Cusick JE (1987) Linkage map of hexaploid wheat. In: Wheat and Wheat Improvement. Ed. EG Heyne. American Society of Agronomy, Madison, WI. Pp. 289-297.

McIntosh RA, Hart GE, Devos KM, Gale MD, Rogers WJ (1998) Catalogue of gene symbols for wheat. In: Proceedings of the 9th International Wheat Genetics Symposium. Vol. 5. University of Saskatchewan Extension Press, Saskatoon, SK. Pp. 117.

McMullen M, Jones R, Gallenberg D (1997) Scab of wheat and barley: a re-emerging disease of devastating impact. Plant Dis 81:1340-1348.

McMullen M, Bergstrom G, de Wolf E, Dill-Macky R, Hershamn D, Shaner G, van Sanford D (2012) A unified effort to fight an enemy of wheat and barley: fusarium head blight. Plant Dis 96:1712-1728.

Mesterhazy A (1995) Breeding for resistance to Fusarium head blight in wheat. *In*: Fusarium Head Blight: Global Status and Future Prospects. HJ Dubin, L. Gilchrist, J. Reeves, A. McNab (eds.) CIMMYT, Mexico. pp. 79-85.

Mesterhazy A (2003) Control of Fusarium head blight of wheat by fungicides. *In:* Leonard KJ, Bushnell WR (eds.). Fusarium head blight of wheat and barley. The American Phytopathological Society, St. Paul, MN. pp. 363-380.

Mesterhazy A, Bartok T, Mirocha CG, Komoroczy AR (1999) Nature of wheat resistance to Fusarium head blight and the role of deoxynivalenol for breeding. Plant Breed 118:97-110.

Mesterhazy A, Bartok T, Lamper C (2003) Influence of wheat cultivar, species of *Fusarium*, and isolate aggressiveness on the efficacy of fungicides for control of Fusarium head blight. Plant Dis 87:1107-1115.

Mesterházy Á (2014) Breeding wheat for Fusarium head blight resistance in Europe. *In*: J.F. Leslie and A.F. Logrieco (eds.), Mycotoxins Reduction in Grain Chains. Wiley Blackwell, Ames, Iowa, USA. pp. 189-208.

Mesterhazy A, Varga M, Toth B, Kotai C, Bartok T, Veha A, Acs K, Vagvolgyi C, lehoczki-Krsjak S (2018) Reduction of deoxynivalenol (DON) contamination by improved

fungicide use in wheat. Part 1. Dependence on epidemic severity and resistance level in small plot tests with artificial inoculation. Eur J Plant Pathol 151:39-55.

Miedaner T, Wilde F, Steiner B, Buerstmayr H, Korzun V, Ebmeyer E (2006) Stacking quantitative trait loci (QTL) for Fusarium head blight resistance from non-adapted sources in an European elite spring wheat background and assessing their effects on deoxynivalenol (DON) content and disease severity. Theor Appl Genet 112:562-569. Doi:10.1007/s00122-005-0163-4.

Miedaner T, Voss HH (2008) Effect of dwarfing *Rht* genes on Fusarium head blight resistance in two sets of near-isogenic lines of wheat and check cultivars. Crop Sci 48:2115-2122.

Miedaner T, Longin CFH (2014) Genetic variation for resistance to Fusarium head blight in winter durum material. Crop Pasture Sci 65:46-51.

Miller LM, Dumas P (2006) Chemical imaging of biological tissue with synchrotron infrared light. Biochim Biophys Acta 1758:846-857.

Miller JD, Young JC, Sampson RD (1985) Deoxynivalenol and Fusarium head blight resistance in spring cereals. Phytopathol 113:359-367.

Miller JD, Stack RW, Joppa LR (1998) Evaluation of *Triticum turgidum* L. var. *dicoccoides* for resistance to Fusarium head blight and stem rust. In: Slinkard AE (ed) Proceedings of the 9th International Wheat Genetics Symposium. Saskatoon, SK, 2-7 Aug. 1998. University of Saskatchewan Ext. Press, Saskatoon, SK Canada, pp 292-293.

Miller S, Chabot DMP, Ouellet T, Harris LJ, Fedak G (2004) Use of a *Fusarium graminearum* strain transformed with green fluorescent protein to study infection in wheat (*Triticum aestivum*). Can J Plant Pathol 26:453-463.

Milus EA (1994) Evaluation of foliar fungicides for controlling fusarium head blight of wheat. Plant Dise 78:697.

Nakajima T (2010) Fungicides application against Fusarium head blight in wheat and barley for ensuring food safety. In: O. Carisse (Ed.), Fungicides. Intech. Pp. 139-156.

Nesbitt M (1998) Where was einkorn wheat domesticated? Trends Plant Sci 3:1360-1385.

Newman LH (1928) The history and present status of wheat production in Canada. Department of Agriculture, Ottawa, ON. Pamphlet #89.

Nishio Z, Onoe C, Ito M, Tabiki T, Nagasava K, Miura H (2016) Mapping a QTL conferring resistance to Fusarium head blight on chromosome 1B in winter wheat (*Triticum aestivum* L.). Breeding Sci 66:668-675. [Abstr].

O'Brien TP, Sammut ME, Lee JW, Smart MG (1985) The vascular system of the wheat spikelet. Aust J Plant Physiol 12:487-511.

Oliver RE, Stack RW, Miller JD, Cai X (2007) Reaction of wild emmer wheat accessions to Fusarium head blight. Crop Sci 47:893-899.

Oplinger ES, Wiersma DW, Grau CR, Kelling KA (1985) Intensive wheat management. University of Wisconsin – Extension, Pamphlet #A3337. [Accessed from: https://coolbean.info/pdf/small_grains/library/grain_production/Intensive_Wheat_Management.pdf, in October 2018].

Osborne LE, Stein JM (2007) Epidemiology of Fusarium head blight on small-grain cereals. Int J Food Microbiol 119: 103-108.

Otto CD, Kianian SF, Elias EM, Stack RW, Joppa LR (2002) Genetic dissection of a major Fusarium head blight QTL in tetraploid wheat. Plant Mol Biol 48:625-632.

Paul PA, McMullen MP, Hershmann DE, Madden LV (2010) Meta-analysis of the effects of triazole-based fungicides on wheat yield and test weight as influenced by Fusarium head blight intensity. Phytopathol 100:160-171.

Paul PA, Bradley CA, Madden LV, et al. (2018) Effects of pre- and post-anthesis applications of demethylation inhibitor fungicides on Fusarium head blight and deoxynivaelnol in spring and winter wheat. Plant Dis. https://doi.org/10.1094/PDIS-03-18-0466-RE

Paux E, Roger D, Badaeva E, Gay G, Bernard M, Sourdille P, Feuillet C (2006) Characterizing the composition and evolution of homoeologous genomes in hexaploid wheat through BAC-end sequencing on chromosome 3B. Plant J 48:463-474.

Pena-Bautista RT, Hernandez-Espinosa N, Jones JM, Guzman C, Braun HJ (2017) Wheat-based foods: their global and regional importance in the food supply, nutrition, and health. Cereal Food World 62(5):231-249.

Pereyra SA, Dill-Macky R (2008) Colonization of the residues of diverse plant species by *Gibberella zeae* and their contribution to Fusarium head blight inoculum. Plant Dis 92:800-807.

Peterson S, Lyerly JH, Maloney PV, Brown-Guedira G, Cowger C, Costa JM, Dong Y, Murphy JP (2016) Mapping of *Fusarium* head blight resistance quantitative trait loci in winter wheat cultivar NC-Neuse. Crop Sci 56:1473-1483.

Peiris KHS, Bockus WW, Dowell FE (2012) Infrared spectral properties of germ, pericarp, and endosperm sections of sound wheat kernels and those damaged by *Fusarium graminearum*. Appl Spectroscopy 66:1053-1060.

Peterson S, Lyerly JH, McKendry AL et al. (2017) Validation of Fusarium head blight resistance QTL in US winter wheat. Crop Sci 57:1-12.

Pirseyedi SM (2014) QTL analysis for Fusarium head blight resistance in Tunisian-derived durum wheat populations. PhD Dissertation, North Dakota State University, December 2013.

Poland JA, Brown PJ, Sorrells ME, Jannink J (2012) Development of high-density genetic maps of barley and wheat using a novel two-enzyme genotyping-by-sequencing approach. PLoS One 7:e32253.

Prat N, Buerstmayr M, Steiner B, Robert O, Burestmayr H (2014) Current knowledge on resistance to Fusarium head blight in tetraploid wheat. Mol Breeding. 34:1689-1699.

Prat N, Guilbert C, Prah U, Wachter E, Steiner B, Langin T, Robert O, Buerstmayr H (2017) QTL mapping of Fusarium head blight resistance in three related durum wheat populations. Theor Appl Genet 130:13-27.

Pugh GW, Johann H, Dickson JG (1933) Factors affecting infection of wheat heads by *Gibberella saubinetti*. J Agric Res 46:771-791.

Pumphrey MO, Bernardo R, Anderson JA (2007) Validating the *Fhb1* QTL for Fusarium head blight resistance in near-isogenic wheat lines developed from breeding populations. Crop Sci 47:200-206. Doi:10.2135/cropsci2006.03.0206.

Qi L, Pumphrey M, Friebe B, Chen P, Gill B (2008) Molecular cytogenetic characterization of alien introgressions with gene *Fhb3* for resistance to Fusarium head blight disease of wheat. Theor Appl Genet 117:1155-1166.

R Core Team (2016) R: A language and environment for statistical computing, Vol. 2016. R Foundation for Statistical Computing, Vienna, Austria.

Rawat N, Pumphrey MO, Liu S et al. (2016) Wheat *Fhb1* encodes a chimeric lectin with agglutinin domians and a pore-forming toxin-like domain conferring resistance to Fusarium head blight. Nat Genet 48:1576-1580.

Ren J, Wang Z, Du Z, Che M, Zhang Y, Quan W, Wang Y, Jiang X, Zhang Z (2018) Detection and validation of a novel major QTL for resistance to Fusarium head blight from *Triticum aestivum* in the terminal region of chromosome 7DL. Theor Appl Genet http://doi.org/10.1007/s00122-018-3213-4.

Ribichich KF, Lopez SE, Vegetti AC (2000) Histopathological spikelet changes produced by *Fusarium graminearum* in susceptible and resistant wheat cultivars. Plant Dis 84:794-802.

Ruan Y, Comeau A, Langevin F, Hucl P, Clarke JM, Brule-Babel A, Pozniak CJ (2012) Identification of novel QTL for resistance to Fusarium head blight in a tetraploid wheat population. Genome 55:853-864.

Salameh A, Buerstmayr M, Steiner B, Neumayer A, Lemmens M, Buerstmayr H (2011) Effects of introgression of two QTL for fusarium head blight resistance from Asian spring wheat by marker-assisted backcrossing into European winter wheat on fusarium head blight resistance, yield and quality traits. Mol Breed 28:485-494. Doi:10.1007/s11032-010-9498-x.

Salas B, Dill-Macky R (2005) Effect of residue management and host resistance on the epidemiology of Fusarium head blight. Phytopathol 95:S92 [Abstr.].

Sari E, Berraies S, Knox RE et al. (2018) High density genetic mapping of Fusarium head blight resistance QTL in tetraploid wheat. PLoS One 13(10):e0204362.

Samad-Zamini M, Schweiger W, Nussbaumer T, Mayer KFX, Buerstmayr H (2017) Time-corse expressin QTL-atlas of the global transcriptional response of wheat to *Fusarium graminearum*. Plant Biotechnol J 15:1453-1464.

Scala V, Aureli G, Cesarano G, Incerti G, Fanelli C, Scala F, Reverberi M, Bonanomi G (2016) Climate, soil management, and cultivar affect Fusarium head blight incidence and deoxynivalenol accumulation in durum wheat of southern Italy. Front Microbiol Doi: 10.3389/fmicb.2016.01014.

Schaafsma AW, Hooker DC (2007) Climatic models to predict occurrence of *Fusarium* toxins in wheat and maize. Int J Food Microbiol 119:116-125.

Schroeder H, Christensen J (1963) Factors affecting resistance of wheat to scab caused by *Gibberella zeae*. Phytopathol 53:831-838.

Schweiger W, Steiner B, Vautrin S et al. (2016) Suppressed recombination and unique candidate genes in the divergent haplotype encoding *Fhb1*, a major Fusarium head blight resistance locus in wheat. Theor Appl Genet 129(8):1607-1623.

Schweiger W, Steiner B, Ametz C et al. (2013) Transcriptomic characterization of two major *Fusarium* resistance quantitative trait loci (QTLs), *Fhb1* and *Qfhs.ifa-5A*, identifies novel candidate genes. Mol Plant Pathol 14(8):772-785.

Segneanu AE, Gozescu I, Dabici A, Sfirloaga P, Szabadai Z (2012) Organic compounds FT-IR spectroscopy. In: Macro to Nano Spectroscopy (ed J. Uddin) InTech pp. 145-164.

Shah L, Ali A, Yahya M, et al. (2017) Integrated control of fusarium head blight and deoxynivalenol mycotoxin in wheat. Plant Pathol 67:532-548.

Shewry PR (2009) Wheat. J Exp Bot 60(6):1537-1553.

Shen CM, Hu YC, Sun HY, Li W, Guo JH, Chen HG (2012) Geographic distribution of trichothecene chemotypes of the *Fusarium graminearum* species complex in major winter wheat production areas of China. Plant Dis 96:1172-1178.

Sinha RC, Savard ME, Lau R (1995) Production of monoclonal antibodies for the specific detection of deoxynivalenol and 15-acetyldeoxynivalenol by ELISA. J Agric Food Chem 43:1740-1744.

Singh AK, Knox RE, Clarke FR, Clarke JM, Somers DJ, Fedak G, Singh A, DePauw R (2008) Fusarium head blight QTL mapping in durum wheat and *Triticum carthlicum* sources of resistance. *In*: Proceedings of the 11th International Wheat Genetics Symposium, Brisbane, QLD, Australia, 24-29 August 2008. Vol 3. Edited by R. Apples, R. Eastwood, E. Lagudah, P. Langridge, M. Mackay, L. McIntyre, P. Sharp. Sydney University Press, Sydney, pp. 845-847.

Skinnes H, Semagn K, Tarkegne Y, Maroy AG, Bjornstad A (2010) The inheritance of anther extrusion in hexaploid wheat and its relationship to *Fusarium* head blight resistance and deoxynivalenol content. Plant Breeding 129:149-155.

Somers DJ, Fedak G, Clarke J, Cao W (2006) Mapping of FHB resistance QTLs in tetraploid wheat. Genome. 49:1586-1593.

Soresi D, Zappacosta D, Garayalde A, Irigoyen I, Basualdo J, Carrera A (2017) A valuable QTL for Fusarium head blight resistance from *Triticum turgidum* L. ssp. *dicoccoides* has a stable expression in durum wheat cultivars. Cereal Res Commun 45(2):234-247.

Srinivasachary, Gosman N, Steed A, et al. (2009) Semi-dwarfing *Rht-B1* and *Rht-D1* loci of wheat differ significantly in their influence on resistance to Fusarium head blight. Theor Appl Genet 118:695-702.

Stack RW, Elias EM, Fetch JM, Miller JD, Joppa LR (2002) Fusarium head blight reaction of Langdon durum-*Triticum dicoccoides* chromosome substitution lines. Crop Sci 42:637-642.

Stack RW (2003) History of Fusarium head blight with emphasis on North America. *In:* Leonard KJ, Bushnell WR (eds.). Fusarium head blight of wheat and barley. The American Phytopathological Society, St. Paul, MN. pp. 1-34.

Stack RW, McMullen MP (1998) A visual scale to estimate severity of Fusarium head blight in wheat. North Dakota State University Extension Service: Small Grains Publications. Online Publication/PP-1095. https://library.ndsu.edu/ir/handle/10365/9187.

Steiner B, Kurz H, Lemmens M, Buerstmayr H (2009) Differential gene expression of related wheat lines with contrasting levels of head blight resistance after *Fusarium graminearum* inoculation. Theor Appl Genet 118:753-764.

Strange RN, Smith H (1971) Fungal growth stimulant in anthers which predisposes wheat to attack by *Fusarium graminearum*. Physiol Plant Pathol 1(2):141-145.

Strange RN, Majer JR, Smith H (1974) The isolation and identification of choline and betaine as the two major components in anthers and wheat germ that stimulate *Fusarium graminearum* in vitro. Physiol Plant Pathol 4(2):277-290.

Suchecki R, Watson-Haigh NS, Baumann U (2017) POTAGE: a visualization tool for speeding up gene discovery in wheat. Sci Rep 7:14315.

Sun J, Ohm HW, Poland JA, Williams CE (2016) Mapping four quantitative trait loci associated with Type I Fusarium head blight resistance in winter wheat 'INW0412'. Crop Sci 56:1163-1172.

Sutton JC (1982) Epidemiology of wheat head blight and maize ear rot caused by *Fusarium graminearum*. Can J Plant Pathol 4:195-209.

Suzuki T, Sato M, Takeuchi T (2012) Evaluation of the effects of five QTL regions on Fusarium head blight resistance and agronomic traits in spring wheat (*Triticum aestivum* L.). Breed Sci 62:11-17. DOI: 10.1270/jsbbs.62.11.

Szabo-Hever A, Lehoczki-Krsjak S, Toth B, Purnhauser L, Buerstmayr H, Steiner B, Mesterhazy A (2012) Identification and validation of fusarium head blight and *Fusarium*-damaged kernel QTL in a Frontana/Remus DH mapping population. Can J Plant Pathol 34(2):224-238.

Talas F, Longin F, Miedaner T (2011) Sources of resistance to Fusarium head blight within Syrian durum wheat landraces. Plant Breeding 130:398-400.

Tamburic-Ilincic L (2012) Effect of 3B, 5A and 3A QTL for Fusarium head blight resistance on agronomic and quality performance of Canadian winter wheat. Plant Breeding 131:722-727.

Tanino K, Willick IR, Hamilton K, et al. (2017) Chemotyping using synchrotron mid-infrared and X-ray spectroscopy to improve agricultural production. Can J Plant Sci 97:982-996.

Taoutaou A, Socaciu C, Pamfil D, Fetea F, Balazs E, Botez C (2012) New markers for potato late blight resistance and susceptibility using FTIR spectroscopy. Not Bot Horti Agrobo 40:150-154.

Tian X, Wen W, Xie L et al. (2017) Molecular mapping of reduced plant height gene *Rht24* in bread wheat. Front Plant Sci 8:1379.

Trail F, Gaffoor I, Vogel S (2005) Ejection mechanics and trajectory of the ascospores of *Gibberella zeae* (anamorph: *Fusarium graminearum*). Fungal Genet Biol 42:528-533.

Turner MK, DeHaan LR, Jin Y, Anderson JA (2013) Wheatgrass-wheat partial amphiploids as a novel source of stem rust and Fusarium head blight resistance. Crop Sci 53:1994-2005.

Van Berloo R (2008) GGT 2.0: Versatile software for visualization and analysis of genetic data. J Heredity 99:232-236.

Van Ooijen JW (2006) JoinMap® 4, software for the calculation of genetic linkage maps in experimental populations. Kyazma BV, Wageningen.

Verges VL, Van Sanford D, Brown-Guedira G (2006) Heritability estimates and response to selection for Fusarium head blight resistance in soft red winter wheat. Crop Sci 46:1587-1594.

Vijayan P, Willick I, Lahlali R, Karunakaran C, Tanino KK (2015) Synchrotron radiation sheds fresh light on plant research: the use of powerful techniques to probe structure and composition of plants. Plant Cell Physiol DOI:10.1093/pcp/pcv080.

Von der Ohe C, Ebmeyer E, Korzun V, Miedaner T (2010) Agronomic and quality performance of winter wheat backcross populations carrying non-adapted Fusarium head blight resistance QTL. Crop Sci 50:2283-2290.

Vorwerk S, Somerville S, Somerville C (2004) The role of plant cell wall polysaccharide composition in disease resistance. Trends Plant Sci 9:203-209.

Voss HH, Holzapfel J, Hartl L, et al. (2008) Effect of the *Rht-D1* dwarfing locus on Fusarium head blight rating in three segregating populations of winter wheat. Plant Breeding 127:333-339.

Walter S, Nicholson P, Doohan FM (2010) Action and reaction of host and pathogen during Fusarium head blight disease. New Phytol 185:54-66.

Wan YF, Yen C, Yang JL, Lin DC (1997) The diversity of resources resistant to scab in *Triticeae* (*Poaceae*). Wheat Information Service 84:7-12.

Wang YZ, Miller JD (1988) Effect of *Fusarium graminearum* metabolites on wheat tissue in relation to Fusarium head blight resistance. J Phytopathol 122:118-125.

Wang S, Basten CJ, Zeng ZB (2012) Windows QTL Cartographer 2.5. Department of Statistics, North Carolina State University, Raleigh, NC, USA.

Wang S, Wong D, Forrest K et al. (2014) Characterization of polyploid wheat genomic diversity using a high-density 90 000 single nucleotide polymorphism array. Plant Biotechnol J 12:787-796.

Ward TJ, Clear RM, Rooney AP, O'Donnell K, Gaba D, Patrick S, Starkey DE, Gilbert J, Geiser DM, Nowicki TW (2008) An adaptive evolutionary shift in Fusarium head blight

pathogen populations is driving the rapid spread of more toxigenic *Fusarium graminearum* in North America. Fungal Genet Biol 45:473-484.

Wegulo SN, Bockus WW, Hernandez Nopsa J, De Wolf ED, Eskridge KM, Peiris KHS, Dowell FE (2011) Effects of integrating cultivar resistance and fungicide application on Fusarium head blight and deoxynivalenol in winter wheat. Plant Dis 95:554-560.

Wegulo SN, Baenziger PS, Nopsa JH, Bockus WW, Hallen-Adams H (2015) Management of Fusarium head blight of wheat and barley. Crop Protection 73:100-107.

Westneat MW, Socha JJ, Lee W-K (2008) Advances in biological structure, function, and physiology using synchrotron X-ray imaging. Ann Rev Physiol 70:119-142.

Whingwiri EE, Kuo J, Stern WR (1981) The vascular system in the rachis of wheat ear. Ann Bot 48:189-201.

Willyerd KT, Li C, Madden LV, et al. (2012) Efficacy and stability of integrating fungicide and cultivar resistance to manage Fusarium head blight and deoxynivalenol in wheat. Plant Dis 96:957-967.

Wong LSL, Tekauz A, Leisle D, Abramson D, McKenzie RIH (1992) Prevalence, distribution, and importance of fusarium head blight in wheat in Manitoba. Can J Plant Pathol 14:233-238.

Xiao J, Jin X, Wang H, et al. (2013) Transcriptome-based discovery of pathways and genes related to resistance against Fusarium head blight in wheat landrace Wangshuibai. BMC Genomics 14:197.

Xu X (2003) Effects of environmental conditions on the development of *Fusarium* ear blight. Eur J Plant Pathol 109:683-689.

Xu S, Jia Z (2007) Genomewide analysis of epistatic effects for quantitative traits in barley. Genetics 175:1955-1963.

Xue S, Li G, Jia H, Xu F, Lin F, Tang M, Wang Y, An X, Xu H, Zhang L (2010a) Fine mapping *Fhb4*, a major QTL conditioning resistance to Fusarium infection in bread wheat (*Triticum aestivum* L.). Theor Appl Genet 121 :147-156.

Xue S, Li G, Jia H et al. (2010b) Marker-assisted development and evaluation of near-isogenic lines for scab resistance QTLs of wheat. Mol Breeding 25 :397-405. Doi :10.1007/s11032-009-9339-y.

Xue S, Xu F, Tang M et al. (2011) Precise mapping *Fhb5*, a major QTL conditioning resistance to Fusarium infection in bread wheat (*Triticum aestivum* L.). Theor Appl Genet 123 :1055-1063. Doi :10.1007/s00122-011-1647-z.

Yan W, Tinker NA (2006) Biplot analysis of multi-environment trial data: principles and applications. Can J Plant Sci 86:623-645.

Ye Z, Brûlé-Babel AL, Graf RJ, Mohr R, Beres BL (2017) The role of genetics, growth habit, and cultural practices in the mitigation of Fusarium head blight. Can J Plant Sci 97:316-328.

Yi X, Cheng J, Jiang Z et al. (2018) Genetic analysis of Fusarium head blight resistance in CIMMYT bread wheat line C615 using traditional and conditional QTL mapping. Front Plant Sci 9:573. Doi: 10.3389/fpls.2018.00573.

Yu QL, Liu TR, Liu YX, Jia GX (1996) Pathological anatomy of the rachis in wheat varieties with resistance against scab. J Heilongjiang August First Land Reclam Univ 8:42-45.

Yu L-X, Lorenz A, Rutkoski J, Singh RP, Bhavani S, Huerta-Espino J, Sorrells ME (2011) Association mapping and gene-gene interaction for stem rust resistance in CIMMYT spring wheat germplasm. Theor Appl Genet 123:1257-1268. Doi:10.1007/s00122-011-1664-y.

Yu L-X, Morgounov A, Wanyera R, Keser M, Singh SK, Sorrells M (2012) Identification of Ug99 stem rust resistance loci in winter wheat germplasm using genome-wide association analysis. Theor Appl Genet 125:749-758. Doi:10.1007/s00122-012-1867-x.

Zeng J, Cao W, Hucl P, Yang Y, Xue A, Chi D, Fedak G (2013) Molecular cytogenetic analysis of wheat-*Elymus repens* introgression lines with resistance to Fusarium head blight. Genome 56:75-82.

Zhang YH, Ye HZ (1993) A study of histology of resistance of wheat to head scab (*Fusarium graminearum*). J Sichuan Agric Univ 11:444-450.

Zhang X, Van De Lee T, Dufrense M, Liu T-G, Lu W-Z, Yu D-Z, Ma H-X (2008) Infection of green fluorescence protein-tagged Fusarium graminearum on wheat and barley spikes. Cereal Res Comm 36 Suppl. B, 465-469.

Zhang M, Zhang R, Yang J, Luo P (2010) Identification of a new QTL for Fusarium head blight resistance in the wheat genotype “Wang shui-bai”. Mol Biol Rep 37:1031-1035.

Zhang X, Pan H, Bai G (2012a) Quantitative trait loci responsible for Fusarium head blight resistance in Chinese landrace Baishanyuehuang. Theor Appl Genet 125:495-502.

Zhang X, Bai G, Bockus W, Ji X, Pan H (2012b) Quantitative trait loci for Fusarium head blight resistance in U.S. hard winter wheat cultivar Heyne. Crop Sci 52:1187-1194.

Zhang X, Fu J, Hiromasa Y, Pan H, Bai G (2013) Differentially expressed proteins associated with Fusarium head blight resistance in wheat. PLoS One 8:282079.

Zhang Q, Axtman JE, Faris JD, Chao S, Zhang Z, Friesen TL, Zhong S, Cai X, Elias EM, Xu SS (2014) Identification and molecular mapping of quantitative trait loci for Fusarium head blight resistance in emmer and durum wheat using a single nucleotide polymorphism-based linkage map. Mol Breeding 34:1677-1687.

Zhang W, Francis T, Gao P, Boyle K, Jiang F, Eudes F, Cuthbert R, Sharpe A, Fobert PR (2018) Genetic characterization of type II Fusarium head blight resistance derived from transgressive segregation in a cross between Eastern and Western Canadian spring wheat. Mol Breeding 38:13 http://doi.org/10.1007/s11032-017-0761-2.

Zhao M, Wang G, Leng Y, Wanjugi H, Xi P, Grosz M, Mergoum M, Zhong S (2018) Molecular mapping of Fusarium head blight resistance in the spring wheat line ND2710. Phytopathol https://doi.org/10.1094/PHYTO-12-17-0392-R.

Zhou WC, Kolb FL, Bai GH, Domier LL, Yao JB (2002) Effect of individual Sumai 3 chromosomes on resistance to scab spread within spikes and deoxynivalenol accumulation within kernels in wheat. Hereditas 137:81-89.

Zhu Z, Bonnett D, Ellis M, He X, Heslot N, Dreisigacker S, Gao C, Singh P (2016a) Characterization of Fusarium head blight resistance in a CIMMYT synthetic-derived bread wheat line. Euphytica 208:367-375.

Zhu X, Zhong S, Cai X (2016) Effects of D-genome chromosomes and their A/B-genome homoeologus on Fusarium head blight resistance in durum wheat. Crop Sci 56:1049-1058.

APPENDICES

Appendix A. Procedure for Neogen enzyme linked immune-sorbent assay (ELISA) for deoxynivalenol (DON) quantification in Fusarium head blight infected grains.

Extraction procedure

Grind the sample to the consistency of finely ground coffee, or so that at least 75% can pass through a 20-mesh sieve.

1. Weigh out 10 g of the homogenous ground sample into the supplied extraction cup or other suitable receptacle.
2. Add 100 mL of deionized or distilled water to the sample.
3. Shake vigorously for 3 minutes.
4. Filter at least 5 mL of extract through a Neogen filter syringe or a filter funnel and filter paper.
5. Collect the filtered extract using the supplied sample collection tubes. Sample is now ready for testing.

Test procedure

1. Warm all reagents to room temperature 18-30 °C (64-86 °F) prior to use.
2. Remove one red-marked mixing well for each sample to be tested, plus five red-marked wells to be used for controls. Place these wells in a microwell holder.
3. Remove an equal number of antibody-coated wells. Immediately return antibody wells that will not be used to the foil pack with desiccant. Reseal the foil pack to protect the antibody. Mark one end of the strip so that the wells can be identified after washing.
4. Mix each reagent by swirling the reagent bottle prior to use.
5. Place 100 µL of conjugate from the blue-labeled bottle in each mixing well.
6. Place 100 µL of each control and sample extraction to the mixing wells as shown below. Use a new pipette tip for each transfer. *(Up to 24 wells may be run at once).*

Strip 1: 0 0.5 1 2 6 S1 S2 S3 S4 S5 S6 S7

Strip 2: S8 S9 S10 S11 S12 S13 S14 S15 S16 S17 S18 S19

7. Using a 12-channel pipettor, mix the wells by pipetting the liquid up and down in the tips 3-4 times. Transfer 100 µL to the antibody wells and mix by sliding the microwell holder back and forth on a flat surface for 30 seconds. Incubate 2 minutes at room temp. Discard red-marked mixing wells.
8. Dump out the contents of the antibody wells. With a wash bottle or running stream of water, fill each antibody well with deionized or distilled water and then dump the water out. Repeat this step 5 times, then turn wells upside down and tap out on a paper towel until the remaining

water has been removed.

9. Pour only the needed volume of substrate from the green-labeled bottle into a clean reagent boat. Using new tips, pipette 100 µL of substrate into the wells and mix 30 seconds. Incubate for 3 minutes at room temp. Discard remaining substrate and rinse the reagent boat with water.

10. Pour the needed volume of red stop solution from the red-labeled bottle into a clean reagent boat. Pipette 100 µL red stop to each well and mix thoroughly by sliding back and forth to eliminate the layering effect. Discard tips.

11. Wipe bottom of microwells with a dry cloth or towel and read within 20 minutes, in a microwell reader using a 650 nm filter.

Appendix B.

Table B. 1. Proportions of the recurrent parent (RP) and donor parent (DP) genomes in the near-isogenic lines for CDC Go and CDC Alsask streams based on 81,587 SNP markers from the 90K iSelect assay (Wang et al. 2014). Here: A, B, H, U represent recurrent parent, donor parent, heterozygous, and unknown alleles, respectively.

	Total map (14.5 Gb)				3B (829.5 Mb; carrying *Fhb1*)				5A (709.8 Mb; carrying *Fhb5*)				6B (721.0 Mb; carrying *Fhb2*)			
Line	**A (%)**	**B (%)**	**H (%)**	**U (%)**	**A (%)**	**B (%)**	**H (%)**	**U (%)**	**A (%)**	**B (%)**	**H (%)**	**U (%)**	**A (%)**	**B (%)**	**H (%)**	**U (%)**
CDC Go (RP)	100.0	0	0	0	100.0	0	0	0	100.0	0	0	0	100.0	0	0	0
04GC0139 (DP)	89.4	10.65	0.00	0.00	78.1	21.95	0.00	0.00	83.7	16.32	0.00	0.00	78.8	21.20	0.00	0.00
Go1	99.2	0.66	0.00	0.10	98.7	1.26	0.00	0.08	97.6	2.34	0.00	0.06	99.8	0.11	0.00	0.08
Go2	99.3	0.68	0.00	0.03	99.1	0.86	0.00	0.05	94.0	5.93	0.00	0.06	99.8	0.08	0.00	0.11
Go3	99.6	0.42	0.00	0.02	97.8	2.17	0.00	0.00	99.7	0.28	0.00	0.03	99.9	0.03	0.00	0.03
Go4	99.1	0.87	0.00	0.02	99.1	0.86	0.00	0.05	93.3	6.68	0.00	0.03	99.7	0.19	0.00	0.08
Go5	99.4	0.59	0.00	0.06	99.1	0.88	0.00	0.00	99.3	0.37	0.06	0.22	99.9	0.05	0.00	0.05
Go6	99.7	0.26	0.03	0.06	99.7	0.19	0.05	0.05	98.8	0.75	0.12	0.31	98.5	1.50	0.03	0.00
Go7	99.3	0.66	0.00	0.03	99.1	0.86	0.00	0.08	93.2	6.68	0.00	0.09	98.3	1.61	0.03	0.05
Go8	99.4	0.61	0.01	0.02	99.7	0.19	0.05	0.05	93.2	6.77	0.00	0.06	98.3	1.58	0.03	0.05
Go9	99.4	0.59	0.01	0.03	99.7	0.19	0.05	0.03	93.3	6.68	0.00	0.06	98.3	1.58	0.03	0.05
Go10	99.7	0.29	0.01	0.04	98.6	1.28	0.05	0.03	99.6	0.34	0.00	0.03	98.4	1.53	0.03	0.08
Go11	99.3	0.65	0.00	0.02	98.0	1.95	0.00	0.03	93.3	6.71	0.00	0.03	99.8	0.08	0.00	0.14
Go12	99.4	0.57	0.00	0.08	98.8	1.12	0.00	0.08	94.5	5.21	0.00	0.25	99.6	0.11	0.00	0.25
Go14	99.5	0.46	0.00	0.02	100.0	0.00	0.00	0.03	97.3	2.62	0.00	0.03	99.9	0.03	0.00	0.08
Go15	99.8	0.18	0.00	0.04	100.0	0.03	0.00	0.00	99.6	0.34	0.00	0.03	99.8	0.11	0.00	0.11
Go16	99.5	0.44	0.00	0.09	98.7	1.28	0.00	0.05	99.4	0.53	0.00	0.06	99.9	0.05	0.00	0.05
Go17	99.6	0.32	0.02	0.08	99.8	0.13	0.00	0.03	99.3	0.53	0.00	0.12	98.4	1.50	0.03	0.08
Go19	99.0	0.93	0.01	0.04	97.8	2.14	0.05	0.03	93.2	6.74	0.00	0.06	99.7	0.14	0.00	0.16
Go20	99.6	0.41	0.00	0.03	100.0	0.00	0.00	0.03	98.7	1.25	0.00	0.06	98.4	1.50	0.03	0.08
Go21	99.2	0.73	0.00	0.03	100.0	0.03	0.00	0.00	93.1	6.86	0.00	0.03	99.8	0.11	0.00	0.08
Go22	99.6	0.34	0.01	0.10	98.6	1.31	0.05	0.05	99.7	0.31	0.00	0.03	99.9	0.03	0.00	0.08
Go23	99.3	0.68	0.01	0.04	97.8	2.09	0.05	0.08	99.4	0.56	0.00	0.00	98.4	1.53	0.03	0.05
Go24	99.5	0.39	0.00	0.15	98.9	0.86	0.00	0.29	99.3	0.41	0.00	0.25	98.1	1.53	0.03	0.35
Go25[a]	-	-	-	-	-	-	-	-	-	-	-	-	-	-	-	-
Go26	99.3	0.64	0.00	0.04	99.1	0.86	0.00	0.03	95.1	4.84	0.00	0.09	98.2	1.63	0.03	0.14
Go27	99.2	0.77	0.01	0.03	97.8	2.17	0.05	0.00	93.2	6.65	0.00	0.12	99.8	0.08	0.00	0.11
Go28	99.1	0.78	0.01	0.10	98.4	1.28	0.05	0.21	93.3	6.61	0.00	0.12	98.1	1.58	0.03	0.25
Go29	99.5	0.44	0.00	0.04	99.1	0.86	0.00	0.05	96.6	3.34	0.00	0.06	99.8	0.08	0.00	0.14
Go30	99.7	0.30	0.00	0.04	99.9	0.00	0.00	0.05	98.0	1.81	0.03	0.12	98.3	1.53	0.03	0.11
Go31	99.5	0.39	0.02	0.07	99.8	0.03	0.05	0.13	97.3	2.68	0.00	0.06	99.8	0.05	0.00	0.11
Go32	99.7	0.30	0.01	0.03	98.6	1.28	0.05	0.03	99.6	0.34	0.00	0.03	98.4	1.53	0.03	0.03
Go33	99.1	0.89	0.01	0.02	97.8	2.17	0.05	0.00	93.3	6.68	0.00	0.03	98.2	1.63	0.03	0.14
Go34	99.0	0.84	0.01	0.11	99.3	0.11	0.05	0.53	93.2	6.65	0.00	0.12	98.2	1.66	0.03	0.08
Go35	99.4	0.50	0.01	0.05	97.8	2.11	0.05	0.08	99.1	0.90	0.00	0.03	99.8	0.03	0.00	0.14
Go36	99.2	0.75	0.01	0.05	97.7	2.17	0.05	0.08	93.3	6.65	0.00	0.06	99.8	0.08	0.00	0.08
Go37	99.2	0.74	0.01	0.02	97.8	2.17	0.05	0.00	93.1	6.86	0.00	0.03	99.9	0.08	0.00	0.00
Go38	99.4	0.58	0.01	0.03	98.7	1.28	0.05	0.00	99.5	0.53	0.00	0.00	99.9	0.05	0.00	0.03
Go39	99.1	0.82	0.02	0.05	98.6	1.36	0.05	0.00	93.3	6.65	0.00	0.06	98.3	1.58	0.03	0.14
Go40	99.5	0.49	0.00	0.04	99.9	0.00	0.00	0.08	99.5	0.37	0.00	0.09	99.8	0.05	0.00	0.11

	Total map (14.5 Gb)				3B (829.5 Mb; carrying *Fhb1*)				5A (709.8 Mb; carrying *Fhb5*)				6B (721 Mb; carrying *Fhb2*)			
	A (%)	**B (%)**	**H (%)**	**U (%)**	**A (%)**	**B (%)**	**H (%)**	**U (%)**	**A (%)**	**B (%)**	**H (%)**	**U (%)**	**A (%)**	**B (%)**	**H (%)**	**U (%)**
CDC Alsask (RP)	100.0	0	0	0	100.0	0	0	0	100.0	0	0	0	100.0	0	0	0
04GC0139 (DP)	87.1	12.91	0.00	0.00	81.8	18.18	0.00	0.00	83.3	16.68	0.00	0.00	77.6	22.40	0.00	0.00
Alsask1	98.0	1.71	0.05	0.21	94.9	4.87	0.08	0.16	93.7	6.20	0.06	0.06	89.2	9.73	0.25	0.82
Alsask2	98.4	1.55	0.05	0.03	91.4	8.50	0.11	0.00	98.2	1.75	0.03	0.03	98.2	1.74	0.03	0.05
Alsask3	98.6	1.37	0.03	0.01	92.7	7.30	0.03	0.00	98.3	1.66	0.03	0.00	97.8	2.18	0.03	0.00
Alsask4	98.4	1.54	0.03	0.01	92.4	7.62	0.03	0.00	98.1	1.85	0.03	0.00	97.6	2.40	0.03	0.00
Alsask5	98.4	1.44	0.04	0.07	91.4	7.78	0.21	0.59	98.5	1.41	0.06	0.03	97.7	2.07	0.05	0.14
Alsask6	98.4	1.56	0.01	0.01	92.9	6.98	0.08	0.00	89.4	10.55	0.03	0.00	98.7	1.23	0.03	0.00
Alsask7	98.7	0.89	0.06	0.32	96.5	2.30	0.24	0.99	95.9	1.66	0.47	1.97	99.0	0.60	0.00	0.35
Alsask8	98.3	1.58	0.05	0.05	96.2	3.29	0.13	0.37	98.0	1.63	0.16	0.25	88.0	11.83	0.08	0.05
Alsask9	98.2	1.66	0.04	0.10	95.6	4.09	0.11	0.21	97.8	2.10	0.06	0.06	88.3	11.53	0.05	0.14
Alsask10	97.2	2.46	0.05	0.25	91.6	8.13	0.05	0.24	90.1	9.70	0.06	0.16	87.0	12.29	0.11	0.60
Alsask11	97.3	2.45	0.07	0.19	91.4	8.42	0.05	0.13	89.9	9.98	0.09	0.03	86.9	12.48	0.05	0.57
Alsask12	97.7	1.75	0.16	0.39	92.1	7.51	0.13	0.21	90.4	9.26	0.16	0.19	89.9	2.43	2.34	5.29
Alsask13	97.7	2.16	0.04	0.12	91.7	8.10	0.08	0.11	92.0	7.82	0.03	0.16	87.6	12.05	0.14	0.22
Alsask14	97.9	2.05	0.05	0.05	96.6	3.34	0.03	0.00	98.0	1.85	0.06	0.09	87.7	12.18	0.08	0.05
Alsask15	97.9	1.97	0.04	0.06	92.0	7.75	0.08	0.16	97.5	2.44	0.06	0.03	88.0	11.77	0.08	0.16
Alsask16	98.6	1.33	0.03	0.03	92.6	7.41	0.03	0.00	98.3	1.66	0.03	0.03	97.7	2.18	0.03	0.05
Alsask17	97.6	2.39	0.04	0.01	91.7	8.26	0.03	0.00	97.3	2.57	0.06	0.03	87.2	12.59	0.08	0.08
Alsask18	99.1	0.89	0.02	0.02	97.1	2.89	0.00	0.00	93.8	6.17	0.00	0.00	99.3	0.65	0.03	0.05
Alsask19	98.8	1.15	0.02	0.01	97.8	2.17	0.00	0.00	90.1	9.83	0.06	0.03	99.1	0.93	0.00	0.00
Alsask20	97.6	2.41	0.02	0.00	90.6	9.25	0.11	0.00	89.5	10.42	0.06	0.00	87.7	12.24	0.08	0.00
Alsask21	97.2	2.74	0.04	0.03	91.2	8.69	0.05	0.05	89.5	10.33	0.09	0.06	87.5	12.37	0.08	0.05
Alsask22	97.1	2.88	0.04	0.02	90.1	9.81	0.08	0.00	88.3	11.58	0.09	0.00	87.2	12.62	0.05	0.08
Alsask23	98.8	1.08	0.05	0.04	96.8	3.07	0.13	0.00	99.0	0.94	0.03	0.03	99.0	0.90	0.03	0.11
Alsask24	98.5	1.47	0.04	0.01	96.7	3.16	0.11	0.00	90.0	9.92	0.06	0.00	98.8	1.17	0.00	0.00
Alsask25	97.5	2.17	0.11	0.20	96.7	2.91	0.11	0.24	90.5	9.23	0.13	0.13	92.2	3.79	1.25	2.73
Alsask26	98.2	1.72	0.03	0.00	96.1	3.74	0.11	0.00	90.5	9.39	0.06	0.00	98.7	1.25	0.00	0.00
Alsask27	98.1	1.78	0.03	0.09	89.9	9.92	0.08	0.11	95.7	4.29	0.00	0.03	94.6	4.85	0.05	0.46
Alsask28	97.3	2.61	0.04	0.02	95.7	4.20	0.08	0.00	88.3	11.61	0.09	0.00	89.6	10.28	0.05	0.03
Alsask29	98.6	1.22	0.08	0.11	96.4	2.99	0.24	0.32	90.5	7.61	0.78	1.06	99.0	0.93	0.05	0.05
Alsask30	98.0	1.85	0.07	0.11	91.6	6.87	0.51	1.07	89.1	10.61	0.06	0.19	98.3	1.50	0.14	0.05
Alsask31	98.2	1.72	0.04	0.01	96.1	3.74	0.11	0.00	90.5	9.39	0.06	0.00	98.7	1.25	0.00	0.00
Alsask32	98.0	1.97	0.04	0.02	96.7	3.16	0.05	0.05	89.1	10.70	0.09	0.06	90.9	9.02	0.08	0.00

Appendix C. Graphical presentation of introgressed segments in all chromosomes, except 3B, 6B, and 5A, from 04GC0139 (resistance donor parent, yellow segments) into CDC Alsask (red segments) near-isogenic lines. Each bar represents a genotype. The grey and blue segments indicate unknown and heterozygous alleles, respectively.

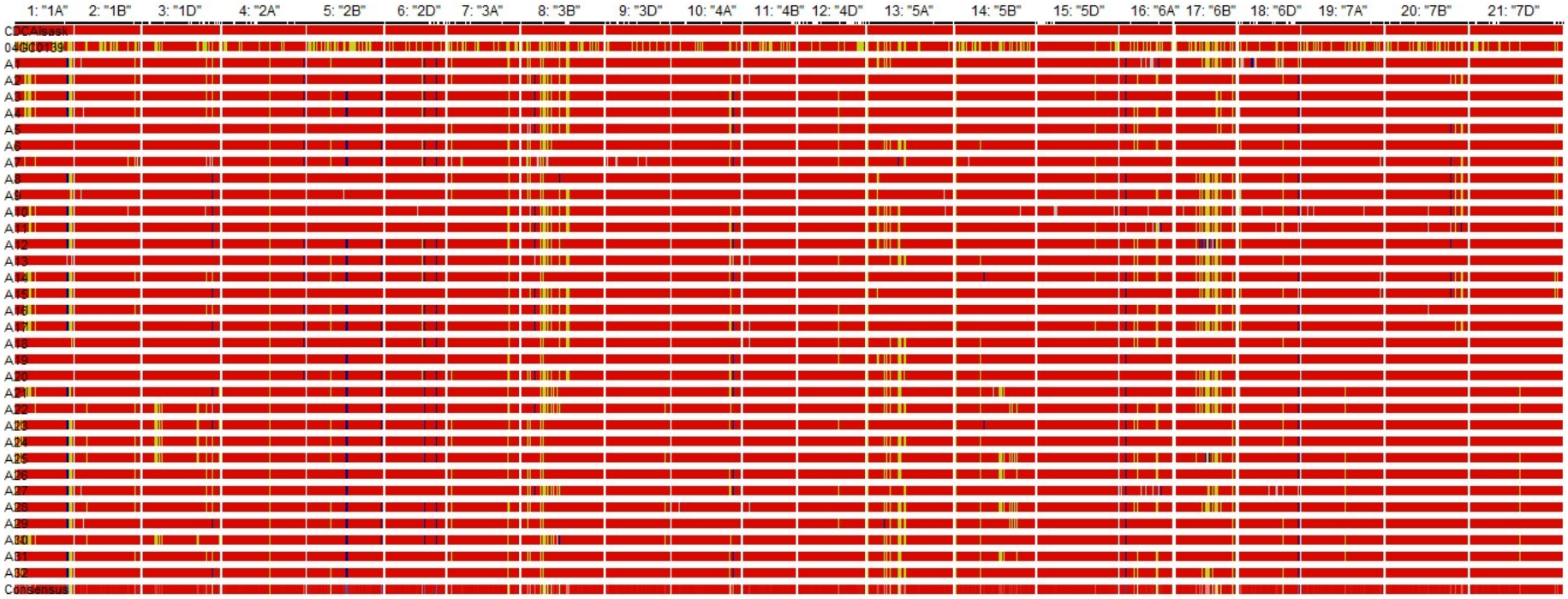

Appendix D. Graphical presentation of introgressed segments in all chromosomes, except 3B, 6B, and 5A, from 04GC0139 (resistance donor parent, yellow segments) into CDC Go (red segments) near-isogenic lines. Each bar represents a genotype. The grey and blue segments indicate unknown and heterozygous alleles, respectively.

Appendix E.

Table E. 1. Pearson's correlation coefficients among agronomic and end-use quality traits from CDC Alsask yield and quality performance trials in 2016 and 2017.

	Heading	Maturity	Plant height	Grain yield	Test weight	Thousand kernel weight	SDS-sedimentation	Hagberg falling number	Grain protein	Lodging
					2016					
Heading	-									
Maturity	0.61***	-								
Plant height	0.52***	ns	-							
Grain yield	ns	-0.32***	0.30***	-						
Test weight	ns	ns	ns	0.36***	-					
Thousand kernel weight	ns	-0.13*	-0.14**	0.49***	0.35***	-				
SDS-sedimentation	-0.27***	-0.32***	ns	0.26***	0.29***	0.37***	-			
Hagberg falling number	-0.25***	-0.28***	ns	ns	0.32***	ns	0.50***	-		
Grain protein	0.32***	0.19***	ns	-0.40***	ns	ns	0.12*	0.37***	-	
Lodging	ns	ns	0.45***	-0.34***	-0.45***	-0.39***	0.26***	0.25***	0.22***	-
					2017					
Heading	-									
Maturity	0.64***	-								
Plant height	0.30***	0.28***	-							
Grain yield	-0.39***	ns	0.29***	-						
Test weight	-0.48***	-0.13*	-0.12*	0.54***	-					
Thousand kernel weight	-0.20***	ns	ns	0.47***	0.27***	-				
SDS-sedimentation	-0.33***	-0.30***	0.39***	0.35***	0.12*	0.21***	-			
Hagberg falling number	ns	ns	ns	ns	0.28***	ns	ns	-		
Grain protein	0.31***	0.13*	0.38***	ns	-0.34***	ns	0.54***	ns	-	
Lodging	0.53***	0.34***	0.36***	-0.30***	-0.67***	-0.13**	0.15**	0.13**	0.61***	-

Note: *, **, *** indicates statistical significance at $P = 0.05, 0.001, 0.0001$, respectively; ns - not significant.

Appendix F.

Table F. 1. Pearson's correlation coefficients among agronomic and end-use quality traits from CDC Go yield and quality performance trials in 2016 and 2017.

	Heading	Maturity	Plant height	Grain yield	Test weight	Thousand kernel weight	SDS-sedimentation	Hagberg falling number	Grain protein	Lodging
					2016					
Heading	-									
Maturity	0.16**	-								
Plant height	0.10*	0.20***	-							
Grain yield	ns	-0.35***	0.38***	-						
Test weight	0.10*	-0.15**	0.30***	0.20***	-					
Thousand kernel weight	ns	-0.30***	0.16**	0.40***	0.72***	-				
SDS-sedimentation	-0.13**	-0.35***	-0.48***	ns	-0.27***	ns	-			
Hagberg falling number	-0.09*	-0.44***	-0.18***	0.21***	ns	ns	0.34***	-		
Grain protein	ns	0.32***	-0.40***	-0.50***	-0.39***	-0.26***	0.43***	ns	-	
Lodging	ns	0.19*	0.17*	ns	-0.53***	-0.30***	0.23*	ns	0.32***	-
					2017					
Heading	-									
Maturity	0.61***	-								
Plant height	0.52***	ns	-							
Grain yield	ns	-0.32***	0.30***	-						
Test weight	ns	ns	ns	0.36***	-					
Thousand kernel weight	ns	-0.13*	ns	0.49***	0.35***	-				
SDS-sedimentation	-0.27***	-0.32***	ns	0.26***	0.29***	0.37***	-			
Hagberg falling number	-0.25***	-0.28***	ns	ns	0.32***	ns	0.50***	-		
Grain protein	0.32***	0.19***	ns	-0.40***	ns	ns	0.12*	0.37***	-	
Lodging	ns	ns	ns	-0.25***	-0.74***	-0.40***	0.35***	-0.17*	0.56***	-

Note: *, **, *** indicates statistical significance at $P = 0.05, 0.001, 0.0001$, respectively; ns - not significant.

Appendix G.

Table G. 1. Pearson's correlation coefficients among Fusarium head blight (FHB) resistance traits from field and greenhouse evaluations for the BGRC3487/2*DT735 population.

Trait	FLD-IND08	FLD-IND09	FLD-IND10	FLD-IND16	FLD-SEV08	FLD-SEV09	FLD-SEV10	FLD-SEV16	FLD-INC08	FLD-INC09	FLD-INC10	FLD-INC16	FLD-VRI09	GH09	GH17
FLD-IND08	-														
FLD-IND09	0.29***	-													
FLD-IND10	0.38***	0.31***	-												
FLD-IND16	0.56***	0.39***	0.53***	-											
FLD-SEV08	0.98***	0.23**	0.39***	0.50***	-										
FLD-SEV09	0.29***	0.98***	0.31***	0.37***	0.23**	-									
FLD-SEV10	0.41***	0.34***	0.96***	0.55***	0.40***	0.33***	-								
FLD-SEV16	0.52***	0.31***	0.50***	0.91***	0.48***	0.30***	0.53***	-							
FLD-INC08	0.81***	0.31***	0.36***	0.58***	0.76***	0.29***	0.38***	0.54***	-						
FLD-INC09	ns	0.78***	0.18*	0.25**	ns	0.71***	0.24**	0.18*	0.20**	-					
FLD-INC10	0.16*	0.04 ns	0.62***	0.20*	0.20**	ns	0.41***	0.17*	ns	ns	-				
FLD-INC16	0.43***	0.38***	0.42***	0.77***	0.35***	0.35***	0.43***	0.57***	0.50***	0.33***	ns	-			
FLD-VRI09	0.47***	0.42***	0.48***	0.53***	0.45***	0.42***	0.48***	0.51***	0.49***	0.29***	0.24**	0.46***	-		
GH09	0.22**	ns	0.22**	0.23**	0.22**	ns	0.21**	0.26**	ns	ns	ns	ns	ns	-	
GH17	0.26**	ns	0.22**	0.29***	0.26**	ns	0.21*	0.32***	0.26**	0.16*	ns	0.26**	0.27**	0.40***	-

Here: FLD-IND – FHB index (%) from field evaluation; FLD-SEV – FHB severity (%) from field evaluation; FLD-INC – FHB incidence (%) from field evaluation; FLD-VRI – FHB field variable rating index (%); GH – FHB severity from greenhouse evaluation following point inoculation with *Fusarium graminearum* (50,000 spores/ml). ***, **, * represent statistical significance at $P = 0.001, 0.01, 0.05$ respectively; ns – not significant.

Appendix H.

Table H. 1. The number of parental (non-recombinant) chromosomes in 160 BCRILs for each of the 14 chromosomes and distribution for each of the two parental alleles (BGRC3487 and DT735). Total chromosome*BCRILs combinations = 2240. Average number of parental chromosomes = 14.5.

Chromosome	DT735	BGRC3487	Parental Chr. No.	% BCRILs
1A	47	0	47	29.4
1B	17	0	17	10.6
2A	62	5	67	41.9
2B	7	0	7	4.4
3A	13	1	17	10.6
3B	11	0	10	6.2
4A	16	0	21	13.1
4B	34	0	32	20.0
5A	17	0	17	10.6
5B	14	0	23	14.4
6A	46	3	49	30.6
6B	13	0	22	13.8
7A	27	2	25	15.5
7B	22	1	20	12.5

Appendix I.

Table I. 1. Correlation of parental chromosome numbers with chromosome length (cM) and number of skeletal markers.

Chromosome	No. of parental Chr.	Chromosome length	No. of skeletal markers
1A	47	52.3	69
1B	17	135.7	194
2A	67	45.8	55
2B	7	288.6	280
3A	17	149.1	93
3B	10	142.6	184
4A	21	79.7	66
4B	32	110.4	84
5A	17	157.9	106
5B	23	165.0	98
6A	49	85.5	116
6B	22	154.2	143
7A	25	118.4	132
7B	20	137.6	157
		-0.64 (*P* <0.05)	**-0.76 (*P* <0.05)**

Appendix J. Genetic linkage maps for BGRC3487/2*DT735 population. The position of centromere for linkage groups is highlighted in red (where known).

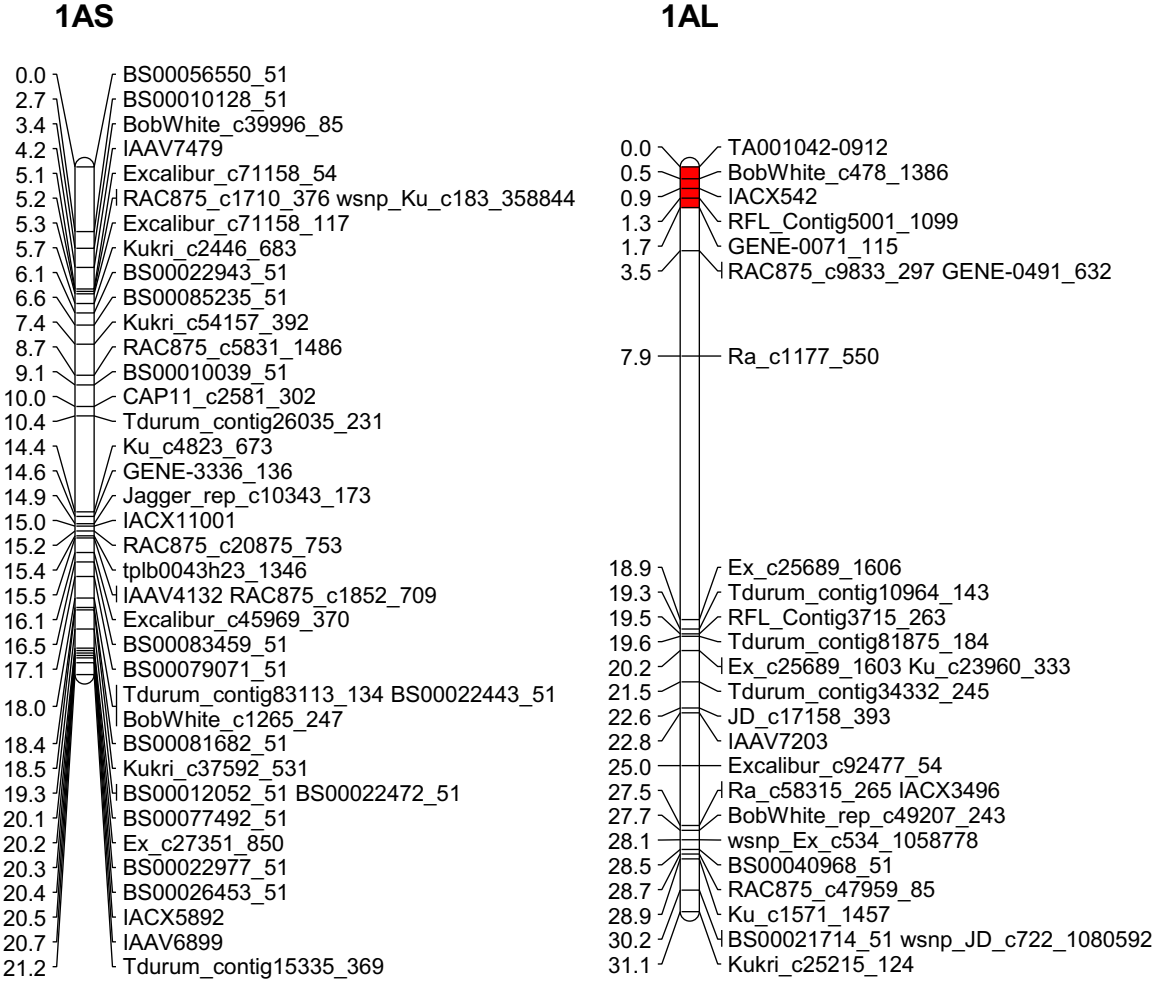


1BS
0.0 GENE-0412_1045
0.5 BS00022504_51
2.5 TA001594-0748
2.7 BS00082565_51
3.1 RAC875_c30399_406
3.4 Excalibur_rep_c110099_126
3.5 Kukri_c37738_417
4.0 Kukri_c38553_67
6.0 Excalibur_c43567_913
6.2 IAAV8117
6.6 RAC875_c40444_84 TA006040-0724
7.4 RAC875_c16981_691
9.0 wsnp_BE405749B_Ta_2_1
9.1 BS00022101_51
10.3 BS00065487_51
10.5 BS00022429_51
10.9 BS00080212_51
12.2 Kukri_c92979_195
12.6 Excalibur_c27135_1212
13.0 BS00081734_51
13.1 wsnp_Ku_rep_c103074_89905152
13.6 BobWhite_c17559_105
14.8 Excalibur_c28255_482
15.0 BS00023177_51
15.2 Ku_c36151_460
18.9 BS00067097_51
21.3 BS00025964_51 BS00025965_51
21.6 Kukri_c76307_182
23.3 BS00108057_51
23.7 TA003247-1072
33.4 BS00066682_51
34.0 Tdurum_contig78972_316
34.5 Tdurum_contig50667_671 Tdurum_contig50667_306
35.1 RAC875_c41114_486
39.4 Kukri_c67384_56
39.8 D_GA8KES402HUUGV_172
41.0 Kukri_c54054_511
42.4 D_contig70818_696
43.3 Excalibur_c415_844 Kukri_c8390_276
44.1 Excalibur_c3270_1566
44.5 Tdurum_contig41904_446
44.6 Tdurum_contig403_290
48.0 Tdurum_contig44861_237
48.1 Tdurum_contig44861_581
48.8 Kukri_c51861_262
50.4 BS00067012_51
51.7 tplb0030l11_244 BS00067169_51
51.8 BS00073199_51
51.9 Tdurum_contig29380_201
52.1 RFL_Contig4520_770
52.8 Ku_c2820_1430 wsnp_BE405834B_Ta_2_3
56.5 Tdurum_contig34049_172
56.9 Tdurum_contig83093_132
57.3 BS00065053_51
57.7 Excalibur_c95656_129 BS00081195_51
58.1 BS00070668_51
58.4 GENE-3653_580
58.6 Kukri_c6409_317
58.8 IAAV3590
62.0 Kukri_c4376_388 BS00087784_51
62.2 Tdurum_contig82187_189
62.4 Tdurum_contig5501_176
62.5 Tdurum_contig28940_690
62.6 Excalibur_c26936_636
63.0 BS00067507_51
63.5 BS00110546_51 BS00022255_51
64.1 wsnp_Ex_c28287_37424983
67.3 RAC875_c79370_378
70.0 Kukri_c20010_849 BS00022281_51
BS00022902_51
70.4 BS00083533_51
70.8 BS00022916_51
71.5 BS00067290_51
72.1 BS00068456_51
73.0 Kukri_c45137_137
73.4 wsnp_Ku_c2115_4089288 Tdurum_contig20702_326
74.3 IAAV8440
74.7 IACX8417 BS00022104_51
75.1 BS00061923_51 BS00018461_51
75.5 Tdurum_contig11692_131 Ex_c6028_1602
76.5 RAC875_c31921_322
76.8 IACX8373
77.0 BS00042054_51 IAAV3828
77.1 Ku_c2115_541
77.2 BS00047700_51 BS00108806_51
77.4 BS00106581_51
77.7 RAC875_c37031_312 BS00022317_51
77.9 Ra_c3837_797
78.1 wsnp_Ra_c21132_30487331
78.2 BobWhite_c22266_315
78.4 Kukri_rep_c91496_1320
78.5 Kukri_c12936_1505
84.0 Tdurum_contig83096_345
1BL1
0.0 BS00010148_51
0.7 Excalibur_c94658_59 TA004690-1102
0.8 wsnp_Ex_c6378_11087794
1.6 Excalibur_c3557_66
5.5 RAC875_c39401_502 RAC875_c39401_229
6.4 wsnp_Ex_c29186_38247956 Excalibur_rep_c107047_605
6.6 Excalibur_c44818_109
6.8 Tdurum_contig96049_200
7.5 BS00069341_51
7.6 BS00023071_51
7.7 RAC875_c39401_277
8.1 Tdurum_contig56281_261
8.5 wsnp_RFL_Contig2744_2471775
11.2 IACX8280 RAC875_c67771_805
11.8 Kukri_c19247_711
11.9 Kukri_c19247_53
12.6 RFL_Contig2736_827
12.9 IACX1891 BS00066278_51
wsnp_Ex_c3147_5816957
13.3 BS00085821_51
13.8 BS00063928_51
14.3 BS00108257_51
14.7 BS00067024_51
17.3 BS00069829_51
17.4 RAC875_c47427_235
17.5 BobWhite_c42716_71
17.6 Excalibur_rep_c96924_118
17.7 BS00067436_51
19.9 JD_c9300_552
21.0 Tdurum_contig25486_89
21.1 Tdurum_contig61863_130
21.2 Tdurum_contig67368_157
22.3 wsnp_BF200640B_Ta_2_1
27.1 BobWhite_c4375_347
30.0 BobWhite_rep_c54139_273
31.8 BobWhite_c20621_541
32.6 BS00021941_51
34.4 BS00065108_51 Excalibur_c56999_109
35.0 Excalibur_rep_c70674_83
35.1 Ra_c7324_527
35.2 BS00084216_51
35.7 BobWhite_c5655_300
36.1 BS00022176_51
36.5 RAC875_c13258_955
36.9 Tdurum_contig43232_811
37.1 Tdurum_contig15410_446
37.3 TA004523-0997 RAC875_c4190_337
37.5 BobWhite_c36862_84
37.6 RAC875_c30786_411
37.8 Kukri_c44191_452
42.0 wsnp_RFL_Contig2171_1489615
44.2 Tdurum_contig52075_807
1BL2
0.0 wsnp_Ex_c649_1279852
2.8 BS00010807_51
3.0 Excalibur_c55186_277 Excalibur_c55186_351
3.3 Tdurum_contig10099_538
3.5 Excalibur_c35345_476
3.9 BS00027006_51
4.2 BS00001128_51
4.5 wsnp_Ex_c750_1474300
5.0 Kukri_c16608_761
5.2 Tdurum_contig58710_516 Excalibur_c25640_110
5.4 RFL_Contig2550_679
5.6 Tdurum_contig1631_240 Tdurum_contig92835_177
6.0 Tdurum_contig83965_208
6.2 Tdurum_contig42960_865
6.4 BobWhite_c7691_195
6.8 Ku_c11537_539
7.1 Tdurum_contig49509_456
7.3 TA001659-0748 RAC875_c5882_307
7.4 IACX9428 Kukri_rep_c111174_132
7.5 wsnp_Ex_c955_1827567

2AS **2AL**

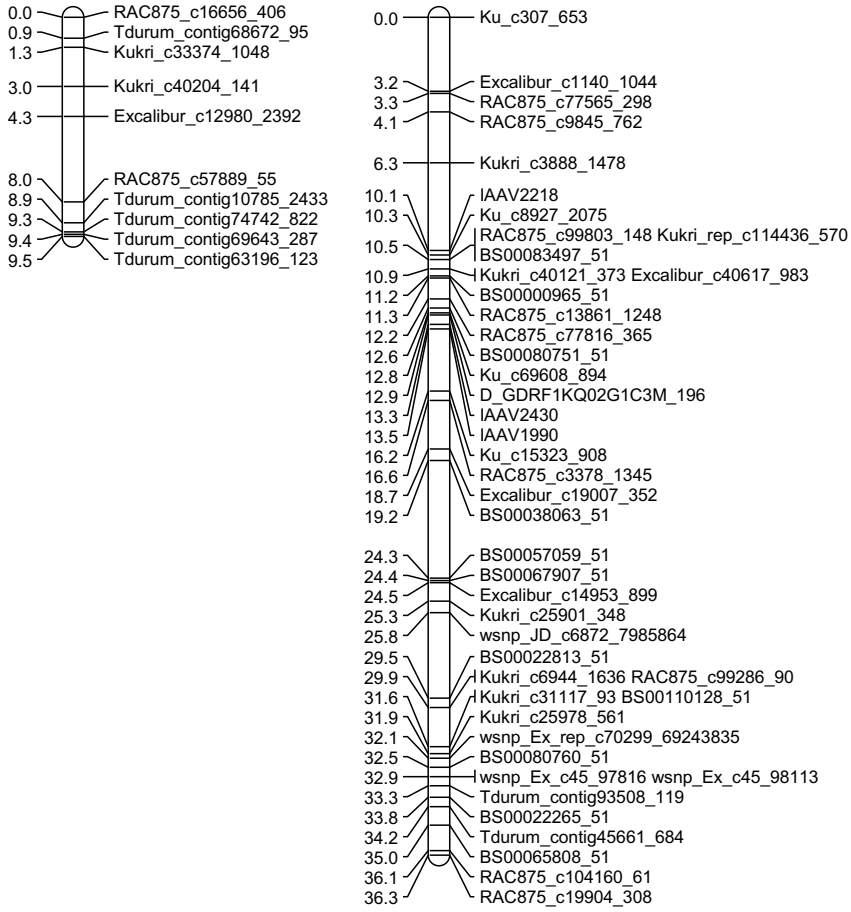
0.0 RAC875_c16656_406
0.9 Tdurum_contig68672_95
1.3 Kukri_c33374_1048
3.0 Kukri_c40204_141
4.3 Excalibur_c12980_2392
8.0 RAC875_c57889_55
8.9 Tdurum_contig10785_2433
9.3 Tdurum_contig74742_822
9.4 Tdurum_contig69643_287
9.5 Tdurum_contig63196_123
0.0 Ku_c307_653
3.2 Excalibur_c1140_1044
3.3 RAC875_c77565_298
4.1 RAC875_c9845_762
6.3 Kukri_c3888_1478
10.1 IAAV2218
10.3 Ku_c8927_2075
10.5 RAC875_c99803_148 Kukri_rep_c114436_570
BS00083497_51
10.9 Kukri_c40121_373 Excalibur_c40617_983
11.2 BS00000965_51
11.3 RAC875_c13861_1248
12.2 RAC875_c77816_365
12.6 BS00080751_51
12.8 Ku_c69608_894
12.9 D_GDRF1KQ02G1C3M_196
13.3 IAAV2430
13.5 IAAV1990
16.2 Ku_c15323_908
16.6 RAC875_c3378_1345
18.7 Excalibur_c19007_352
19.2 BS00038063_51
24.3 BS00057059_51
24.4 BS00067907_51
24.5 Excalibur_c14953_899
25.3 Kukri_c25901_348
25.8 wsnp_JD_c6872_7985864
29.5 BS00022813_51
29.9 Kukri_c6944_1636 RAC875_c99286_90
31.6 Kukri_c31117_93 BS00110128_51
31.9 Kukri_c25978_561
32.1 wsnp_Ex_rep_c70299_69243835
32.5 BS00080760_51
32.9 wsnp_Ex_c45_97816 wsnp_Ex_c45_98113
33.3 Tdurum_contig93508_119
33.8 BS00022265_51
34.2 Tdurum_contig45661_684
35.0 BS00065808_51
36.1 RAC875_c104160_61
36.3 RAC875_c19904_308

2B_Part1

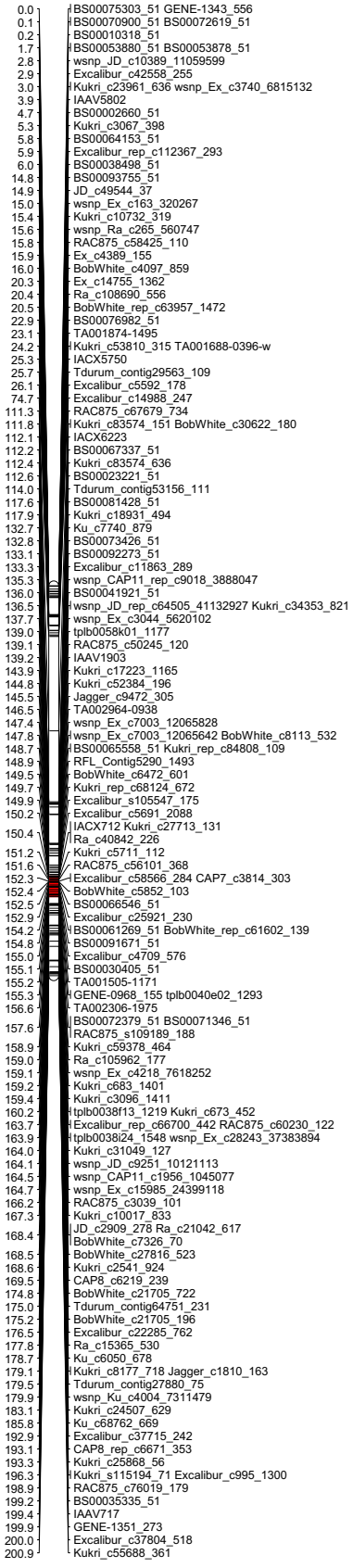

2B_Part2

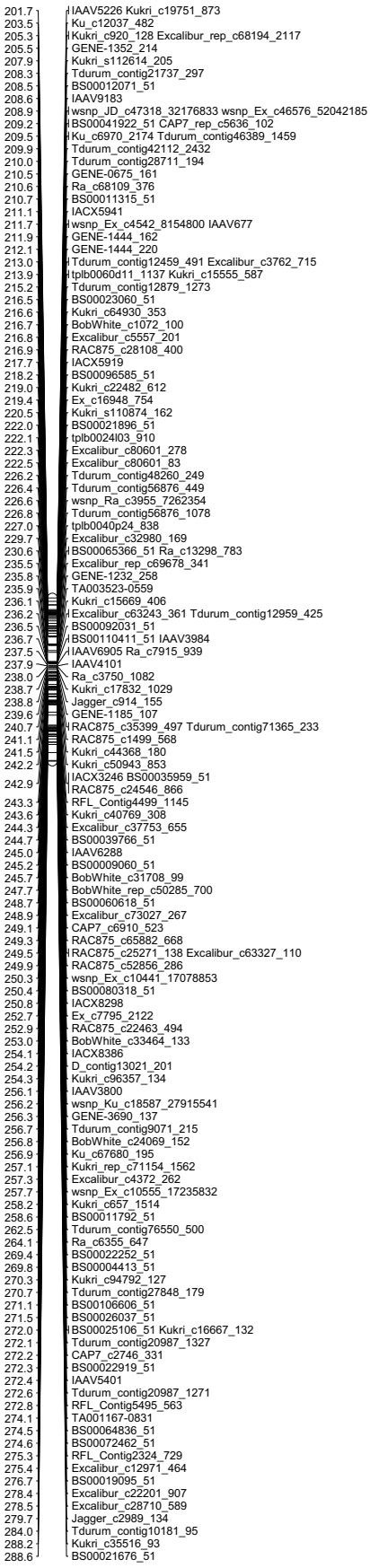

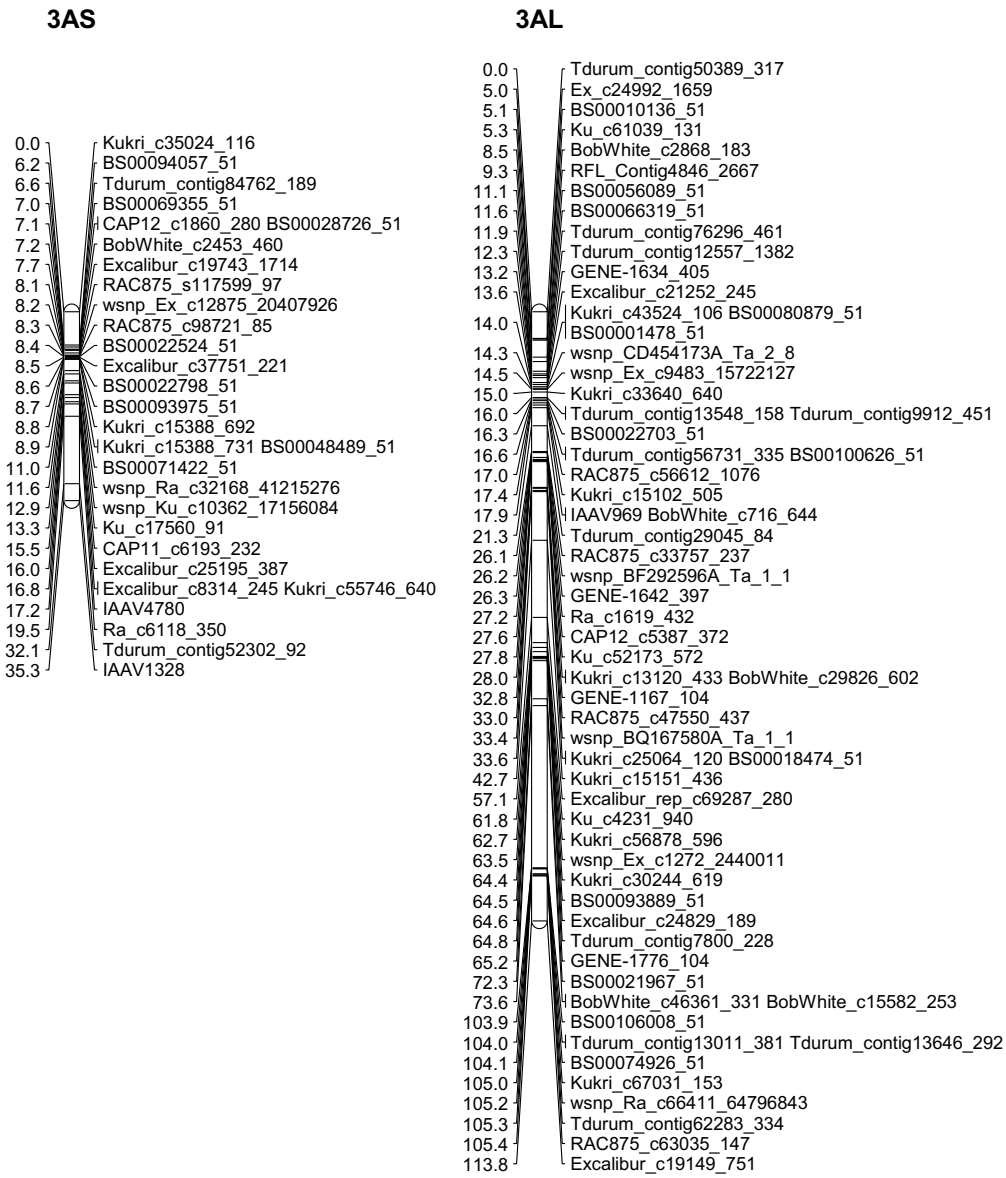
3AS
0.0 Kukri_c35024_116
6.2 BS00094057_51
6.6 Tdurum_contig84762_189
7.0 BS00069355_51
7.1 CAP12_c1860_280 BS00028726_51
7.2 BobWhite_c2453_460
7.7 Excalibur_c19743_1714
8.1 RAC875_s117599_97
8.2 wsnp_Ex_c12875_20407926
8.3 RAC875_c98721_85
8.4 BS00022524_51
8.5 Excalibur_c37751_221
8.6 BS00022798_51
8.7 BS00093975_51
8.8 Kukri_c15388_692
8.9 Kukri_c15388_731 BS00048489_51
11.0 BS00071422_51
11.6 wsnp_Ra_c32168_41215276
12.9 wsnp_Ku_c10362_17156084
13.3 Ku_c17560_91
15.5 CAP11_c6193_232
16.0 Excalibur_c25195_387
16.8 Excalibur_c8314_245 Kukri_c55746_640
17.2 IAAV4780
19.5 Ra_c6118_350
32.1 Tdurum_contig52302_92
35.3 IAAV1328
3AL
0.0 Tdurum_contig50389_317
5.0 Ex_c24992_1659
5.1 BS00010136_51
5.3 Ku_c61039_131
8.5 BobWhite_c2868_183
9.3 RFL_Contig4846_2667
11.1 BS00056089_51
11.6 BS00066319_51
11.9 Tdurum_contig76296_461
12.3 Tdurum_contig12557_1382
13.2 GENE-1634_405
13.6 Excalibur_c21252_245
14.0 Kukri_c43524_106 BS00080879_51
BS00001478_51
14.3 wsnp_CD454173A_Ta_2_8
14.5 wsnp_Ex_c9483_15722127
15.0 Kukri_c33640_640
16.0 Tdurum_contig13548_158 Tdurum_contig9912_451
16.3 BS00022703_51
16.6 Tdurum_contig56731_335 BS00100626_51
17.0 RAC875_c56612_1076
17.4 Kukri_c15102_505
17.9 IAAV969 BobWhite_c716_644
21.3 Tdurum_contig29045_84
26.1 RAC875_c33757_237
26.2 wsnp_BF292596A_Ta_1_1
26.3 GENE-1642_397
27.2 Ra_c1619_432
27.6 CAP12_c5387_372
27.8 Ku_c52173_572
28.0 Kukri_c13120_433 BobWhite_c29826_602
32.8 GENE-1167_104
33.0 RAC875_c47550_437
33.4 wsnp_BQ167580A_Ta_1_1
33.6 Kukri_c25064_120 BS00018474_51
42.7 Kukri_c15151_436
57.1 Excalibur_rep_c69287_280
61.8 Ku_c4231_940
62.7 Kukri_c56878_596
63.5 wsnp_Ex_c1272_2440011
64.4 Kukri_c30244_619
64.5 BS00093889_51
64.6 Excalibur_c24829_189
64.8 Tdurum_contig7800_228
65.2 GENE-1776_104
72.3 BS00021967_51
73.6 BobWhite_c46361_331 BobWhite_c15582_253
103.9 BS00106008_51
104.0 Tdurum_contig13011_381 Tdurum_contig13646_292
104.1 BS00074926_51
105.0 Kukri_c67031_153
105.2 wsnp_Ra_c66411_64796843
105.3 Tdurum_contig62283_334
105.4 RAC875_c63035_147
113.8 Excalibur_c19149_751

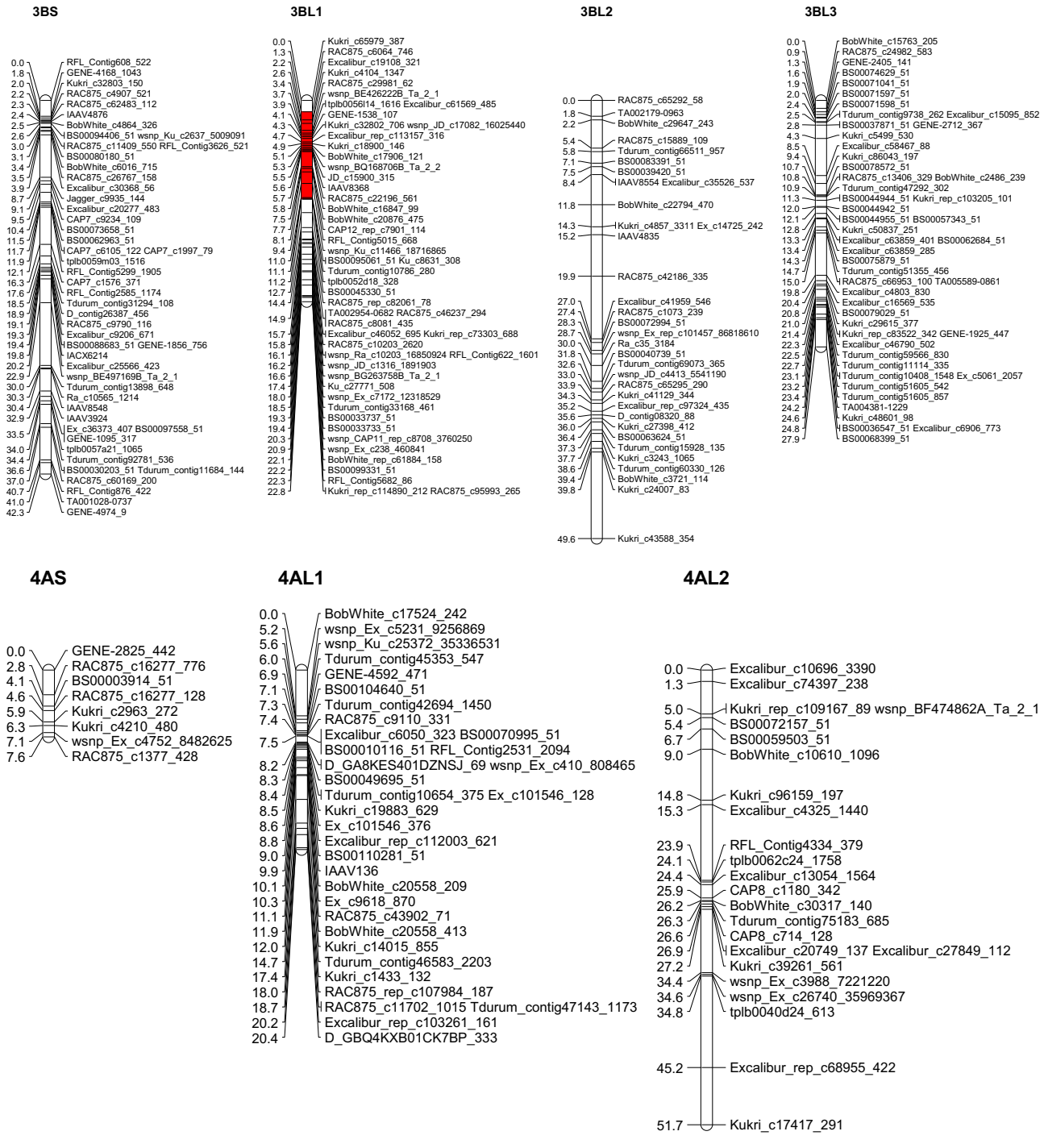
3BS
0.0 RFL_Contig608_522
1.8 GENE-4168_1043
2.0 Kukri_c32803_150
2.2 RAC875_c4907_521
2.3 RAC875_c62483_112
2.4 IAAV4876
2.5 BobWhite_c4864_326
2.6 BS00094406_51 wsnp_Ku_c2637_5009091
3.0 RAC875_c11409_550 RFL_Contig3626_521
3.1 BS00080180_51
3.4 BobWhite_c6016_715
3.5 RAC875_c26767_158
3.9 Excalibur_c30368_56
8.7 Jagger_c9935_144
9.1 Excalibur_c20277_483
9.5 CAP7_c9234_109
10.4 BS00073658_51
11.5 BS00062963_51
11.7 CAP7_c6105_122 CAP7_c1997_79
11.9 tplb0059m03_1516
12.1 RFL_Contig5299_1905
16.3 CAP7_c1576_371
17.6 RFL_Contig2585_1174
18.5 Tdurum_contig31294_108
18.9 D_contig26387_456
19.1 RAC875_c9790_116
19.3 Excalibur_c9206_671
19.4 BS00088683_51 GENE-1856_756
19.8 IACX6214
20.2 Excalibur_c25566_423
22.9 wsnp_BE497169B_Ta_2_1
30.0 Tdurum_contig13898_648
30.3 Ra_c10565_1214
30.4 IAAV8548
32.9 IAAV3924
33.5 Ex_c36373_407 BS00097558_51
GENE-1095_317
34.0 tplb0057a21_1065
34.4 Tdurum_contig92781_536
36.6 BS00030203_51 Tdurum_contig11684_144
37.0 RAC875_c60169_200
40.7 RFL_Contig876_422
41.0 TA001028-0737
42.3 GENE-4974_9
3BL1
0.0 Kukri_c65979_387
1.3 RAC875_c6064_746
2.2 Excalibur_c19108_321
2.6 Kukri_c4104_1347
3.4 RAC875_c29981_62
3.7 wsnp_BE426222B_Ta_2_1
3.9 tplb0056l14_1616 Excalibur_c61569_485
4.1 GENE-1538_107
4.3 Kukri_c32802_706 wsnp_JD_c17082_16025440
4.7 Excalibur_rep_c113157_316
4.9 Kukri_c18900_146
5.1 BobWhite_c17906_121
5.3 wsnp_BQ168706B_Ta_2_2
5.5 JD_c15900_315
5.6 IAAV8368
5.7 RAC875_c22196_561
5.8 BobWhite_c16847_99
7.5 BobWhite_c20876_475
7.7 CAP12_rep_c7901_114
8.1 RFL_Contig5015_668
9.4 wsnp_Ku_c11466_18716865
11.0 BS00095061_51 Ku_c8631_308
11.1 Tdurum_contig10786_280
11.2 tplb0052d18_328
12.7 BS00045330_51
14.4 RAC875_rep_c82061_78
14.9 TA002954-0682 RAC875_c46237_294
IRAC875_c8081_435
15.7 Excalibur_c46052_695 Kukri_rep_c73303_688
15.8 RAC875_c10203_2620
16.1 wsnp_Ra_c10203_16850924 RFL_Contig622_1601
16.2 wsnp_JD_c1316_1891903
16.6 wsnp_BG263758B_Ta_2_1
17.4 Ku_c27771_508
18.0 wsnp_Ex_c7172_12318529
18.5 Tdurum_contig33168_461
19.3 BS00033737_51
19.4 BS00033733_51
20.3 wsnp_CAP11_rep_c8708_3760250
20.9 wsnp_Ex_c238_460841
22.1 BobWhite_rep_c61884_158
22.2 BS00099331_51
22.3 RFL_Contig5682_86
22.8 Kukri_rep_c114890_212 RAC875_c95993_265
3BL2
0.0 RAC875_c65292_58
1.8 TA002179-0963
2.2 BobWhite_c29647_243
5.4 RAC875_c15889_109
5.8 Tdurum_contig66511_957
7.1 BS00083391_51
7.5 BS00039420_51
8.4 IAAV8554 Excalibur_c35526_537
11.8 BobWhite_c22794_470
14.3 Kukri_c4857_3311 Ex_c14725_242
15.2 IAAV4835
19.9 RAC875_c42186_335
27.0 Excalibur_c41959_546
27.4 RAC875_c1073_239
28.3 BS00072994_51
28.7 wsnp_Ex_rep_c101457_86818610
30.0 Ra_c35_3184
31.8 BS00040739_51
32.6 Tdurum_contig69073_365
33.0 wsnp_JD_c4413_5541190
33.9 RAC875_c65295_290
34.3 Kukri_c41129_344
35.2 Excalibur_rep_c97324_435
35.6 D_contig08320_88
36.0 Kukri_c27398_412
36.4 BS00063624_51
37.3 Tdurum_contig15928_135
37.7 Kukri_c3243_1065
38.6 Tdurum_contig60330_126
39.4 BobWhite_c3721_114
39.8 Kukri_c24007_83
49.6 Kukri_c43588_354
3BL3
0.0 BobWhite_c15763_205
0.9 RAC875_c24982_583
1.3 GENE-2405_141
1.6 BS00074629_51
1.9 BS00071041_51
2.0 BS00071597_51
2.4 BS00071598_51
2.5 Tdurum_contig9738_262 Excalibur_c15095_852
2.8 BS00037871_51 GENE-2712_367
4.3 Kukri_c5499_530
8.5 Excalibur_c58467_88
9.4 Kukri_c86043_197
10.7 BS00078572_51
10.8 RAC875_c13406_329 BobWhite_c2486_239
10.9 Tdurum_contig47292_302
11.3 BS00044944_51 Kukri_rep_c103205_101
12.0 BS00044942_51
12.1 BS00044955_51 BS00057343_51
12.8 Kukri_c50837_251
13.3 Excalibur_c63859_401 BS00062684_51
13.4 Excalibur_c63859_285
14.3 BS00075879_51
14.7 Tdurum_contig51355_456
15.0 RAC875_c66953_100 TA005589-0861
19.8 Excalibur_c4803_830
20.4 Excalibur_c16569_535
20.8 BS00079029_51
21.0 Kukri_c29615_377
21.4 Kukri_rep_c83522_342 GENE-1925_447
22.3 Excalibur_c46790_502
22.5 Tdurum_contig59566_830
22.7 Tdurum_contig11114_335
23.1 Tdurum_contig10408_1548 Ex_c5061_2057
23.2 Tdurum_contig51605_542
23.4 Tdurum_contig51605_857
24.2 TA004381-1229
24.6 Kukri_c48601_98
24.8 BS00036547_51 Excalibur_c6906_773
27.9 BS00068399_51
4AS
0.0 GENE-2825_442
2.8 RAC875_c16277_776
4.1 BS00003914_51
4.6 RAC875_c16277_128
5.9 Kukri_c2963_272
6.3 Kukri_c4210_480
7.1 wsnp_Ex_c4752_8482625
7.6 RAC875_c1377_428
4AL1
0.0 BobWhite_c17524_242
5.2 wsnp_Ex_c5231_9256869
5.6 wsnp_Ku_c25372_35336531
6.0 Tdurum_contig45353_547
6.9 GENE-4592_471
7.1 BS00104640_51
7.3 Tdurum_contig42694_1450
7.4 RAC875_c9110_331
7.5 Excalibur_c6050_323 BS00070995_51
BS00010116_51 RFL_Contig2531_2094
8.2 D_GA8KES401DZNSJ_69 wsnp_Ex_c410_808465
8.3 BS00049695_51
8.4 Tdurum_contig10654_375 Ex_c101546_128
8.5 Kukri_c19883_629
8.6 Ex_c101546_376
8.8 Excalibur_rep_c112003_621
9.0 BS00110281_51
9.9 IAAV136
10.1 BobWhite_c20558_209
10.3 Ex_c9618_870
11.1 RAC875_c43902_71
11.9 BobWhite_c20558_413
12.0 Kukri_c14015_855
14.7 Tdurum_contig46583_2203
17.4 Kukri_c1433_132
18.0 RAC875_rep_c107984_187
18.7 RAC875_c11702_1015 Tdurum_contig47143_1173
20.2 Excalibur_rep_c103261_161
20.4 D_GBQ4KXB01CK7BP_333
4AL2
0.0 Excalibur_c10696_3390
1.3 Excalibur_c74397_238
5.0 Kukri_rep_c109167_89 wsnp_BF474862A_Ta_2_1
5.4 BS00072157_51
6.7 BS00059503_51
9.0 BobWhite_c10610_1096
14.8 Kukri_c96159_197
15.3 Excalibur_c4325_1440
23.9 RFL_Contig4334_379
24.1 tplb0062c24_1758
24.4 Excalibur_c13054_1564
25.9 CAP8_c1180_342
26.2 BobWhite_c30317_140
26.3 Tdurum_contig75183_685
26.6 CAP8_c714_128
26.9 Excalibur_c20749_137 Excalibur_c27849_112
27.2 Kukri_c39261_561
34.4 wsnp_Ex_c3988_7221220
34.6 wsnp_Ex_c26740_35969367
34.8 tplb0040d24_613
45.2 Excalibur_rep_c68955_422
51.7 Kukri_c17417_291

4B

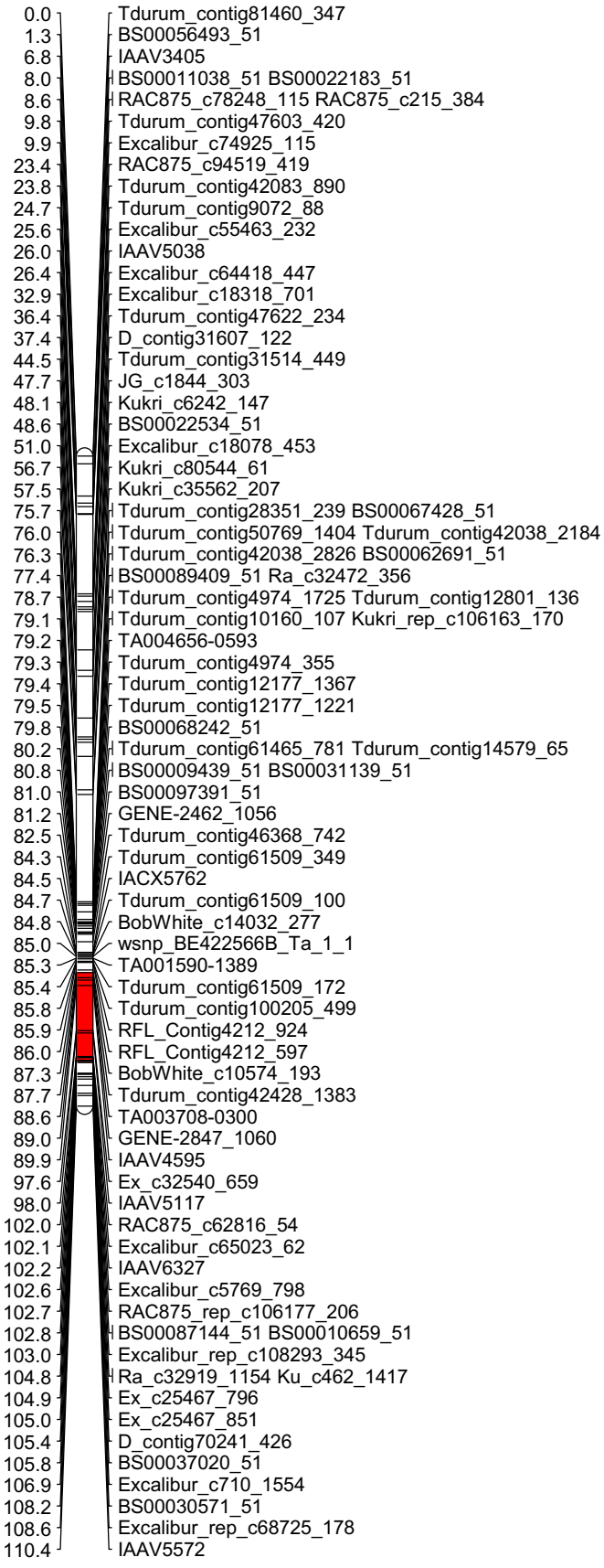
0.0 Tdurum_contig81460_347
1.3 BS00056493_51
6.8 IAAV3405
8.0 BS00011038_51 BS00022183_51
8.6 RAC875_c78248_115 RAC875_c215_384
9.8 Tdurum_contig47603_420
9.9 Excalibur_c74925_115
23.4 RAC875_c94519_419
23.8 Tdurum_contig42083_890
24.7 Tdurum_contig9072_88
25.6 Excalibur_c55463_232
26.0 IAAV5038
26.4 Excalibur_c64418_447
32.9 Excalibur_c18318_701
36.4 Tdurum_contig47622_234
37.4 D_contig31607_122
44.5 Tdurum_contig31514_449
47.7 JG_c1844_303
48.1 Kukri_c6242_147
48.6 BS00022534_51
51.0 Excalibur_c18078_453
56.7 Kukri_c80544_61
57.5 Kukri_c35562_207
75.7 Tdurum_contig28351_239 BS00067428_51
76.0 Tdurum_contig50769_1404 Tdurum_contig42038_2184
76.3 Tdurum_contig42038_2826 BS00062691_51
77.4 BS00089409_51 Ra_c32472_356
78.7 Tdurum_contig4974_1725 Tdurum_contig12801_136
79.1 Tdurum_contig10160_107 Kukri_rep_c106163_170
79.2 TA004656-0593
79.3 Tdurum_contig4974_355
79.4 Tdurum_contig12177_1367
79.5 Tdurum_contig12177_1221
79.8 BS00068242_51
80.2 Tdurum_contig61465_781 Tdurum_contig14579_65
80.8 BS00009439_51 BS00031139_51
81.0 BS00097391_51
81.2 GENE-2462_1056
82.5 Tdurum_contig46368_742
84.3 Tdurum_contig61509_349
84.5 IACX5762
84.7 Tdurum_contig61509_100
84.8 BobWhite_c14032_277
85.0 wsnp_BE422566B_Ta_1_1
85.3 TA001590-1389
85.4 Tdurum_contig61509_172
85.8 Tdurum_contig100205_499
85.9 RFL_Contig4212_924
86.0 RFL_Contig4212_597
87.3 BobWhite_c10574_193
87.7 Tdurum_contig42428_1383
88.6 TA003708-0300
89.0 GENE-2847_1060
89.9 IAAV4595
97.6 Ex_c32540_659
98.0 IAAV5117
102.0 RAC875_c62816_54
102.1 Excalibur_c65023_62
102.2 IAAV6327
102.6 Excalibur_c5769_798
102.7 RAC875_rep_c106177_206
102.8 BS00087144_51 BS00010659_51
103.0 Excalibur_rep_c108293_345
104.8 Ra_c32919_1154 Ku_c462_1417
104.9 Ex_c25467_796
105.0 Ex_c25467_851
105.4 D_contig70241_426
105.8 BS00037020_51
106.9 Excalibur_c710_1554
108.2 BS00030571_51
108.6 Excalibur_rep_c68725_178
110.4 IAAV5572

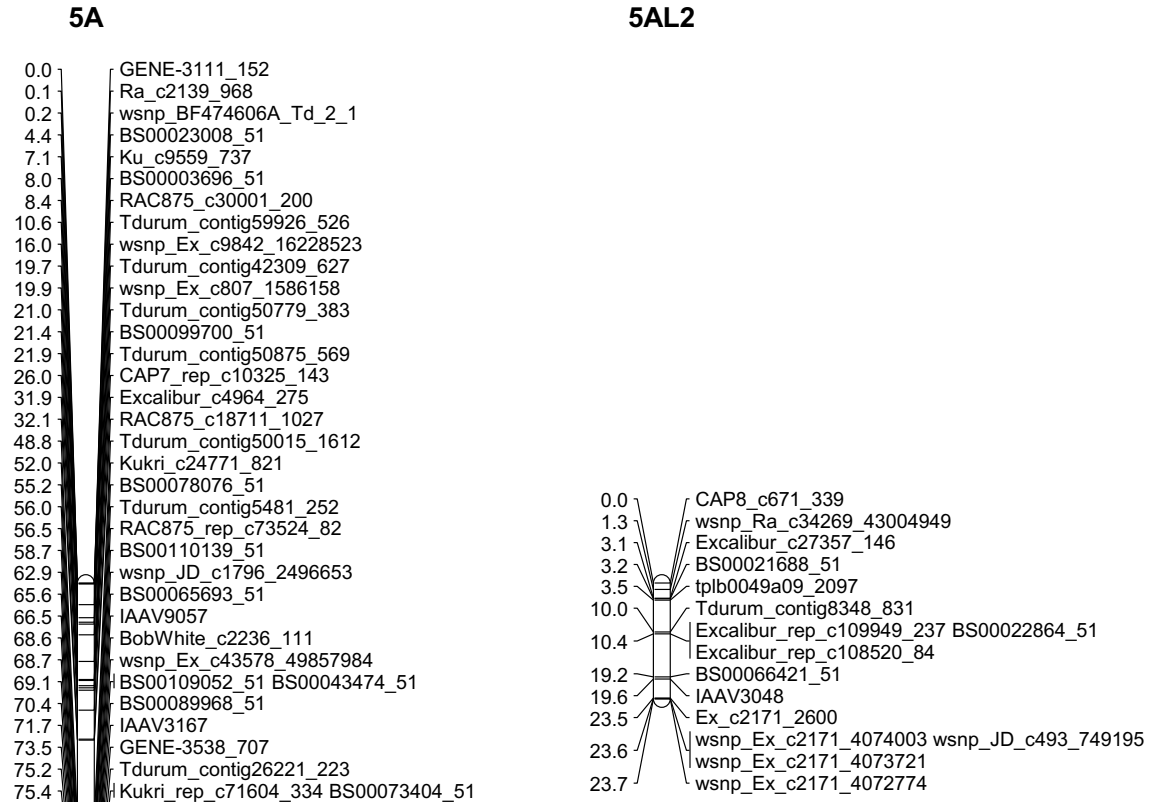
5A
0.0 GENE-3111_152
0.1 Ra_c2139_968
0.2 wsnp_BF474606A_Td_2_1
4.4 BS00023008_51
7.1 Ku_c9559_737
8.0 BS00003696_51
8.4 RAC875_c30001_200
10.6 Tdurum_contig59926_526
16.0 wsnp_Ex_c9842_16228523
19.7 Tdurum_contig42309_627
19.9 wsnp_Ex_c807_1586158
21.0 Tdurum_contig50779_383
21.4 BS00099700_51
21.9 Tdurum_contig50875_569
26.0 CAP7_rep_c10325_143
31.9 Excalibur_c4964_275
32.1 RAC875_c18711_1027
48.8 Tdurum_contig50015_1612
52.0 Kukri_c24771_821
55.2 BS00078076_51
56.0 Tdurum_contig5481_252
56.5 RAC875_rep_c73524_82
58.7 BS00110139_51
62.9 wsnp_JD_c1796_2496653
65.6 BS00065693_51
66.5 IAAV9057
68.6 BobWhite_c2236_111
68.7 wsnp_Ex_c43578_49857984
69.1 BS00109052_51 BS00043474_51
70.4 BS00089968_51
71.7 IAAV3167
73.5 GENE-3538_707
75.2 Tdurum_contig26221_223
75.4 Kukri_rep_c71604_334 BS00073404_51
77.4 BS00076190_51 Tdurum_contig48658_802
78.9 Ex_c6161_335
87.3 Tdurum_contig69079_300
87.6 RFL_Contig1929_805 Kukri_c5046_198
88.4 BobWhite_rep_c48815_538
89.3 Excalibur_c17268_243
89.5 BS00060939_51 BobWhite_c5748_756
89.7 RAC875_c29072_75
90.1 tplb0026e04_1730
90.5 Tdurum_contig43093_1179 RAC875_c9130_154
90.7 RFL_Contig1917_221
90.9 BS00022191_51 BS00004202_51
91.4 RAC875_c1219_1258
91.8 BS00082002_51
92.9 wsnp_Ku_c14275_22535576 BS00107192_51
BobWhite_rep_c61813_322
93.4 Kukri_c14275_674
93.5 IAAV3514 BobWhite_c13238_386
95.9 CAP11_c528_76
96.0 wsnp_Ex_c17268_25935536
96.4 wsnp_Ra_c21347_30731133
97.0 TA002501-1291
98.9 Excalibur_c47321_138
100.6 Kukri_rep_c77459_316
100.8 RAC875_c35993_308
101.0 IACX5879 wsnp_Ex_c31017_39858962
Tdurum_contig49187_601
101.9 Tdurum_contig11933_1503
106.1 wsnp_Ex_c1279_2451582 Ku_c47168_563
107.0 Ex_c9327_1907
107.2 Ex_c9327_1198
107.4 Ex_c9327_1750 IAAV6488
115.1 wsnp_Ku_c15816_24541162
115.5 BobWhite_c9057_118
116.8 Kukri_s112067_110
116.9 BS00065313_51
117.0 BobWhite_c5457_1440
119.3 BS00066143_51
119.4 BS00023076_51
119.5 Ex_c5317_662
125.6 Tdurum_contig68445_462
128.1 wsnp_Ex_c19519_28487099
129.4 Tdurum_contig48760_112
134.2 Tdurum_contig30246_179
5AL2
0.0 CAP8_c671_339
1.3 wsnp_Ra_c34269_43004949
3.1 Excalibur_c27357_146
3.2 BS00021688_51
3.5 tplb0049a09_2097
10.0 Tdurum_contig8348_831
10.4 Excalibur_rep_c109949_237 BS00022864_51
Excalibur_rep_c108520_84
19.2 BS00066421_51
19.6 IAAV3048
23.5 Ex_c2171_2600
23.6 wsnp_Ex_c2171_4074003 wsnp_JD_c493_749195
wsnp_Ex_c2171_4073721
23.7 wsnp_Ex_c2171_4072774

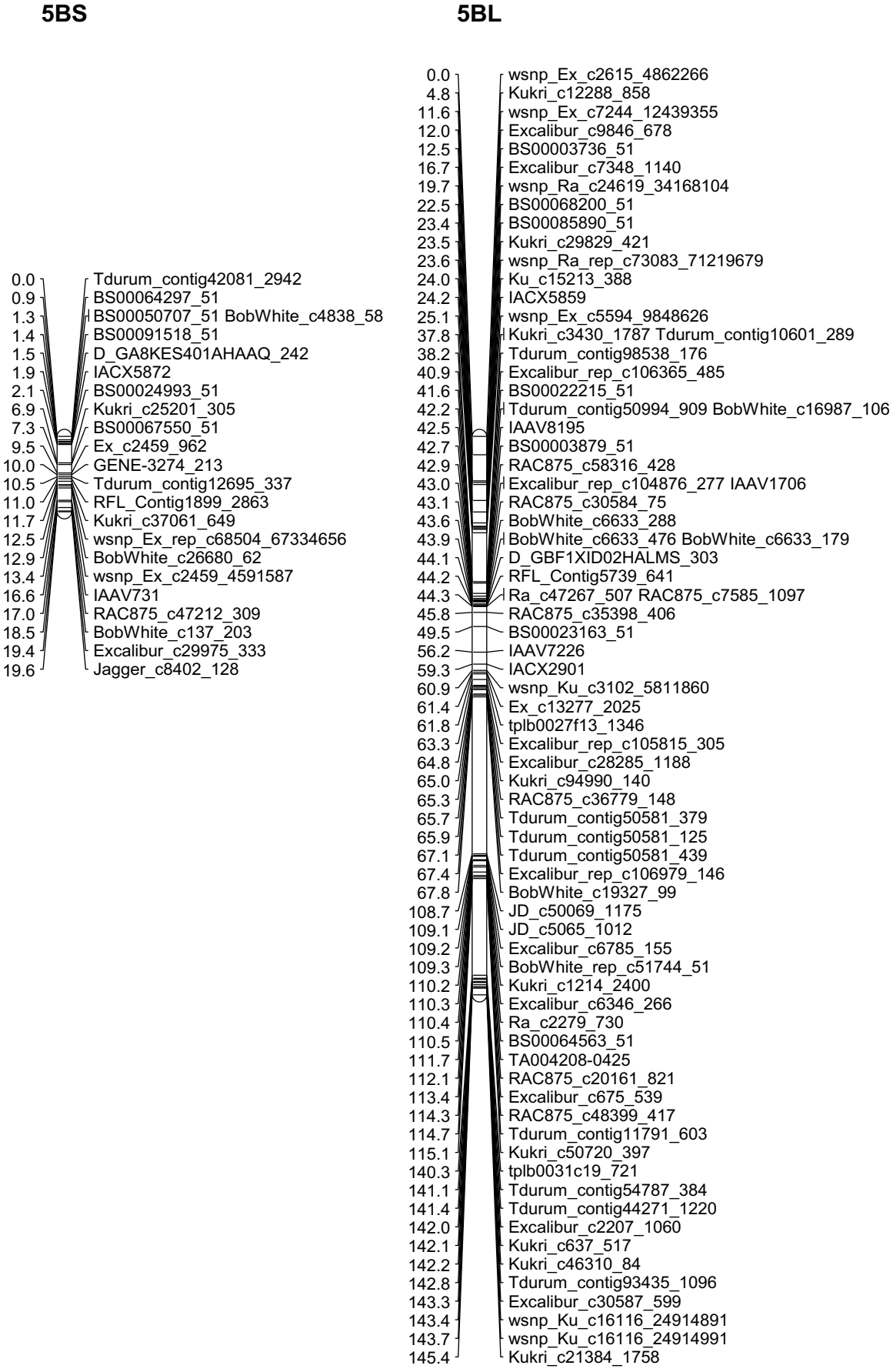
5BS
5BL
0.0 Tdurum_contig42081_2942
0.9 BS00064297_51
1.3 BS00050707_51 BobWhite_c4838_58
1.4 BS00091518_51
1.5 D_GA8KES401AHAAQ_242
1.9 IACX5872
2.1 BS00024993_51
6.9 Kukri_c25201_305
7.3 BS00067550_51
9.5 Ex_c2459_962
10.0 GENE-3274_213
10.5 Tdurum_contig12695_337
11.0 RFL_Contig1899_2863
11.7 Kukri_c37061_649
12.5 wsnp_Ex_rep_c68504_67334656
12.9 BobWhite_c26680_62
13.4 wsnp_Ex_c2459_4591587
16.6 IAAV731
17.0 RAC875_c47212_309
18.5 BobWhite_c137_203
19.4 Excalibur_c29975_333
19.6 Jagger_c8402_128
0.0 wsnp_Ex_c2615_4862266
4.8 Kukri_c12288_858
11.6 wsnp_Ex_c7244_12439355
12.0 Excalibur_c9846_678
12.5 BS00003736_51
16.7 Excalibur_c7348_1140
19.7 wsnp_Ra_c24619_34168104
22.5 BS00068200_51
23.4 BS00085890_51
23.5 Kukri_c29829_421
23.6 wsnp_Ra_rep_c73083_71219679
24.0 Ku_c15213_388
24.2 IACX5859
25.1 wsnp_Ex_c5594_9848626
37.8 Kukri_c3430_1787 Tdurum_contig10601_289
38.2 Tdurum_contig98538_176
40.9 Excalibur_rep_c106365_485
41.6 BS00022215_51
42.2 Tdurum_contig50994_909 BobWhite_c16987_106
42.5 IAAV8195
42.7 BS00003879_51
42.9 RAC875_c58316_428
43.0 Excalibur_rep_c104876_277 IAAV1706
43.1 RAC875_c30584_75
43.6 BobWhite_c6633_288
43.9 BobWhite_c6633_476 BobWhite_c6633_179
44.1 D_GBF1XID02HALMS_303
44.2 RFL_Contig5739_641
44.3 Ra_c47267_507 RAC875_c7585_1097
45.8 RAC875_c35398_406
49.5 BS00023163_51
56.2 IAAV7226
59.3 IACX2901
60.9 wsnp_Ku_c3102_5811860
61.4 Ex_c13277_2025
61.8 tplb0027f13_1346
63.3 Excalibur_rep_c105815_305
64.8 Excalibur_c28285_1188
65.0 Kukri_c94990_140
65.3 RAC875_c36779_148
65.7 Tdurum_contig50581_379
65.9 Tdurum_contig50581_125
67.1 Tdurum_contig50581_439
67.4 Excalibur_rep_c106979_146
67.8 BobWhite_c19327_99
108.7 JD_c50069_1175
109.1 JD_c5065_1012
109.2 Excalibur_c6785_155
109.3 BobWhite_rep_c51744_51
110.2 Kukri_c1214_2400
110.3 Excalibur_c6346_266
110.4 Ra_c2279_730
110.5 BS00064563_51
111.7 TA004208-0425
112.1 RAC875_c20161_821
113.4 Excalibur_c675_539
114.3 RAC875_c48399_417
114.7 Tdurum_contig11791_603
115.1 Kukri_c50720_397
140.3 tplb0031c19_721
141.1 Tdurum_contig54787_384
141.4 Tdurum_contig44271_1220
142.0 Excalibur_c2207_1060
142.1 Kukri_c637_517
142.2 Kukri_c46310_84
142.8 Tdurum_contig93435_1096
143.3 Excalibur_c30587_599
143.4 wsnp_Ku_c16116_24914891
143.7 wsnp_Ku_c16116_24914991
145.4 Kukri_c21384_1758

6A

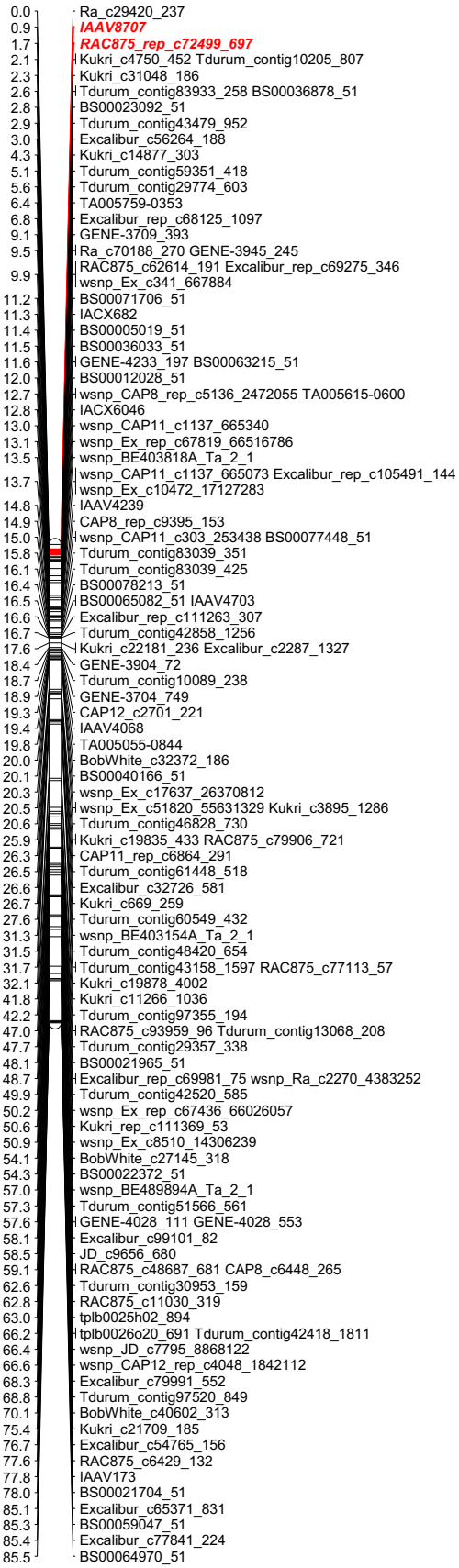
0.0 Ra_c29420_237
0.9 IAAV8707
1.7 RAC875_rep_c72499_697
2.1 Kukri_c4750_452 Tdurum_contig10205_807
2.3 Kukri_c31048_186
2.6 Tdurum_contig83933_258 BS00036878_51
2.8 BS00023092_51
2.9 Tdurum_contig43479_952
3.0 Excalibur_c56264_188
4.3 Kukri_c14877_303
5.1 Tdurum_contig59351_418
5.6 Tdurum_contig29774_603
6.4 TA005759-0353
6.8 Excalibur_rep_c68125_1097
9.1 GENE-3709_393
9.5 Ra_c70188_270 GENE-3945_245
9.9 RAC875_c62614_191 Excalibur_rep_c69275_346
wsnp_Ex_c341_667884
11.2 BS00071706_51
11.3 IACX682
11.4 BS00005019_51
11.5 BS00036033_51
11.6 GENE-4233_197 BS00063215_51
12.0 BS00012028_51
12.7 wsnp_CAP8_rep_c5136_2472055 TA005615-0600
12.8 IACX6046
13.0 wsnp_CAP11_c1137_665340
13.1 wsnp_Ex_rep_c67819_66516786
13.5 wsnp_BE403818A_Ta_2_1
13.7 wsnp_CAP11_c1137_665073 Excalibur_rep_c105491_144
wsnp_Ex_c10472_17127283
14.8 IAAV4239
14.9 CAP8_rep_c9395_153
15.0 wsnp_CAP11_c303_253438 BS00077448_51
15.8 Tdurum_contig83039_351
16.1 Tdurum_contig83039_425
16.4 BS00078213_51
16.5 BS00065082_51 IAAV4703
16.6 Excalibur_rep_c111263_307
16.7 Tdurum_contig42858_1256
17.6 Kukri_c22181_236 Excalibur_c2287_1327
18.4 GENE-3904_72
18.7 Tdurum_contig10089_238
18.9 GENE-3704_749
19.3 CAP12_c2701_221
19.4 IAAV4068
19.8 TA005055-0844
20.0 BobWhite_c32372_186
20.1 BS00040166_51
20.3 wsnp_Ex_c17637_26370812
20.5 wsnp_Ex_c51820_55631329 Kukri_c3895_1286
20.6 Tdurum_contig46828_730
25.9 Kukri_c19835_433 RAC875_c79906_721
26.3 CAP11_rep_c6864_291
26.5 Tdurum_contig61448_518
26.6 Excalibur_c32726_581
26.7 Kukri_c669_259
27.6 Tdurum_contig60549_432
31.3 wsnp_BE403154A_Ta_2_1
31.5 Tdurum_contig48420_654
31.7 Tdurum_contig43158_1597 RAC875_c77113_57
32.1 Kukri_c19878_4002
41.8 Kukri_c11266_1036
42.2 Tdurum_contig97355_194
47.0 RAC875_c93959_96 Tdurum_contig13068_208
47.7 Tdurum_contig29357_338
48.1 BS00021965_51
48.7 Excalibur_rep_c69981_75 wsnp_Ra_c2270_4383252
49.9 Tdurum_contig42520_585
50.2 wsnp_Ex_rep_c67436_66026057
50.6 Kukri_rep_c111369_53
50.9 wsnp_Ex_c8510_14306239
54.1 BobWhite_c27145_318
54.3 BS00022372_51
57.0 wsnp_BE489894A_Ta_2_1
57.3 Tdurum_contig51566_561
57.6 GENE-4028_111 GENE-4028_553
58.1 Excalibur_c99101_82
58.5 JD_c9656_680
59.1 RAC875_c48687_681 CAP8_c6448_265
62.6 Tdurum_contig30953_159
62.8 RAC875_c11030_319
63.0 tplb0025h02_894
66.2 tplb0026o20_691 Tdurum_contig42418_1811
66.4 wsnp_JD_c7795_8868122
66.6 wsnp_CAP12_rep_c4048_1842112
68.3 Excalibur_c79991_552
68.8 Tdurum_contig97520_849
70.1 BobWhite_c40602_313
75.4 Kukri_c21709_185
76.7 Excalibur_c54765_156
77.6 RAC875_c6429_132
77.8 IAAV173
78.0 BS00021704_51
85.1 Excalibur_c65371_831
85.3 BS00059047_51
85.4 Excalibur_c77841_224
85.5 BS00064970_51

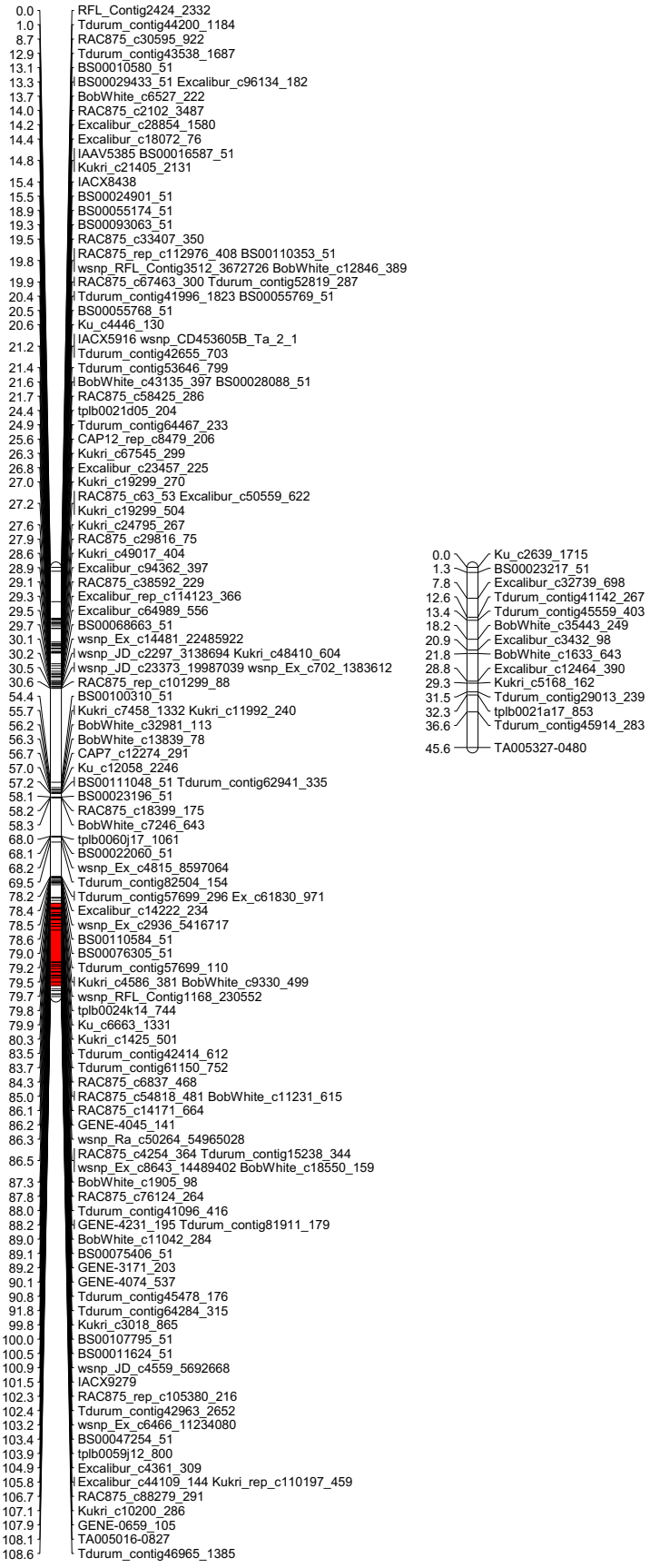
6BS
6BL
0.0 RFL_Contig2424_2332
1.0 Tdurum_contig44200_1184
8.7 RAC875_c30595_922
12.9 Tdurum_contig43538_1687
13.1 BS00010580_51
13.3 BS00029433_51 Excalibur_c96134_182
13.7 BobWhite_c6527_222
14.0 RAC875_c2102_3487
14.2 Excalibur_c28854_1580
14.4 Excalibur_c18072_76
14.8 IAAV5385 BS00016587_51
Kukri_c21405_2131
15.4 IACX8438
15.5 BS00024901_51
18.9 BS00055174_51
19.3 BS00093063_51
19.5 RAC875_c33407_350
19.8 RAC875_rep_c112976_408 BS00110353_51
wsnp_RFL_Contig3512_3672726 BobWhite_c12846_389
19.9 RAC875_c67463_300 Tdurum_contig52819_287
20.4 Tdurum_contig41996_1823 BS00055769_51
20.5 BS00055768_51
20.6 Ku_c4446_130
21.2 IACX5916 wsnp_CD453605B_Ta_2_1
Tdurum_contig42655_703
21.4 Tdurum_contig53646_799
21.6 BobWhite_c43135_397 BS00028088_51
21.7 RAC875_c58425_286
24.4 tplb0021d05_204
24.9 Tdurum_contig64467_233
25.6 CAP12_rep_c8479_206
26.3 Kukri_c67545_299
26.8 Excalibur_c23457_225
27.0 Kukri_c19299_270
27.2 RAC875_c63_53 Excalibur_c50559_622
Kukri_c19299_504
27.6 Kukri_c24795_267
27.9 RAC875_c29816_75
28.6 Kukri_c49017_404
28.9 Excalibur_c94362_397
29.1 RAC875_c38592_229
29.3 Excalibur_rep_c114123_366
29.5 Excalibur_c64989_556
29.7 BS00068663_51
30.1 wsnp_Ex_c14481_22485922
30.2 wsnp_JD_c2297_3138694 Kukri_c48410_604
30.5 wsnp_JD_c23373_19987039 wsnp_Ex_c702_1383612
30.6 RAC875_rep_c101299_88
54.4 BS00100310_51
55.7 Kukri_c7458_1332 Kukri_c11992_240
56.2 BobWhite_c32981_113
56.3 BobWhite_c13839_78
56.7 CAP7_c12274_291
57.0 Ku_c12058_2246
57.2 BS00111048_51 Tdurum_contig62941_335
58.1 BS00023196_51
58.2 RAC875_c18399_175
58.3 BobWhite_c7246_643
68.0 tplb0060j17_1061
68.1 BS00022060_51
68.2 wsnp_Ex_c4815_8597064
69.5 Tdurum_contig82504_154
78.2 Tdurum_contig57699_296 Ex_c61830_971
78.4 Excalibur_c14222_234
78.5 wsnp_Ex_c2936_5416717
78.6 BS00110584_51
79.0 BS00076305_51
79.2 Tdurum_contig57699_110
79.5 Kukri_c4586_381 BobWhite_c9330_499
79.7 wsnp_RFL_Contig1168_230552
79.8 tplb0024k14_744
79.9 Ku_c6663_1331
80.3 Kukri_c1425_501
83.5 Tdurum_contig42414_612
83.7 Tdurum_contig61150_752
84.3 RAC875_c6837_468
85.0 RAC875_c54818_481 BobWhite_c11231_615
86.1 RAC875_c14171_664
86.2 GENE-4045_141
86.3 wsnp_Ra_c50264_54965028
86.5 RAC875_c4254_364 Tdurum_contig15238_344
wsnp_Ex_c8643_14489402 BobWhite_c18550_159
87.3 BobWhite_c1905_98
87.8 RAC875_c76124_264
88.0 Tdurum_contig41096_416
88.2 GENE-4231_195 Tdurum_contig81911_179
89.0 BobWhite_c11042_284
89.1 BS00075406_51
89.2 GENE-3171_203
90.1 GENE-4074_537
90.8 Tdurum_contig45478_176
91.8 Tdurum_contig64284_315
99.8 Kukri_c3018_865
100.0 BS00107795_51
100.5 BS00011624_51
100.9 wsnp_JD_c4559_5692668
101.5 IACX9279
102.3 RAC875_rep_c105380_216
102.4 Tdurum_contig42963_2652
103.2 wsnp_Ex_c6466_11234080
103.4 BS00047254_51
103.9 tplb0059j12_800
104.9 Excalibur_c4361_309
105.8 Excalibur_c44109_144 Kukri_rep_c110197_459
106.7 RAC875_c88279_291
107.1 Kukri_c10200_286
107.9 GENE-0659_105
108.1 TA005016-0827
108.6 Tdurum_contig46965_1385
0.0 Ku_c2639_1715
1.3 BS00023217_51
7.8 Excalibur_c32739_698
12.6 Tdurum_contig41142_267
13.4 Tdurum_contig45559_403
18.2 BobWhite_c35443_249
20.9 Excalibur_c3432_98
21.8 BobWhite_c1633_643
28.8 Excalibur_c12464_390
29.3 Kukri_c5168_162
31.5 Tdurum_contig29013_239
32.3 tplb0021a17_853
36.6 Tdurum_contig45914_283
45.6 TA005327-0480

7AS

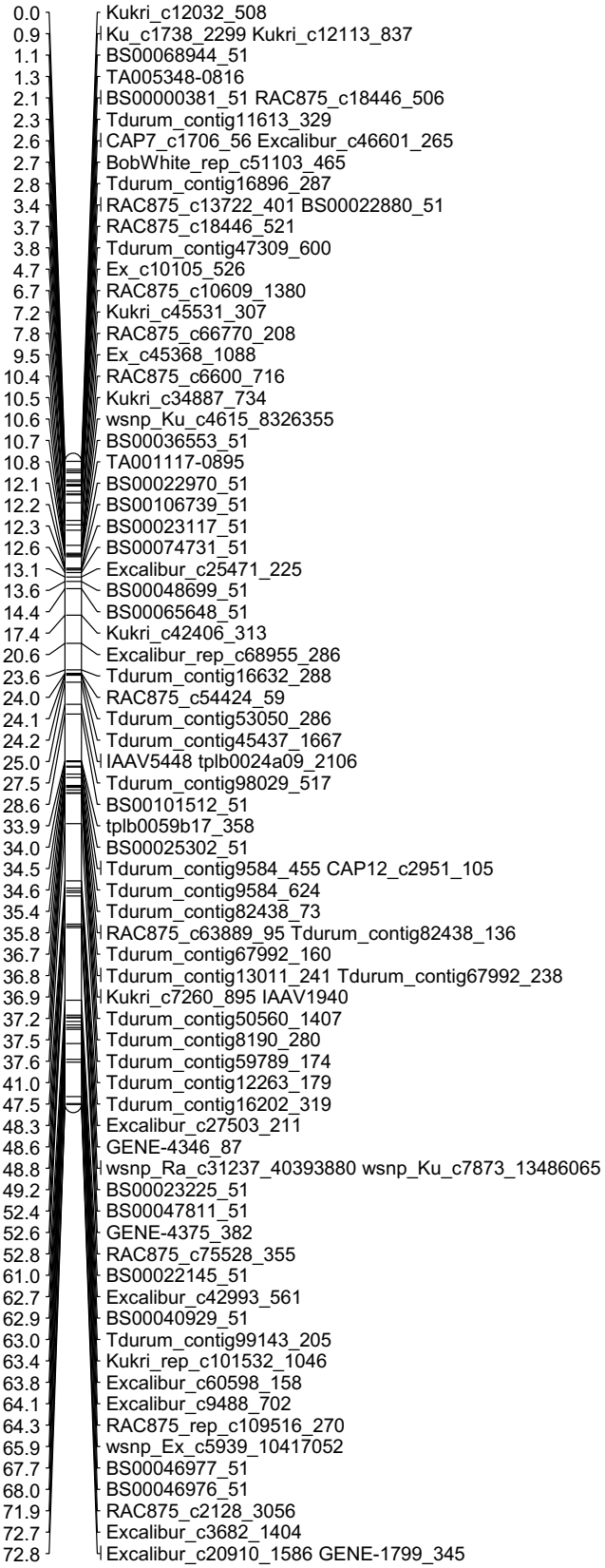
0.0 Kukri_c12032_508
0.9 Ku_c1738_2299 Kukri_c12113_837
1.1 BS00068944_51
1.3 TA005348-0816
2.1 BS00000381_51 RAC875_c18446_506
2.3 Tdurum_contig11613_329
2.6 CAP7_c1706_56 Excalibur_c46601_265
2.7 BobWhite_rep_c51103_465
2.8 Tdurum_contig16896_287
3.4 RAC875_c13722_401 BS00022880_51
3.7 RAC875_c18446_521
3.8 Tdurum_contig47309_600
4.7 Ex_c10105_526
6.7 RAC875_c10609_1380
7.2 Kukri_c45531_307
7.8 RAC875_c66770_208
9.5 Ex_c45368_1088
10.4 RAC875_c6600_716
10.5 Kukri_c34887_734
10.6 wsnp_Ku_c4615_8326355
10.7 BS00036553_51
10.8 TA001117-0895
12.1 BS00022970_51
12.2 BS00106739_51
12.3 BS00023117_51
12.6 BS00074731_51
13.1 Excalibur_c25471_225
13.6 BS00048699_51
14.4 BS00065648_51
17.4 Kukri_c42406_313
20.6 Excalibur_rep_c68955_286
23.6 Tdurum_contig16632_288
24.0 RAC875_c54424_59
24.1 Tdurum_contig53050_286
24.2 Tdurum_contig45437_1667
25.0 IAAV5448 tplb0024a09_2106
27.5 Tdurum_contig98029_517
28.6 BS00101512_51
33.9 tplb0059b17_358
34.0 BS00025302_51
34.5 Tdurum_contig9584_455 CAP12_c2951_105
34.6 Tdurum_contig9584_624
35.4 Tdurum_contig82438_73
35.8 RAC875_c63889_95 Tdurum_contig82438_136
36.7 Tdurum_contig67992_160
36.8 Tdurum_contig13011_241 Tdurum_contig67992_238
36.9 Kukri_c7260_895 IAAV1940
37.2 Tdurum_contig50560_1407
37.5 Tdurum_contig8190_280
37.6 Tdurum_contig59789_174
41.0 Tdurum_contig12263_179
47.5 Tdurum_contig16202_319
48.3 Excalibur_c27503_211
48.6 GENE-4346_87
48.8 wsnp_Ra_c31237_40393880 wsnp_Ku_c7873_13486065
49.2 BS00023225_51
52.4 BS00047811_51
52.6 GENE-4375_382
52.8 RAC875_c75528_355
61.0 BS00022145_51
62.7 Excalibur_c42993_561
62.9 BS00040929_51
63.0 Tdurum_contig99143_205
63.4 Kukri_rep_c101532_1046
63.8 Excalibur_c60598_158
64.1 Excalibur_c9488_702
64.3 RAC875_rep_c109516_270
65.9 wsnp_Ex_c5939_10417052
67.7 BS00046977_51
68.0 BS00046976_51
71.9 RAC875_c2128_3056
72.7 Excalibur_c3682_1404
72.8 Excalibur_c20910_1586 GENE-1799_345

7AL

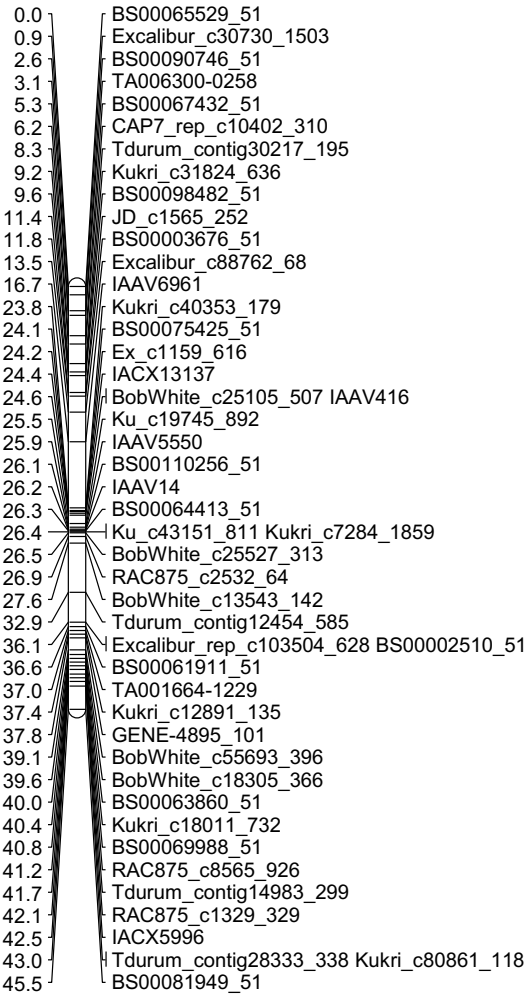
0.0 BS00065529_51
0.9 Excalibur_c30730_1503
2.6 BS00090746_51
3.1 TA006300-0258
5.3 BS00067432_51
6.2 CAP7_rep_c10402_310
8.3 Tdurum_contig30217_195
9.2 Kukri_c31824_636
9.6 BS00098482_51
11.4 JD_c1565_252
11.8 BS00003676_51
13.5 Excalibur_c88762_68
16.7 IAAV6961
23.8 Kukri_c40353_179
24.1 BS00075425_51
24.2 Ex_c1159_616
24.4 IACX13137
24.6 BobWhite_c25105_507 IAAV416
25.5 Ku_c19745_892
25.9 IAAV5550
26.1 BS00110256_51
26.2 IAAV14
26.3 BS00064413_51
26.4 Ku_c43151_811 Kukri_c7284_1859
26.5 BobWhite_c25527_313
26.9 RAC875_c2532_64
27.6 BobWhite_c13543_142
32.9 Tdurum_contig12454_585
36.1 Excalibur_rep_c103504_628 BS00002510_51
36.6 BS00061911_51
37.0 TA001664-1229
37.4 Kukri_c12891_135
37.8 GENE-4895_101
39.1 BobWhite_c55693_396
39.6 BobWhite_c18305_366
40.0 BS00063860_51
40.4 Kukri_c18011_732
40.8 BS00069988_51
41.2 RAC875_c8565_926
41.7 Tdurum_contig14983_299
42.1 RAC875_c1329_329
42.5 IACX5996
43.0 Tdurum_contig28333_338 Kukri_c80861_118
45.5 BS00081949_51

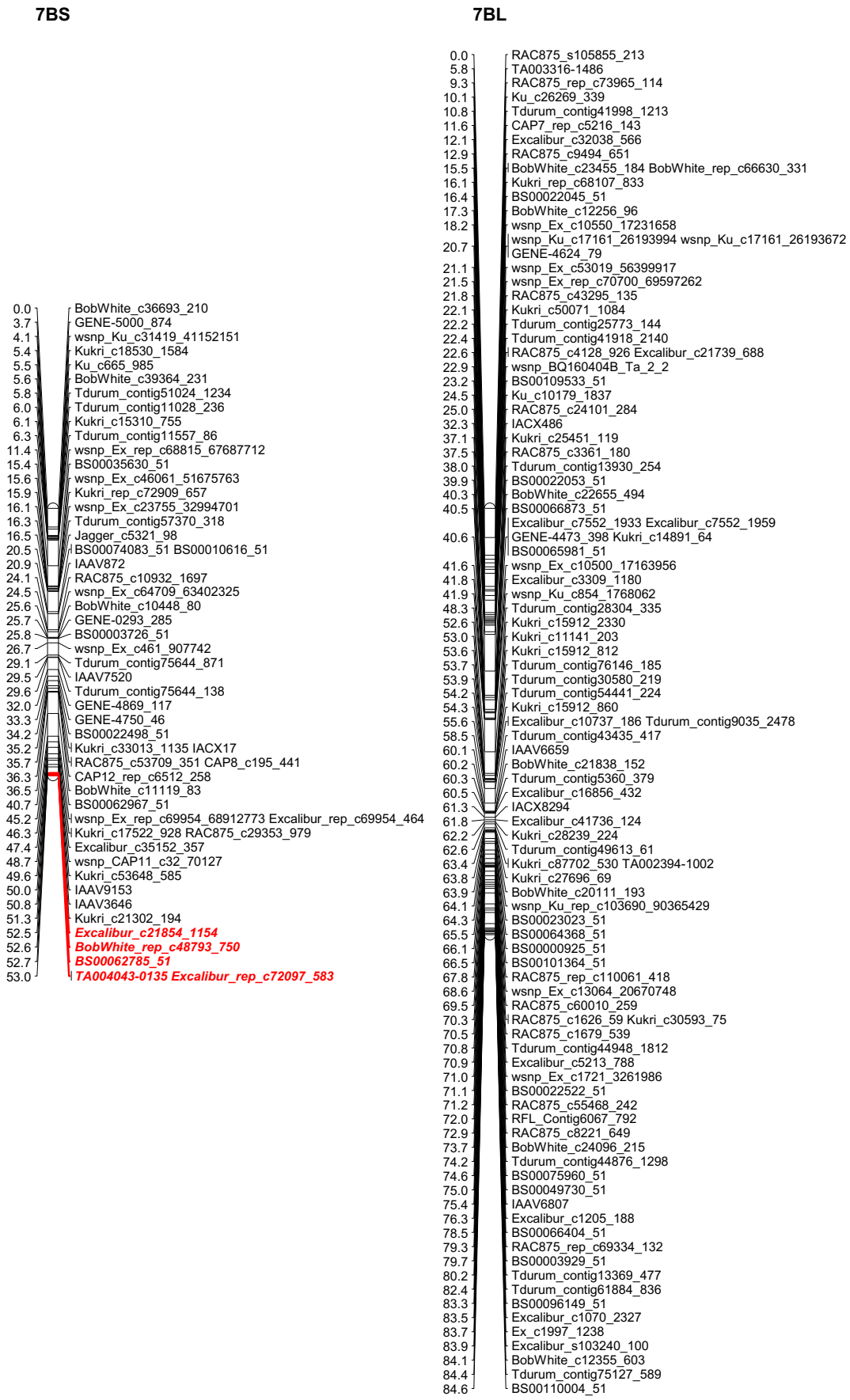
7BS
0.0 BobWhite_c36693_210
3.7 GENE-5000_874
4.1 wsnp_Ku_c31419_41152151
5.4 Kukri_c18530_1584
5.5 Ku_c665_985
5.6 BobWhite_c39364_231
5.8 Tdurum_contig51024_1234
6.0 Tdurum_contig11028_236
6.1 Kukri_c15310_755
6.3 Tdurum_contig11557_86
11.4 wsnp_Ex_rep_c68815_67687712
15.4 BS00035630_51
15.6 wsnp_Ex_c46061_51675763
15.9 Kukri_rep_c72909_657
16.1 wsnp_Ex_c23755_32994701
16.3 Tdurum_contig57370_318
16.5 Jagger_c5321_98
20.5 BS00074083_51 BS00010616_51
20.9 IAAV872
24.1 RAC875_c10932_1697
24.5 wsnp_Ex_c64709_63402325
25.6 BobWhite_c10448_80
25.7 GENE-0293_285
25.8 BS00003726_51
26.7 wsnp_Ex_c461_907742
29.1 Tdurum_contig75644_871
29.5 IAAV7520
29.6 Tdurum_contig75644_138
32.0 GENE-4869_117
33.3 GENE-4750_46
34.2 BS00022498_51
35.2 Kukri_c33013_1135 IACX17
35.7 RAC875_c53709_351 CAP8_c195_441
36.3 CAP12_rep_c6512_258
36.5 BobWhite_c11119_83
40.7 BS00062967_51
45.2 wsnp_Ex_rep_c69954_68912773 Excalibur_rep_c69954_464
46.3 Kukri_c17522_928 RAC875_c29353_979
47.4 Excalibur_c35152_357
48.7 wsnp_CAP11_c32_70127
49.6 Kukri_c53648_585
50.0 IAAV9153
50.8 IAAV3646
51.3 Kukri_c21302_194
52.5 Excalibur_c21854_1154
52.6 BobWhite_rep_c48793_750
52.7 BS00062785_51
53.0 TA004043-0135 Excalibur_rep_c72097_583
7BL
0.0 RAC875_s105855_213
5.8 TA003316-1486
9.3 RAC875_rep_c73965_114
10.1 Ku_c26269_339
10.8 Tdurum_contig41998_1213
11.6 CAP7_rep_c5216_143
12.1 Excalibur_c32038_566
12.9 RAC875_c9494_651
15.5 BobWhite_c23455_184 BobWhite_rep_c66630_331
16.1 Kukri_rep_c68107_833
16.4 BS00022045_51
17.3 BobWhite_c12256_96
18.2 wsnp_Ex_c10550_17231658
20.7 wsnp_Ku_c17161_26193994 wsnp_Ku_c17161_26193672 GENE-4624_79
21.1 wsnp_Ex_c53019_56399917
21.5 wsnp_Ex_rep_c70700_69597262
21.8 RAC875_c43295_135
22.1 Kukri_c50071_1084
22.2 Tdurum_contig25773_144
22.4 Tdurum_contig41918_2140
22.6 RAC875_c4128_926 Excalibur_c21739_688
22.9 wsnp_BQ160404B_Ta_2_2
23.2 BS00109533_51
24.5 Ku_c10179_1837
25.0 RAC875_c24101_284
32.3 IACX486
37.1 Kukri_c25451_119
37.5 RAC875_c3361_180
38.0 Tdurum_contig13930_254
39.9 BS00022053_51
40.3 BobWhite_c22655_494
40.5 BS00066873_51
40.6 Excalibur_c7552_1933 Excalibur_c7552_1959 GENE-4473_398 Kukri_c14891_64 BS00065981_51
41.6 wsnp_Ex_c10500_17163956
41.8 Excalibur_c3309_1180
41.9 wsnp_Ku_c854_1768062
48.3 Tdurum_contig28304_335
52.6 Kukri_c15912_2330
53.0 Kukri_c11141_203
53.6 Kukri_c15912_812
53.7 Tdurum_contig76146_185
53.9 Tdurum_contig30580_219
54.2 Tdurum_contig54441_224
54.3 Kukri_c15912_860
55.6 Excalibur_c10737_186 Tdurum_contig9035_2478
58.5 Tdurum_contig43435_417
60.1 IAAV6659
60.2 BobWhite_c21838_152
60.3 Tdurum_contig5360_379
60.5 Excalibur_c16856_432
61.3 IACX8294
61.8 Excalibur_c41736_124
62.2 Kukri_c28239_224
62.6 Tdurum_contig49613_61
63.4 Kukri_c87702_530 TA002394-1002
63.8 Kukri_c27696_69
63.9 BobWhite_c20111_193
64.1 wsnp_Ku_rep_c103690_90365429
64.3 BS00023023_51
65.5 BS00064368_51
66.1 BS00000925_51
66.5 BS00101364_51
67.8 RAC875_rep_c110061_418
68.6 wsnp_Ex_c13064_20670748
69.5 RAC875_c60010_259
70.3 RAC875_c1626_59 Kukri_c30593_75
70.5 RAC875_c1679_539
70.8 Tdurum_contig44948_1812
70.9 Excalibur_c5213_788
71.0 wsnp_Ex_c1721_3261986
71.1 BS00022522_51
71.2 RAC875_c55468_242
72.0 RFL_Contig6067_792
72.9 RAC875_c8221_649
73.7 BobWhite_c24096_215
74.2 Tdurum_contig44876_1298
74.6 BS00075960_51
75.0 BS00049730_51
75.4 IAAV6807
76.3 Excalibur_c1205_188
78.5 BS00066404_51
79.3 RAC875_rep_c69334_132
79.7 BS00003929_51
80.2 Tdurum_contig13369_477
82.4 Tdurum_contig61884_836
83.3 BS00096149_51
83.5 Excalibur_c1070_2327
83.7 Ex_c1997_1238
83.9 Excalibur_s103240_100
84.1 BobWhite_c12355_603
84.4 Tdurum_contig75127_589
84.6 BS00110004_51

Appendix K. Diagrammatic experimental workflow of X-ray phase contrast imaging (PCI) and computed tomography (CT) at the synchrotron.

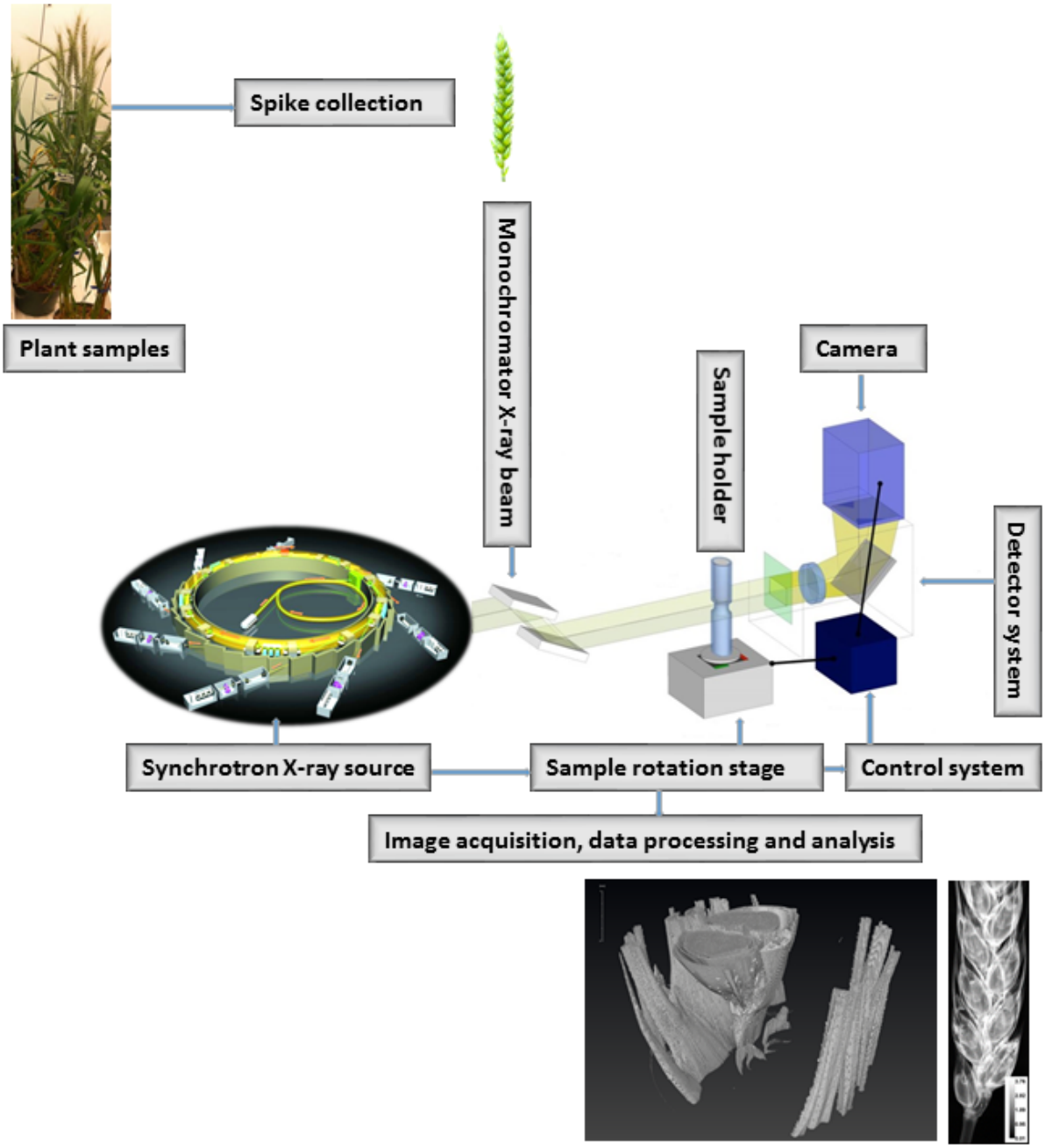

Appendix L. Positioning of cylindrical cropping volume to remove seed from the floret to isolate the rachilla + rachis node. The area inside the cylinder was removed prior to downstream analyses.

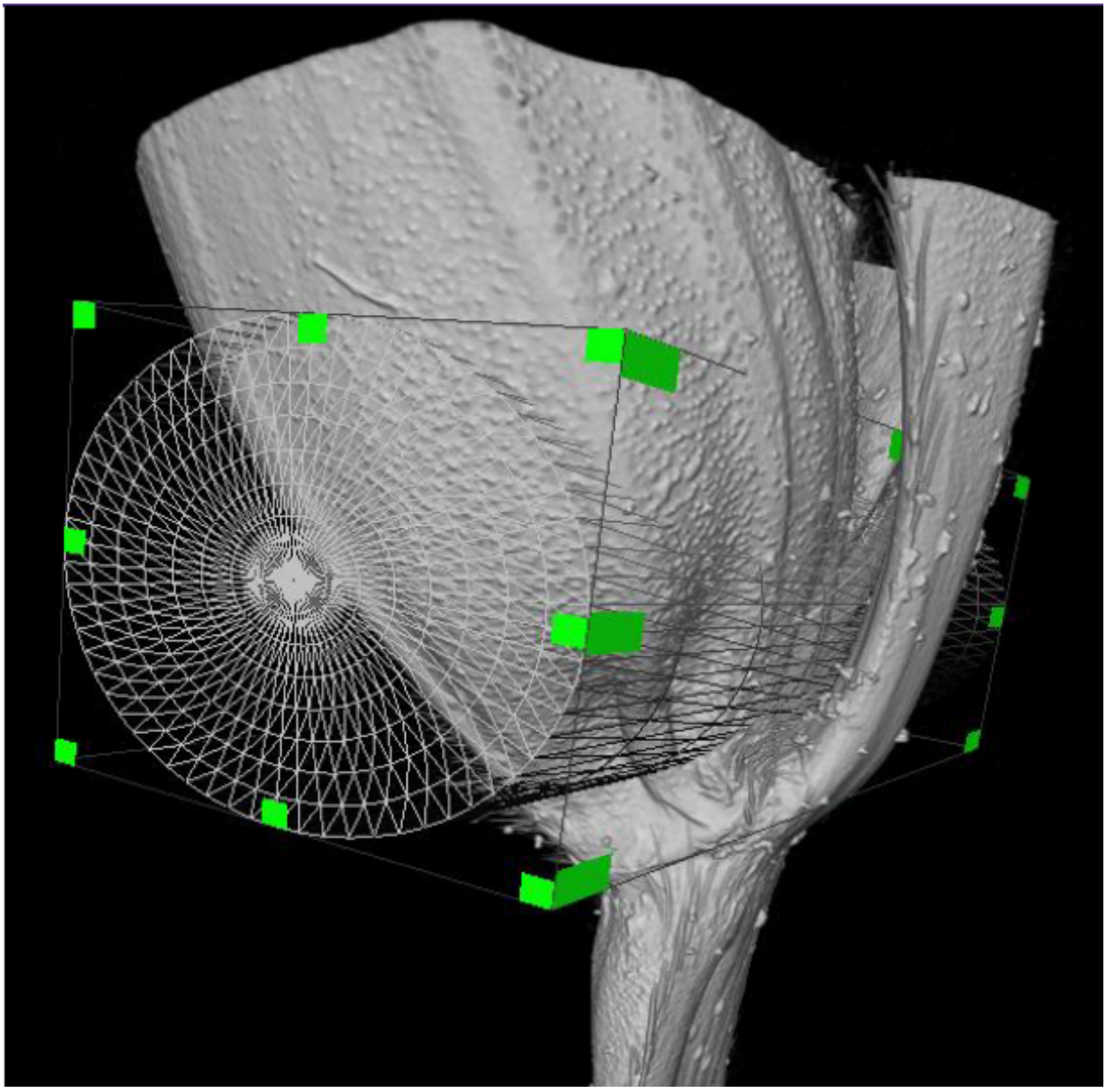

Appendix M. A voxel intensity histogram representing grayscale value for air.

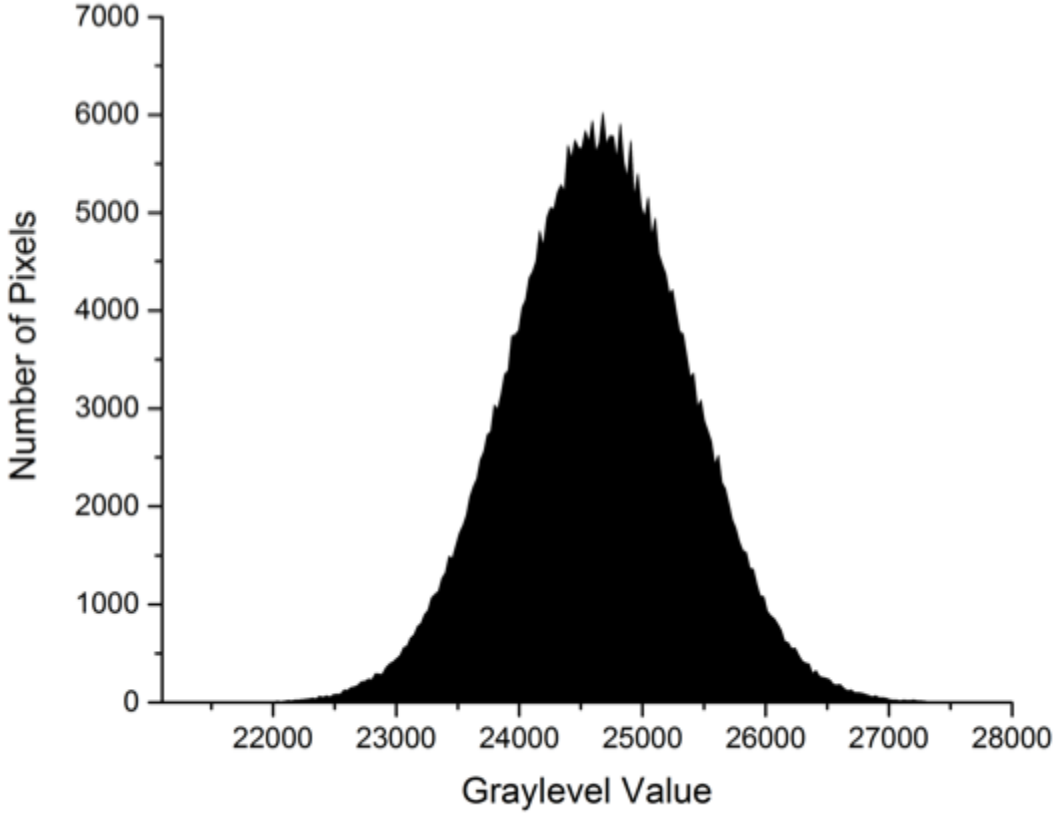

Appendix N. Second-derivative Fourier transform mid infrared (FTIR) spectra of seven wheat genotypes at 12 days post-inoculation with *Fusarium graminearum* (*Fg*). Genotypes were either challenged with *Fg* at 10^5 spores/ml or mock-inoculated with distilled water.

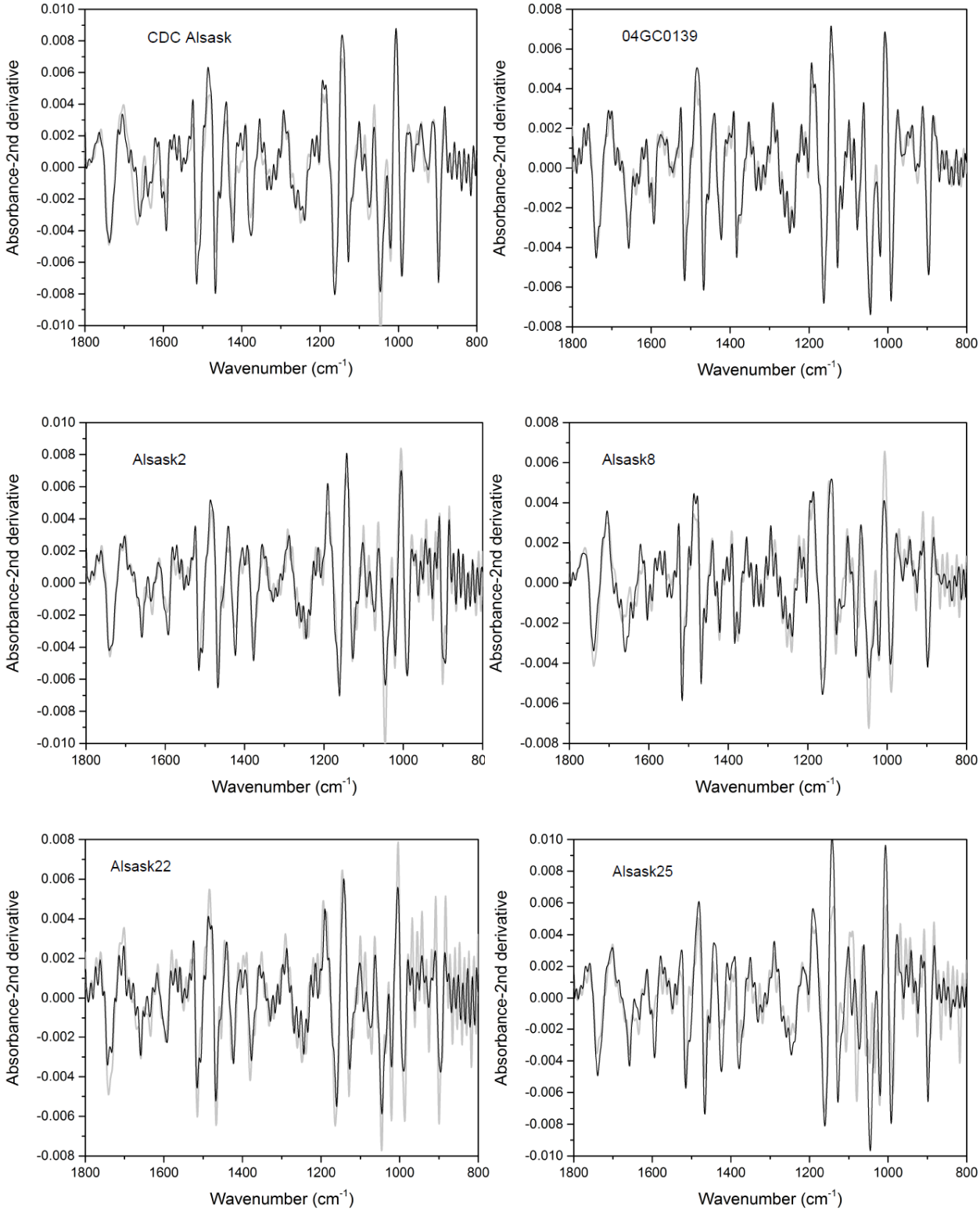

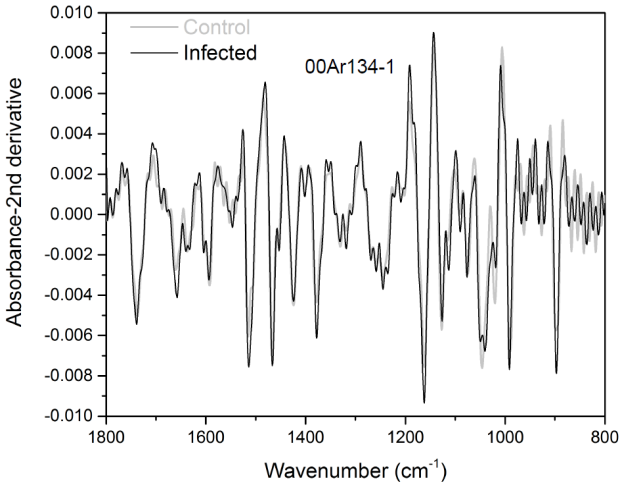
Control
Infected
00Ar134-1
Absorbance-2nd derivative
0.010
0.008
0.006
0.004
0.002
0.000
-0.002
-0.004
-0.006
-0.008
-0.010
1800
1600
1400
1200
1000
800
Wavenumber (cm-1)